UNIVERSITÉ DE SHERBROOKE

Faculté de génie

Département de génie électrique et de génie informatique

SURVEILLANCE PHOTONIQUE DES ACTIVITÉS BIOLOGIQUES DE BACTÉRIES IMMOBILISÉES SUR DES SURFACES DES SEMICONDUCTEURS QUANTIQUES BIOFUNCTIONNALISÉES

PHOTONIC MONITORING OF BIOLOGICAL ACTIVITIES OF BACTERIA IMMOBILIZED ON BIOFUNCTIONALIZED SURFACES OF QUANTUM SEMICONDUCTORS

Thèse de doctorat

Spécialité: Génie électrique

Elnaz NAZEMI

Jury : Jan J. DUBOWSKI (Directeur)

Eric H. FROST (Co-directeur)

Paul G. CHARETTE (Rapporteur)

Patrick VERMETTE (Examinateur)

Azam F. TAYABALI (Examinateur)

Sherbrooke (Québec) Canada January 2017

À mon mari et mes parents

RÉSUMÉ

Le suivi de la viabilitié, la croissance et le métabolisme cellulaire des bactéries peut contribuer de manière significative au diagnostic précoce de la maladie, mais peut aussi aider à améliorer le rendement des produits bactériens dans des expériences industrielle ou à petite echelle. Les méthodes conventionnelles utilisées pour l'étude de la sensibilité des bactéries aux antibiotiques sont basées principalement sur la culture, une technique qui prend au moins 12 heures pour rendre un résultat. Ce retard conduit au surtraitement d'un large éventail d'infections par des antibiotiques à large spectre, ce qui est coûteux et peut conduire à l'apparition de résistance à ces antibiotiques précieux, tandis que la détection rapide d'une infection virale ou l'absence de bactéries pourrait prévenir de tels traitements et, dans le cas d'une infection bactérienne, l'identification de la sensibilité aux antibiotiques pourrait permettre l'utilisation d'antibiotiques à spectre étroit. Le projet décrit dans le présent document vise à surveiller les activités biologiques des bactéries vivantes immobilisées sur les surfaces biofonctionnalisées de microstructures composées de semi-conducteurs quantiques (QS). Le procédé dépend de la sensibilité de la photoluminescence (PL) émise par des semi-conducteurs à la perturbation du champ électrique induit par la charge électrique des bactéries immobilisées sur la surface de ces structures. Dans la première phase du projet, nous avons étudié une méthode innovante impliquant la surveillance par PL de l'effet de photocorrosion dans des hétérostructures GaAs/AlGaAs. Le maintien d'un équilibre entre la sensibilité et la stabilité du biocapteur dans l'environnement aqueux nous a permis de détecter *Escherichia coli* K12 dans des solutions salines tamponnées au phosphate (PBS) avec une limite de détection attrayante de 10^3 UFC/ml en moins de 2 heures. Suite à cette recherche, nous avons émis l'hypothèse que ces hétérostructures pourraient être utilisés pour développer une méthode à faible coût et quasiment en temps reel de la croissance et de la sensibilité des bactéries aux antibiotiques. L'un des éléments clés dans le développement de cette plate-forme de biocapteurs était de démontrer que le GaAs (001), normalement utilisé pour recouvrir les hétérostructures de GaAs/AlGaAs, ne nuira pas à la croissance des bactéries. Dans la deuxième phase du projet, nous avons exploré la capture et la croissance de *E. coli* K12 sur des surfaces nues et biofonctionnalisées de GaAs (001). Il a été déterminé que la couverture initiale et les taux de croissance de bactéries dépendent de l'architecture de biofonctionnalisation utilisée pour capturer les bactéries: les surfaces biofonctionnalisées avec d'anticorps présentaient une efficacité de capture significativement plus élevée. En outre, on a trouvé que pour des suspensions contenant des bactéries à moins de 10^5 UFC/ml, la surface des plaquettes de GaAs ne supportait pas la croissance des bactéries, quel que soit le type d'architecture de biofonctionnalisation. Dans la troisième phase du projet, nous avons suivi la croissance et la sensibilité aux antibiotiques de *E. coli* K12 et *E. coli* HB101. Tandis que la présence de bactéries retardaient d'apparition du maximum de PL, la croissance des bactéries retardaient encore plus ce maximum. Par contre, en presence d'antibiotiques efficaces, la croissance des bactéries était arrêtée et le maximum de PL est arrivé plus tôt. Ainsi, nous avons pu distinguer entre des *E. coli* sensibles ou résistantes à la pénicilline ou à la ciprofloxacine en moins de 3h. En raison de la petite taille, du faible coût et de la réponse rapide du biocapteur, l'approche proposée a le potentiel d'être appliquée dans les laboratoires de diagnostic clinique pour le suivi rapide de la sensibilité des bactéries aux antibiotiques.

Mots clés: Semi-conducteurs quantiques, Photoluminescence, Photocorrosion, GaAs/AlGaAs hétérostructures, *Escherichia coli*, Détection bactérienne, Croissance bactérienne, Sensibilité aux antibiotiques des bactéries

ABSTRACT

Monitoring the viability, growth and cellular metabolism of bacteria can contribute significantly to the early diagnosis of disease, but can also help improve yield of bacterial products in industrial- or small-scale experiments. Conventional methods applied for investigation of antibiotic sensitivity of bacteria are mostly culture-based techniques that are time-consuming and take at least 12 h to reveal results. This delay leads to overtreatment of a wide range of infections with broad spectrum antibiotics which is costly and may lead to the development of resistance to these precious antibiotics, whereas rapid detection of a viral infection or absence of bacteria could prevent such treatments and, in the case of bacterial infection, identification of antibiotic susceptibility could allow use of narrow spectrum antibiotics. The project outlined in this document aims at monitoring biological activities of live bacteria immobilized on biofunctionalized surfaces of quantum semiconductor (QS) microstructures. The method takes advantage of the sensitivity of photoluminescence (PL) emitting semiconductors to the perturbation of the electric field induced by the electric charge of bacteria immobilized on the surface of these structures. Our hypothesis was that bacteria growing on the surface of biofunctionalized QS biochips would modify their PL in a different, and measurable way in comparison with inactivated bacteria. In the first phase of the project, we investigated an innovative method involving PL monitoring of the photocorrosion effect in GaAs/AlGaAs heterostructures. Maintaining the balance between device sensitivity and stability in the biosensing (aqueous) environment allowed us to detect *Escherichia coli* K12 in phosphate buffered saline solutions (PBS) at an attractive limit of detection of 10^3 CFU/mL in less than 2 hours. Following this research, we hypothesised that these heterostructures could be employed to develop a method for inexpensive and quasi-real time monitoring of the growth and antibiotic susceptibility of bacteria. One of the key elements in the development of this biosensing platform was to demonstrate that GaAs (001), normally used for capping PL emitting GaAs/AlGaAs heterostructures, would not inhibit the growth of bacteria. In the second phase of the project, we explored the capture and growth of *E. coli* K12 on bare and biofunctionalized surfaces of GaAs (001). It has been determined that the initial coverage, and the subsequent bacterial growth rates are dependent on the biofunctionalization architecture used to capture bacteria, with antibody biofunctionalized surfaces exhibiting significantly higher capture efficiencies. Moreover, for suspensions containing bacteria at less than 10^5 CFU/mL, it has been found that the surface of GaAs wafers could not support the growth of bacteria, regardless of the type of biofunctionalization architecture. In the third phase of the project, we used PL to monitor the growth and antibiotic susceptibility of *E. coli* K12 and *E. coli* HB101 bacteria. While immobilization of bacteria on the surface of GaAs/AlGaAs heterostructures retards the PL monitored photocorrosion, growth of these bacteria further amplifies this effect. By comparing the photocorrosion rate of QS wafers exposed to bacterial solutions with and without antibiotics, the sensitivity of bacteria to the specific antibiotic could be determined in less than 3 hours. Due to the small size, low cost and rapid response of the biosensor, the proposed approach has the potential of being applied in clinical diagnostic laboratories for quick monitoring of antibiotic susceptibility of different bacteria.

Key words: Quantum semiconductors; Photoluminescence; Photocorrosion; GaAs/AlGaAs heterostructures; *Escherichia coli*; Bacterial detection; Bacterial growth; Antibiotic susceptibility of bacteria

ACKNOWLEDGMENT

I would like to offer my deepest and sincerest gratitude to my supervisor, Professor Jan J. Dubowski, who has supported me through this work with his expertise, motivation, valuable guidance and thoughtful advice. I appreciate his vast knowledge and skills in many areas and I am extremely thankful to him for providing me with an excellent atmosphere to do my research project.

I would like to express my special appreciation and thanks to my co-supervisor, Professor Eric H. Frost, for sharing his enthusiasm and knowledge with me. I would like to thank him for his valuable comments and insightful suggestions.

I would also like to warmly thank my committee members, Professor Paul G. Charette, Professor Patrick Vermette and Professor Azam F. Tayabali, for their precise and valuable comments.

I take this opportunity to thank Dr. Khalid Moumanis and Dr. Walid M. Hassen for their care, kindness and great assistance throughout this work.

I also want to thank all the members of the QS group at UdeS, who have been good colleagues and more than that good friends. Being a part of this group was a pleasure for me.

Last, but certainly not least, I would like to thank my friends and my family for their support. Especially I would like to thank my parents and my lovely sister for supporting me spiritually throughout my life, all I am or I hope to be is because of them. Words cannot express how grateful I am to them.

Finally, my tremendous and deep thanks belongs to my husband, Mohsen Rohani, who always stood by me through the good times and bad. Without his never ending support, encouragement and love, I would not have been able to finish my thesis.

TABLE OF CONTENTS

LIST of FIGURES

LIST of TABLES

LIST of ACRONYMS

Acronyms	Definition
Ab	Antibody
AFM	Atomic force microscopy
ars	Arsenic resistance determinant
AS	Ammonium sulfide
AST	Antibiotic susceptibility test
ATP	Adenosine 5′-triphosphate
ATR	Attenuated total reflectance
b-Ab	Biotinylated antibody
BCP	Bacterial cytological profiling
BGM	Bacterial growth monitoring
BioFET	Biosensing field effect transistor
b-PEG	Biotinylated polyethylene glycol
BSA	Bovine serum albumin

CBCM	Charge based capacitive measurement
CBE	Conduction band edge
CE	Capillary electrophoresis
CF	Cystic fibrosis
CFU	Colony forming unit
CPE	Constant phase element
DC	Duty cycle
DGMOSFET	Dual-gate MOSFET
DIC	Differential interference contrast
DI H_2O	Deionized water
EDC	1-ethyl-3-(3-dimethylaminopropyl)-carbodiimide
EIA	Enzyme immunoassay
EIS	Electrochemical impedance spectroscopy
ELISA	Enzyme-linked immunosorbent assay
EOT	Extraordinary optical transmission
FBI	Food-borne illness

FET	Field-effect transistor
FL	Fermi level energy
FREDFET	Fast-reverse epitaxial diode FET
FRET	Fluorescence resonance energy transfer
FTIR	Fourier transform infrared
GFP	Green Fluorescent Protein-Expressing
HDT	1-hexadecanethiol
HGT	Horizontal gene transfer
HI-PLM	Hyperspectral imaging PL mapper
IDL	Interfacial dipole layer
IHL	Inner Helmholtz layer
ISFET	Ion-sensitive FET
LB	Luria Bertani
LED	Light-emitting diode
LIF	Laser induced fluorescence
LOD	Limit of detection

LPCVD	Low pressure chemical vapor deposition
MAC	Microfluidic agarose channel
MEMS	Microelectromechanical systems
MHDA	16-mercaptohexadecanoic acid
MIC	Minimum inhibitory concentration
MOCSER	Molecular controlled semiconductor resistor
MOSFET	Metal-oxide-semiconductor FET
MUDA	11-mercaptoundecanoic acid
MUDO	11-mercapto-1-undecanol
NA	Neutravidin
NHS	N-hydroxysuccinimide
OD	Optical density
OHL	Outer Helmholtz layer
PBS	Phosphate buffered saline solution
PC	Photonic crystal
PCR	Polymerase chain reaction

PECVD	Plasma enhanced chemical vapor deposition
PEG	Polyethylene glycol
PL	Photoluminescence
PVD	Physical vapor deposition
QCM	Quartz crystal microbalance
QD	Quantum dot
QS	Quantum semiconductor
QSPB	Quantum semiconductor photonic biosensor
QW	Quantum well
RMS	Root mean square
SAM	Self-assembled monolayer
SCR	Space charge region
SEM	Scanning electron microscope
SERS	Surface-enhanced Raman spectroscopy
SLB	Supported lipid bilayers
SPM	Scanning probe microscopy

SPR	Surface plasmon resonance
SRV	Surface recombination velocity
TATP	Triacetone triperoxide
TEM	Transmission electron microscope
TFET	Tunnel FET
UDT	1-undecanethiol
VBE	Valance band edge
VBG	Volume Bragg grating
VEGF	Vascular endothelial growth factor
XPS	X-ray photoelectron spectroscopy

CHAPTER 1: Introduction

1.1 Project outline

Bacterial infections are one the major causes of human and animal diseases ranging from food poisoning to respiratory infections and death. Food poisoning or food-borne illness (FBI) are one of the most common diseases throughout the world today (Addis and Sisay 2015). FBI is caused by bacteria, viruses, moulds, parasites and some chemicals present in foods. Although the majority of bacteria are harmless and some of them are even helpful for production of some foods such as cheese and yogurt, pathogenic bacteria are the main cause of food poisoning. It has been reported that 66% of FBI are caused by bacteria (Adams and Moss 2008; Addis and Sisay 2015; CDC 2011). According to the report provided by Centers for Disease Control and Prevention (CDC), around 48 million people got sick and 3,000 died from FBI in USA in 2011 (CDC 2011). Water-borne disease is another type of illness which is transmitted through drinking or industrial water. Circulating cooling water systems provide desirable conditions for growth of bacteria due to the favourable pH (generally between 7-9) and temperature (between 20° C-40° C). Cooling towers are favourable environments for growth of *Legionella* which causes Legionnaires' disease (a dangerous type of lung infection) (CDC 2016b). Plumbing systems, especially hospital plumbing can harbour *Pseudomonas, Mycobacteria,* and *Legionella* (Falkinham et al. 2015). Typhoid fever, bacillary dysentery and cholera are the most important bacterial water-borne illnesses (Cabral 2010). Water-borne diseases don't threaten only developing countries. Developed countries are also affected by this type of illness, e.g., around 12,000 people die from water-borne diseases in USA per year (Cabral 2010; Medema et al. 2003).

Antibiotics play a vital role in treating infections and saving patients' lives. They are also of great importance in achievement of significant advances in medicine and surgery fields (Gould and Bal 2013). The first prescription of antibiotics for treating severe infections goes back to 1940s (CDC 2016a). During World War II penicillin succeeded to treat bacterial infections among soldiers (Sengupta et al. 2013). However, by the 1950s resistance of bacteria to penicillin

became a clinical problem and threatened the prior advances in this field (Spellberg and Gilbert 2014). To control this crisis, new beta-lactam antibiotics were introduced and developed (Sengupta et al. 2013; Spellberg and Gilbert 2014), however, shortly thereafter, methicillin-resistant bacteria were identified in the United Kingdom and USA in 1960s (Sengupta et al. 2013). Nowadays, antibiotic-resistance has been recognized as a major clinical problem that threatens human lives (Ventola 2015; WHO 2016). It has been reported that at least 2 million people become infected with antibiotic-resistant bacteria and at least 23,000 people die directly because of these infections each year in the USA (CDC 2016a).

There are several factors leading to antibiotic-resistance such as overuse and inappropriate prescription of antibiotics (Ventola 2015). Generally bacteria could inherit genes from relatives or receive them through horizontal gene transfer (HGT). Through HGT genes responsible for resistance of bacteria to antibiotics, which are usually found in plasmids, could be transferred among various types of bacteria and make them antibiotic-resistant. Resistance of bacteria to antibiotics could spread naturally when antibiotics remove drug-sensitive competitors of bacteria and fail to stop bacterial growth or kill bacteria (Read and Woods 2014). It has been reported that prescription of antibiotics in 30% to 60% of cases is not appropriate or necessary in intensive care units (ICUs) (Bergmans et al. 1997; Kollef 2001; Kollef and Fraser 2001; Roberts et al. 2014). This is often due to the fact that treatment must be started before antibiotic sensitivity is known or even bacteria identified.

The main methods used for investigation of antibiotic susceptibility of bacteria are broth microdilution and Kirby-Bauer disk diffusion tests. In the broth microdilution method, bacteria are inoculated into broth with increasing concentrations of antibiotic. The lowest concentration of the antibiotic that inhibits the growth of bacteria is called the minimum inhibitory concentration (MIC). In this method, the growth of bacteria in the presence of the antibiotic is evaluated according to the turbidity of the bacterial suspension. In the Kirby-Bauer method, the bacteria are evenly inoculated in the Petri dish and then paper disks containing precise amounts of the antibiotics are placed in the Petri dish. If the antibiotic is effective against the bacteria, a circle without bacterial growth is observed around the paper disk. The larger the circle, the more the bacteria is sensitive to the antibiotic (Jorgensen and Ferraro 2009; Poupard et al. 1994; Versalovic et al. 2011). These techniques are time-consuming and require controlled laboratory

conditions. A variety of nanomethods like surface plasmon resonance (SPR) (Chiang et al. 2009), impedance (Rieder et al. 2009; Zavizion et al. 2010), and cytological methods (Quach et al. 2016) have been developed to assess antibiotic sensitivity more rapidly. However, they often rely on very subtle changes and so may be difficult to bring to hospital laboratories without highly specialized technicians. Therefore, development of a simple, rapid and sensitive method for detection of growth and antibiotic sensitivity of bacteria at low cost remains an attractive but elusive goal for clinical diagnostics, food and water control industries.

Photoluminescence-emitting semiconductors have great potential of being applied in biosensing fields due to the sensitivity of their PL signal to the phenomena taking place at the surface of these materials (Adamowicz et al. 1998; Gfroerer 2006; Lebedev 2001; Moumanis et al. 2006; Tomkiewicz et al. 2009). For instance, immobilization of electrically charged molecules at the surface of a semiconductor modifies the bending of energy bands near the surface which could affect PL of such a material (Seker et al. 2000; Zhang and Yates 2012). Syshchyk et al. (Syshchyk et al. 2015) employed PL emission of nanoporous Si layers to detect different concentrations of glucose and urea.

The goal of this thesis was to develop a photonic method for monitoring biological activities of bacteria immobilized on the surfaces of biofunctionalized quantum semiconductor (QS) microstructures. The approach of this thesis was based on measuring the photoluminescence signal from specially designed QS microstructures that is highly sensitive to the amount of negative electric charge accumulated on the surface of these devices. Previous PL studies of functionalized QS biochips have been focused on detection of *E. coli* K12 bacteria. It has been reported that the negative electric charge of bacteria immobilized on the GaAs/AlGaAs biochips increased the intensity of the PL signal emitted from these microstructures (Duplan et al. 2011). Following this research, we hypothesized that bacteria growing on the surface of biofunctionalized GaAs/AlGaAs biochips would modify their PL in a different, and measurable way in comparison with inactivated bacteria. Our hypothesis was that the local field interactions between the bacteria and the QS substrate on which the bacteria were immobilized would induce changes in the PL of QS and allow us to monitor some activities of bacteria such as growth and their reactions to antibiotics. Using the PL emission of semiconductors to study biological activities of bacteria is a relatively novel approach, and the first challenge was to demonstrate if bacteria, indeed, could grow on surfaces of the investigated biochips.

1.2 Research project objectives

The principal objective of the project was to investigate an Ab-based architecture for immobilization of *E. coli* K12 bacteria in order to develop a GaAs/AlGaAs-based photonic biosensor for monitoring biological activity of bacteria. The first hypothesis was that bacteria can grow on a biofunctionalized surface of GaAs. The second hypothesis was that photoluminescence of bulk GaAs or epitaxial GaAs/AlGaAs microstructures could be used to monitor bacterial growth. The third hypothesis was that sensitivity of a photoluminescence-based biosensor allows detecting differences between growth rates of intact and antibiotic affected bacteria. To achieve the principal objective of the project, it was necessary to define and fulfill specific intermediate objectives.

1.2.1 Optimization of the biofunctionalization architecture to immobilize bacteria

The first step of the project was to find an efficient bio-architecture to functionalize the surface of GaAs/AlGaAs heterostructures. This step was of high importance to improve the ability of the surface to capture bacteria. In order to be able to monitor growth and antibiotic susceptibility of bacteria by using PL emission of the GaAs/AlGaAs biochip, the bacteria should first be immobilized on the surface of the biochip, therefore, improving biofunctionalization methods to increase the ability of the biosensor to capture the bacteria and improve sensitivity was needed in this project.

1.2.2 Detection of bacteria using PL emission of GaAs/AlGaAs heterostructures

Before monitoring the biological activity of bacteria immobilized on the biofunctionalized surfaces of GaAs/AlGaAs heterostructures, we should investigate the effect of bacterial immobilization on the PL of these structures. Although the detection of *E. coli* K12 bacteria based on PL emission of GaAs/AlGaAs heterostructures has been carried out before (Duplan et al. 2011), we should investigate the effect of bacterial immobilization on PL of the biochips functionalized with our optimized bio-architecture.

1.2.3 Growth of bacteria on bare and biofunctionalized surfaces of GaAs

One of the key elements in the development of the proposed photonic biosensor to monitor growth and antibiotic susceptibility of bacteria is investigation of growth of bacteria on the surface of GaAs, our material of interest for capping GaAs/AlGaAs heterostructures. Due to the toxic properties of arsenic (As) and gallium (Ga) (Tanaka 2004), we should find the minimum bacterial concentration that could grow on GaAs surfaces while the biochips are kept in darkness or irradiated under laser light.

1.2.4 Photonic monitoring of bacterial growth

After investigation of bacterial growth on the surfaces of GaAs samples, we intended to monitor the growth of bacteria using PL emission of GaAs/AlGaAs heterostructures. The growth of bacteria would be investigated by comparison of PL emission of the samples exposed to live bacteria and growth medium with that of UV-killed bacteria and growth medium.

1.2.5 Photonic monitoring of bacterial susceptibility to antibiotics

The final goal of the project was to investigate antibiotic susceptibility of bacteria using PL emission of GaAs/AlGaAs heterostructures. The reaction of bacteria to a specific antibiotic would be interpreted from the PL curves showing the PL emission of the biofunctionalized GaAs/AlGaAs heterostructures exposed to (1) bacteria and growth medium and (2) bacteria, growth medium containing antibiotics.

1.3 Thesis plan

The thesis is structured in 7 chapters.

In the present chapter an introduction to the subject of the thesis is provided. After discussion of bacterial threats to human health and the emerging antibiotic resistance problem, the general outline of the project and the objectives of the project are presented.

In Chapter 2 an introduction to bacteria and their adhesion to solid surfaces are described. Moreover, we review different methods, including conventional and biosensing approaches, applied to investigate bacterial adhesion and monitor antibiotic susceptibility of bacteria. In this chapter, semiconductor-based sensors and the importance of surface functionalization of semiconductors for biosensing purposes are also discussed.

Chapter 3 demonstrates the detection of *E. coli* at different concentrations by PL monitoring of the photocorrosion effect from GaAs/AlGaAs heterostructures functionalized with self-assembled monolayers (SAMs) of alkanethiols, post-processed in an ammonium sulfide solution and exposed to neutravidin and biotinylated antibodies against *E. coli*. The formation of surface oxides and dissolution of a limited thickness of the GaAs cap material results in the appearance of a characteristic maximum in temporal PL plots collected over time. The position of the PL maximum (the photocorrosion rate) depends on the concentration of the electric charge immobilized in the vicinity of the surface of PL emitting semiconductor biochips, and is delayed with increasing concentrations of bacteria in PBS solutions surrounding the antibody functionalized biochips. Post-processing of alkanethiol SAM functionalized biochips with ammonium sulphide increases their photonic stability in a biological environment, and enables us to demonstrate detection of *E. coli* in PBS at 10^3 CFU/mL, which represents a one-order improved limit of detection in comparison to that reported in 2011 without the use of ammonium sulphide (Duplan et al. 2011). This chapter has been published in Sensors and Actuators B: Chemical.

Chapter 4 studies growth of *E. coli* on bare and biofunctionalized surfaces of GaAs (001) and gold samples using microscopy to count adherent bacteria. We observed that, as long as the GaAs wafers were exposed to bacterial suspensions at concentrations of at least 10^5 CFU/mL, bacteria could grow on the surface of wafers, regardless of the type of the biofunctionalization architecture used to capture the bacteria. However, the initial coverage and the subsequent bacterial growth rate were found to depend on the bio-architecture, with antibody functionalized surfaces clearly being more efficient in capturing bacteria and providing better conditions for bacterial growth. In this chapter, we have compared the initial capture and growth rate of bacteria at different initial concentrations ranging from 10^5-10^8 CFU/mL using

biofunctionalization architectures based on SAMs of 16-mercaptohexadecanoic acid (MHDA) thiols. This chapter has been submitted to Journal of Biological Engineering.

Based on our success in showing microscopic growth of bacteria on GaAs and gold surfaces, in chapter 5, growth and antibiotic sensitivity of *E. coli* have been investigated by PL monitoring of photocorroding GaAs/AlGaAs heterostructures. While bacteria captured on the surface of biochips retard the PL maximum, growth of these bacteria further delays the PL maximum. By monitoring the formation of PL maxima of biofunctionalized GaAs/AlGaAs biochips exposed to different bacterial and antibiotic solutions, we demonstrated the functionality of the biochips for monitoring the growth and antibiotic sensitivity of penicillin-sensitive and penicillin-resistant *E. coli* at ambient temperature in less than 3 hours. This chapter has been published in Biosensors and Bioelectronics. The extended abstract of this chapter has also been accepted for publication in Procedia Technology (PROTCY).

In Chapter 6 mechanisms of bacterial interactions with semiconductor surfaces and the experimental results complementary to Chapters 3-5 are presented. Section 6.3 of this chapter describes principal points of a related patent application (publication number of WO2015113164A1).

Chapter 7 summarizes an overview of the research project. In addition, the perspectives and the proposed future work are also explained.

CHAPTER 2: State of the art

The first step to achieve the main goal of the project is immobilization of bacteria on the surface of GaAs which is a material of interest for capping GaAs/AlGaAs heterostructures. Since there is no literature discussing this subject, in this chapter we are presenting an introduction of bacterial adherence to other surfaces, mechanisms of adherence and factors influencing adhesion of bacteria to solid surfaces. This chapter also draws a picture of different methods applied to investigate bacterial adhesion and monitor their activities. In this chapter different techniques including conventional methods and biosensing approaches applied to monitor activities of bacteria such as growth and antibiotic susceptibility are discussed. At the end, a review of the methods employed to functionalize the surface of semiconductors is also provided.

2.1 Bacteria and their adhesion to surfaces

2.1.1 Bacterial characteristics relevant for biosensor technology

Bacteria are unicellular prokaryotic microorganisms that are invisible to the naked eye, except for a few cases such as *Thiomargarita namibiensis* that have been discovered with diameter of up to 0.75 mm (Planck 1999; Schulz et al. 1999). Bacteria can be found in almost all environments and play an important role in recycling the materials and production of different types of biomolecules such as amino acids, enzymes, hormones and etc. The majority of bacteria are beneficial or harmless, however, some of them are pathogenic and threaten human health (Doyle et al. 2013; Lim et al. 2010; Mead et al. 1999; Wanke 2001).

The genome (genetic material) of most bacteria consists of a single circular DNA molecule. They also can have smaller pieces of circular DNA called plasmids that often carry genes conferring resistance to substances like Hg or antibiotics. Plasmids can be transferred from the donor bacterium to a recipient bacterium through the conjugation or transformation processes (Bennett 2008; Grohmann et al. 2003). These processes are responsible for the appearance and dissemination of antibiotic-resistant bacteria, particularly multiple drug resistant enteric bacteria like some recent isolates of *E. coli* (McGann et al. 2016; Ruppé et al. 2015). Antibiotic resistance has become a world problem (Carlet et al. 2014; CDC 2013; Gootz 2010; WHO 2015).

Bacteria are generally classified into two groups of gram-positive and gram-negative based on the composition of their cell walls. Gram-positive bacteria have a rigid layer of peptidoglycan that is 15-80 nm thick on top of the plasma membrane. For gram-negative bacteria, the peptidoglycan layer is thinner (1-2 nm) and it is sandwiched between the plasma membrane and the outer membrane (Kleijin and van Leeuwen 2000; Poortinga et al. 2002; Tsien et al. 1978) (see Figure 1). The general method applied to differentiate between these two species is called Gram staining or Gram's method in which type of the bacteria is identified based on bacterial colour after staining.

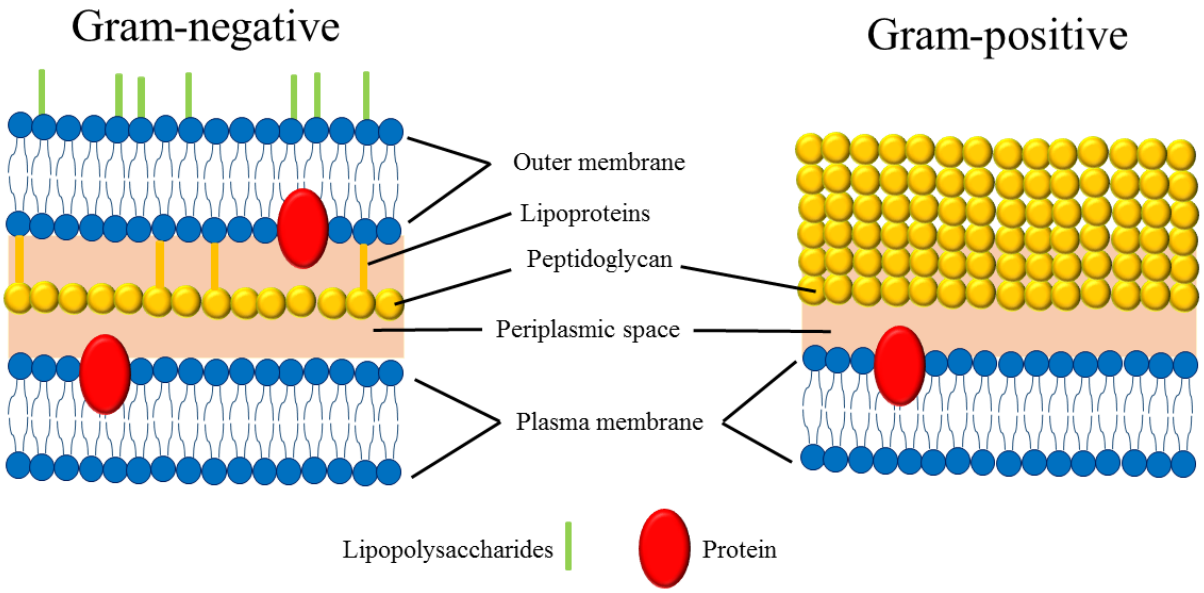

Figure 1. Schematic illustration of gram-positive and gram-negative bacteria (scales are not accurate). Adapted from (Istockphoto LP 2015).

There are various types of structural features on the surface of the outer membrane in gram-negative and on top of the peptidoglycan layer in gram-positive bacteria. The ability of bacteria to adhere to solid surfaces is associated with their surface appendages and surface macromolecules. Flagella, fibrils and fimbriae are the most important surface features that are mostly involved in bacterial movement and bacterial attachment to solid surfaces. Flagella are threadlike appendages that are made of several polypeptides. They are around 20 nm in diameter and 10-20 µm in length. Fimbriae are proteinaceous appendages that are found in many gram-negative and gram-positive bacteria. They can be rigid or flexible and are about 0.2-2.0 µm in

length and 2-10 nm in diameter. Fibrils are another type of appendages that are less than 0.2 μm long and small variable width (Busscher et al. 2000; Poortinga et al. 2002). In addition to these appendages, there are lipopolysaccharides in gram-negative bacteria, and proteins, polysaccharides and many other macromolecules on the surface of bacteria involved in energy (ATP) production, transport into and out of the bacteria and other bacterial functions including synthesis and assemblage of the outer membrane and flagella. Some pathogenic bacteria are also surrounded by a capsule made of polysaccharides that prevents white blood cells from ingesting the bacteria and antibodies from binding to the proteins underneath. Some bacteria use their surface appendages to adhere to surfaces and survive, for example oral bacteria use their fibrils or fimbriae to adhere to tooth surfaces for their survival and not to be swallowed (Poortinga et al. 2002; Sjollema and Busscher 1989). However, in some cases surface macromolecules block adherence of bacteria to surfaces, e.g., presence of capsular polysaccharide colonic acid on the surface of uropathogenic *E. coli* blocks adhesion of bacteria on both hydrophilic and hydrophobic surfaces (Hanna et al. 2003). We will need to use these surface molecules to attach bacteria to semiconductor surfaces.

2.1.2 Bacterial adhesion to solid surfaces

Bacterial adhesion is an important phenomenon in soil ecology, the food industry and in medical fields related to human life. In general, bacteria can exist freely in solutions (planktonic bacteria) or can adhere to solid substrates and form biofilms (Garrett et al. 2008). Bacteria produce biofilms to be protected from antimicrobial agents such as antibiotics (Goldberg 2002) and disinfectants (Peng et al. 2002). Biofilms have become a serious problem in many industries such as oil (Nemati et al. 2001), maritime (Busscher and van Der Mei 1995), food (Srey et al. 2013) and water systems (Bott 1998). Some of the problems caused by biofilms are speeding up the corrosion of steel, blocking the pores of membranes and decreasing the trans-membrane pressure, and contamination of water and food products (Mortensen 2014). Research into bacterial adhesion is also of great importance in healthcare and pharmaceutical fields because adhesion of bacteria to human tissue surfaces is considered as the first step of the pathologic process (An and Friedman 2000; Gristina and Costerton 1985). If they do not adhere, they will be swept away by host defenses. In addition, study of bacterial adhesion and investigation of

the factors influencing adhesion of bacteria to surfaces plays an important role in the biosensing field, because the first step in performance of most of the biosensors applied for detection and/or monitoring biological activities of bacteria is adhesion of bacteria to the biosensing elements.

Stable attachment of bacteria to a solid surface requires the following processes: movement to the vicinity of the surface, attachment to the surface and resistance of detachment in the presence of any forces by means of molecular and cellular interactions. In general, adhesion of bacteria to solid substrates is described as a two-phase process: reversible physiochemical interactions (phase I) and irreversible intimate molecular and cellular interactions (phase II) (Deupree 2009; Gristina 1987; Quirynen et al. 2000). Phase I happens quickly where a set of mechanical processes including gravity, Brownian motion and chemotaxis are first responsible for bringing the bacteria close to the surface. After that, attachment of the bacteria to the surface happens via long- and short-range reversible physiochemical interactions including electrostatic attractions, hydrophobic interactions and van der Waals forces. These interactions happen along vectors perpendicular to the surface (Deupree 2009; van Loosdrecht et al. 1990). Bacterial attachment enters the second phase if the net attractions exceed the repulsive forces in the first phase. During phase II, macromolecules on the surface of the bacteria, if present, may attach to the substrate via cellular and molecular interactions, as illustrated in Figure 2.

There are some parameters affecting adhesion of bacteria to biomaterial surfaces such as surface free energy, charge and hydrophobicity of surface and charge and hydrophobicity of bacteria (Busscher et al. 1984; Dutta et al. 2012; Merritt and An 2000; Reynolds and Wong 1983). In addition, surface roughness also plays an important role in bacterial immobilization rates on solid surfaces (Merritt and An 2000), e. g., it has been suggested to use intraoral hard surfaces with optimal smoothness to reduce the rate of bacterial immobilization (Quirynen et al. 1993).

The adhesion of bacteria to solid substrates can be predicted by the thermodynamic approach. On the basis of this rule, neglecting the electrical charge interactions, adhesion of bacteria to a solid surface may be expected only if (Absolom et al. 1983; Busscher et al. 1984),

$$AF_{adh} = \gamma_{sb} - \gamma_{sl} - \gamma_{bl} < 0 \qquad (2.1)$$

where AF_{adh} is the interfacial free energy of adhesion, γ_{sb} is the solid-bacterium interfacial free energy, γ_{sl} is the solid-liquid interfacial free energy and γ_{bl} is the bacterium-liquid interfacial free energy.

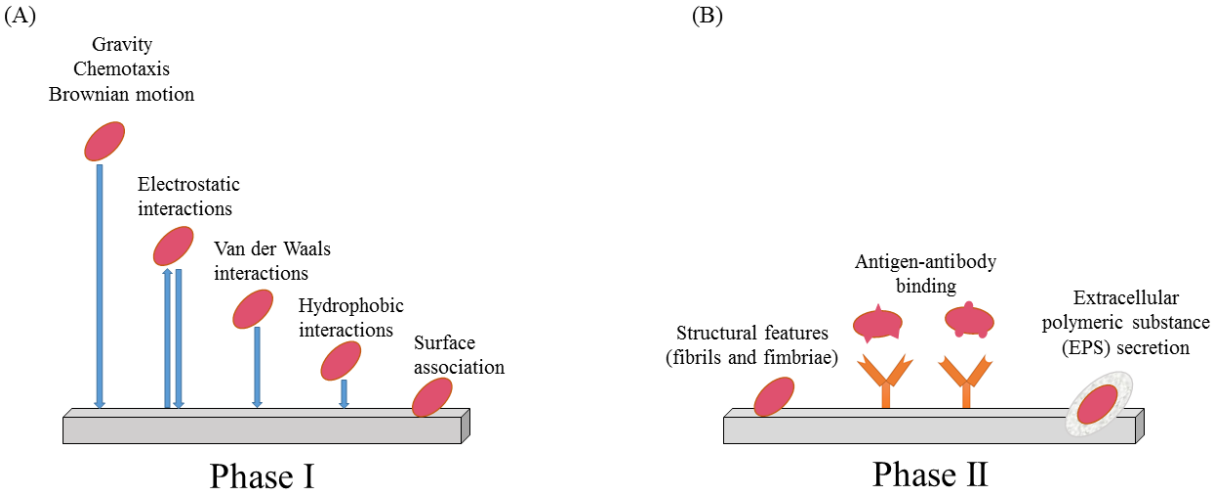

Figure 2. Schematic illustration of attachment of bacteria to solid surfaces including reversible physiochemical interactions (phase I) (A) and irreversible intimate molecular and cellular interactions (phase II) (B). Adapted from (Deupree 2009).

Another parameter affecting adhesion of bacteria to solid substrates is the charge of the surface and the bacteria. It should be noted that most bacteria are negatively charged at a pH greater than 4. The negative charge mainly arises from the excess number of carboxyl and phosphate groups compared with the amino groups (Poortinga et al. 2002). When bacteria are suspended in a solution, like PBS (1X), the bacterial surface would be surrounded by positively charged counter ions present in the solution as presented in Figure 3. For a bacterial surface with N_1 acid (like -COOH) and N_2 base (like $-NH_2$) uncharged groups per unit volume with dissociation constants of K_{a1} and K_{a2}, a space charge density fixed to the cell surface is determined by equation (2.2) (Healy and White 1978; Poortinga et al. 2002),

$$\rho_{fix} = eN_1 \frac{-Ka_1}{K_{a1} + [H^+]\exp(-e\psi/kT)} + eN_2 \frac{[H^+]exp(-e\psi/kT)}{K_{a2} + [H^+]exp(-e\psi/kT)} \quad (2.2)$$

where e is the charge of electron, $[H^+]$ is the concentration of proton, ψ is the electric potential at the location of the ionisable surface group, k is Boltzmann constant and T is the absolute temperature.

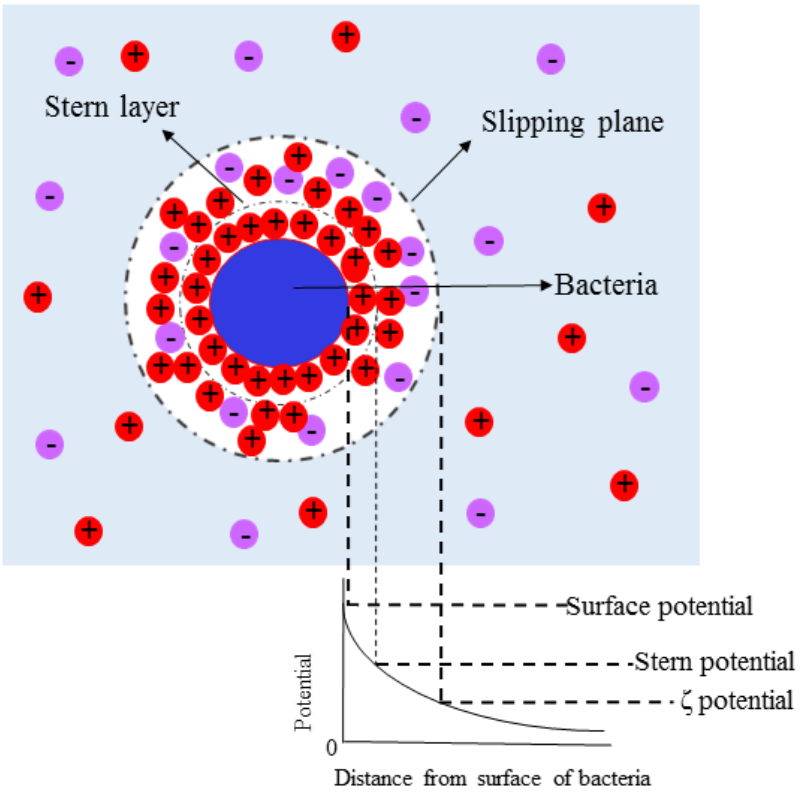

Figure 3. Immobilization of positively charged counter ions on the surface of a negatively charged bacterium. The diagram shows the electric potential as the function of distance from the bacterium surface. Adapted from (Larryisgood 2012).

The surface of bacteria is dynamic and responds strongly to environmental changes. Changes in the pH of the environment cause association or dissociation of charged groups (carboxyl, phosphates and amino groups) present on the surface of bacteria (Poortinga et al. 2002) and change the zeta potential of bacteria. It has been reported that the zeta potential of *E.coli* is not affected by the pH in the range of pH 6.0 to 10.0, while it is strongly dependent on the pH when the pH is less than 6.0. In the range of pH 3.0 to 6.0 the zeta potential of *E. coli* varies from +15 mV to around -35 mV, respectively (Lin et al. 2003).

As it was discussed before, adhesion of bacteria to solid surfaces is also influenced by hydrophobicity of both bacteria and the receiving surface. Bacterial hydrophobicity is determined by the molecules and components present on the surface of bacteria (Merritt and An 2000), such as polypeptides (Jenkinson 1986) and fimbriae (Gibbons et al. 1983). Surface hydrophobicity of bacteria is of great importance when the solid substrates are either hydrophobic or hydrophilic. For example, it has been reported that hydrophobic *P. aeruginosa* bacteria are immobilized more on silicone hydrogel lenses compared with HEMA-based lenses because the hydrophobicity of silicone hydrogel lenses is higher than HEMA-based lenses (Dutta et al. 2012).

2.2 Methods applied to detect bacteria, monitor their activities and their adhesion

2.2.1 Conventional methods

2.2.1.1 Culture-based methods to monitor antibiotic sensitivity

The culture-based method is a central technique used in biology labs to monitor bacterial growth and investigate susceptibility of bacteria to different antibiotics. This method is based on the ability of bacteria to form visible colonies with or without the presence of antibiotics. There are four possible ways to investigate the sensitivity of bacteria to antibiotics. In the first approach bacteria are inoculated in the series of Petri dishes containing increasing amounts of the antibiotic. Alternatively, in the second approach which is called broth microdilution method, employed in most automatic apparatus, bacteria may be inoculated into broth with increasing concentrations of antibiotic. The lowest concentration of the antibiotic that prevents the bacterial growth is called the minimum inhibitory concentration (MIC). The main advantage of this method is its reproducibility and the potential of providing quantitative results such as MIC. In addition, presence of prepared panels in automated apparatus have made this technique as one of the most convenient methods for investigation of antibiotic susceptibility of bacteria. However, this method is time-consuming and it cannot provide same-day results.

In the third approach, called the Kirby-Bauer method, bacteria are evenly inoculated in the Petri dish and then paper disks containing precise amounts of the antibiotics are placed on the Petri dish. If the antibiotic is effective on the bacteria, a circle without bacterial growth is observed around the paper disk after bacterial growth. The larger the circle, the more sensitive the bacteria is to the antibiotic (Jorgensen and Ferraro 2009; Poupard et al. 1994; Versalovic et al. 2011). This method is simple, inexpensive and does not need any specific equipment. The disadvantage of this method is that it could not provide same-day results. In addition, this technique could not be automated (Jorgensen and Ferraro 2009).

In the fourth approach, called antimicrobial gradient method or epsilometry (E-test), an antimicrobial concentration gradient is placed on a plastic strip that is added to a Petri dish inoculated evenly with bacteria. Following overnight incubation, the MIC is evaluated at the place of intersection of the growth inhibition area with the lowest concentration of antibiotic marked on the strip. This method is time-consuming and expensive if more than a few antimicrobials are investigated (Jorgensen and Ferraro 2009).

2.2.1.2 Enumerating bacterial adhesion to surfaces

2.2.1.2.1 Culture methods

Culture-based methods can also be employed for investigation of bacterial adhesion. For that purpose, after bacteria have attached to a surface, they can be counted by detaching them from the surface, culturing on Petri dishes, and counting the colonies to obtain colony forming units (CFU). This reflects the number of bacteria immobilized on the surface. This technique is simple and straightforward and does not require the application of specific and complicated technologies. However, there are potential disadvantages to this method as well, e. g., the detachment process may be incomplete and it may also damage the bacteria (Christensen et al. 2000). Moreover, the bacteria can aggregate and single colonies can arise from more than one bacterium.

2.2.1.2.2 Light microscope

Light microscopy provides an inexpensive and simple technique for investigation of bacterial attachment to surfaces. Under the appropriate circumstances, this method is the fastest way to

investigate the number of bacteria immobilized on solid substrates. However, this method has some disadvantages as well. The first limitation is that the investigated surface should be planar and optically clear. Furthermore, this method does not provide any information about the viability of bacteria (Christensen et al. 2000) unless a series of examinations are performed over time to demonstrate increases in the number of bacteria. Finally, bacteria are very small and pleomorphic, so particles that resemble bacteria may also be present and it is difficult to distinguish them from bacteria, resulting in possible over- or under-estimations.

2.2.1.2.3 Transmission electron microscope

Transmission electron microscope (TEM) operates like the light microscope but here instead of light, electrons operate. This microscope has a high potential for visualization and characterization of bacterial attachment (Knutton 1995). In this microscope, a beam of electrons is transmitted through a specimen and the image is constructed from the specimen-electron interaction (Wang 2000). This technique has a higher resolution than light microscopy and allows the researchers to investigate small details in the cells. The disadvantage of this method is that for soft-bodied organisms like bacteria or cells, chemical fixation is required. In addition, this microscope cannot assess the viability of bacteria (Christensen et al. 2000). Another disadvantage is that this method requires a lot of time for each individual specimen and so throughput is quite slow.

2.2.1.2.4 Scanning electron microscope

Scanning electron microscopy (SEM) allows researchers to observe adhesion of bacteria to surfaces in good detail (Knutton 1995). With this microscope, the surface of the sample is scanned by a beam of electrons and information about the surface morphology is obtained based on interaction of specimen and electrons (Reimschuessel 1972). Like TEM, imaging of soft-bodied organisms requires chemical fixation which may cause artifacts (Matthysse 1995). Furthermore, this technique has slow throughput and cannot provide information about viability of bacteria.

2.2.1.2.5 Atomic force microscope

Atomic force microscopy (AFM) is one of the techniques applied for observation of bacterial attachment and is ideally suited for observing biological activities of bacteria in physiological environments, e. g., imaging interactions of bacteria during formation of biofilms (Meyer et al. 2010) or monitoring interaction of drugs with cell membranes of bacteria (Li et al. 2015). AFM could also be employed to investigate roughness of the samples such as root mean square (RMS) roughness. The critical point in AFM imaging of biological specimens is that the specimens should be well attached to the surface to resist removal through the force of the cantilever (Dufrene 2002). In addition, the process of AFM imaging of each individual specimen is time-consuming and so throughput is quite slow.

AFM could operate in contact, tapping and non-contact modes. In contact mode, the tip of the cantilever is dragged across the surface of the specimen. In this mode, which is the general operation mode of AFM, images are constructed based on the deflections of the cantilever. In non-contact mode, the tip does not touch the surface and just hovers at a distance above the surface. In this mode, the tip oscillates quite close to the surface and the images are constructed based on the amplitude or frequency changes of the oscillation. In tapping mode, like non-contact mode, the tip oscillates up and down in the close distance of the surface. However, the amplitude of oscillation in this mode is much higher than non-contact mode, so the tip taps the surface and does not damage the surface of the sample. Tapping mode is an ideal mode for imaging of soft and fragile specimens (Li 1997).

2.2.1.3 Optical density measurements

One of the common techniques used in microbiology to monitor bacterial growth is optical density (OD) measurement. In this method, a spectrophotometer is employed to measure the OD of the bacterial suspension at a specific wavelength of irradiation which is normally at 600 nm. Growth of bacteria results in increase of the number of bacteria present in the suspension which causes enhancement of scattered light. Therefore, most of the light does not reach the photoelectric cell and the amount of the electric current decreases compared with a cell-free

suspension or a suspension with lower number of bacteria. The electric current is then transformed to an OD value which reflects the turbidity of the suspension (see Figure 4).

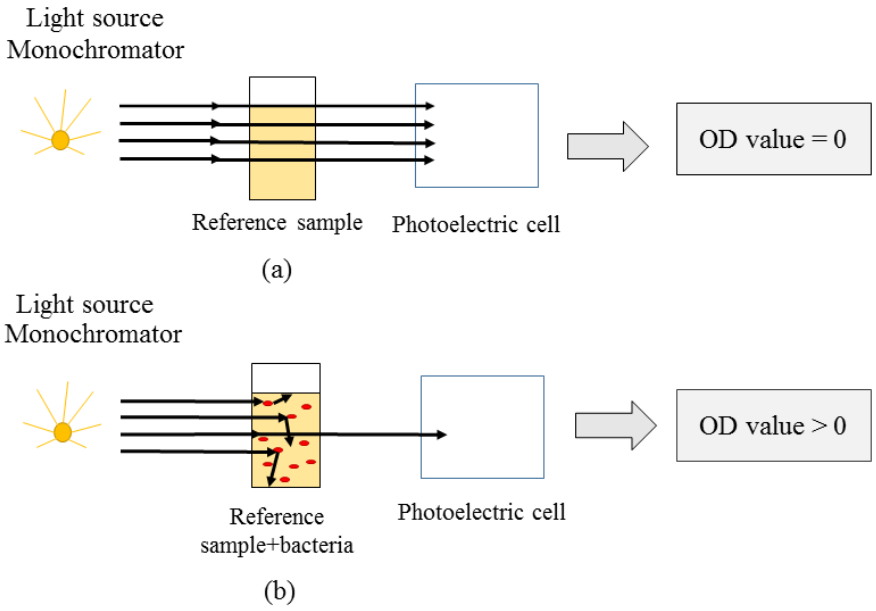

Figure 4. Schematic illustration of the basis of a spectrophotometer. The scattering of light is assumed to be zero in the reference experiment and the photoelectric cell records all the irradiated light (a).The irradiated light is scattered by the bacteria present in the suspension and the photoelectric cell records less light which results in decrease of the electric current. The electric current is then transformed to an OD value (b). Adapted from (Widdel 2007).

If we assume that N_0 represents the initial number of bacteria in the suspension and t_d shows the generation time of bacteria, the number of bacteria reaches N in the period of t following Eq. (2.3) (Widdel 2007),

$$N = N_0 2^{t/t_d} = N_0 (e^{\ln 2})^{t/t_d} \tag{2.3}$$

If we define $\mu = \frac{\ln 2}{t_d}$, Eq. (2.3) could be written as follows,

$$N = N_0 e^{\mu t} \tag{2.4}$$

The cell density or cell concentration is defined as the number of cells per volume unit, as presented in Eq. (2.5),

$$\frac{N}{V} = \text{cell density} \tag{2.5}$$

According to Eq. (2.4), cell density could be written as follows,

$$\frac{N}{V} = \frac{N_0 e^{\mu t}}{V} \tag{2.6}$$

In addition, optical density (turbidity) of the bacterial suspension is proportional to the cell density ($\frac{N}{V} \sim OD$), consequently, Eq. (2.6) could be written as follows,

$$OD = OD_0 e^{\mu t} \tag{2.7}$$

Therefore, OD of the bacterial suspension could be followed by optical measurements and plotted vs. time to obtain the growth curve of bacteria and calculate the bacterial generation time. A typical bacterial growth curve shows four phases which are lag phase, exponential or log phase, stationary phase and death phase (Atlas 1988) (see Figure 5). During the lag phase bacteria prepare to produce proteins and cellular enzymes and the size of bacteria increases, though no growth occurs in this stage (Garbutt 1997). When the log phase is reached, the bacterial growth (biomass accumulation) begins and the number of bacteria doubles every period of time (Akerlund et al. 1995). During the stationary phase, the rates of bacterial growth and bacterial death are equal and no increase is observed in the number of viable cells (Akerlund et al. 1995). Finally when the death phase is reached bacterial lysis happens which is mainly because of augmentation of inhibitory products and environmental factors such as pH changes (Garbutt 1997).

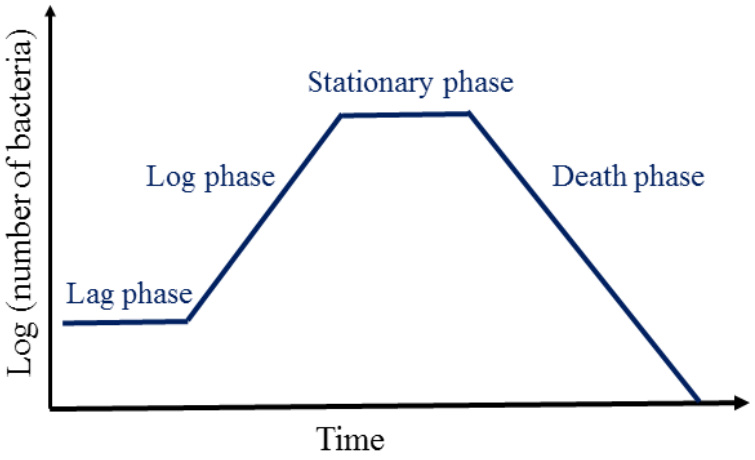

Figure 5. A typical bacterial growth curve consisting of lag phase, exponential or log phase, stationary phase and death phase. Adapted from (Komorniczak 2009).

OD measurement could also be employed for investigation of bacterial adhesion. For that purpose, bacteria are removed actively from the surface of the substrate by sonication and the OD of the bacterial solution is measured. This approach is simple, well standardized and applicable to a wide variety of bacteria with different shapes (Christensen et al. 2000; Wengrovitz et al. 1991). The drawback of this method is that it does not distinguish between live and dead bacteria (Matlock et al.) and it is only sensitive to large numbers of bacteria (> 10^6).

2.2.1.4 McFarland standards

One of the most convenient techniques to monitor bacterial growth and investigate the antibiotic susceptibility of bacteria is using McFarland standards. In this method, the density of the bacterial suspension is estimated by visual or spectrophotometric comparison of the turbidity of the bacterial sample with one of the McFarland standard solutions. McFarland standards are made by mixing different concentrations of barium chloride and sulfuric acid numbered from 0.5 to 6. Each number of McFarland standards corresponds to a specific bacterial concentration so the bacterial suspension can be diluted or concentrated to be compared to one of the McFarland standards (McFarland 1907).

2.2.2 Conventional biosensing methods

The general operation of a biosensor is comprised of capture of a specific analyte by applying a sensing element and detection of the captured analyte by use of a unique transducer device (Sin et al. 2014; Thakur and Ragavan 2013; Turner et al. 1987). Antibodies, enzymes, cell receptors and nucleic acids can be considered as some usual examples of sensitive biological elements. Biological elements capture the analyte by forming lock-and-key complexes such as antigen-antibody, enzyme-reaction and DNA hybridization (Moina and Ybarra 2012) which have been schematically shown in Figure 6. The performance of a biosensor is measured statistically by sensitivity and specificity. Sensitivity depends on the efficacy inherent in the sensing process and is affected by several parameters such as signal to noise ratio and stability of the biosensor. Specificity describes the ability of the biosensor to distinguish and recognize a specific analyte in the environment of operation, for example, to detect a particular type of bacteria among other kinds of bacteria. Moreover, short response time and sensor linearity are also considered as important parameters (Marshall 2011; Thakur and Ragavan 2013).

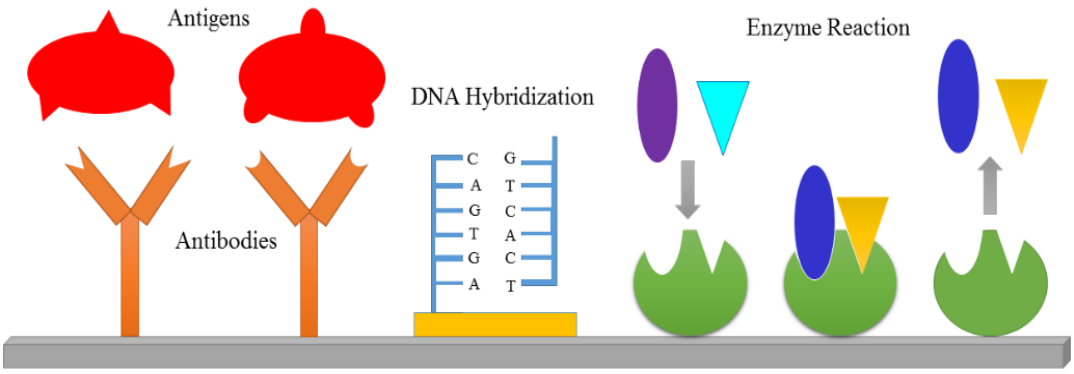

Figure 6. Three common examples of biosensing complexes including antigen-antibody, DNA hybridization and enzyme reaction. Adapted from (Marshall 2011).

The glucose sensor is the best-known and most commercially successful device based on the concept of a transduction mechanism. In this biosensor, the input elements are glucose and oxygen that are converted to gluconic acid and hydrogen peroxide (H_2O_2) in the presence of the enzyme glucose oxidase. The transduction mechanism is based on the reduction of the H_2O_2 product at the cathode that results in a measurable current. Thus, the glucose sensor is an amperometric device taking advantage of enzymatic reactions. The amperometric sensors based

on the concept of enzymatic reactions are considered as the first developed biosensors (Clark and Lyons 1962; Marshall 2011). In 1985 when Elsevier launched the principle journal in the field of biosensing, *Biosensors and Bioelectronics*, the journal published around 30 papers out of the total number of 100 papers published in this field in the world. The number of biosensor publications reached approximately 4500 in 2011. This number accounts for more than 10% of all the publications in this field from 1980 to 2011 which shows the phenomenal growth of the biosensing field during this period (see Figure 7) (Turner 2013).

In spite of publication of many interesting academic papers and patents in the biosensing field, only a small number of biosensors have been commercialized. The commercial success of biosensors is limited by their cost and some technical problems such as reliability, sensitivity and stability (Luong et al. 2008). In addition, small size, simplicity of operation and the potential of being automated also play important roles in commercial success of biosensors. As an example, the glucose sensor comprises around 85% of the biosensing market (Newman and Turner 2005) and its success can be considered as the consequence of low cost, ease of use, rapidity and reliability of the biosensor (Newman and Turner 2005; Yoo and Lee 2010). Biosensing is a wide and rapidly progressing field and has great potential applications in medical diagnostics, environmental monitoring, pharmaceutical fields, food and agricultural industries (Turner 2013).

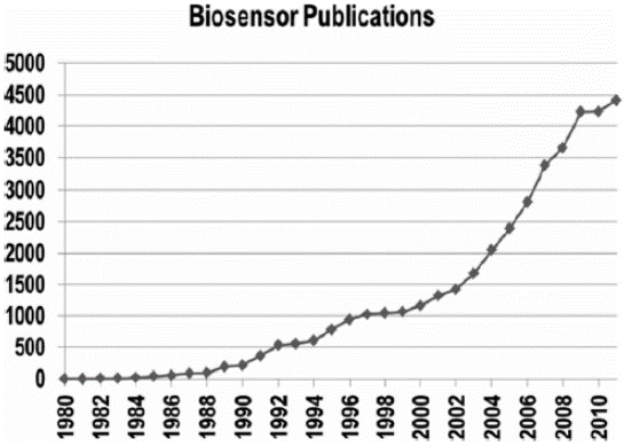

Figure 7. Approximate number of biosensor publications from 1980 to 2010. Reproduced from (Turner 2013) with permission of The Royal Society of Chemistry (http://dx.doi.org/10.1039/C3CS35528D).

In general, biosensors are classified based on their transduction mechanisms. Table 1 briefly demonstrates general types of biosensors and some common examples (Marshall 2011; Moina and Ybarra 2012).

Table 1. Classification of biosensors according to their transduction mechanism (Marshall 2011; Moina and Ybarra 2012).

Classification of biosensors	Transducer effect	Example
Electrochemical	Amperometric/Potentiometric /Conductimetric	*In vivo* electrode
Optical	Colourimetric/ Spectroscopic/Mode dispersion	Fluorescence resonance energy transfer (FRET)/Surface plasmon resonance (SPR)
Piezoelectric	Mass increase	Quartz crystal microbalance (QCM)/Bio-Micro electro mechanical systems (Bio-MEMS)
Semiconductor	Channel conductance/ Photoluminescence	Biosensing field effect transistor (BioFET)/Quantum dots

Electrochemical biosensors monitor changes of the electrical signal due to the redox reactions happening in the vicinity of the electrode surface. The name "electrochemical" has been chosen for this type of biosensors because their operation is based on measuring the variations of the electrical signal induced by the chemical reactions. These changes can be measured as variations in the current (amperometric), in the voltage (potentiometric) or in the conductivity (conductimetric) (Moina and Ybarra 2012). In optical biosensors the recognition of the analyte can generate an optical signal such as colour, or it can change the optical properties of the device (Moina and Ybarra 2012). One of the popular types of optical biosensors is surface plasmon resonance (SPR) devices. In SPR sensors, surface plasmons are excited at a specific (resonance) angle or wavelength of the incident light, which results in attenuation of the intensity of the reflected light. Immobilization of an analyte on the surface of the SPR device changes the refractive index in the vicinity of the surface and results in the modification of the resonance angle (Liu et al. 2012). In piezoelectric biosensors capture of the analyte causes mass increase which is detectable with piezoelectric devices (Moina and Ybarra 2012). Cantilevered MEMs (Raiteri et al. 2001) and QCMs (Kaewphinit et al. 2012) are the best known examples of this

kind of biosensor. Semiconductor-based sensors are divided into channel conductance-based and photoluminescence-based sensors which are described in detail in Sec.2.2.3.

In the following sections, we present a review of the biosensors applied to investigate bacterial adhesion to surfaces and to monitor bacterial activities such as their reactions to antibiotics.

2.2.2.1 Polymerase chain reaction

The polymerase chain reaction (PCR) is a technique developed by Kary Mullis in the 1980s (Bartlett and Stirling 2003) which is based on the exponential synthesis of copies of a specific DNA sequence which doubles for every cycle of PCR. This method can be applied for different purposes such as bacterial detection (Zariffard et al. 2002) and diagnosis of infectious diseases (Atkins and Clark 2004; Speers et al. 2003). It can also be used to produce large amounts of fragments of a specific gene that can be sequenced or otherwise analysed to infer antibiotic sensitivity (Baz et al. 2007; Ge et al. 2013) or genetic disorders such as cystic fibrosis (CF) (Vrettou et al. 2002). The PCR technique is a rapid, sensitive and specific method for monitoring bacterial growth (Wittwer and Kusukawa 2004). PCR can also be used for determination of sensitivity of bacteria to different antibiotics either by detecting resistance genes or by measuring the number of DNA copies in the presence or absence of a specific antibiotic. Hombach et al. (Hombach et al. 2010) employed real-time PCR methods to detect the *mec*A gene responsible for resistance of *Staphylococcus aureus* to methicillin. Rolain et al. (Rolain et al. 2004) used PCR to detect antibiotic susceptibilities of different bacterial strains, e.g., *Streptococcus pneumoniae* and *E. coli*. If the bacteria are resistant to the antibiotic, the number of DNA copies is similar to the growth control test without the antibiotic and if the bacteria are sensitive to the antibiotic, the number of DNA copies is lower than the growth control test. In spite of considerable benefits of PCR over culture-based methods including rapidity, the cost and complexity of the method limits its application to specialized laboratory environments (Toze 1999). Automation of PCR has brought this method to clinical laboratories, but only for specific antibiotic sensitivity determinations like *S. aureus* resistant to methicillin (Grisold et al. 2002). Another major disadvantage of PCR is its inability to detect living versus dead bacteria.

2.2.2.2 Fluorescence-based assays

Fluorescence-based assays are one of the salient techniques which are applied to investigate bacterial adhesion. Adhesion of bacteria could be investigated by using fluorescent bacteria or adding fluorescent molecules such as antibodies after immobilization of bacteria. For example, Lorenzetti et al. (Lorenzetti et al. 2015) applied green fluorescent protein-expressing (GFP) *E. coli* to investigate adhesion of these bacteria to titanium substrates and Müller et al. (Müller et al. 2007) investigated adhesion of biotinylated *Streptococcus gordonii*, *Streptococcus mitis* and *Staphylococcus aureus* on silicon wafers by using fluorescence-labelled avidin-D. This method is highly selective, however, it has some disadvantages such as photobleaching of the fluorophores.

Over the past two decades, a number of fluorescence-based assays have been described for detection of live vs. dead bacteria and analysis of antibiotic susceptibility of bacteria (Boi et al. 2015; Braga et al. 2003; Pore 1994; Quach et al. 2016; Roth et al. 1997). Quantum dots (QDs) are a new class of fluorescent material which has been introduced to improve these assays (Borchert et al. 2003). The main advantage of QDs over fluorophores is that they have a narrow emission spectrum and the spectral location of the emission band is tunable by the size of QDs (Resch-Genger et al. 2008), however, toxicity of QDs (Lewinski et al. 2008) limits their application in biological fields. Meyer et al. (Meyer et al. 2010) employed SYTO9 and propidium iodide fluorophores to assess the viability of *Staphylococcus sciuri* immobilized on glass surfaces using polyphenolic adhesive protein. The viability of bacteria was distinguishable by this method because live and dead bacteria stained green (with SYTO9) and red (with propidium iodide), respectively. This method has also been accompanied with flow cytometry to evaluate antibiotic susceptibility of different strains of *E. coli* (Boi et al. 2015). Flow cytometry is a laser-based technology that is applied for cell counting and cell sorting. In the method applied by Boi et al. (Boi et al. 2015) bacteria were stained with SYTO9 and propidium iodide fluorophores before and after incubation with antibiotics and the antibiotic susceptibility of bacteria was determined by the degree of decrease in the intensity of the light emitted by green (viable) bacteria.

Quach et al. (Quach et al. 2016) employed bacterial cytological profile (BCP) to rapidly investigate antibiotic susceptibility of *Staphylococcus aureus*. In this approach, bacteria were incubated with antibiotics for 1-2 h, stained with fluorophores and observed under a fluorescence microscope. WGA-Cy5 (red) and DAPI (blue) were used to stain cell walls and DNA of bacteria, respectively. SYTOX (green) was also used to analyse membrane permeability of bacteria. The data obtained by the fluorescence microscope was then used to create BCP that showed cytological parameters of bacteria. By comparison between BCP of antibiotic-treated and non-treated bacteria, the sensitivity of bacteria to antibiotics could be determined.

2.2.2.3 Colourimetric biosensors

In colourimetric biosensors, the interaction of an optical dye with the analyte causes changes in the absorption band of the optical dye and changes its colour or opacity (Yotter et al. 2004). Colourimetric biosensors are of great importance because they do not require complicated and expensive technologies (Sharma 2010). Some of the products of metabolic activities of biological cells that can be monitored using these biosensors are oxygen, carbon dioxide, glucose, adenosine triphosphate (ATP) and pH variations (Yotter et al. 2004). The disadvantage of colorimetric approaches is that a high number of biological cells should be present in the environment to produce a colorimetric reaction. Besides that, these methods are time-consuming.

Enzyme-linked immunosorbent assay (ELISA) is one of the colourimetric techniques employed to verify the number of attached bacteria. For that purpose, anti-bacterial antibody (usually raised in a mouse or rabbit) is added to the medium to bind to the attached bacteria. After washing off unbound antibody, a second, enzyme-linked, antibody directed against mouse or rabbit antibodies is added which binds to the bound antibody. Then, the enzyme substrate is added and the reaction produces a colour change which is measured by a spectrophotometer. By monitoring the amount of the colour change, the number of bacteria attached to the substrate can be estimated. ELISA is also employed as a diagnostic tool to detect the presence of specific proteins such as antibodies (Gudino and Miller 1981). The critical point in this technique is that the antibody should be highly specific and should not attach specifically or non-specifically to

the substrate. The disadvantage of this method is that, like other biologic assays, each experiment should be standardized to correlate the amount of the colour change to the number of attached bacteria (Christensen et al. 2000).

2.2.2.4 Surface plasmon resonance biosensors

Due to the sensitivity of SPR biosensors to the refractive index changes at the surface of these structures, these biosensors can also be applied for investigation of bacterial adhesion and biofilm growth. For example, Zagorodko et al. (Zagorodko et al. 2015) used the SPR method to investigate the effet of flow rate changes on adhesion of *E. coli* on aminoheptyl α-D-mannopyranoside-coated gold surfaces. The SPR biosensors have also been applied for monitoring activities of biological cells. Liu et al. (Liu et al. 2012) used a SPR biosensor for monitoring secretions of vascular endothelial growth factor (VEGF) from SKOV-3 ovarian cancer cells. Secretion of VEGF protein and capture of this protein by the sensitive surface of the SPR biosensor causes a shift in the SPR angle. Cuerrier et al. (Cuerrier et al. 2008) employed SPR to monitor cellular activity of HEK-293 cells stimulated by angiotensin (Ang) II. HEK-293 cells, with AngII receptor, were seeded on gold-coated glass substrates and exposed to different concentrations of AngII. As presented in Figure 8 (a), immediately after stimulation of the cells with AngII, a decrease in the SPR signal is observed. Thereafter, the SPR signal increases and exceeds the baseline. The magnitude of the SPR signal depends on the concentration of AngII and enhances by increasing the concentration of AngII. Figure 8 (b) shows the dependency of the reflectance variation on the concentration of AngII. As it is presented in this figure, by increasing the concentration of AngII the reflectance variation increases.

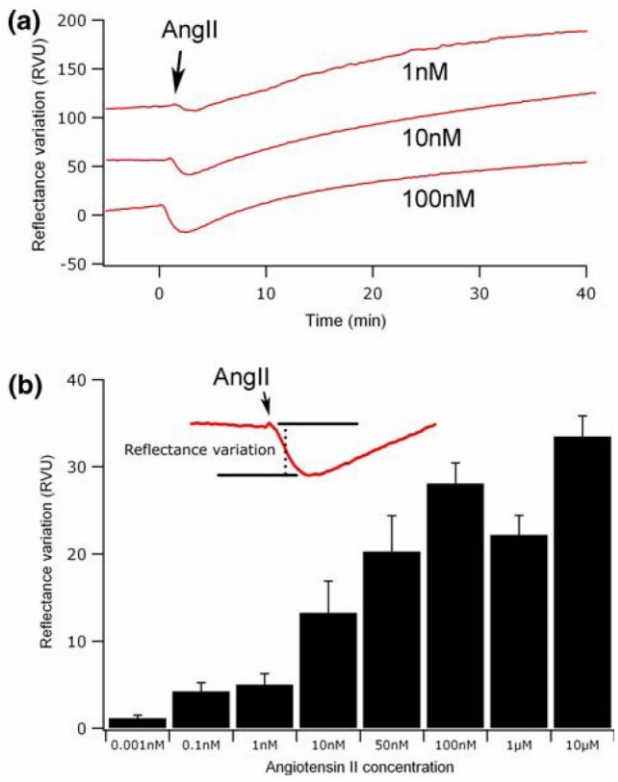

Figure 8. (a) SPR signal measured for increasing AngII concentrations (1, 10 and 100 nM). (b) The amplitude of the initial decrease (inset) was used to generate a concentration response graphic of the AngII receptor activation graphic of the AngII receptor activation (Cuerrier et al. 2008)[1].

Chiang et al. (Chiang et al. 2009) employed a SPR biosensor to determine susceptible and resistant strains of *Staphylococcus epidermidis* and *E. coli* to tetracycline and ampicillin. In this approach, bacteria were immobilized on poly-l-lysine-coated gold substrates and exposed to DI-water and Luria Bertani (LB). Thereafter, another washing step was applied and then bacteria were exposed to antibiotic solution. The amount of SPR angle shift after incubation of bacteria with the antibiotic revealed information about resistance or susceptibility of bacteria to the antibiotic. The SPR angle shift in the case of susceptible bacteria was higher than the one

[1] Cellular and Molecular Bioengineering, Surface Plasmon Resonance Monitoring of Cell Monolayer Integrity: Implication of Signaling Pathways Involved in Actin-Driven Morphological Remodeling, 1(4), 2008, 229-239, C. M. Cuerrier, V. Chabot, S. Vigneux, V. Aimez, E. Escher, F. Gobeil, P. G. Charette, M. Grandbois, "With permission of Springer" (http://dx.doi.org/10.1007/s12195-008-0028-4).

observed for resistant bacteria. For example, in the case of ampicillin-resistant *E. coli* the SPR angle shift was around -0.00154, while for ampicillin-sensitive *E. coli* was -0.01608.

Kee et al. (Kee et al. 2013) used a plasmonic nanohole sensing platform for monitoring growth and antibiotic susceptibility of *E. coli*. The performance of the biosensor is based on the extraordinary optical transmission (EOT) phenomenon shift in plasmonic nanoholes as a result of refractive index changes in the vicinity of the biosensor surface. Figure 9 illustrates the structure of the biosensor and the transmission spectra of the sensor at different stages of measurement. The transmission spectra of the blank biosensor, after antibody immobilization, after 1 h and after 3 h of bacteria seeding is shown in Figure 10 (a). When the immobilized bacteria are exposed to a growth medium, the bacteria grow and the increased number of bacteria on the surface cause a shift in the transmission peak to higher wavelengths. This shift provides a method of monitoring bacterial growth. Figure 10 (b) shows susceptibility of *E. coli* to two types of antibiotics. After exposure of the bacteria to ampicillin solution, *E. coli* continue to grow and the resonant wavelength shift increases with time. This indicates resistance of the bacteria to this type of antibiotic. In the case of exposure to a tetracycline solution, bacterial growth is stopped and a plateau is observed in the resonant wavelength shift curve.

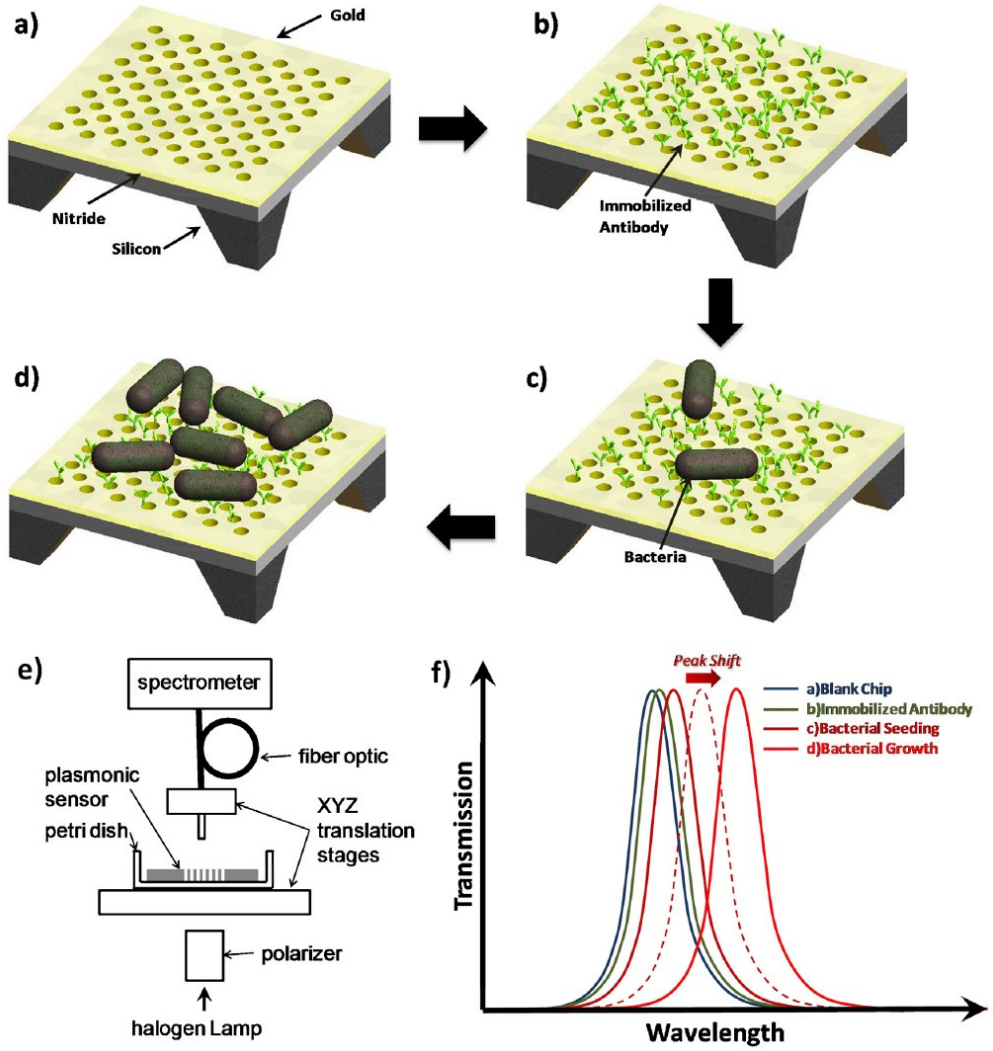

Figure 9. Schematic illustration of the biosensor structure and its transmission spectra, bare plasmonic nanohole sensor platform (a), immobilization of antibody on the surface of the biosensor (b), immobilization of bacteria on the surface of the biosensor (c), growth of bacteria on the surface of the biosensor (d), experimental setup applied for monitoring growth and antibiotic susceptibility of bacteria (e) and transmission spectra of plasmonic nanohole structure at different stages of the measurement (f) (Kee et al. 2013)[2].

[2] "Reprinted from Sensors and Actuators B: Chemical, Vol. 182, J. S. Kee, S. Y. Lim, A. P. Perera, Y. Zhang, M. K. Park, Plasmonic nanohole arrays for monitoring growth of bacteria and antibiotic susceptibility test, Pages 576–583, Copyright (2013), with permission from Elsevier." (http://dx.doi.org/10.1016/j.snb.2013.03.053).

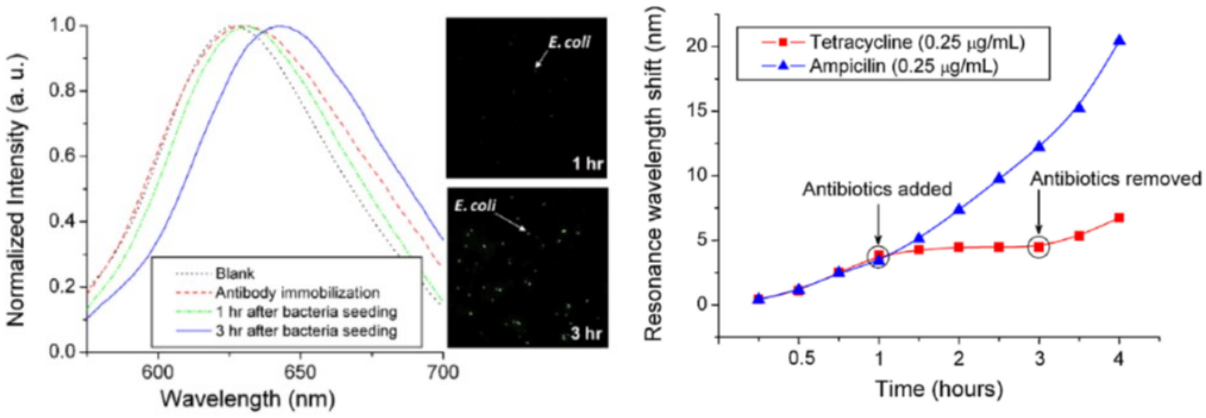

(a) (b)

Figure 10. Transmission spectra of the biosensor measured for blank structure, after antibody immobilization, after 1 h and after 3 h of bacterial seeding. Inset shows fluorescence microscopic images of bacteria immobilized on the biosensor surface (a), monitoring antibiotic susceptibility of *E. coli* to ampicillin and tetracycline by measuring the resonant wavelength shift (b) (Kee et al. 2013)[3].

2.2.2.5 Fourier transform infrared spectroscopy and Raman spectroscopy

Fourier transform infrared (FTIR) spectroscopy is a fast, sensitive and reliable method for investigation of chemical compositions on the surface of a sample. The absorption or transmission of IR for each molecule is specific, so investigating the spectral location and intensity of FTIR signal helps us to detect the molecules on the surface of the sample (Griffiths and de Haseth 1986; ThermoNicoletCorporation 2001). The disadvantage of this method is that the FTIR spectrum is highly affected by the environmental conditions, therefore, numerous scans of the sample and background scans are needed to obtain the accurate spectrum (Davis and Mauer 2010). Over the past two decades, this technique has been applied for analyzing variations in morphology and chemical compositions of biological cells (Cohenford et al. 1998; Rigas et al.

[3] "Reprinted from Sensors and Actuators B: Chemical, Vol. 182, J. S. Kee, S. Y. Lim, A. P. Perera, Y. Zhang, M. K. Park, Plasmonic nanohole arrays for monitoring growth of bacteria and antibiotic susceptibility test, Pages 576–583, Copyright (2013), with permission from Elsevier." (http://dx.doi.org/10.1016/j.snb.2013.03.053).

1990). Gasparri et al. (Gasparri and Muzio 2003) applied the FTIR method based on attenuated total reflectance (ATR) to monitor apoptosis of HL60 (human promyelocytic leukaemia) cells. Apoptosis causes many biochemical and biophysical changes in the proteins of the cells. During apoptosis, changes in localization and folding of the proteins affect the IR absorption range of the peptidic bonds.

Raman spectroscopy is another spectroscopic technique which uses a scattering mechanism to identify molecules (Matthäus et al. 2008). In this technique, a sample is irradiated with a laser beam and the photons interact with the molecular vibrations. The changes in the energy of the scattered photons compared with the laser photons reveal information about the vibrational modes of the molecules. This method has the potential of being applied to monitor biological activities of cells. Lo et al. (Lo et al. 2011) used Raman spectroscopy to monitor the maturation process of an oral mucosa equivalent (EVPOME). Spectroscopic techniques are also of great importance in the field of biofilm research (Wolf et al. 2002), e.g., ATR/FTIR spectroscopy has been applied to monitor biofilm formation on a germanium internal reflection element (IRE) (Bremera and Geesey 1991). Tinham et al. (Tinham and Bott 2003) employed an IR monitor to investigate formation of biofilms in flowing systems. Due to the dependence of the amount of the absorbed IR by the biofilm to the thickness of the biofilm, effect of pH and flow rates were investigated on the biofilm growth.

2.2.2.6 Impedance spectroscopy

Impedance spectroscopy is a promising tool for monitoring the physiological state and activities of biological cells in culture (Ehret et al. 1997). In this method, electrical properties of materials placed between the electrodes or immobilized on the surface of the electrodes are measured at a specific frequency range. Ghafar-Zadeh et al. (Ghafar-Zadeh et al. 2008) applied the charge based capacitive measurement (CBCM) to monitor the growth of *E. coli*. By placing two sensing electrodes in the bacterial suspension and measurement of the standing impedance between the electrodes, the bacterial growth was monitored. Electrochemical approaches have also been employed for investigation of antibiotic susceptibility of bacteria. Besant et al. (Besant et al. 2015) monitored the electrochemical reduction of resazurin, a redox-active molecule, and based on this reaction, the antibiotic susceptibility of *E. coli* was evaluated in less than 1 hour. If the

bacteria were resistant to the antibiotic, they continued to grow in the presence of the antibiotic and created a reducing environment in which resazurin was reduced to resorufin. When bacteria were sensitive to the antibiotic, bacterial growth was inhibited and reduction of the dye was prevented.

Mach et al. (Mach et al. 2011) applied an electrochemical approach based on the detection of bacterial 16S rRNA to investigate antibiotic susceptibility of *E. coli* isolated from clinical samples. In their approach, bacteria were incubated with different antibiotics and the amount of the output current of the biosensor was measured for each test. If the output current was comparable with the growth control test (in the absence of the antibiotic), the bacteria were resistant to the antibiotic and if the output current was lower than the growth test, the bacteria were affected by the antibiotic.

Zavizion et al. (Zavizion et al. 2010) investigated stress responses of *E. coli* and *S. aureus* by monitoring dielectric permittivity of the bacterial suspension. Their approach was applied to monitor antibiotic susceptibility of bacteria and responses of bacteria to heat shock and chemical stresses induced by Triton X-100 or H_2O_2. Differential impedance sensing methods were applied to directly evaluate the dielectric permittivity of the bacterial suspension which was represented as the normalized impedance response (NIR). When the bacteria were affected by the antibiotic or exposed to the heat or chemicals, the NIR decreased continuously. If the bacteria were resistant to the antibiotic, the NIR slightly increased, similar to the growth control test. One example of NIR monitoring of *E. coli* suspension exposed to different concentrations of gentamicin is presented in Figure 11. A continuous decrease is observed for the antibiotic-treated bacteria. This decrease is more considerable for higher concentrations of the antibiotic. NIR monitoring was also applied by Rieder et al. (Rieder et al. 2009) to investigate susceptibility of *M. tuberculosis* H37Ra to anti-tuberculous drugs such as rifampicin and pyrazinamide.

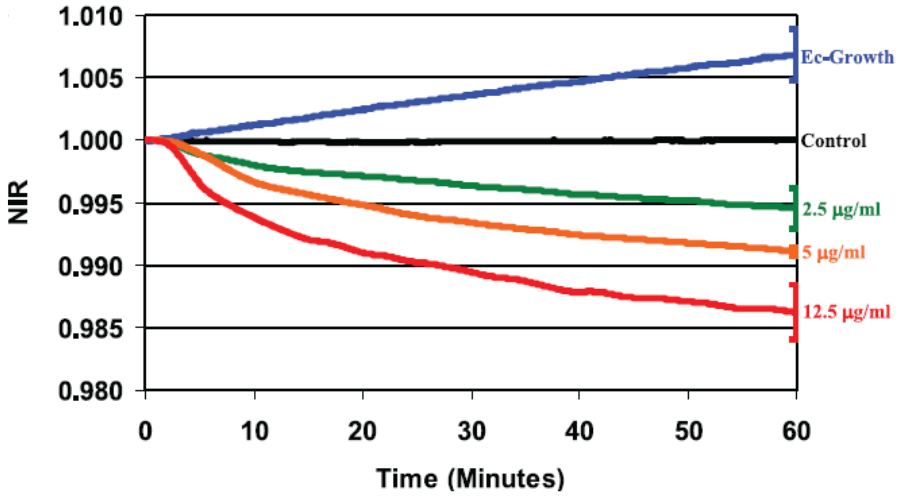

Figure 11. NIR monitoring of *E. coli* exposed to different concentrations of gentamicin. E_c-Growth shows the NIR of the bacterial suspension in the absence of the antibiotic and control shows the NIR of the medium without the bacteria. Reproduced from (Zavizion et al. 2010).

Impedance spectroscopy could be employed for investigation of bacterial adhesion and biofilm growth. Kim et al. (Kim et al. 2011) developed an electrochemical approach based on monitoring the double-layer capacitance variations to investigate bacterial adhesion and biofilm maturation. As presented in Figure 12, the adhesion and/or growth of bacteria on the sensing electrode results in a considerable change in the double layer capacitance.

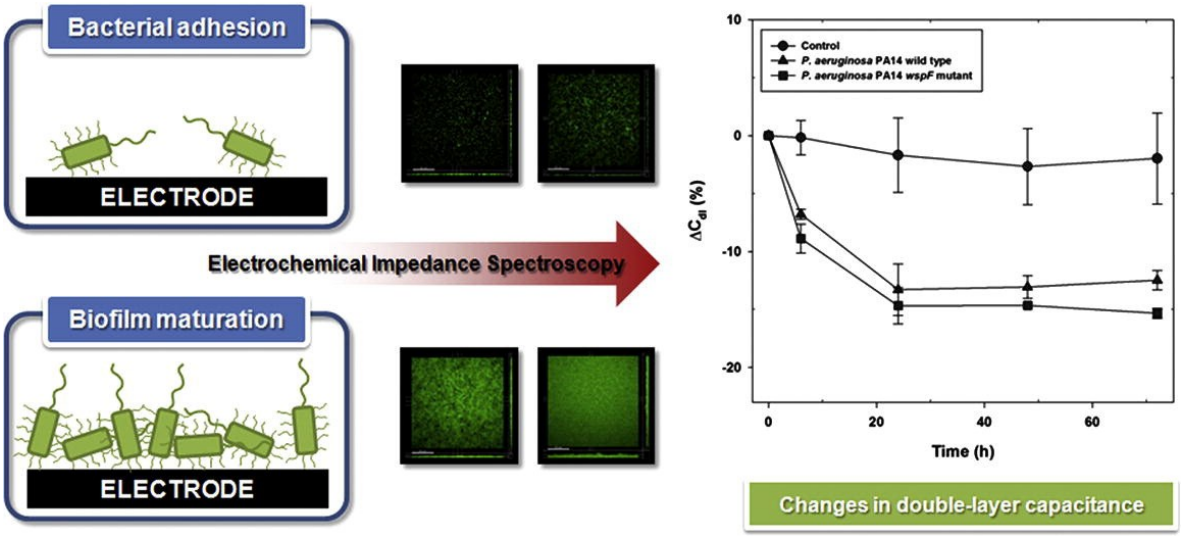

Figure 12. Changes in the double-layer capacitance as the result of the bacterial adhesion and biofilm maturation (Kim et al. 2011)[4].

2.2.2.7 Optical time-lapse assays

Optical time-lapse assays are other approaches which have the potential of being applied to investigate antibiotic susceptibility of bacteria. Fredborg et al. (Fredborg et al. 2013) developed an optical screening system (oCelloScope) to evaluate antibiotic sensitivity of different bacteria such as *E. coli*, *S. aureus* and *Streptococcus pneumoniae* based on digital time-lapse spectroscopy of bacteria-antibiotic suspension. They applied an optical source, a lens and a camera to get multiple optical images of bacteria and evaluated the bacterial growth while they were exposed to antibiotics. They succeeded in determining antibiotic susceptibility of *E. coli* within 6 min for monoculture and within 30 min for complex samples isolated from pigs with urinary tract infections. In another study, the same setup was employed to evaluate antibiotic susceptibility of methicillin-resistant *S. aureus* within the net average time of 108 min (Fredborg et al. 2015).

[4] "Reprinted from Water Research, Vol. 45, T. Kim, J. Kang, J-H. Lee, J. Yoon, Influence of attached bacteria and biofilm on double-layer capacitance during biofilm monitoring by electrochemical impedance spectroscopy, Pages 4615-4622, Copyright (2011), with permission from Elsevier." (http://dx.doi.org/10.1016/j.watres.2011.06.010)

Choi et al. (Choi et al. 2013) employed a microfluidic agarose channel (MAC) system to incubate bacteria with antibiotics and used a time-lapse assay to investigate antibiotic sensitivity of *P. aeruginosa* and *S. aureus* within 3-4 h. As presented in Figure 13, multiple images of bacteria were taken as they were exposed to different concentrations of gentamicin for different incubation times. Based on the time-lapse images, the growth rate of bacteria was calculated and the minimum inhibitory concentration (MIC) of the antibiotic was determined for each test. For example *S. aureus* was able to grow when the concentration of gentamicin was lower than 1 µg/mL, but for this concentration and higher concentrations the bacterial growth was inhibited even after 3 h of incubation with the antibiotic.

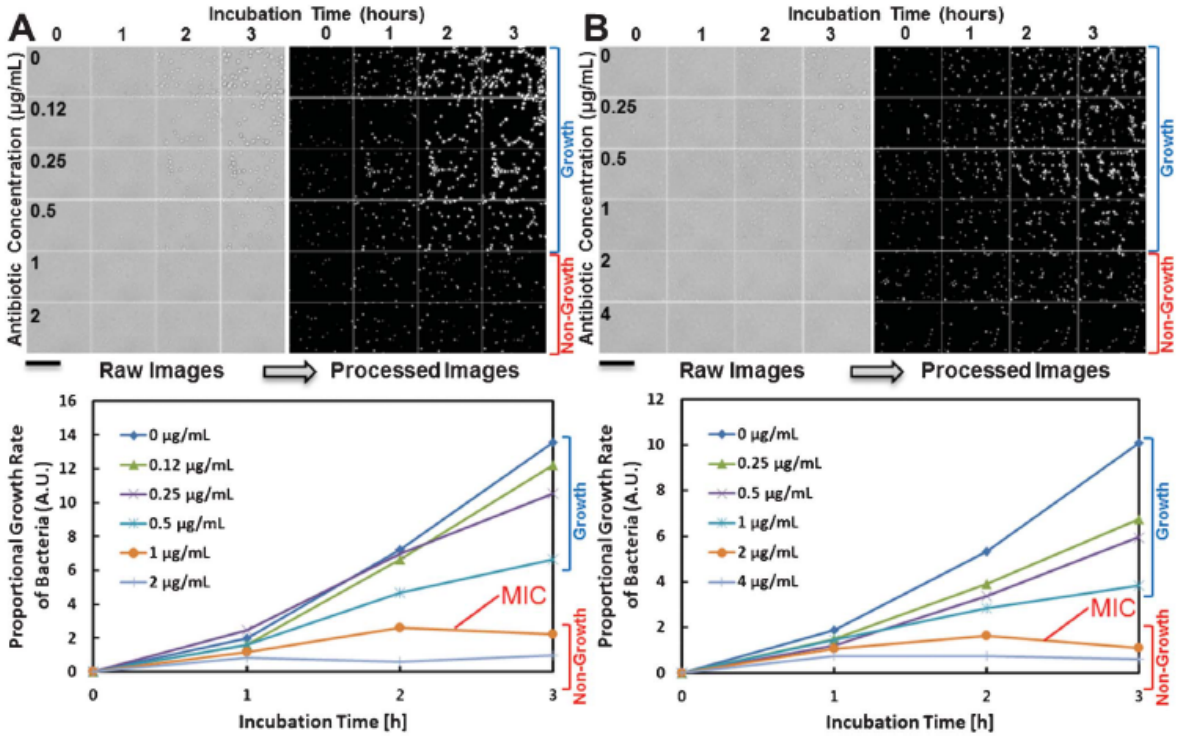

Figure 13. Time-lapse microscopy of *S. aureus* (A*)* and *P. aeruginosa* (B) incubated for different times with different concentrations of gentamicin. Based on the time-lapse images the MIC of the antibiotic was determined for each bacteria. Reproduced from (Choi et al. 2013) with permission of The Royal Society of Chemistry (http://dx.doi.org/ 10.1039/C2LC41055A).

2.2.3 Semiconductor-based sensors

2.2.3.1 Channel conductance-based sensors

A field-effect transistor (FET) is a three terminal unipolar semiconductor device which controls the flow of charge carriers from the source to the drain by affecting the conductivity of the channel by application of the voltage applied across the gate and source terminals (Streetman and Banerjee 1999). FETs could be employed in the biosensing field to detect a wide range of targets. A FET-based biosensor (bio-FET) is a biosensing platform which consists of a FET and a biosensing element (Lee et al. 2014; Matsumoto and Miyahara 2013). In bio-FETs, the channel region is functionalized to capture a specific analyte. Immobilization of the analyte on the channel region changes the electrical properties of the bio-FET (Lee et al. 2009). Two main derivatives of bio-FETs are ion-sensitive FETs (ISFET) and molecular controlled semiconductor resistor (MOCSER) devices which are described in the following paragraphs.

ISFETs have been historically developed by Bergveld (Bergveld 1970). The ISFET devices are like metal oxide semiconductor FETs (MOSFET) but the metal gate connection in these devices is in the form of a reference electrode in an electrolyte solution which is in contact with the gate oxide. The schematic illustration of one type of MOSFET and ISFET devices and their electronic diagram are shown in Figure 14 (Bergveld 2003).

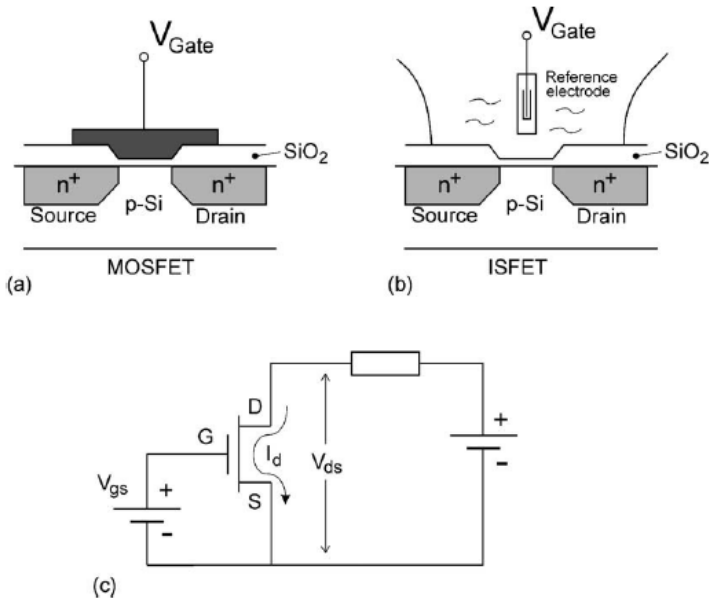

Figure 14. Schematic illustration of (a) MOSFT, (b) ISFET and (c) their electronic diagram (Bergveld 2003)[5].

The drain current in MOSFET and ISFET devices in the non-saturated mode can be calculated by equation (2.8) (Bergveld 2003),

$$I_d = C_{OX}\mu\frac{W}{L}\left[(V_{gs} - V_t)V_{ds} - \frac{1}{2}V_{ds}^2\right] \tag{2.8}$$

where C_{OX} is the oxide capacity per unit area, μ is the mobility of electrons in the channel, W and L are width and length of the channel respectively, V_{gs} is the gate-source voltage, V_{ds} is the drain-source voltage, and V_t is the threshold voltage. As equation (2.8) shows that the drain current can be a unique function of V_{gs} if V_t, V_{ds} and the geometric sensitivity parameter $\beta=C_{OX}\mu W/L$ are constant. By definition V_t is described by equation (2.9) for MOSFET devices (Bergveld 2003),

[5] "Reprinted from Sensors and Actuators B, Vol. 88, P. Bergveld, Thirty years of ISFETOLOGY What happened in the past 30 years and what may happen in the next 30 years, Pages 1-20, Copyright (2003), with permission from Elsevier." (http://dx.doi.org/10.1016/S0925-4005(02)00301-5)

$$V_t = \frac{\Phi_{M-}\Phi_{Si}}{q} - \frac{Q_{OX} + Q_{SS} + Q_B}{C_{OX}} + 2\phi_f \tag{2.9}$$

where the first term is the difference in workfunction between the gate metal (Φ_M) and silicon (Φ_{Si}), the second term is related to the collected charge in the oxide (Q_{OX}), at the oxide-silicon interface (Q_{SS}) and the depletion charge in silicon (Q_B), and the third term depends on the doping level of silicon. For ISFET the observed ion sensitivity is described as an additional parameter in definition of V_t and the threshold voltage is expressed by equation (2.10) (Bergveld 2003),

$$V_t = E_{ref} - \psi + \chi^{sol} - \frac{\Phi_{Si}}{q} - \frac{Q_{OX} + Q_{SS} + Q_B}{C_{OX}} + 2\phi_f \tag{2.10}$$

where E_{ref} and χ^{sol} describe the potential of the reference electrode and surface potential of the solvent, respectively, and have constant values. The parameter ψ in equation (2.10) describes the chemical input parameter which is a function of pH of the solution. It should be noted that parameter Φ_M is hidden in E_{ref} term and does not appear in this equation. Note that the potential of the reference electrode and V_{ds} are held constant, ISFET devices can be operated as a sensor sensitive to the pH of the electrolyte (Bergveld 2003).

As it was discussed in the beginning of this section, another derivative of bio-FET is MOCSER device in which no reference electrode is needed. Naaman et al. (Naaman et al. 2013) employed a MOCSER device to detect triacetone triperoxide (TATP) vapors in gaseous mixtures. The schematic illustration of the MOCSER device is shown in Figure 15. By applying a constant potential between two conduction pads, the current change is monitored when the device is exposed to gaseous mixtures containing vapors of the target. Absorption of the target molecules on the sensing layer causes charge transfer from the substrate and results in current variations.

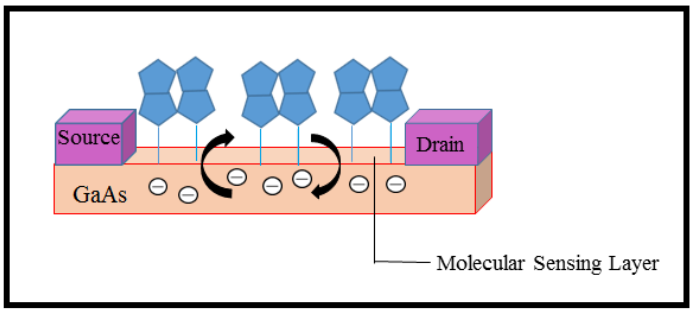

Figure 15. Schematic illustration of the MOCSER device used for detection of TATP in gaseous mixtures. Adapted from (Naaman et al. 2013).

2.2.3.2 Semiconductor optical (photoluminescence) sensors

Absorption of a photon with energy greater than the bandgap energy of a semiconductor raises electrons from the valance band to the conduction band. Photoluminescence (PL) is the radiative recombination of excited conduction band electrons and valance band holes that happens after the electrons move down to the valance band. Non-radiative recombination of electrons and holes happens as the result of diffusion movement of minority carriers and occurs within a thin layer near the surface, typically less than a few hundred nanometers thick. The surface recombination velocity (SRV) is determined by the surface conditions and dominates the rate of non-radiative recombination. Radiative and non-radiative recombination of electrons and holes are schematically shown in Figure 16.

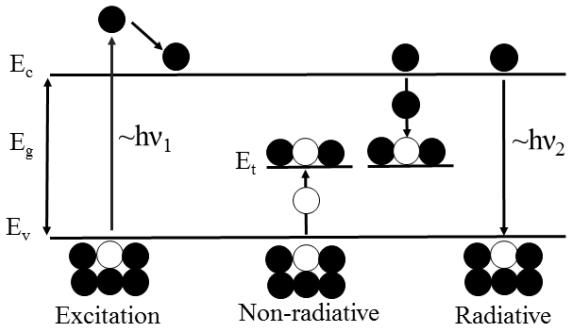

Figure 16. Schematic illustration of recombination processes in GaAs. Absorbing photons of higher energy than bandgap energy of GaAs excites electrons and raises them to the conduction band. Electrons relax to the edge of the conduction band by releasing phonons. Non-radiative recombination is the result of diffusion movement of minority carriers while radiative recombination is the result of direct transition of excited conduction band electrons to the valance band which leads to emission of photons. Adapted from (Marshall 2011).

The overall recombination rate is inversely proportional to the minority carrier life time (τ) which is defined by the reciprocal sum of radiative and non-radiative recombination terms (equation 2.11). For n-type material, the radiative and non-radiative recombination rates are approximately defined by equations (2.12) and (2.13), respectively. A similar equation can be written for p-type semiconductors (Yacobi 2003),

$$\frac{1}{\tau} = \frac{1}{\tau_r} + \frac{1}{\tau_{nr}} \tag{2.11}$$

$$r_r = \tau_r^{-1} \approx \beta(n_0 + \Delta n) = \beta n \tag{2.12}$$

$$r_{nr} = \tau_{nr}^{-1} = \sigma_p v_{th,p} N_t \tag{2.13}$$

In equation (2.12) β is the radiative recombination rate which is defined under non-degenerate injection conditions (Lambert et al. 1990), n_0 is defined as the equilibrium majority carrier (electron) concentration and Δn is the photo-generated excess concentration because of electron-hole generation. In equation (2.13), defined by Shockley-Read-Hall recombination theory (Shockley and Read 1952), σ_p, $v_{th,p}$ and N_t are the minority carrier (holes) capture cross-section, minority carrier thermal velocity and trap density, respectively. The PL intensity can be quantified by the internal quantum efficiency (γ_{PL}) which is defined in terms of radiative and non-radiative recombination rates (Yacobi 2003). According to equation (2.14) any change in the radiative and/or non-radiative recombination rates alters the PL intensity which is considered as the suitable metric in PL-based sensors.

$$\gamma_{PL} = \frac{r_r}{r_r + r_{nr}} \tag{2.14}$$

Discontinuity of bulk properties of semiconductors such as GaAs results in presence of significant number of surface states at the surface of these materials. Consequently, when these materials are exposed to air, water or other medium, additional bending occurs of the energetic

bands approaching the surface. As the result, a space charge region (SCR) is formed near the surface of semiconductors. The associated electric field separates electrons (e^-) and holes (h^+) produced in this layer and thus, it decreases the chance of radiative recombination rate of electrons and holes and reduces PL intensity. For n-type semiconductors the associated electric field drives photo-excited holes to the surface and the photo-excited electrons toward the bulk (Yu and Cardona 2010).

The basis of PL based biosensors relies on changes in the energy distribution, trapping and/or occupation of surface state defects. Variations in radiative and non-radiative recombination and as the result changes in the PL intensity depend on changes in these parameters. Figure 17 schematically illustrates the band bending at the surface of an n-type semiconductor. The surface barrier height ($q\Phi_{sb}$), built-in electric field (E), space charge density (qN_d), space charge region (SCR), depletion depth (Z_d), surface charge density (Q_{ss}), surface trapped charge (-), ionized donors (+), conduction/valance bands (CB/VB) and Fermi level energy (FL) are also shown in this figure.

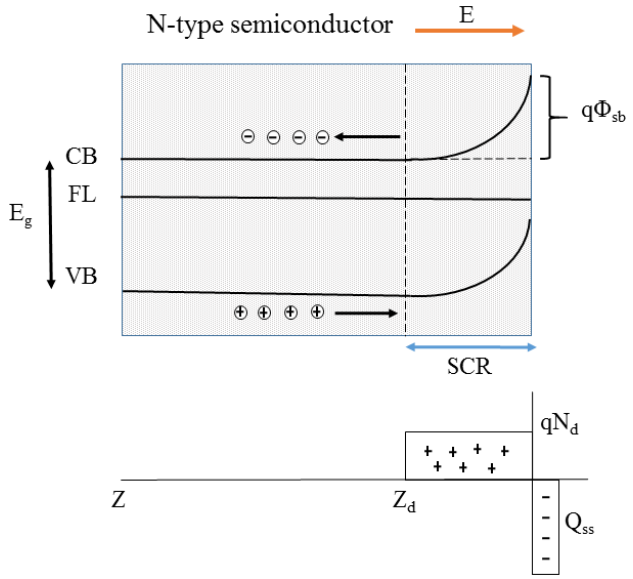

Figure 17. The schematic illustration of the near-surface band structure in a typical n-type semiconductor. The photo-excited minority carriers (⊕) are driven towards the surface by drift and diffusion movements. The surface barrier height ($q\Phi_{sb}$), built-in electric field (E), space charge density (qN_d), space charge region (SCR), depletion depth (Z_d), surface charge density (Q_{ss}), surface trapped charge (-), ionized donors (+), conduction/valance bands (CB/VB) and Fermi level energy (FL) are also indicated in the figure. Adapted from (Marshall et al. 2011).

PL-based sensors have the potential of being applied for chemical sensing (Seker et al. 2000) such as ammonia detection (Luebker et al. 1991). In PL-based sensors, analytes can be immobilized either on the surface directly, or on the surface coated with a transducer film. Transducer films are employed to functionalize the surface of semiconductors and are able to change the PL intensity by affecting surface conditions of the biosensing device (Seker et al. 2000). An example is a Si_3N_4-coated surface of GaAs which was employed to detect *E. coli* bacteria in aqueous solutions (Duplan et al. 2011). In the direct adsorption type sensor, the analyte is adsorbed on the semiconductor surface via physical attraction. For example, exposure of a single-crystal n-CdSe sensor to gaseous amines results in adduct formation between the semiconductor surface and the gaseous amines which causes reduction of the depletion width and enhancement of PL (Meyer et al. 1988). An example of a more recent PL-based sensor is a GaAs-aptamer device applied for detection of adenosine 5′-triphosphate (ATP) (Budz et al. 2010). During the ATP-aptamer formation, the aptamer probes fold and adopt a tertiary structure simulating a stem and loop. Formation of this structure on the surface of the sensor changes the charge distribution on the GaAs surface, decreases the width of the depletion region and increases the PL intensity. Another example of PL-based sensor is a III–V quantum semiconductor (QS) device which has been applied for rapid detection of *E. coli* bacteria in phosphate buffered saline solution (PBS) (Duplan et al. 2011). Immobilization of electrically charged bacteria on the biofunctionalized surface of the device modifies the band bending of the semiconductor and increases the PL intensity. Figure 18 shows PL emission of QS samples as they are exposed to different concentrations of bacteria in PBS. After 2 hours of PL measurement, the difference in the intensity of PL signals can be used for calibration of the biosensor. A negative control test with *Lactococcus lactis* bacteria shows the specificity of the biosensor functionalized with *E. coli* antibody.

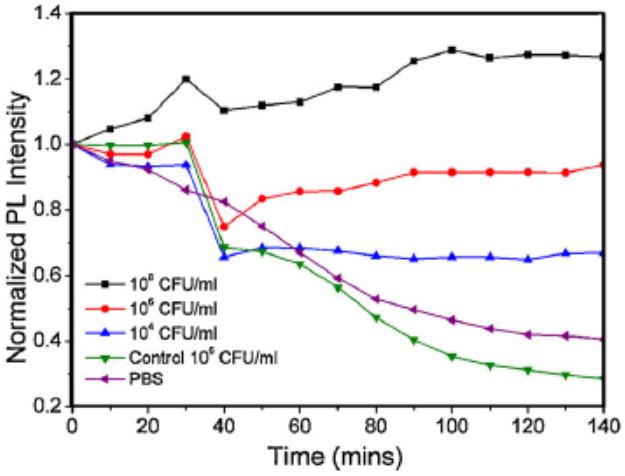

Figure 18. *In situ* PL intensity of biofunctionalized QS samples exposed to PBS (purple line) and different concentrations of *E. coli* (black, red and blue lines) or *L. lactis* (green line) (Duplan et al. 2011)[6].

The systems employed for PL measurements are composed of an optical source to excite the sample, lenses to concentrate the irradiation light and the PL signal, filters to isolate the irradiation light from the PL signal, a spectrometer, and a photo-detector. The intensity of the PL signal, which depends on the number of photo-excited electrons and holes, is directly proportional to the intensity of the irradiation light. By increasing the power of the excitation source the intensity of the PL signal increases until it reaches a saturation level (Gfroerer 2006; Marshall et al. 2011).

In our project we employed two custom designed PL reader systems, hyperspectral imaging photoluminescence mapper (HI-PLM) and quantum semiconductor photonic biosensor (QSPB) reader, to record the PL emission of QS biochips at room temperature. In the HI-PLM, the whole sample is irradiated with a green laser (at 532 nm) and PL emissions from the sample are collected and separated spectrally by using a volume Bragg grating (VBG). This results in production of multiple images of the sample, each image at a different wavelength of PL set by

[6] "Reprinted from Sensors and Actuators B: Chemical, Vol. 160, V. Duplan, E. Frost, J. J. Dubowski, A photoluminescence-based quantum semiconductor biosensor for rapid in situ detection of *Escherichia coli*, Pages 46-51, Copyright (2011), with permission from Elsevier."(http://dx.doi.org/10.1016/j.snb.2011.07.010)

the user (Lepage et al. 2010). The images are then stacked in three dimensional arrays (x,y,z) called raw cubes. The x, y position of the cube corresponds to the position of the sample and z shows the wavelength. It should be noted that every taken image is not at an accurate wavelength. The center of the image is at the desired wavelength set by the user and the sides are at ±60 nm difference. Therefore, the system should scan 60 more nm to provide images at the precise wavelength and construct rectified cubes. To eliminate the effect of background, the system creates background cubes with the laser shutter closed. The final PL map is then built by subtraction of the background cubes from the rectified cubes. The schematic illustration of the HI-PLM used in our project is presented in Figure 19.

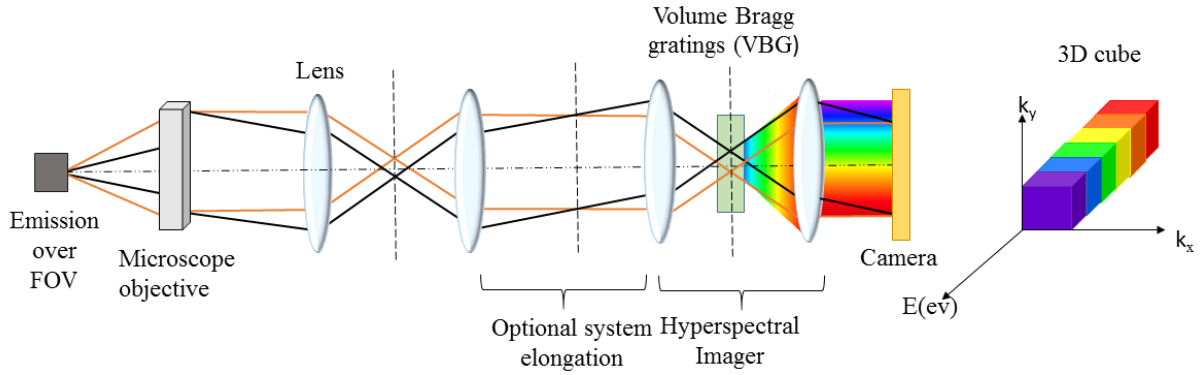

Figure 19. The schematic illustration of the HI-PLM used in our project to record PL emission of QS biochips. Adapted from (Lepage et al. 2010).

The operation of the QSPB reader is similar to a fluorescence microscope. The system does not record the PL spectrum, but it acquires images of PL emission intensity in a wavelength band determined by an emission filter. The schematic illustration of the QSPB reader employed in our project is shown in Figure 20. In this system a light-emitting diode (LED) operating near 660 nm is used to excite the samples. In HI-PLM and QSPB systems, the exposure time of the samples is controlled by a computer-programmed shutter and the PL maps are recorded by a CCD camera. In addition, the intensity of the irradiation light could be controlled manually in both systems.

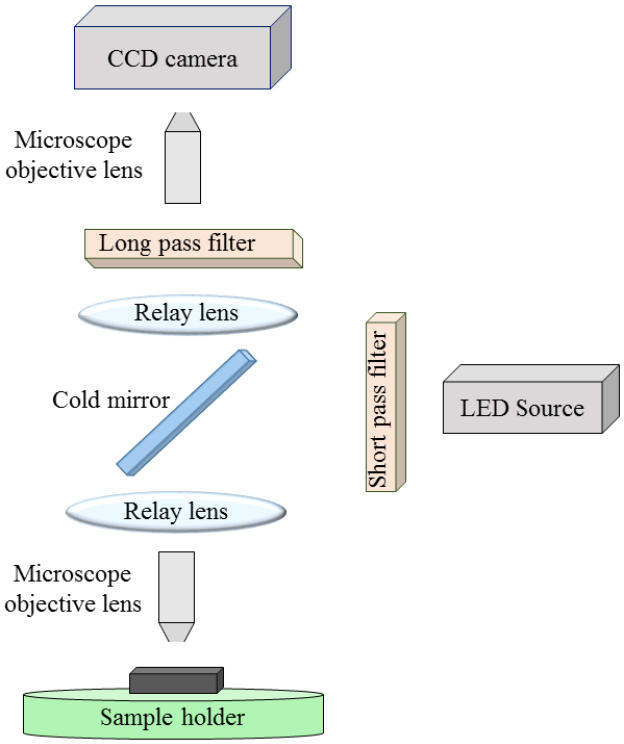

Figure 20. Schematic illustration of the QSPB reader used in our project to record PL emission of QS biochips. Adapted from (Aziziyan et al. 2016).

In Table 2, basic features of conventional biosensing techniques introduced for the evaluation of antibiotic susceptibility of bacteria have been compared. Although culture-based techniques, such as broth microdilution and Kirby-Bauer disk diffusion, are inexpensive and reproducible, these methods are time-consuming and labour intensive (Chiang et al. 2009; Kee et al. 2013; Versalovic et al. 2011). Polymerase chain reaction (PCR) techniques offer considerable benefits over culture-based methods including rapidity, however, these techniques are expensive and they need the presence of highly qualified personnel for both sample preparation and interpretation of the data (Toze 1999). In addition, resistance of bacteria to antibiotics might be related to the presence of different genes, while the PCR technique only evaluates the presence of specific genes (Cockerill 1999). Electrochemical impedance spectroscopy (EIS) represents another approach to rapidly detect antibiotic susceptibility of bacteria (Zavizion et al. 2010). However, the sample preparation procedure in this technique is time consuming. Moreover, the EIS analysis suffers due to the difficulties in accurate interpretation of experimental data and assigning a correct modeling (Lasia 2014). Surface plasmon resonance (SPR) (Chiang et al.

2009) and fluorescence-based assays (Boi et al. 2015; Roth et al. 1997) are other approaches introduced to rapidly investigate antibiotic susceptibility of bacteria. However, the cost of sensitive SPR systems (Lazcka et al. 2007) and technical complexity of fluorescent dye use are inhibitory factors restricting application of these techniques to laboratory environments. Therefore, development of a simple, rapid and inexpensive method for detection of antibiotic sensitivity of bacteria remains an attractive but elusive goal for clinical diagnostics, food and water control industries.

Table 2. Characteristics of different methods introduced to investigate antibiotic susceptibility of bacteria

Method	Time to result	Ease of use	Potential for automation	Cost	Ref.
Broth microdilution	Overnight	Simple	Could be combined with automated panel reader	$10 to $22 each panel	(Jorgensen and Ferraro 2009)
Disk diffusion	16–24 h	Simple	No	$2.50–$5 per test	(Jorgensen and Ferraro 2009)
Antimicrobial gradient	Overnight	Simple	No	$2–$3 each strip	(Jorgensen and Ferraro 2009)
PCR	2 h for Gram-negative bacilli 4 h for Gram-positive cocci	Complex	Yes	Expensive	(Rolain et al. 2004)
Fluorescence-based	1–2 h for methicillin-susceptible and -resistant *S. aureus*	Complex	Yes	Expensive	(Quach et al. 2016)

SPR	2 h for *E. coli*	Relatively complex	Yes	Expensive	(Kee et al. 2013)
Electrochemical	1 h for *E. coli*	Complex	No	Not quoted	(Besant et al. 2015)
Optical-time lapse	3-4 h for *P. aeruginosa* and *S. aureus*	Relatively simple	Yes	Not quoted	(Choi et al. 2013)
Photoluminescence -based	Less than 3 h for *E. coli*	Relatively simple	Yes	inexpensive	This work

2.2.4 Surface functionalization of semiconductors

Development of an efficient and low-cost method to functionalize the surface of semiconductors is of great importance to the operation of electronic and optoelectronic devices made with these materials (Jaouad et al. 2004). In addition to efficiently capturing a specific target molecule, it is highly desirable in sensing applications to protect cleaned and etched surfaces of semiconductors from oxidization and absorption of unwanted molecules (Adlkofer et al. 2000). There are numerous methods applied for surface functionalization of semiconductors including deposition of organic molecules and coating the surface with vacuum evaporated dielectric films such as Si_3N_4. In the following, some of the functionalization methods used for GaAs will be discussed.

2.2.4.1 Organic thiols

An effective approach to functionalize the surface of semiconductors is deposition of self-assembled monolayers (SAMs) of organic thiols (Dassa et al. 2006; Lunt et al. 1991b; Schvartzman et al. 2001). One type of SAMs used widely for this purpose is *n*-alkanethiol [$HS(CH_2)_nR$]. This type of SAMs is of high interest for passivation of GaAs due to the ability of this thiol to make a covalent bond with the surface of GaAs through formation of S–As and S-Ga bonds. In addition, the terminal group (R) of alkanethiols can be used for selective attachment and identification of different types of biomolecules (Bienaime et al. 2013; Budz et

al. 2009; Ding and Dubowski 2005; Dubowski et al. 2010; Lee et al. 2008; Voznyy and Dubowski 2008). Some common examples of terminal groups are COOH (carboxylic acid), OH (hydroxyl), NH_2 (amine) and $C_{10}H_{16}N_2O_3S$ (biotin).

In practice, a mixture of OH-terminated and biotinylated polyether alkanethiols shown in Figure 21 are often used to form a mixed monolayer. The advantage of mixing these two types of thiols is that the OH-terminated thiols space out the biotin coupling sites of polyether alkanethiols to reduce steric hindrance and thus provide better conditions for binding of streptavidin (Mittler-Necher et al. 1995). Alkanethiol-based SAMs with biotin functional groups are widely used for coupling with proteins, such as neutravidin or streptavidin. These proteins can be used as linkers for immobilization of other biotinylated species such as biotinylated antibodies (Cho et al. 2007; Hirsch and Haugland 2005; Mao 2010; Orth et al. 2003). Biotinylated polyethylene glycol thiols have been applied successfully for specific immobilization of *E. coli* bacteria and influenza A virus on GaAs surfaces (Duplan et al. 2011; Duplan et al. 2009).

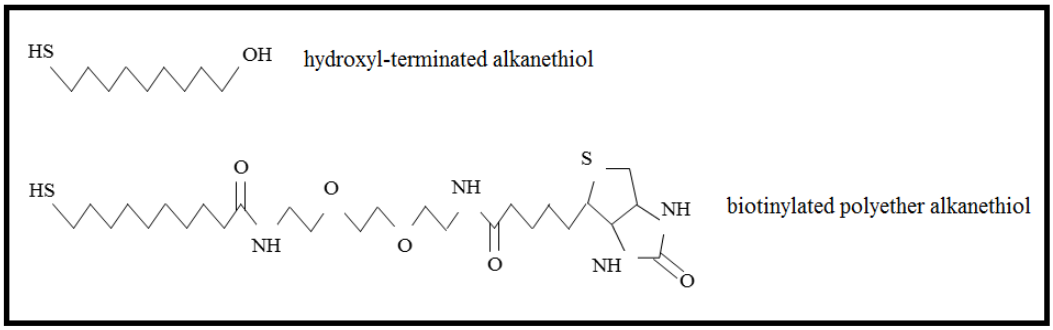

Figure 21. Schematic illustration of OH-terminated and biotinylated polyether alkanethiols that can be mixed to form a monolayer for immobilization of streptavidin or neutravidin. Adapted from (Marshall 2011).

It has been reported that surface passivation of semiconductors with SAMs leads to an enhancement of their photoluminescence (Adlkofer et al. 2002; Adlkofer et al. 2003; Dassa et al. 2006; Ding et al. 2006; Liu and Kauffman 1995; Lunt et al. 1991a; Schvartzman et al. 2001). The reason is that the electric field of the interfacial dipole layer (IDL) formed by the SAMs interacts with the electric field in the depletion layer of the semiconductor and decreases the rate of non-radiative e^--h^+ recombination, which results in an increase in the PL signal (Marshall et al. 2011). The rate of PL increase depends on the length of the molecule chain and

hydrophobicity of its terminal group (Ding et al. 2006). Wieliczka, Ding, and Dubowski (Wieliczka et al. 2006) have investigated the efficiency of 5 types of alkanethiols on surface passivation of GaAs: 11-mercapto-1-undecanol (MUDO, HS(CH2)11OH), 11-mercaptoundecanoic acid (MUDA, $HS(CH_2)_{10}CO_2H$), 1-hexadecanethiol (HDT, $HS(CH_2)_{15}CH_3$), 1-undecanethiol (UDT, $HS(CH_2)_{10}CH_3$) and 16-mercaptohexadecanoic acid (MHDA, $HS(CH_2)_{15}CO_2H$). According to X-ray photoelectron spectroscopy (XPS) of O1s core levels of the GaAs samples, the relative oxygen intensity is weaker for the SAMs with hydrophobic terminal groups (HDT and UDT) than hydrophilic thiols (MHDA, MUDA, MUDO), which means that SAMs with hydrophobic terminal groups are more efficient in protecting the surface of GaAs from ambient oxygen (Wieliczka et al. 2006). It is worthwhile to mention that besides the role of length and terminal group of alkanethiols, the surrounding solvent environment also plays an important role in efficiency of surface passivation (Bain et al. 1989; Sur and Lakshminarayanan 2004). It has been reported that aqueous solutions create favourable situations for formation of well-organized alkanethiols on GaAs and Au surfaces (Dai et al. 2008; Huang and Dubowski 2014).

It is claimed that although thiols can bind to both Ga and As, they are able to cover only 50% of the available sites (Voznyy and Dubowski 2008). Therefore, new methods are necessary to improve surface passivation and stabilization. In that context, Arudra et al. (Arudra et al. 2012) proposed post-growth processing of alkanethiol SAM coated GaAs (001) in ammonium sulfide (AS). According to XPS and PL data, this treatment increases surface concentration of sulfur atoms reacting with Ga and As, which has a positive effect on the photonic stability of GaAs in aqueous environments.

2.2.4.2 Coating with silicon nitride

Deposition of silicon nitride (Si_3N_4) on the surface of GaAs is an attractive way to passivate GaAs because Si_3N_4 films are optically transparent and chemically inert (Jaouad et al. 2004). Thin films of Si_3N_4 have often been used in the fabrication of integrated circuits to electrically isolate different structures and provide a barrier against water molecules, oxygen and sodium ions that are considered to be three major sources of corrosion in microelectronics (Yota 2009).

There are two methods mainly applied for silicon nitride deposition on the surface of solid substrates (Nishi and Doering 2007). The first method is low pressure chemical vapor deposition (LPCVD) which operates at high temperatures up to 600° C (Harbeke et al. 1984). In the LPCVD method, gaseous species are transported to the substrate, absorb on the surface and produce a solid phase film on the surface of the wafer (Stoffel et al. 1996). The second method is plasma enhanced chemical vapor deposition (PECVD) in which high-quality Si_3N_4 films could be fabricated at lower temperatures than those of the standard LPCVD technique. The use of plasma improves also the rates of chemical reactions between different precursors (Alayo et al. 2002; Lazerand and Lishan 2014).

Thin films of Si_3N_4 have been studied for sensing applications because they can be chemically modified relatively easily to produce sensitive surfaces (Headrick and Berrie 2004; Kruchinin et al. 1995). As an example, following etching of Si_3N_4 coated GaAs samples with HF, it was possible to exploit the reactivity of the silicon-hydrogen ($Si\text{-}H_x$) bonds and follow further functionalization procedures with antibodies designed for detection of bacteria (Duplan et al. 2011).

Surface of GaAs could also be passivated with Ga_2O_3. This oxide could be deposited on the surface of GaAs by a physical vapor deposition (PVD) method. Thin oxide films, nanometers to millimetres thick, are fabricated by evaporation of a source material in a vacuum (Diaspro et al. 2006; Guo-Ping and Ruda 1998; Mattox 2010). It has been demonstrated that formation of a Ga_2O_3/GaAs interface decreases the number of surface states responsible for non-radiative recombination and increases the PL emission of GaAs (Passlack et al. 1995).

CHAPTER 3: Avant-Propos

Auteurs et affiliation:

- ***Elnaz Nazemi: Étudiante au doctorat, Université de Sherbrooke, Faculté de génie, Département de génie électrique et informatique.***

- Srivatsa Aithal : Étudiant au doctorat, Université de Sherbrooke, Faculté de génie, Département de génie électrique et informatique.
- Walid M. Hassen : Assistant de recherche, Université de Sherbrooke, Faculté de génie, Département de génie électrique et informatique.
- Eric H. Frost: Professeur, Université de Sherbrooke, Faculté de médecine et des sciences de la santé, Département de microbiologie et d'infectiologie.
- Jan J. Dubowski: Professeur, Titulaire de la Chaire de recherche du Canada en semiconducteur quantiques, Université de Sherbrooke, Faculté de génie, Département de génie électrique et informatique.

Date de publication: Novembre 2014

Revue: Sensors and Actuators B: Chemical, Vol. 207, pp. 556-562

Titre français:

Biocapteur photonique à base de hétérostructure GaAs / AlGaAs pour la détection rapide d'*Escherichia coli* dans une solution saline tamponnée au phosphate.

Résumé français :

Nous avons étudié la détection de bactéries avec un biocapteur photonique basé sur la photoluminescence (PL) des hétérostructures GaAs/AlGaAs. Cette méthode profite de la sensibilité de la PL de GaAs à la perturbation du champ électrique induite par la charge des

bactéries immobilisées à la surface du semiconducteur. Le maintien d'un équilibre entre la sensibilité et la stabilité du biocapteur dans un environnement aqueuse est l'un des paramètres essentiels permettant la biodétection réussie. Pour immobiliser les bactéries, nous avons utilisé un réseau d'anticorps biotinylés retenu à la surface du semiconducteur à l'aide d'une monocouche autoassemblée de thiol polyéthylène glycol biotinylés par les liens fournis par la neutravidine. Les surfaces ont reçu un post-traitement avec le sulfure d'ammonium pour augmenter la stabilité des architectures de biodétection et pour augmenter la sensibilité de la biodétection. *Escherichia coli* a été détectée dans une solution saline tamponnée au phosphate à 10^3 UFC/ml; toutefois, il apparaît que les niveaux de sensibilité encore plus grandes sont possibles avec cette technique.

CHAPTER 3: GaAs/AlGaAs heterostructure based photonic biosensor for rapid detection of *Escherichia coli* in phosphate buffered saline solution

3.1. Abstract

We have investigated photonic biosensing of bacteria based on photoluminescence (PL) of GaAs/AlGaAs heterostructures. The method takes advantage of the GaAs PL sensitivity to the perturbation of the semiconductor near-surface electric field induced by the charge of bacteria immobilized in its vicinity. Maintaining the balance between device sensitivity and stability in the biosensing (aqueous) environment is one of the key parameters allowing successful biosensing. To immobilize bacteria, we have employed a network of biotinylated antibodies interfaced with biotinylated polyethylene glycol thiols through the link provided by neutravidin. Post-processing of thiolated samples in ammonium sulfide was applied to increase the stability of the biosensing architectures while allowing biosensing at an attractive level of detection. *Escherichia coli* was detected in phosphate buffered saline solutions at 10^3 CFU/mL; however, it appears that even greater sensitivity levels are feasible with this technique.

3.2. Introduction

The need to detect pathogenic bacteria rapidly and with high sensitivity is well documented in the literature (Deininger and Lee 2005; Turner 2013; Velusamy et al. 2010). While traditional bacteria detection techniques involving culture-based methods (Fratamico 2003) are sensitive and relatively inexpensive (Velusamy et al. 2010), they are time-consuming and labour intensive (Lazcka et al. 2007; Leonard et al. 2003; Wang et al. 2014). The polymerase chain reaction (PCR) (Pau et al. 2010) offers considerable benefits over culture based methods including rapidity and equivalent sensitivity; however, the complexity of this technique and the requirement of highly qualified personnel for both sample preparation and interpretation make it unattractive for many users (Toze 1999). Automated PCR systems are expensive and target a

limited number of microorganisms. Piezoelectric biosensors (Babacan et al. 2002) hold good potential for detection of food-born and water-born microorganisms, but they are affected by relatively low sensitivity (Wang et al. 2014). Electrochemical impedance spectroscopy (EIS) represents a sensitive approach to detect pathogenic microorganisms with a low limit of detection and a large linear range (Barreiros dos Santos et al. 2013; Li et al. 2014; Mannoor et al. 2010). However, the EIS analysis, in addition to time consuming sample preparation procedure, has suffered due to the difficulties in accurate interpretation of experimental data and assigning a correct modeling (Lasia 2014). Thus, the fabrication of an EIS device capable of delivering attractive results has remained an elusive task (see, e.g., (Wang et al. 2012) and references therein). In that context, the surface plasmon resonance (SPR) technique has demonstrated detection of pathogenic microorganisms, such as *O157:H7* (Taylor et al. 2005), but the cost and the generally large size of SPR instruments limit their application to the laboratory environment (Lazcka et al. 2007). Table 3 illustrates typical detection limits and time to detection of *L. pneumophila*, *E. coli* and *Salmonellae* bacteria achieved with common detection techniques. It is worth mentioning that the requirement of a low limit of detection could result in a significantly increased time to detection. For instance, it takes around 3 hours for a dual wavelength fluorometry technique to detect 10^3 CFU/mL of *Enterococcus faecalis*, whereas detection of these bacteria at less than 10^2 CFU/mL requires more than 5½ hours (Noble and Weisberg 2005).

Table 3. Typical detection limits and time to detection of selected bacteria achieved with some common detection techniques.

Detection Technique	Bacteria	Time of Analysis	Detection Range (CFU mL^{-1})	Detection Limit (CFU mL^{-1})	Ref.
Colony count	*L. pneumophila*	5-14 days	2.5-994	1	(Villari et al. 1998)
Enzyme-linked immunosorbent assay (ELISA)	*E. coli*	Next day	10^3-10^4	1.2×10^3	(Blais et al. 2004)
PCR-ELISA	*E. coli*	5 h	10^0-10^4	10^2	(Daly et al. 2002)
PCR-electrophoresis	*E. coli*	2 h	10^1-10^4	10^3	(Daly et al. 2002)
Real-time PCR	*E. coli*	5 h 20 min	$5\text{-}5 \times 10^4$	5	(Fu et al. 2005)

Piezoelectric	*E. coli*	30-50 min	10^3-10^8	10^3	(Su and Li 2004)
Quartz Crystal Microbalance (QCM)	*Salmonellae*	60 min	10^5–5×10^8	10^4	(Wong et al. 2002)
QCM	*E. coli*	170 min	10^3-10^8	10^3	(Brooks et al. 2004)
EIS	*E. coli*	Not quoted	3×10^1-3×10^4	2	(Barreiros dos Santos et al. 2013)
SPR	*E. coli*	10-30 min	10^4-10^8	10^4	(Taylor et al. 2005)
SPR	*L. pneumophila*	2 h 20 min	10^2-10^9	10^2	(Oh et al. 2003)

Photoluminescence (PL) emitting semiconductors offer an attractive alternative in developing biosensing devices due to the sensitivity of the PL effect to the presence of electrically charged molecules, such as viruses or bacteria trapped in the vicinity of the semiconductor surface. Examples of devices built on such a principle include colloidal QDs of CdSe, ZnS, CdS, ZnSe, CdTe and PbSe (Gao et al. 2002; Mattoussi et al. 2000; Medintz et al. 2005; Stringer et al. 2008) and bulk GaAs (Budz et al. 2010; Seker et al. 2000; Tang et al. 2013). Protection (passivation) of cleaned and etched surfaces of semiconductors from oxidization plays an important role in functioning of PL-based biosensors (Adlkofer et al. 2000), and investigation of electronic or photonic properties of semiconductors surrounded by aqueous environments (Baumgartner et al. 1995; Herman and Terry Jr. 1992; Tkachev et al. 2013). The common approach in passivation of GaAs involves sulfurization from ammonium sulfide (Bessolov et al. 1997; Carpenter et al. 1989) or coating with vacuum evaporated Ga_2O_3 (Guo-Ping and Ruda 1998) and Si_3N_4 films (Duplan et al. 2011; Jaouad et al. 2004). Deposition of self-assembled monolayers (SAMs) of n-alkanethiols [$HS(CH_2)_nR$] on the surface of GaAs is attractive because the SAM head group (HS) provides means of sulfurization while its terminal group (R) could be implicated in building biosensing architectures (Arudra et al. 2012; Dubowski et al. 2010; Lee et al. 2008; Voznyy and Dubowski 2008). While full chemical passivation of GaAs has been successfully achieved and demonstrated, e.g., in the operation of molecular controlled semiconductor resistor (MOCSER) devices (Tkachev et al. 2013), working with a not entirely passivated GaAs surface allows to investigate the role of the photocorrosion effect for biosensing. This is possible since electrically charged molecules, if immobilized in the vicinity of the semiconductor surface,

could modify both band bending of a semiconductor and the concentration of photo-holes generated at the semiconductor surface. A detailed discussion of this approach has been published elsewhere (Dubowski et al. 2015).

Previously, we used SAM functionalized GaAs/AlGaAs microstructures and demonstrated PL-based detection of *Escherichia coli* in phosphate buffered saline (PBS) solution at 10^4 CFU/mL (Duplan et al. 2011). In the present study, we have investigated detection of *E. coli* using SAM functionalized GaAs/AlGaAs microstructures with their surface also coated with sulfur precipitated from an ammonium sulfide (AS) solution. This additional processing step yields microstructures with the increased photonic stability (Arudra et al. 2012) expected to play an important role while addressing detection of bacteria at reduced concentrations.

3.3 Experimental methods

3.3.1 Materials

A nominally undoped epitaxial GaAs/$Al_xGa_{1-x}As$ (x=0.35) heterostructure used in this study (J0149) comprised a 500 nm thick layer of GaAs that emitted a strong PL signal at 869 nm excited with a homogenized beam of a 532 nm laser. Grown above that layer were 3 and 8 nm thick GaAs layers separated by 100 and 10 nm thick $Al_xGa_{1-x}As$ layers. Figure 22 shows schematically a cross-section of the device and a typical PL emission plot observed at 869 nm during photocorrosion of the GaAs cap.

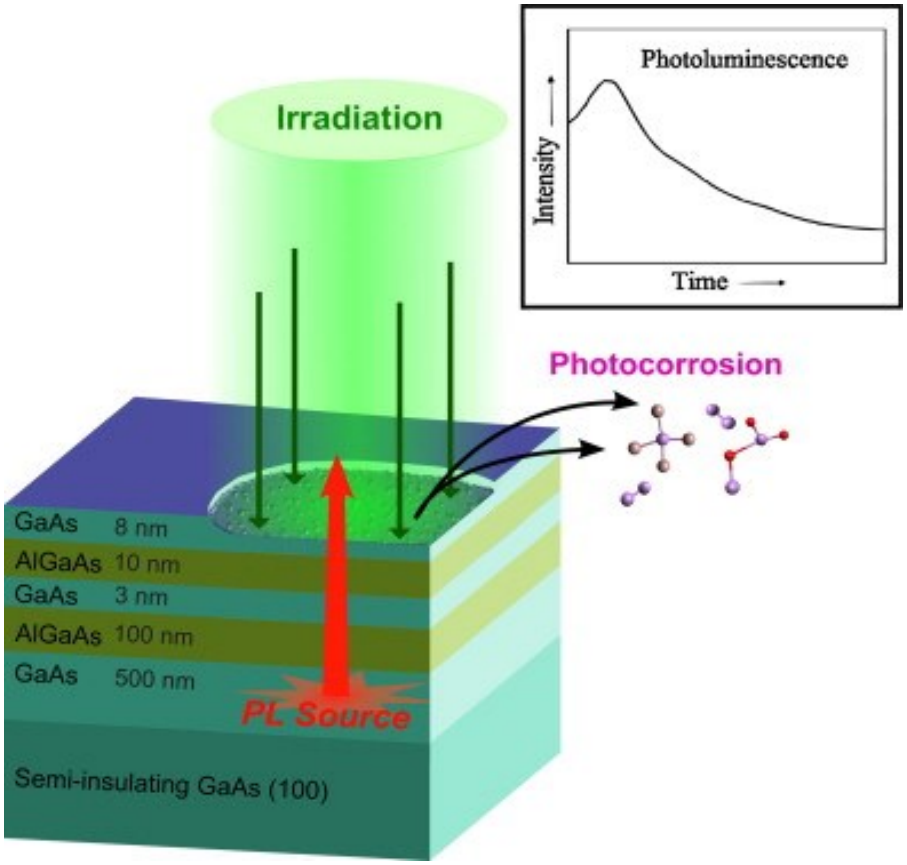

Figure 22. Schematic of the GaAs/$Al_{0.35}Ga_{0.65}As$ heterostructure employed for biosensing. The inset shows PL emission at 869 nm observed during photoocorrosion of the GaAs cap.

Biotinylated polyethylene glycol (PEG) thiols and hexadecane thiols (HDT) were obtained from Prochimia Surfaces (Gdansk, Poland) and Sigma-Aldrich (Ontario, Canada), respectively. Polyclonal biotinylated antibodies against *E. coli* were purchased from ViroStat, Inc. (Portland, ME) and a PBS solution (10X, pH 7.4) was purchased from Sigma (Oakville, Canada). Neutravidin was bought from Molecular Probes (Invitrogen, Burlington, Canada). The solvents used to remove impurities from the surface of the samples are OptiClear (National Diagnostics (Mississauga, Canada)), acetone (ACP, Montréal, Canada) and isopropanol (2-propanol) (Fisher Scientific, Ottawa, Canada). Ammonium hydroxide 28% (NH_4OH) was purchased from Anachemia (Richmond, Canada) and ammonium sulfide (48%) from Sigma-Aldrich (Ontario, Canada). The streptavidin-coated microbeads used in a modeling study of bacteria immobilization were purchased from Bangs Laboratories, Inc. (Indiana, United States). *Escherichia coli* K12 and *Bacillus subtilis* bacteria were obtained from the Department of

Biology of the Université de Sherbrooke (Quebec, Canada). The *E. coli* and *B. subtilis* bacteria were grown in Luria Bertani (LB) and minimal broths, respectively. Before use, the bacteria were stored in 50% glycerol at −26 °C.

3.3.2 Preparation of the GaAs (001) surface and biofunctionalization

Semiconductor samples of 2 mm ×2 mm were cleaned using OptiClear, acetone and isopropanol in an ultrasonic bath (5 min for each). After the cleaning step, the samples were dried using a flow of nitrogen and then etched in a concentrated solution of ammonium hydroxide (28%) for 2 min at room temperature to remove native oxides. Following rinsing with deoxygenized ethanol, the samples were incubated for 20 h at room temperature in a mixture of biotinylated PEG thiol and HDT (1:15) diluted in the deoxygenized ethanol at a final concentration of 2 mM. PEG-based thiols were used because they are known to decrease non-specific binding (Nagasaki et al. 2007). After the thiolation step, the samples were rinsed with deoxygenized ethanol to remove surplus thiol molecules physisorbed on the surface. Thereafter, the samples with biotin terminated SAMs were exposed to 0.1% AS for 15 min and then rinsed with deionized (DI) water. The preparation process continued by incubation of the samples for 2 h in PBS (1X) solution containing 0.2 mg/mL of neutravidin. This step was followed by the exposure of the neutravidin-coated samples to biotinylated antibodies against *E. coli* diluted in PBS (1X) at 0.1 mg/mL, corresponding to a concentration of 0.625 1 μM. The samples were stored for 1 hour in antibody (Ab) solution at room temperature After the Ab coating step, the samples were exposed to different concentrations of *E. coli* bacteria suspended in PBS (1X) and their PL emission was recorded by *in situ* measurements. For the negative control tests, the biofunctionalized samples with *E. coli* Ab were exposed to 10^5 CFU/mL of *B. subtilis* bacteria. The structure of the biosensor used for bacteria detection is schematically shown in Figure 23. The validation of a similar PEG-thiol SAM structure for immobilization of influenza A virus was investigated by us previously using Fourier transform IR spectroscopy (FTIR) (Duplan et al. 2009).

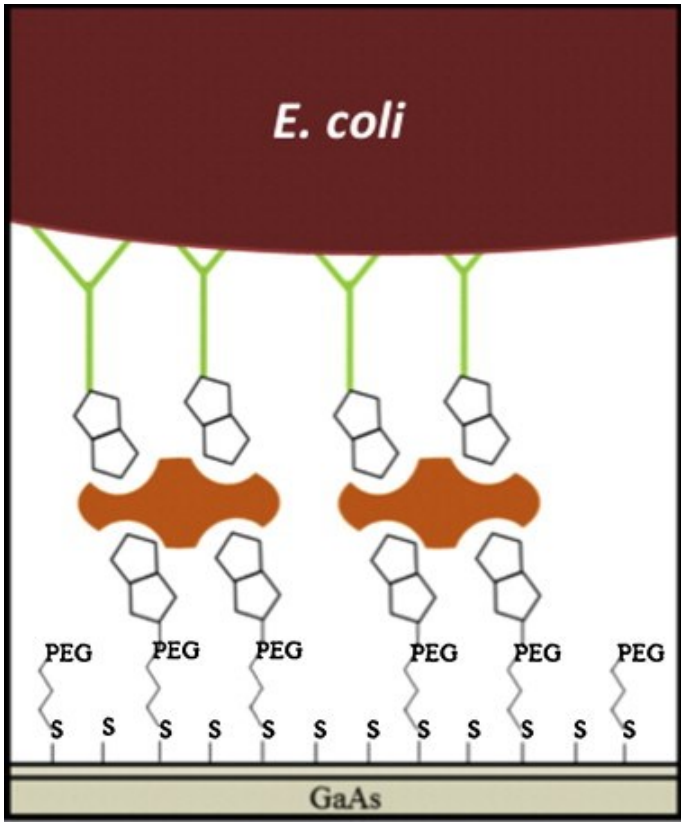

Figure 23. Schematic illustration of the biosensor structure functionalized with PEG SAM and biotin conjugated antibodies exposed to *E. coli* K12.

3.3.3 Immobilization of streptavidin coated microbeads

To investigate the 2-dimensional immobilization efficiency of bacteria on the surface of functionalized biochips, we employed a model consisting of 3 μm diameter microbeads coated with streptavidin and a network of biotinylated PEG thiol SAMs. The SAM formation was achieved by following the standard thiolation procedure. GaAs (001) samples of 2 mm x 2 mm, after etching in ammonium hydroxide (28%) and rinsing with deoxygenized ethanol, were incubated for 20 h at room temperature in a mixture of biotinylated PEG thiols and OH-terminated PEG thiols (1:5) diluted in the deoxygenized ethanol to a final concentration of 2 mM. After this step, the samples were rinsed again with deoxygenized ethanol and exposed for 30 min to beads suspended in PBS (1X) at 10^5 beads/mL. At the final step, the samples were rinsed with PBS (1X) and then with DI water. The microbead-coated samples were analyzed with a ZEISS optical microscope with the total magnification of 500 X working in DIC mode.

The same procedure was applied for the bacteria exposed samples. High-resolution imaging was carried out with an atomic force microscope (AFM, Digital Instruments Dimension 3000). For the AFM images, etched single-crystal silicon tips of around 5-20 nm radius with a rectangular, single beam cantilever (TESP from Digital Instruments) were applied. The cantilever spring constant and the resonance frequency were 20-100 N/m and 200-400 kHz, respectively. For this measurement, the bacteria exposed samples were rinsed with DI-water and the bacteria were fixed with glutaraldehyde (2.5%). The AFM measurement operated in a tapping mode and the measurement has been carried out in an air environment. The AFM images were analysed with WSxM 3.0 software and the brightness and contrast were slightly enhanced using Adobe Photoshop CS4 software.

3.3.4 PL based GaAs/AlGaAs biosensor

Due to the discontinuity of the bulk properties of GaAs and $Al_xGa_{1-x}As$, the presence of significant density surface states is expected on the surface of these materials. This, and the exposure to air, water or other medium will result in a significant band bending of both GaAs and $Al_xGa_{1-x}As$. The associated near-surface electric field plays an important role in the behavior of carriers (electrons and holes) excited in this region. For n-type semiconductors, photo-excited holes (h^+) will be driven towards the interface and photo-excited electrons (e^-) towards the bulk. The net result is a decreased chance of radiative e^-–h^+ recombinations and, consequently, a reduced intensity PL signal (Yu and Cardona 2010). In contrast, the process of surface passivation of III-V semiconductors manifests by an enhanced PL emission due to the reduced concentration of surface states and decreased surface recombination velocity (SRV) of electrons and holes (Arudra et al. 2012; Arudra et al. 2010; Ding et al. 2006; Dubowski et al. 2010; Lunt et al. 1991a; Marshall et al. 2011). An illustration of such a process is enhanced PL observed during thiolation of GaAs samples (Adlkofer et al. 2002; Adlkofer et al. 2003; Ding et al. 2006; Kauffman et al. 1998; Liu and Kauffman 1995; Lunt et al. 1991a). Due to the interaction with the depletion layer of GaAs, the electric field of an interfacial dipole layer formed by SAM decreases the number of non-radiative recombination events and, consequently, results in an increased PL signal (Marshall et al. 2011). The increase of PL emission has also been observed depending on the length of a molecular chain, its wetting characteristics and time

of immersion of GaAs in a thiol solution (Ding and Dubowski 2005). However, it is known that alkanethiol SAMs provide only partial passivation of the GaAs (001) surface (Dubowski et al. 2010; Voznyy and Dubowski 2008), resulting in relatively unstable SAM-GaAs interfaces in a water environment. This instability is related to the formation of photo-holes at the surface GaAs irradiated with photons of energy exceeding its bandgap energy. The photo-holes induce photocorrosion of GaAs via the formation of surface oxides that dissolve into solution due to their thermodynamic instability in an acidic environment. The process, described by the following reaction (Ruberto et al. 1991):

$$GaAs + 2H_2O + 6h^+ \rightarrow Ga^{3+} + HAsO_2 + 3H^+ \tag{3.1}$$

indicates that photocorrosion of an n-type semiconductor strongly dependents on the presence of positively charged minority carriers (h^+) on its surface. To address the problem of a limited surface passivation provided in such a case by SAM, we have investigated post-processing of alkanethiol SAM coated GaAs (001) with AS and, based on X-ray photoelectron spectroscopy and FTIR measurements, we have demonstrated that this treatment increases the number of sulfur atoms reacting with Ga and As without measurable modification of the quality of SAM (Arudra et al. 2012).

The process of photocorrosion was investigated with a custom designed (Photon etc., Montreal) hyperspectral imaging PL mapper (HI-PLM) designed for collecting *in situ* PL spectra of laser irradiated samples (Kim et al. 2009). Normally, GaAs and AlGaAs layers are etched at a rate determined by the parameters of an excitation source (laser) and electrolytes of different etching power, such as PBS, water or ammonium hydroxide. As etching removes surface defects and GaAs and, consequently, reveals the AlGaAs layer, one can expect to observe measurable changes of the PL signal originating from the 500 nm thick GaAs layer of a structure depicted in Figure 22. Furthermore, as positively charged objects, such as bacteria decorated with positive ions extracted from the solution, approach the semiconductor surface, the band bending at the surface is reduced, resulting in reduced transport of photo-excited holes to the surface. This process is expected to slow down photocorrosion with the efficiency increasing with the concentration of bacteria trapped in the vicinity of the semiconductor surface.

3.4 Experimental results and discussion

3.4.1 Immobilization of functionalized microspheres and *E. coli* bacteria on GaAs (001)

Figure 24 shows a uniformly covered surface of GaAs with microbeads following the exposure to a microbead solution at 10^5/mL. The mechanism of attachment of microbeads is based on the streptavidin-biotin interaction characterized by the dissociation constant, K_d of 4×10^{-14} M (Holmberg et al. 2005). A significantly greater dissociation constant, $K_d = 10^{-9}$ M (He et al. 2013) characterizing antigen-antibody complexes, suggests that for a comparable concentration of binding sites, the surface concentration of the investigated microbeads should be greater than that of bacteria.

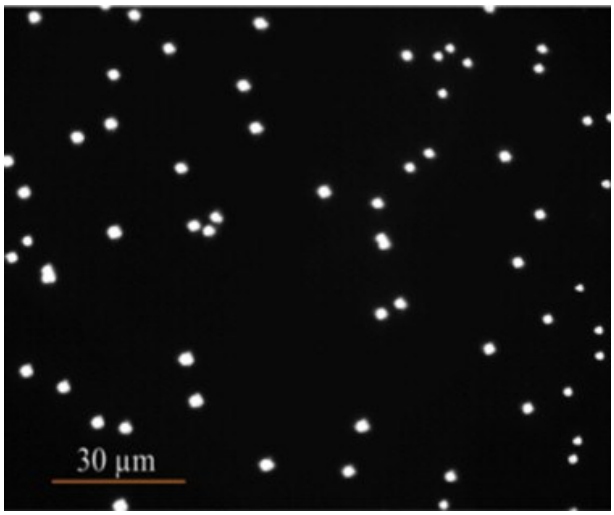

Figure 24. Microscopic image of a functionalized surface of GaAs (001) following the exposure to a PBS solution of streptavidin coated microspheres at 10^5/mL.

In spite of these differences, we systematically observed greater surface coverage with *E. coli* for comparable volume concentrations of microbeads and bacteria. Figure 25 shows examples of optical images obtained for *E. coli* Ab functionalized samples exposed to PBS, 10^5 CFU/mL of *B. subtilis* and 10^5 CFU/mL of *E. coli*. The inset in Figure 25c shows an AFM picture of one of the *E. coli* bacterium immobilized on the Ab functionalized surface of GaAs. The long and short axis of this glutaraldehyde fixed bacterium, respectively 2 and 1 µm, are consistent with the typical dimension of a *E. coli* bacterium reported in literature (Kubitschek 1990; Trueba and

Woldringh 1980). For the negative control test, the maximum number of *B. subtilis* immobilized on the biochip was at 0.13 bacteria/100 μm^2. This compares to 1.1 bacteria/100 μm^2 of *E. coli*, and to 0.5 microbeads/100 μm^2 observed for the same volume concentrations. The average number of bacteria immobilized on the 100 μm^2 of GaAs was 0.9 and 0.09 for 10^5 CFU/mL of *E. coli* and 10^5 CFU/mL *B. subtilis* respectively. The relatively greater surface coverage achieved with *E. coli* in comparison to that with microbeads is surprising given the relatively large dissociation constant characterizing the antibody-bacteria interaction. Our measurements show that the zeta potential of streptavidin coated microbeads in their buffer is around -16 mV, whereas, the zeta potential of *E. coli* in PBS (1X) at pH=7.4 is around -19 mV. Thus, the almost identical zeta potentials of the beads and bacteria cannot account for the observed differences in the surface coverage. Plausible reasons of the reduced binding efficiency of the investigated microbeads could be low concentration of streptavidin sites on surface of microbeads as well as the increased curvature and rigidity of the microbeads surface when compared to *E. coli*. Furthermore, steric hindrance occurring between larger-than-bacteria microbeads and the streptavidin binding sites could also lead to a reduced binding efficiency.

Figure 25. Optical images of the GaAs samples biofunctionalized with *E. coli* Ab and exposed for 30 min to (a) PBS (1×) solution, (b) 10^5 CFU/mL of *B. subtilis* (0.1 bacteria/100 μm^2), and (c) 10^5 CFU/mL of *E. coli* (1.1 bacteria/100 μm^2). Inset shows an AFM image of an individual *E. coli* (AB = 2 μm, CD = 1 μm).

3.4.2 Photonic detection of *E. coli* in PBS

After functionalization of the GaAs/AlGaAs biochips with *E. coli* Ab, as described in Sec. 3.3.2, the samples were exposed either to PBS or to different concentrations of bacteria diluted in PBS, while their PL emission was recorded *in situ* over the period of up to 2 h. Following the initial 30 min exposure to bacteria suspensions, the samples were rinsed with PBS to reduce the

contribution to the PL signal from the bacteria nonreacted with Ab. The 30-min exposure time was assumed sufficient for allowing a reasonable amount of bacteria in the microfluidic chamber to interact with the antibody sites of the biochip surface (Hlady et al. 1990). This step could be refined further, e.g., by increasing the exposure time or recirculating the stream of bacterial solution over the biochip surface.

Figure 26 shows a series of time-dependent PL intensity plots for samples exposed to *E. coli* at 10^3, 10^4 and 10^5 CFU/mL, and to *B. subtilis* at 10^5 CFU/mL. For comparison, we also show a PL plot collected from an Ab biofunctionalized chip exposed to PBS. A characteristic feature of each plot is the presence of a maximum revealed at some time from the onset of the experiment. In agreement with data from the literature (Passlack et al. 1995) and our XPS experiments (Dubowski et al. 2015), the increasing intensity of the PL signal is related to the formation Ga_2O_3 that passivates the surface of GaAs. However, during this process, GaAs is slowly dissolved and the PL signal begins decreasing as the thickness of the GaAs layer falls below the critical level where the etch rate of GaAs exceeds the rate of Ga_2O_3 formation. The photocorrosion rate of the GaAs/AlGaAs heterostructures correlates with the concentration of *E. coli* in solution: the greater the bacteria concentration the slower the photocorrosion rate and the formation of the characteristic maximum is delayed. A plausible mechanism behind this behavior is related to a strong interaction between negatively charged bacteria that become decorated with positive ions available in the PBS solution and, upon immobilization in the vicinity of an Ab functionalized semiconductor surface, attract electrons from the bulk of the semiconductor. This will result in a reduced concentration of photo-excited surface holes and lead to a reduced rate of photocorrosion (Ruberto et al. 1991), in proportion to the average concentration of the positive charge of the object immobilized in the vicinity of the semiconductor. Additionally, immobilized bacteria could reduce mass transfer of the products of photocorrosion from the semiconductor surface, changing the chemical environment and reducing photo-oxidation rates. Figure 26 shows an example of normalized PL intensity plots measured *in situ* for a series of samples exposed to different concentrations of bacteria. Note that the *E. coli* antibody functionalized biochip exposed to *B. subtilis* generated PL response comparable to that from the biochip exposed just to PBS. This result confirms a highly specific character of the biosensing architecture employed in these experiments.

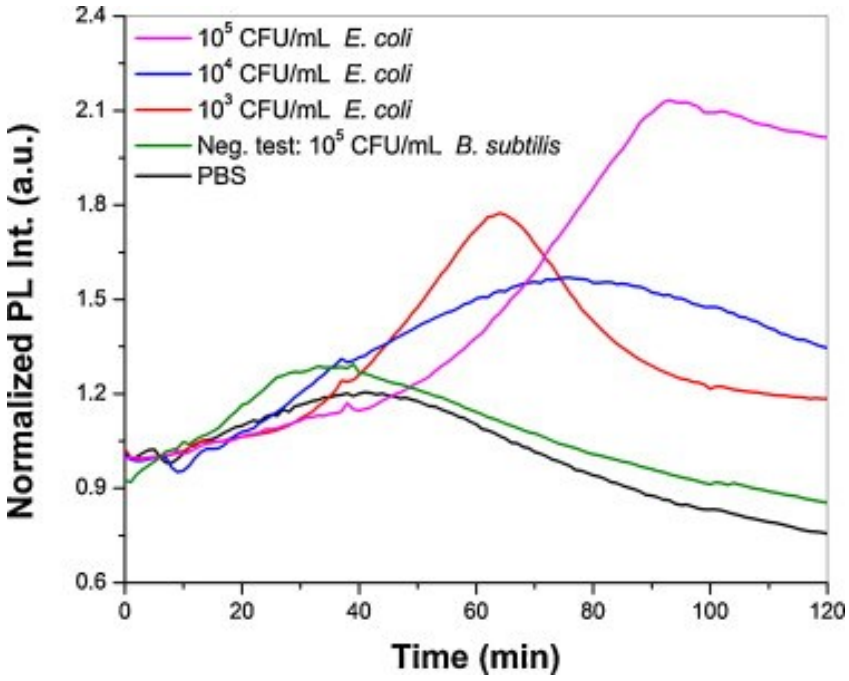

Figure 26. Normalized PL intensity measured *in situ* for the samples exposed to different concentrations of bacteria. The samples were exposed to bacteria at t = 0 and then were rinsed with PBS after 30 min of bacteria exposure.

Similar sets of experiments were repeated 3 times enabling us to determine temporal position of the PL maxima and calibrate response of the biochips, as well as to evaluate an experimental error of the measurements. The results, summarized in Table 4, indicate an attractive reproducibility of the measurements. It can be seen that the PL maximum position related to the negative test has been determined with ±5 % and the error of the maximum position for 10^5 CFU/mL of *E. coli* does not exceed ±3.9 %. A relatively large error of ±25 % related to the position of the maximum observed for the biochips exposed to the PBS solution seems to be related to the more aggressive photocorrosion rate induced in that case and a stronger dependence of the result on the diffusion of a fresh etching medium towards the semiconductor surface.

Table 4. PL peak position for *E. coli* Ab functionalized samples exposed to PBS and different concentrations of *E. coli*. A negative test was carried out for *E. coli* Ab functionalized samples exposed to 10^5 CFU/mL of *B. subtilis*

Medium	Concentration	PL Maximum Position (min)
PBS	1X	32.33±25%
E. coli	10^3 CFU/mL	64.50±1.1%
E. coli	10^4 CFU/mL	77.00±1.8%
E. coli	10^5 CFU/mL	90.50±3.9%
B. Subtilis	10^5 CFU/mL	41.33±5%

Figure 27 shows a semi-logarithmic plot of the position of PL maxima as a function of the investigated concentrations of bacteria. Both specificity and detection at 10^3 CFU/mL are well illustrated. It appears that a direct detection of bacteria in less concentrated solutions should be feasible pending the development of a protocol for defining the biochip response to the PBS solution with better accuracy. This development, in addition to the introduction of advanced methods for bacteria concentration, e.g., based on filtration, electrophoresis or chemotaxis, has the potential to lead to an effective detection of bacteria at ~1 CFU/mL.

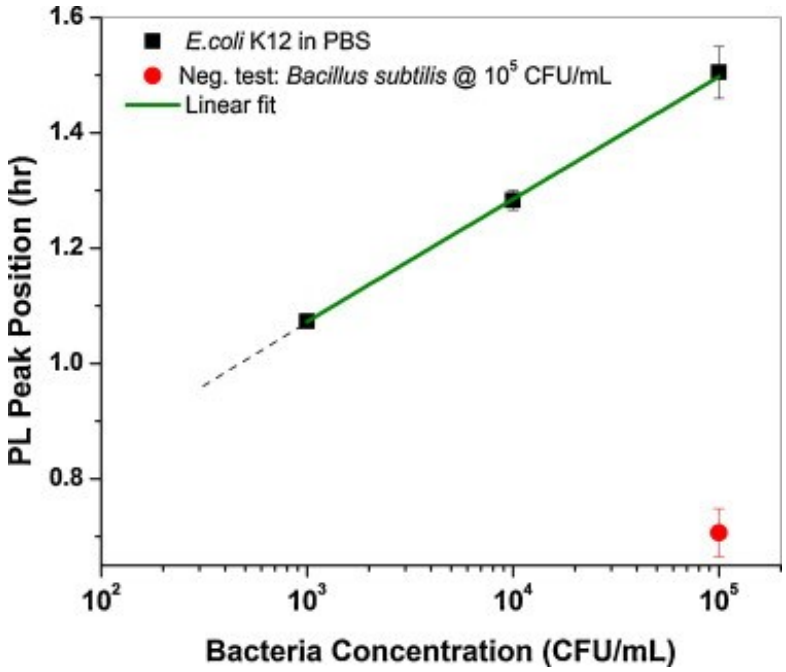

Figure 27. PL peak position vs. different concentrations of bacteria. The PL peak position for the sample exposed to PBS is 32.3 ± 25%.

3.5 Conclusion

We have investigated detection of *E. coli* K12 suspended in PBS solution using an innovative method involving PL monitoring of the photocorrosion effect in GaAs/$Al_xGa_{1-x}As$ nanoheterostructures. The rate of photocorrosion depends on the concentration of the electric charge immobilized in the vicinity of the surface of PL emitting semiconductor biochips, and it slows down with increasing concentrations of bacteria in PBS solutions surrounding the antibody functionalized biochips. Post-processing of alkanethiol SAM functionalized biochips with ammonium sulphide, which increases their photonic stability in a biological environment, enabled us to demonstrate a direct detection of *E. coli* at 10^3 CFU/mL. This represents one order improved limit of detection in comparison to that reported by us previously for the same bacteria (Duplan et al. 2011), but it appears that the detection of an even lower concentration of bacteria should be feasible pending the development of a protocol for defining the biochip response to the PBS solution with better accuracy. This development, in addition to the introduction of advanced methods for bacteria concentration, e.g., based on filtration, electrophoresis or chemotaxis, have the potential to lead to an effective detection of bacteria at ~1 CFU/mL.

3.6 Acknowledgments

This project has been supported by the Canada Research Chair in Quantum Semiconductors Program and the CRIBIQ-MITACS-FRQNT project on "Development of a miniaturized device for optical reading of the QS biosensor". The help of Dr. Kh. Moumanis and the technical staff of the Interdisciplinary Institute for Technological Innovation (3IT) is greatly appreciated. We thank CMC Microsystems (Kingston, Ontario) for subsidizing the manufacturing cost of GaAs/AlGaAs epitaxial microstructures used in this work. We also thank Dr. François Malouin of the Department of Biology, Université de Sherbrooke for kindly supplying *E. coli* and *B. subtilis* bacteria.

CHAPTER 4: Avant-Propos

Auteurs et affiliation:

- ***Elnaz Nazemi: Étudiante au doctorat, Université de Sherbrooke, Faculté de génie, Département de génie électrique et informatique.***

- Walid M. Hassen : Assistant de recherche, Université de Sherbrooke, Faculté de génie, Département de génie électrique et informatique.
- Eric H. Frost: Professeur, Université de Sherbrooke, Faculté de médecine et des sciences de la santé, Département de microbiologie et d'infectiologie.
- Jan J. Dubowski: Professeur, Titulaire de la Chaire de recherche du Canada en semiconducteur quantiques, Université de Sherbrooke, Faculté de génie, Département de génie électrique et informatique.

Date de soumission: Octobre 2016

Revue: Journal of Biological Engineering

Titre français:

La croissance de *Escherichia coli* sur la surface de GaAs (001)

Résumé français :

La détection de bactéries pathogènes et la surveillance de leur capacité à se développer sont importantes dans les domaines de la médecine, la recherche pharmaceutique, ainsi que les industries de l'eau et des produits alimentaires. Dans une tentative de développer un biocapteur photonique pour surveiller la croissance et la sensibilité aux antibiotiques de bactéries en tirant avantage de la photoluminescence (PL) émise de semiconducteurs quantiques (QS) III-V, nous avons exploré la capture et la croissance d'*Escherichia coli* K12 sur des surfaces nues et biofonctionnalisées de GaAs (001) - un matériau d'intérêt pour recouvrir différentes QS III-V.

Nous avons trouvé que des tranches de GaAs placés sur gélose nutritive dans les boîtes de Pétri inoculées avec des bactéries, n'a pas inhibé la croissance des bactéries, indépendamment du fait que les surfaces GaAs étaient nues ou biofonctionnalisées. Nous avons également étudié la capture et la croissance de bactéries sur les surfaces biofonctionnalisées de GaAs tandis que les biopuces ont été maintenus dans une cellule d'écoulement et exposées à différentes concentrations de bactéries et un milieu de croissance. Nous avons observé que, tant que les plaquettes de GaAs ont été exposées à des suspensions bactériennes à des concentrations d'au moins 10^5 UFC/ml, les bactéries peuvent se développer sur la surface des plaquettes, quel que soit le type d'architecture de biofonctionnalisation utilisé pour capturer les bactéries. Cependant, la couverture initiale des surfaces de GaAs avec des bactéries et les taux de croissance des bactéries se sont révélées dépendre de l'architecture de la biofonctionnalisation. Les surfaces revêtues d'anticorps étaient nettement plus efficace pour capturer de bactéries et offraient de meilleures conditions pour la croissance de bactéries.

CHAPTER 4: Growth of *Escherichia coli* on the GaAs (001) surface

4.1 Abstract

Detection of pathogenic bacteria and monitoring their susceptibility to antibiotics are of great importance in the fields of medicine, pharmaceutical research, as well as water and food industries. In order to develop a photonic biosensor for detection and monitoring antibiotic susceptibility of bacteria by taking advantage of photoluminescence (PL) emission of photocorroding III-V quantum semiconductors (QS), we have explored the capture and growth of *Escherichia coli* K12 on bare and biofunctionalized surfaces of GaAs (001) - a material of interest for capping different III-V QS. Once capture and growth of *E. coli* have been demonstrated, future studies with PL will have a rational basis. We found that GaAs or Au wafers placed on nutrient agar Petri dishes inoculated with bacteria did not inhibit bacterial growth as evidenced by counting bacteria with a microscope, regardless of whether the GaAs surfaces were bare or biofunctionalized. However, the capture and growth of bacteria on biofunctionalized surfaces of GaAs wafers kept in a flow cell and exposed to different concentrations of bacteria and growth medium revealed that the initial coverage of the GaAs surfaces with bacteria, and the subsequent bacterial growth rates were dependent on the biofunctionalization architecture, with antibody-coated surfaces clearly being most efficient in capturing bacteria and offering better conditions for growth of bacteria. We observed that, as long as the GaAs wafers were exposed to bacterial suspensions at concentrations of at least 10^5 CFU/mL, bacteria could grow on the surface of wafers, regardless of the type of biofunctionalization architecture used to capture the bacteria. The demonstration that a biofunctionalized surface of GaAs provides conditions attractive for the growth of bacteria is an important step towards advancing an innovative method of photonic monitoring of bacterial activities in different biochemical environments.

4.2 Background

Evaluating growth of bacteria to determine antibiotic susceptibility and metabolic traits is essential to diagnostic microbiology (Versalovic et al. 2011). Monitoring the viability, growth and cellular metabolism of bacteria also plays an important role in yielding bacterial products in industrial- or small-scale experiments (Garneau and Moineau 2011; Kee et al. 2013; Nayak et al. 2009; Schuler and Marison 2012; Sonnleitner et al. 1992). Conventionally, bacterial growth has been investigated by (1) plate counting where colony forming units (CFU) are determined (Sonnleitner et al. 1992), and (2) visualization of growth in broth either by eye or by nephelometry (de Freitas et al. 2003; Joubert et al. 2010; Versalovic et al. 2011). Broth microdilution and Kirby-Bauer disk diffusion are widely applied in clinical laboratories to evaluate the antibiotic susceptibility of bacteria (Poupard et al. 1994; Versalovic et al. 2011). These techniques are time-consuming and labour intensive and, typically, they are not able to provide same-day monitoring (Chiang et al. 2009; Kee et al. 2013; Versalovic et al. 2011). Polymerase chain reaction (PCR) (Cotto et al. 2015; Rolain et al. 2004; Versalovic et al. 2011), surface plasmon resonance (SPR) (Chiang et al. 2009) and fluorescence-based assays (Boi et al. 2015; Roth et al. 1997) have been introduced for rapid evaluation of growth and antimicrobial sensitivity of bacteria. However, the cost of PCR (Mwaigwisya et al. 2015) and SPR systems (Lazcka et al. 2007) and technical complexity of fluorescent dye use are inhibitory factors that limit the application of these methods in clinical laboratories.

Photoluminescence (PL) emitting semiconductors hold a great potential for biosensing applications due to the sensitivity of the PL signal to the surface localized phenomena (Adamowicz et al. 1998; Gfroerer 2006; Lebedev 2001; Moumanis et al. 2006; Tomkiewicz et al. 2009). Electrically charged molecules, if immobilized at the surface of a semiconductor, could affect PL of such a material by modifying bending of its energy bands near the surface (Seker et al. 2000; Zhang and Yates 2012). PL of some semiconductors has been used for chemical sensing (Seker et al. 2000) and detection of biomolecules (Budz et al. 2010). We have demonstrated a successful detection of electrically charged viruses (Dubowski et al. 2014), *Escherichia coli* K12 bacteria (Duplan et al. 2011; Nazemi et al. 2015) and, more recently, *Legionella pneumophila* (Aziziyan et al. 2016) by taking advantage of PL emission of

GaAs/AlGaAs nano-heterostructures. The major advantage of the GaAs/AlGaAs biosensor, in comparison to a variety of biosensors employing Au surfaces, is its low cost (GaAs/AlGaAs microstructures are used by ubiquitous light emitting diodes), also related to its simple (planar) surface structure, a straightforward biofunctionalization protocol and inexpensive hardware for reading the biosensor signal. Furthermore, the microstructures with stacks of GaAs/AlGaAs nano-heterostructures have the potential to be applied as multi-biosensors, each defined by a photocorroding pair of GaAs/AlGaAs. Following this research, we have hypothesised that these nano-heterostructures could be employed to develop a method for inexpensive and quasi-real time monitoring of the growth and antibiotic susceptibility of bacteria. One of the key elements in the development of this innovative biosensing platform is to demonstrate that GaAs (001), normally used for capping PL emitting GaAs/AlGaAs nano-heterostructures, could support the growth of bacteria. We note that GaAs (001) denotes a specific, technologically important surface of a zinc blende crystal structure GaAs material (LaBella et al. 2005; Ohtake 2008) that is well-known in the production of optoelectronic devices (Mokkapati and Jagadish 2009; Wada 1988).

Growth of bacteria on solid surfaces can be affected by biocompatibility of the substrate. Some metal surfaces such as silver (Ag) are well-known to have antimicrobial activity and prevent bacterial colonization (Golubovich and Rabotnova 1974). Silver coating is widely applied for reducing bacterial contamination of medical tools and minimizing nosocomial infections related to operating rooms and other sections of hospitals (Casey et al. 2012). Some gold (Au)-coated nanoparticles were found toxic to bacteria (Zhou et al. 2012), whereas others were not (Williams et al. 2006). Furthermore, arsenic (As) and gallium (Ga) have been reported to affect bacterial viability (DeLeon et al. 2009; Harvey and Crundwell 1996; Mukhopadhyay et al. 2002; Podol'skaia et al. 2002; Rzhepishevska et al. 2011).

To investigate the effect of surface biocompatibility in the growth of bacteria on GaAs, we studied the growth of *E. coli* K12 on bare and biofunctionalized surfaces of GaAs (001) and compared the results with the growth on Au surfaces. Related experiments were carried out as a function of the initial concentration of bacteria to assess the toxicity of GaAs and Au surfaces,

and we addressed the impact of different binding architectures on the capture and growth potential of these bacteria.

4.3 Experimental methods

4.3.1 Materials

Semi-insulating (SI) undoped GaAs (001) wafers (AXTG108-36) were obtained from AXT Inc. (Fremont, USA). OptiClear, acetone and isopropanol (2-propanol) used for cleaning the GaAs wafers were purchased from National Diagnostics (Mississauga, Canada), ACP Chemicals (Montréal, Canada) and Fisher Scientific (Ottawa, Canada), respectively. Anhydrous ethanol was obtained from Commercial Alcohols Inc. (Brampton, Canada). Deionized (DI) water with an electrical resistivity of 18 MΩ.cm was obtained with a Millipore purification custom system built by Culligan (Quebec, Canada). Ultra-high purity nitrogen 5.0 UHP (99.999%) used for deoxygenation the anhydrous ethanol and high purity nitrogen 4.8 HP (99.998%) used for drying the GaAs wafers were both purchased from Praxair Canada Inc. (Mississauga, Canada). Ammonium hydroxide 28% (NH_4OH) was obtained from Anachemia (Richmond, Canada). Ammonium sulfide 48% (AS) was purchased from Sigma-Aldrich (Ontario, Canada). Biotinylated polyethylene glycol (b-PEG) thiols were bought from Prochimia Surfaces (Gdansk, Poland). Luria Bertani (LB) broth, phosphate buffered saline (PBS) solution (10X, pH 7.4), 16-Mercaptohexadecanoic acid (MHDA) thiol, hexadecanethiol (HDT), 1-Ethyl-3-(3-dimethylaminopropyl)-carbodiimide (EDC) and N-hydroxysuccinimide (NHS) were all obtained from Sigma-Aldrich (Ontario, Canada). Non-conjugated polyclonal antibodies (Ab) and polyclonal biotinylated antibodies (b-Ab) against *E. coli* were both bought from ViroStat, Inc (Portland, ME). Neutravidin (NA) was purchased from Molecular Probes (Invitrogen, Burlington, Canada). Live *E. coli* K12 bacteria were obtained from the Department of Biology of the Université de Sherbrooke (Quebec, Canada). The Au-coated samples were made by deposition of a thin layer of Au (40 -50 nm) on glass substrates in the cleanroom of the Interdisciplinary Institute for Technological Innovation (3IT), Université de Sherbrooke (Quebec, Canada).

4.3.2 Biofunctionalization of GaAs (001) and Au surfaces

Samples of 2 mm × 2 mm were cleaved from GaAs (001) wafers and cleaned in an ultrasonic bath with OptiClear, acetone and isopropanol sequentially for 5 min each. Following the cleaning steps, the GaAs samples were dried under a flow of compressed nitrogen and etched in a solution of NH_4OH (28%) for 2 min at room temperature. Three different bio-architectures have been applied to functionalize the surface of freshly etched GaAs (001) samples, as described below. The Au-coated glass samples, 2 mm × 2 mm, were cleaned in OptiClear, acetone and isopropanol, and then dried with a flow of compressed nitrogen. Dried samples were functionalized with MHDA-EDC/NHS-Ab in the same way as the GaAs samples.

4.3.2.1 b-PEG-NA-b-Ab functionalization

Freshly etched GaAs samples were rinsed with deoxygenated anhydrous ethanol and immediately incubated for 20 h at room temperature in a 2 mM mixture of b-PEG (1:15) and HDT (14:15) thiols diluted in deoxygenated anhydrous ethanol. After the thiolation step, the GaAs samples were rinsed with deoxygenated anhydrous ethanol and exposed to AS (0.1%) for 15 min. Following this step, the samples were rinsed with DI water and incubated for 2 h at room temperature in PBS (1X) solution containing 200 µg/mL of neutravidin. Thereafter, the neutravidin-coated samples were immersed for 1 h at room temperature in a solution of biotinylated polyclonal antibodies against *E. coli* diluted in PBS (1X) at 0.1 mg/mL. The antibodies were biotinylated by the manufacturer by covalent attachment of biotin molecules to free amine groups (NH_2) in the antibody structure. Figure 28 shows a schematic illustration of bacteria immobilized on the GaAs (001) surface functionalized with an architecture comprising mixed b-PEG and HDT thiols, neutravidin and biotinylated polyclonal antibodies against *E. coli* (b-PEG-NA-b-Ab). The formation of HDT self-assembled monolayers (SAMs) on the GaAs (001) surface has been investigated with PL (Arudra et al. 2012; Ding et al. 2006; Huang and Dubowski 2014; Kim et al. 2009), ellipsometry (Rosu et al. 2009), X-ray diffraction (McGuiness et al. 2007) and Fourier transform infrared spectroscopy (FTIR) (Arudra et al. 2012). The SAM formation from b-PEG diluted in OH-terminated PEG thiols has also been investigated using FTIR (Duplan et al. 2009). In each case, the intensity and full-width-at-half-maximum of two

peaks in the 2800 to 3000 cm^{-1} region, that are assigned to stretching vibrations of CH_2 in the alkane chains (Arnold et al. 2002), are considered as a measure of the quality of formed SAMs. Mixed SAMs comprising different thiols have also been investigated on Au surfaces (Folkers et al. 1992; Mustafa et al. 2012; Nelson et al. 2001; Olbris et al. 1995; Tarnawski and Ulbricht 2011; Yoshioka et al. 2010), suggesting the feasibility of formation of such architectures on GaAs (001) surfaces as well. We employed the b-PEG-NA-b-Ab architecture to support the growth of bacteria on GaAs samples placed on nutrient LB-agar plates. A similar architecture was previously used by us for detection of *E. coli* K12 bacteria (Duplan et al. 2011; Nazemi et al. 2015).

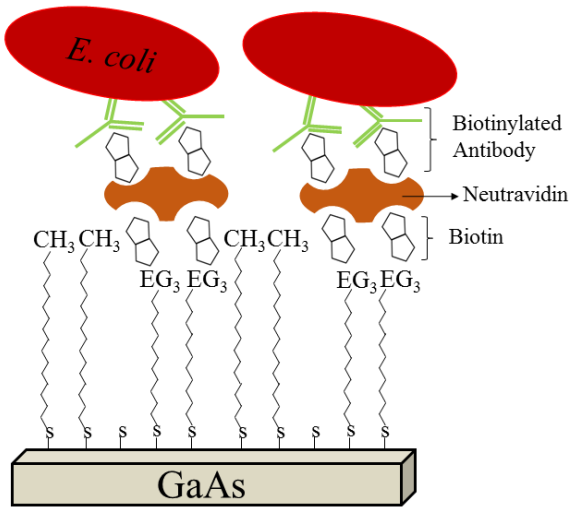

Figure 28. Schematic illustration of a GaAs (001) surface functionalized with a biotinylated PEG-neutravidin-biotinylated antibody architecture for immobilization of *E. coli* bacteria.

4.3.2.2 MHDA-EDC/NHS functionalization

Freshly etched GaAs samples were rinsed with deoxygenated anhydrous ethanol and immediately incubated for 20 h at room temperature in a 2 mM solution of MHDA thiol diluted in deoxygenated anhydrous ethanol. Following this step, the GaAs samples were rinsed with deoxygenated anhydrous ethanol and then PBS (1X). Thereafter, the samples were incubated for 30 min at room temperature in a mixture of 400 mM of EDC and 100 mM of NHS diluted in PBS (1X) to activate the COOH group of the MHDA thiol. A schematic illustration of the

MHDA-EDC/NHS biofunctionalization procedure applied to immobilize *E. coli* bacteria on the GaAs (001) surface is presented in Figure 29. The formation of MHDA SAM on the GaAs (001) surface and activation of COOH group of this thiol with the EDC/NHS step has recently been discussed by Lacour et al. (Lacour et al. 2016). The appearance of a C=O peak at 1741 cm^{-1} in FTIR absorption spectra of MHDA-coated samples that follows the EDC/NHS exposure, confirms the activation of the COOH group of MHDA thiol (Frey and Corn 1996). This process allows direct attachment of bacteria through covalent binding with naturally-occurring NH_2 groups on the bacterial surface (Meyer et al. 2010). The EDC/NHS activated MHDA SAM architecture has been applied to directly capture *E. coli* bacteria on GaAs samples kept in a flow cell.

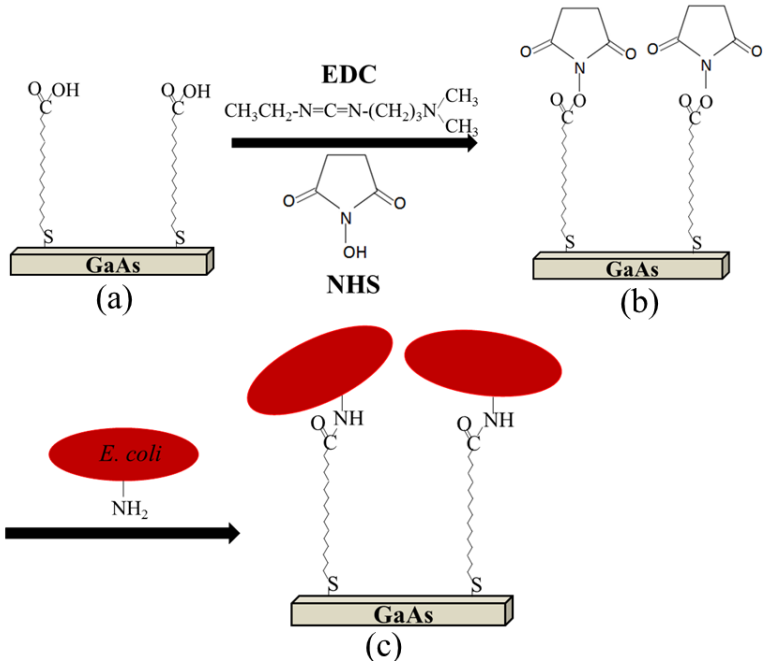

Figure 29. Schematic illustration of the biofunctionalization steps employed for non-specific immobilization of *E. coli* bacteria on the surface of GaAs (001). Following formation of SAM of MHDA thiol on the freshly etched surface of GaAs (001) (a), COOH group of MHDA thiol is activated with EDC/NHS (b), which allows immobilization of *E. coli* via naturally-occurring NH_2 groups on the bacterial surface (c).

4.3.2.3 MHDA-EDC/NHS-Ab functionalization

The fabrication of MHDA-EDC/NHS-Ab bio-architecture on GaAs (001) and Au surfaces included covalent linkage of polyclonal Ab against *E. coli* to COOH groups of MHDA SAM

that had been activated by EDC/NHS, as described in the previous section. The reaction was carried out for 1 h at room temperature from an antibody solution in PBS (1X) at 0.1 mg/mL. The illustration of the biofunctionalization steps employed in this case is presented schematically in Figure 30. The immobilization of antibodies depended on covalent binding of their NH_2 groups with carboxyl-functionalized surfaces activated by EDC/NHS. As demonstrated by Lacour et al. with FTIR measurements (Lacour et al. 2016), the presence of amide A, amide I and amide II bands in the 3300, 1660 and 1520 cm^{-1} regions (Bandekar 1992; Lacour et al. 2016) validate the attachment of *E. coli* Ab to the GaAs (001) surface. This architecture has been applied to specifically capture *E. coli* bacteria on GaAs and Au samples kept in a flow cell. We note that no special procedure was employed to block activated COOH against reaction with bacteria (in MHDA-EDC/NHS bio-architecture) or with antibodies (in MHDA-EDC/NHS-Ab bio-architecture). It is reasonable, however, to expect that the buffers and the LB growth medium contributed to the saturation of free COOH.

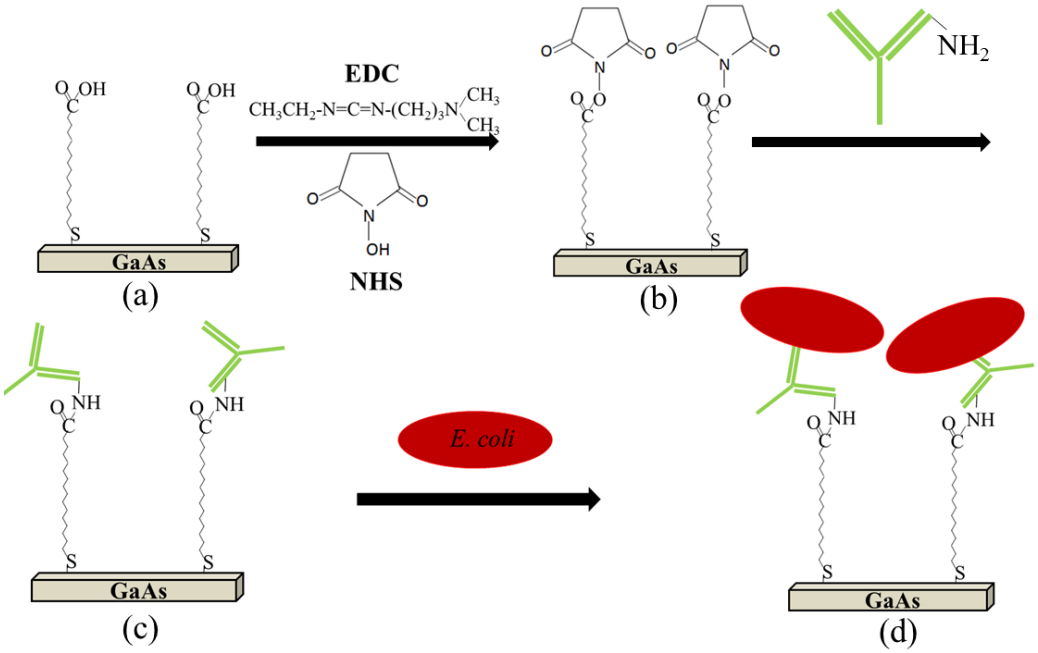

Figure 30. Schematic illustration of the biofunctionalization steps applied for immobilization of *E. coli* bacteria with antibody on the surface of GaAs (001). Following formation of MHDA SAM on the freshly etched surface of GaAs (001) (a), COOH group of MHDA thiol is activated with EDC/NHS (b), followed by immobilization of *E. coli* antibodies whose NH_2 groups react with the EDC/NHS activated carboxyl sites (c), and antibody specific immobilization of *E. coli* bacteria (d).

4.3.3. Growth of *E. coli* on GaAs (001) and Au surfaces in contact with nutrient LB-agar plate

Freshly cultured *E. coli* K12 suspension was prepared by overnight growth of bacteria in LB at 37º C before use the following morning. On the day of the experiment, the concentration of the bacteria was measured with a cell density meter (Fisher Scientific, model 40) operating at 600 nm. Bacteria were then centrifuged in LB for 25 min at 3000 rpm. After that, the medium was removed and the pellets were suspended in PBS (1X) and centrifuged at 3000 rpm for 15 min. Finally, PBS (1X) was removed and the pellets were resuspended in PBS (1X) and diluted to give 10^5 CFU/mL. A group of 8 b-PEG-NA-b-Ab functionalized and 8 bare GaAs (001) samples were placed upside down on a nutrient agar plate that had been inoculated evenly with 100 µL of the bacterial suspension at 10^5 CFU/mL. Assuming homogenous distribution of bacteria on the nutrient agar plate, the initial coverage of the agar plate with bacteria was around 2 bacteria/mm^2. This number was calculated by dividing the total number of bacteria used to inoculate the agar plate (10^4 bacteria) by the total area of the agar plate (45.6 cm^2). Figure 31 schematically illustrates the top and side views of the experimental setup. The plate with GaAs samples was then kept at 37° C for up to 8 hours.

Every hour, one of the bare samples and one of the biofunctionalized samples were removed from the agar plate and adherent bacteria were counted with an optical microscope following the procedure discussed in the Microscopic enumeration of bacteria section. These measurements allowed us to investigate the dynamics of the immobilization process on the surface of both samples. As a control experiment, a series of experiments was also carried out for bare Au samples which are, no doubt, the most commonly used surfaces in biosensor studies (Lazcka et al. 2007) following the methodology applied for GaAs (001) samples. The principle of studying the growth of bacteria on GaAs and Au samples in contact with bacterial cultures on Petri dishes can be compared to a Kirby–Bauer antibiotic sensitivity test (Poupard et al. 1994; Versalovic et al. 2011) where paper disks containing different types of antibiotics are placed on Petri dishes to allow evaluation of the impact of the antibiotics on bacterial growth.

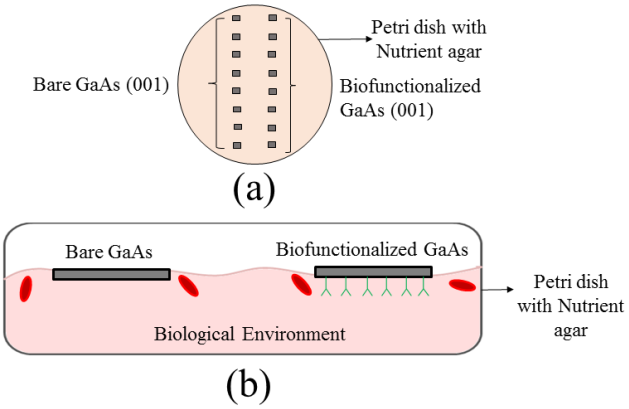

Figure 31. Top view (a) and side view (b) of the setup for studying the growth of *E. coli* in proximity of GaAs samples. The nutrient agar plate was inoculated evenly with 100 µL of *E. coli* K12 bacteria (red ovals in (b)) at 10^5 CFU/mL. Biofunctionalized and bare GaAs (001) samples were placed upside down. The same setup and procedure was applied for bare Au samples.

4.3.4 Growth of *E. coli* on the surface of GaAs (001) and Au in a flow cell

In this approach, growth of *E. coli* K12 bacteria on biofunctionalized GaAs (001) and Au surfaces was investigated for samples kept in an ULTEM^{TM} flow cell and exposed to bacterial suspensions and LB broth, sequentially. A schematic illustration of the setup used in this experiment is presented in Figure 32. It consists of a flow cell with an outer diameter of 38.1 mm and a height of 3.92 mm containing a groove where samples were placed that had a volume of 0.15 mL. This groove could be filled with bacterial solutions and then rinsed with LB medium stored in a dedicated vessel using a peristaltic pump with a 0.89 mm diameter Santoprene tube. This setup is similar to that employed for monitoring PL *in situ* from GaAs/AlGaAs biochips exposed to different bacterial solutions (Aziziyan et al. 2016; Nazemi et al. 2015).

Following 10 min injection of 1 mL of freshly-cultured bacterial suspension into the flow cell using the peristaltic pump (flow rate of 0.1 mL/min), the samples were left in contact with the bacterial suspension for an additional 20 min without any further injection. This resulted in a total of 30 min exposure of the samples to specific bacterial solutions, similar to that used by others for antigen-antibody reactions at liquid/solid interfaces (Hlady et al. 1990). Following this step, LB was injected into the flow cell for 30 min (flow rate of 0.1 mL/min which would replace the liquid volume of the flow cell groove 20 times) to rinse away unattached bacteria

and provide surface-attached bacteria with a growth medium. The bacteria were exposed to LB for an additional 4 h without any further injection while the flow cell was kept at 37° C to stimulate the growth of bacteria. The biochips were analyzed after 30 min exposure to bacterial suspension, and after an additional 4.5 h exposure to LB broth with an optical microscope as described in the Microscopic enumeration of bacteria section. We performed this experiment for bacterial concentrations ranging from 10^4 to 10^8 CFU/mL and GaAs samples functionalized with MHDA-EDC/NHS and MHDA-EDC/NHS-Ab architectures. This allowed investigation of the impact of different binding architectures on the initial capture and the subsequent growth of bacteria. The growth rate of bacteria was also addressed as a function of the initial bacterial concentration for each bio-architecture. As a control, the same setup and procedure were applied for Au samples functionalized with MHDA-EDC/NHS-Ab and exposed to initial bacterial suspensions at 10^4 and 10^5 CFU/mL. Since the first step of our experiments was immobilization of bacteria on the surface of the biochips, we only worked with biofunctionalized GaAs or Au samples and did not employ bare samples which are not able to efficiently capture the bacteria.

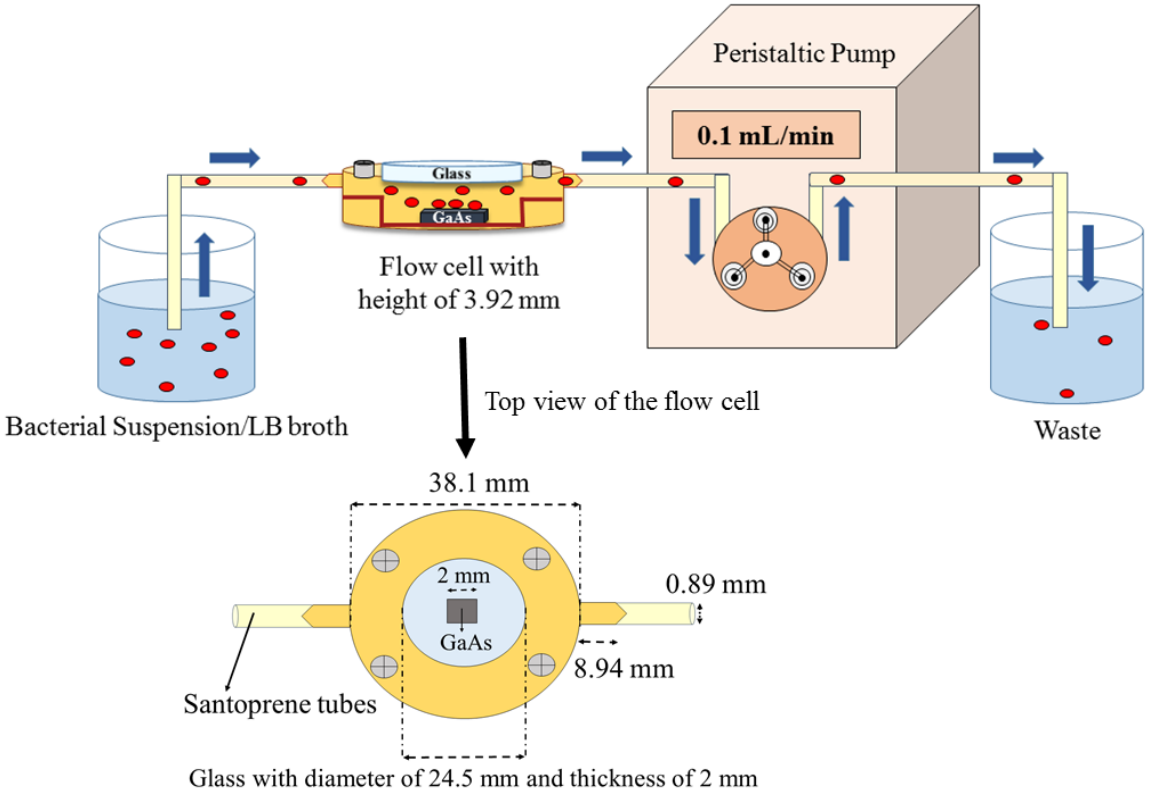

Figure 32. Schematic illustration of the flow cell setup. The biofunctionalized GaAs (001) or Au biochips were placed in the flow cell and exposed to bacterial suspension (red ovals) and LB, sequentially. The bacteria and LB were injected into the flow cell at a flow rate of 0.1 mL/min using the peristaltic pump.

4.3.5 Microscopic enumeration of bacteria

Biochips were removed after each experiment and placed on glass slides with the bacteria exposed surface facing up, for microscopic analysis. Without fixation, washing, or staining, bacteria were observed with an optical microscope (Zeiss, Axiotech) using overhead illumination. Bacteria were readily observed through a 100X lens with supplemental 10X digital enlargement. Total bacteria adherent to the surface in each experiment was estimated by analysing several optical images at magnification of 1000X (each image with the surface area of ~3500 μm^2 per field) collected at different sites of the sample and reported per mm^2.

4.4 Results and discussion

4.4.1 Growth of *E. coli* K12 on the surface of GaAs (001) and Au samples in contact with a nutrient agar plate

The growth of *E. coli* K12 was observed on both bare and b-PEG-NA-b-Ab functionalized surfaces of GaAs (001) biochips placed on nutrient agar plates. Not only was there no inhibition zone around the biochips as has been observed in similar experiments with silver nanoparticles (Naqvi et al. 2013), but neither bare nor functionalized GaAs samples prevented bacteria from multiplying. The time dependent surface density of immobilized bacteria on bare and b-PEG-NA-b-Ab functionalized surfaces of GaAs (001) is shown in Figure 33(a). Each experiment was performed at least in triplicate to obtain average values with standard deviation. The number of bacteria immobilized on the bare GaAs increased from 3±1 bacteria/mm^2 at 1 h to 2687±173 bacteria/mm^2 at 8 h. This compares with 20±3 and 2967±339 bacteria at 1 and 8 h for the biofunctionalized samples. The greater initial concentration of bacteria on the biofunctionalized surface suggests, as expected, more efficient capture of bacteria. The number of bacteria visualized on the GaAs surfaces probably reflected both non-specific and specific capture. It can be seen that initially (1 hour), the number of bacteria captured with Ab-based architectures exceeded ~ 7X the number of non-specifically captured bacteria. However, after 6 hours, in both cases, the surface coverage with bacteria reached a saturation number of around 3×10^3 bacteria/mm^2. The saturation effect might be related to the stationary phase of bacterial growth when the rates of bacterial growth and bacterial death are equal (Akerlund et al. 1995; Fujikawa and Morozumi 2005).

The data in Figure 33(a), fitted with exponential curves, indicate that the number of bacteria doubled every 31 and 44 min on the surface of bare and antibody functionalized GaAs, respectively. This compares to the ability of *E. coli* to double every 20 min under ideal conditions of temperature, oxygen concentration and a rich liquid nutrient medium (Berg 2004). However, for comparable growth rates of bacteria in the exponential phase in liquid and solid environments (agar plates), the longer latency phase of bacteria on solid media could explain the lower rate of bacterial growth on solid substrates than in liquid environments (Fujikawa and

Morozumi 2005). This test demonstrates the feasibility of growing *E. coli* bacteria on GaAs (001) biochips placed on agar plates.

Figure 33(b) illustrates the time dependent surface density of *E. coli* bacteria immobilized on bare GaAs and Au samples. The number of bacteria immobilized on bare Au samples increased from 8±2 bacteria/mm^2 at 1 h to 2955±341 bacteria/mm^2 at 8 h. Fitted with the exponential curve, the number of bacteria in this case doubled every 35 min, which compares to the 31 min required by bacteria to double on the surface of bare GaAs. Thus, the similar growth rates of bacteria on bare GaAs and Au samples indicate that GaAs was no more inhibitory to the growth of *E. coli* bacteria than Au for the biochips placed on nutrient agar Petri dishes inoculated with bacteria.

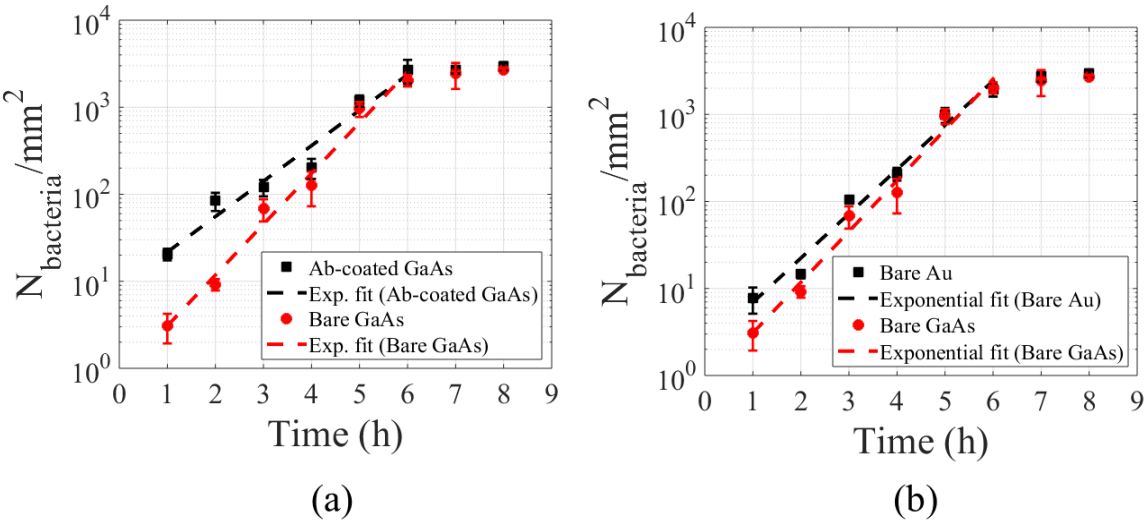

Figure 33. Time dependent surface density of *E. coli* bacteria immobilized on bare and b-PEG-NA-b-Ab functionalized surfaces of GaAs (001) (a) and on bare Au surfaces compared to those of bare GaAs (b).

4.4.2 Growth of *E. coli* K12 on GaAs (001) and Au surfaces in a flow cell

Figure 34 presents the initial surface coverage (after 30 min exposure to a bacterial suspension) and the coverage after a 4.5-h incubation in LB medium for GaAs biochips functionalized with MHDA-EDC/NHS and MHDA-EDC/NHS-Ab (See related data included in Supplementary Material). For the set of bacterial suspensions ranging from 10^5, 10^6, 10^7 and 10^8 CFU/mL, each

experiment was performed at least in triplicate. Examples of optical images for a biochip functionalized with MHDA-EDC/NHS-Ab and exposed to bacterial suspension at 10^6 CFU/mL, before and after incubation in LB, are shown in Figure 35. We noted that the size of the bacteria before and after growth was in good agreement with literature data, indicating increased bacterial length after entering the growth phase (Trueba and Woldringh 1980). All bacteria appeared to be immobilized on the surface and not free in the film of LB medium that surrounded the sample because no bacteria could be seen moving by Brownian or flagella-assisted movement, nor were partially out of the plane of focus. For this reason, we attributed increased coverage with surface growth rather than with growth free in the medium and subsequent attachment.

The average growth rate of bacteria was calculated for each bio-architecture and for each concentration of bacteria, and is presented in Table 5. The average growth rate of bacteria was calculated using the following formula:

$$R = \frac{N_2 / N_1}{T} \tag{4.1}$$

where N_1 and N_2 correspond to the average surface coverage with bacteria before and after bacterial growth, respectively, and T is the duration of the experiment, which is equal to 300 min.

We systematically observed a greater initial surface coverage with *E. coli* using the EDC/NHS-Ab capture method compared with the direct EDC/NHS method for comparable concentrations of bacteria. The difference between the two bio-architectures in terms of the initial surface coverage was more noticeable for lower concentrations of bacteria. This might be related to a limitation in the number of bacteria that the antibody-coated surface is able to capture and saturation of this surface at higher bacterial concentrations. Due to the higher efficiency of antibody-coated surface in initial capture of bacteria, the surface coverage after bacterial growth (see Figure 34), and the bacterial growth rate (see Table 5) were higher compared with the EDC/NHS functionalized surface for each concentration of bacteria. It is also possible that the lower number of bacteria on the EDC/NHS functionalized surface compared with antibody-

coated surface, might be related to the reduced capture of growing bacteria directly on the EDC/NHS functionalized surface due to the inactivation of COO-NHS groups following their reaction with free NH_2 groups of proteins in the LB medium.

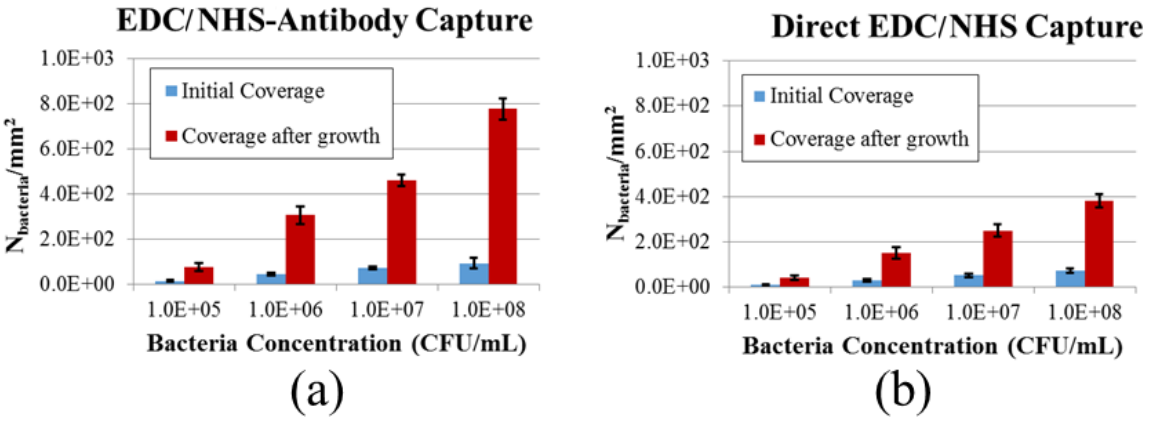

Figure 34. Growth of *E. coli* on GaAs biochips functionalized with EDC/NHS-Ab (a) and EDC/NHS without antibody (b) detected by measuring initial (after 30 min exposure to a bacterial suspension) and final (after 4.5 h in LB) bacterial surface coverage for different concentrations of bacteria.

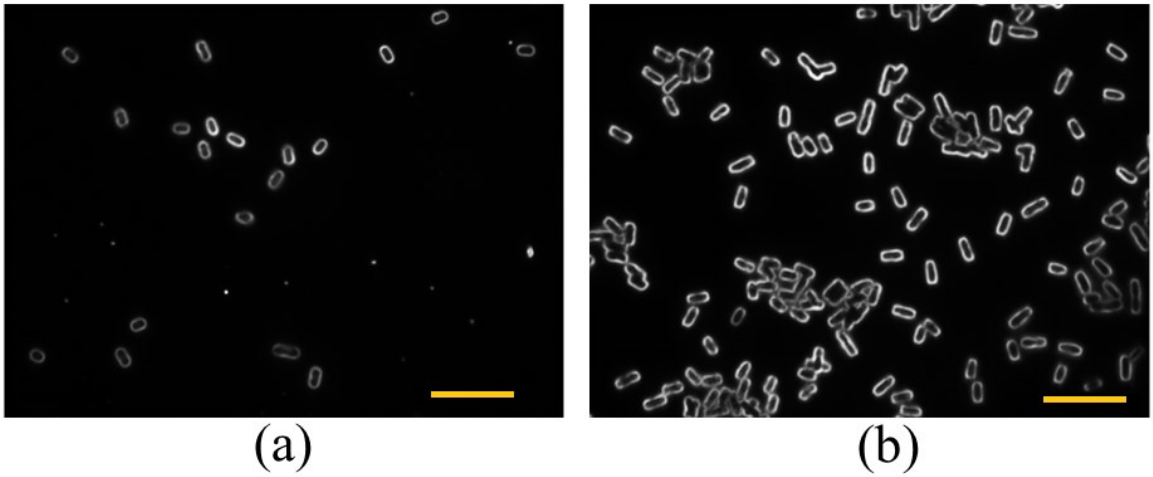

Figure 35. Examples of microscopic images of *E. coli* K12 bacteria immobilized on the MHDA-EDC/NHS-Ab functionalized surface of GaAs (001) exposed for 30 min to a 10^6 CFU/mL solution (a), and after 4.5 h exposure to a growth medium (b). The scale bars correspond to 10 µm.

Table 5. Average growth rate of bacteria on the functionalized surface of GaAs for different bacterial concentrations.

Bacterial Concentration (CFU/mL)	Growth rate using EDC/NHS-Ab Capture method (min^{-1})	Growth rate using EDC/NHS capture method (min^{-1})
10^5	0.016	0.015
10^6	0.023	0.018
10^7	0.021	0.016
10^8	0.028	0.018

We were not able to observe the growth of bacteria on either of the investigated architectures for bacterial concentration of 10^4 CFU/mL. A minimum threshold concentration for bacterial growth might be related to the toxicity of Ga and As ions that are known to affect the viability and/or growth of bacteria (DeLeon et al. 2009; Harvey and Crundwell 1996; Mukhopadhyay et al. 2002; Podol'skaia et al. 2002; Rzhepishevska et al. 2011). The release of these ions is a consequence of GaAs corrosion (Ruberto et al. 1991):

$$GaAs + 2H_2O + 6h^+ \rightarrow Ga^{3+} + HAsO_2 + 3H^+ \quad (4.2)$$

It is possible that for bacterial concentrations below 10^5 CFU/mL, the amount of Ga and/or As ions released per bacteria could reach a toxic dose (Diorio et al. 1995; Podol'skaia et al. 2002) and affect bacterial viability and growth. Moreover, the growth of bacteria might also be inhibited by the antibodies used to capture bacteria in MHDA-EDC/NHS-Ab bio-architecture (Chalghoumi et al. 2009; Lin et al. 1998).

As a control, we investigated the growth of *E. coli* on Au substrates functionalized with MHDA-EDC/NHS-Ab. Following the methodology applied for GaAs samples, the biofunctionalized Au samples were kept in the flow cell and exposed to the bacterial suspension at 10^5 CFU/mL and then to LB medium. The initial coverage of Au samples exposed for 30 min to the bacterial suspension and for 4.5 h to LB medium was at 17±5 and 98±25 bacteria/mm^2, respectively. The average bacterial growth rate of 0.019 min^{-1} on these samples was slightly higher than that of 0.016 min^{-1} on MHDA-EDC/NHS-Ab functionalized GaAs samples, suggesting that for the 10^5 CFU/mL solution, the GaAs substrate had only a minor negative effect on bacterial growth in comparison to the Au substrate. We note that the Petri dish experiments with GaAs (001) and

Au substrates in contact with nutrient agar plates inoculated with bacteria at ~ 2 bacteria/mm^2, revealed comparable growth rates of bacteria on bare both GaAs and Au substrates. This suggests that the concentration of As and/or Ga released to the Petri dish was not sufficient to affect bacterial growth, or that the agar growth medium neutralized any toxicity. Given that some toxicity has been observed with Au in an ionic form (Williams et al. 2006), our inability to observe bacterial growth on both Au and GaAs substrates kept in the flow cell, when initial concentrations of bacteria were below 10^5 CFU/mL, could be due to comparable toxicity of the Au and GaAs substrates. Nevertheless, these results have revealed that the GaAs surface provides conditions satisfactory for the growth of bacteria in a flow cell, which potentially is attractive for photonic monitoring *in situ* of the growth and reaction of bacteria to different biological environments and particularly antibiotics.

4.5 Conclusion

In our endeavor to develop a GaAs-based photonic biosensor for monitoring reaction of bacteria to different biochemical conditions, we have investigated the capture and growth of *E. coli* K12 on surfaces of GaAs (001). The experiments with bare GaAs and Au in contact with nutrient agar plates inoculated with bacteria at ~ 2 bacteria/mm^2 suggested that neither of these substrates inhibited the growth of bacteria. However, the experiments in a flow cell revealed that the initial coverage, and the subsequent bacterial growth rates were dependent on the biofunctionalization architecture used to capture bacteria. Antibody biofunctionalized surfaces exhibited significantly higher capture efficiencies, especially at lower concentrations of bacteria. For suspensions containing bacteria at less than 10^5 CFU/mL, we were not able to observe the growth of bacteria, regardless of the biofunctionalization architecture. This threshold might be related to the toxicity of As and/or Ga released from the GaAs samples. Nevertheless, we have recently demonstrated the successful application of this method for detection of *E. coli* reaction to antibiotics in less than 3 h (Nazemi et al. 2016). We realize that our current approach requires bacterial suspensions at ≥ 10^5 CFU/mL. However, this shortcoming is also present for matrix-assisted laser desorption ionization time of flight mass spectrometry (MALDI-TOF MS) which requires 10^4 – 10^5 cells per assay (van Belkum et al. 2013), yet is about to revolutionize clinical

diagnostic laboratories. Whereas MALDI-TOF MS does not determine antibiotic sensitivity, our approach does and could thus complement MALDI-TOF MS in the same time frame.

4.6 List of abbreviations

CFU**,** Colony forming unit; PCR, Polymerase chain reaction; SPR, Surface plasmon resonance; PL, Photoluminescence; SI, Semi-insulating; DI water, Deionized water; AS, Ammonium sulfide; b-PEG, Biotinylated polyethylene glycol; LB, Luria Bertani; PBS, Phosphate buffered saline; MHDA, 16-Mercaptohexadecanoic acid; HDT, Hexadecanethiol; EDC, 1-Ethyl-3-(3-dimethylaminopropyl)-carbodiimide; NHS, N-hydroxysuccinimide; Ab, Non-conjugated polyclonal antibodies; b-Ab, Polyclonal biotinylated antibodies; NA, Neutravidin; SAM, Self-assembled monolayer; FTIR, Fourier transform infrared spectroscopy

4.7 Declarations

4.7.1 Ethics approval and consent to participate

Not applicable.

4.7.2 Consent for publication

Not applicable.

4.7.3 Availability of data and materials

The data supporting the conclusions of this study are included in this article and in Supplementary Material (available on-line).

4.7.4 Competing interests

The authors declare that they have no competing interests.

4.7.5 Funding

This research was supported by the Canada Research Chair in Quantum Semiconductors Program and the Fonds de recherche Nature et Technologie du Québec (FRQNT) project No 2015-PR-184056.

4.7.6 Authors' contributions

EN carried out the experimental tests, performed the data analysis and drafted the manuscript. WMH provided the materials necessary for the experiments and helped in performing the experiments and revising the manuscript. JJD and EHF supervised the research, contributed in designing the experiments, aided in interpretation of the data and contributed in writing and revising the manuscript. All the authors read and approved the final manuscript.

4.7.7 Acknowledgements

We thank Dr. Khalid Moumanis and the technical staff of the Interdisciplinary Institute for Technological Innovation (3IT) for their assistance. We are also indebted to Dr. François Malouin of the Department of Biology, Université de Sherbrooke for kindly supplying *E. coli* K12.

4.8 Supplementary material

Table 6. Bacterial surface coverage of functionalized GaAs for different bacterial concentrations.

	Bacterial concentration (CFU/mL)			
	10^5	**10^6**	**10^7**	**10^8**
Initial coverage with EDC/NHS-Ab capture method (/mm^2)	16±3	44±5	72±6	93±23
Initial coverage with EDC/NHS capture method (/mm^2)	9±2	28±6	52±8	71±10
Coverage after growth with EDC/NHS-Ab capture method (/mm^2)	76±19	306±39	460±26	776±46
Coverage after growth with EDC/NHS capture method (/mm^2)	40±9	151±25	249±26	382±29

CHAPTER 5: Avant-Propos

Auteurs et affiliation:

- ***Elnaz Nazemi: Étudiante au doctorat, Université de Sherbrooke, Faculté de génie, Département de génie électrique et informatique.***

- Walid M. Hassen : Assistant de recherche, Université de Sherbrooke, Faculté de génie, Département de génie électrique et informatique.
- Eric H. Frost: Professeur, Université de Sherbrooke, Faculté de médecine et des sciences de la santé, Département de microbiologie et d'infectiologie.
- Jan J. Dubowski: Professeur, Titulaire de la Chaire de recherche du Canada en semiconducteur quantiques, Université de Sherbrooke, Faculté de génie, Département de génie électrique et informatique.

Date de publication: January 2017

Revue: Biosensors and Bioelectronics

Titre français:

Surveillance la croissance et la sensibilité aux antibiotiques des *Escherichia coli* avec photoluminescence de GaAs / AlGaAs puits quantique

Résumé français :

Le développement de méthodes rapides et fiables afin d'étudier la sensibilité des bactéries aux antibiotiques est essentiel pour empêcher l'utilisation inappropriée et non ciblée des antibiotiques et de contrôler la crise de la résistance aux antibiotiques. Les auteurs ont développé une approche bon marché, innovante et rapide pour évaluer la sensibilité aux antibiotiques des bactéries en utilisant la photoluminescence (PL) émise lors de la photocorrosion de biopuces GaAs/AlGaAs en puits quantiques (QW). Les biopuces étaient fonctionnalisés avec des

monocouches auto-assemblées de thiols biotinylés de polyéthylène glycol, de neutravidine et d'anticorps biotinylés pour immobiliser les bactéries. L'irradiation d'une biopuce avec le rayonnement au-dessus de la bande interdite conduit à la formation d'oxydes de surface et la dissolution d'une épaisseur limitée du matériau de recouvrement en GaAs (≤10 nm) qui résulte en l'apparition d'un maximum caractéristique dans la PL collectée au fil du temps. La position du maximum PL dépend du taux de la photocorrosion qui, à son tour, dépend de la charge électrique immobilisée à la surface des biopuces GaAs/AlGaAs. Les bactéries capturées à la surface des biopuces retardent l'apparition du maximum PL tandis que la croissance de ces bactéries retarde encore plus le survenu du maximum PL. Pour les bactéries inhibées par les antibiotiques, le maximum PL apparaissait plus rapidement, en comparaison avec les bactéries en croissance. En exposant les bactéries à un bouillon nutritif contenant de la pénicilline ou de la ciprofloxacine, nous avons été en mesure de distinguer les bactéries sensibles et résistantes aux antibiotiques en moins de 3 h, ce qui est beaucoup plus rapide que les méthodes fondées sur la culture. L'émission PL des hétérostructures a été contrôlée avec un lecteur peu coûteux. Cette détermination rapide de la sensibilité des bactéries aux différents antibiotiques pourrait avoir des applications cliniques et de recherche.

CHAPTER 5: Monitoring growth and antibiotic susceptibility of *Escherichia coli* with photoluminescence of GaAs/AlGaAs quantum well microstructures

5.1 Abstract

Development of quick and reliable methods to investigate antibiotic susceptibility of bacteria is vital to prevent inappropriate and untargeted use of antibiotics and control the antibiotic resistance crisis. The authors have developed an innovative, low-cost and rapid approach to evaluate antibiotic susceptibility of bacteria by employing photoluminescence (PL) emission of photocorroding GaAs/AlGaAs quantum well (QW) biochips. The biochips were functionalized with self-assembled monolayers of biotinylated polyethylene glycol thiols, neutravidin and biotinylated antibodies to immobilize bacteria. The illumination of a QW biochip with above bandgap radiation leads to formation of surface oxides and dissolution of a limited thickness of GaAs cap material (≤ 10 nm) that results in the appearance of a characteristic maximum in the PL plot collected over time. The position of the PL maximum depends on the photocorrosion rate which, in turn, depends on the electric charge immobilized on the surface of the GaAs/AlGaAs biochips. Bacteria captured on the surface of biochips retard the PL maximum, while growth of these bacteria further delays the PL maximum. For the bacteria affected by antibiotics a faster occurring PL maximum, compared with growing bacteria, is observed. By exposing bacteria to nutrient broth and penicillin or ciprofloxacin, the authors were able to distinguish *in situ* antibiotic-sensitive and resistant *Escherichia coli* bacteria within less than 3 h, which is considerably more rapid than with culture-based methods. The PL emission of the heterostructures was monitored with an inexpensive reader. This rapid determination of bacterial sensitivity to different antibiotics could have clinical and research applications.

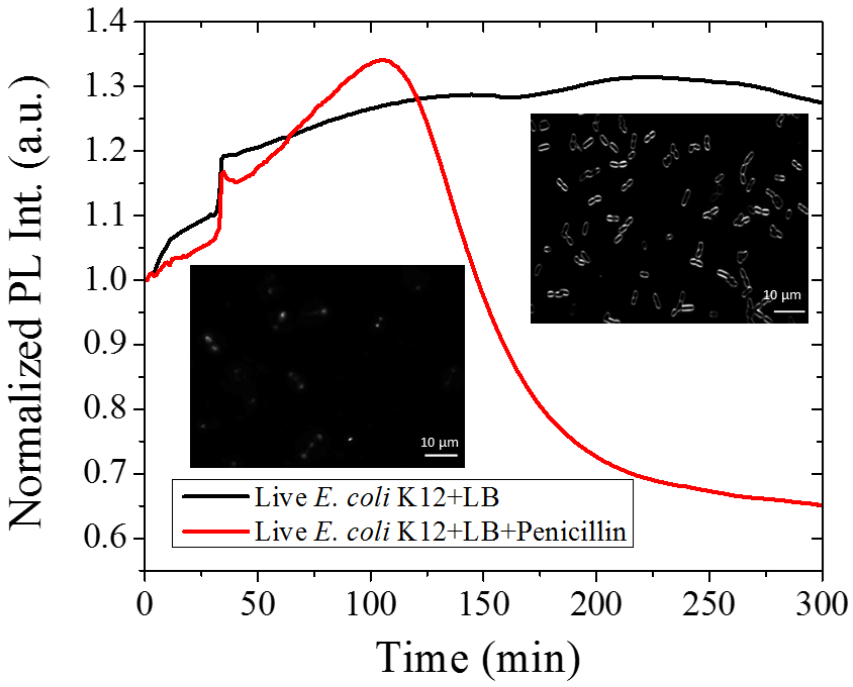

Figure 36. Graphical abstract of the paper on monitoring growth and antibiotic susceptibility of *Escherichia coli* with photoluminescence of GaAs/AlGaAs heterostructures.

5.2 Introduction

Monitoring bacterial growth and reactions to specific environments plays an important role in the fields of medicine, food production, and pharmaceutical research with great importance for small-scale, as well as industrial-scale production of natural or genetically engineered bacterial products such as enzymes or hormones (Garneau and Moineau 2011; Kee et al. 2013; Nayak et al. 2009; Schuler and Marison 2012; Sonnleitner et al. 1992; Versalovic et al. 2011). Antimicrobial resistance has been recognized as a global problem (Gootz 2010) related to inappropriate or untargeted use of antibiotics (Engel 2009; Fleming-Dutra et al. 2016; Kee et al. 2013). Part of the solution lies in effective, rapid and low-cost diagnostic tools to guide optimal use of antibiotics (WHO 2015). Microbiological antibiotic susceptibility tests (AST) help medical personnel predict the reactions of bacteria to specific drugs and allow them to prescribe appropriate treatments (Jorgensen and Ferraro 2009). Conventional techniques such as broth microdilution and Kirby-Bauer disk diffusion tests for AST (Poupard et al. 1994; Versalovic et al. 2011) are analytical diagnostic methods which do not provide same-day results (Chiang et

al. 2009; Kee et al. 2013; Versalovic et al. 2011) nor can they be easily applied outside laboratory settings. The polymerase chain reaction (PCR) can also be applied for investigation of bacterial susceptibility to antibiotics by detecting resistance markers like the *mec*A gene of *Staphylococcus aureus* (Hombach et al. 2010). However, genetic methods require background knowledge of resistance genes (Quach et al. 2016) and they lack standardization (Cockerill 1999). In addition, resistance of bacteria to antibiotics might be related to presence of different genes, while the PCR technique only evaluates the presence of specific genes (Cockerill 1999). An approach based on electrochemical reduction of resazurin, a redox-active molecule, has recently been proposed for evaluation of antibiotic susceptibility of *Escherichia coli* claiming that the results could be delivered in one hour (Besant et al. 2015). Surface plasmon resonance (SPR) and plasmonic nanohole arrays represent other approaches to monitor antibiotic susceptibility of bacteria, with a time-to-result for *E. coli* claimed to be 2 h (Chiang et al. 2009; Kee et al. 2013). However, the cost of sensitive SPR systems (Lazcka et al. 2007) and the demanding fabrication process necessary to make uniform plasmonic nanoholes (Kee et al. 2013) are inhibitory factors restricting application of these techniques to laboratory environments. Clearly, development of a simple, rapid and sensitive method for detection of growth and antibiotic sensitivity of bacteria at low cost remains an attractive but elusive goal for clinical diagnostics, food and water control industries. Photoluminescence (PL) emitting semiconductors have the potential to be applied in the biosensing field due to the sensitivity of the PL signal to reactions taking place at the surface of these materials (Adamowicz et al. 1998; Gfroerer 2006; Lebedev 2001; Moumanis et al. 2006; Tomkiewicz et al. 2009). For instance, Budz et al. (Budz et al. 2010) demonstrated operation of a GaAs-based biosensor for PL detection of adenosine 5′-triphosphate (ATP), and we used a PL-based approach to detect *E. coli* at 10^4 CFU/mL (Duplan et al. 2011). PL spectroscopy has also been employed to characterize photocorrosion of semiconductors, such as laser-induced etching of GaAs (Joshi et al. 2009). Since the photocorrosion of III-V semiconductors is driven by the surface presence of photo-generated holes (Ruberto et al. 1991), electric and/or electrostatic interactions occurring at the semiconductor surface could increase/decrease concentration of photo-generated holes and, consequently, accelerate/delay the photocorrosion process. Based on this approach, we have developed a PL-monitored photocorrosion method for detection of *E. coli*

(Nazemi et al. 2015) and *Legionella pneumophila* (Aziziyan et al. 2016). Furthermore, we have reported that functionalized surfaces of GaAs/AlGaAs biochips remain relatively stable in biological fluids, and provide satisfactory conditions for cultivating *E. coli* (Nazemi et al. 2016). In this report, we discuss the innovative concept of PL monitored photocorrosion of GaAs/AlGaAs biochips for evaluating the growth and susceptibility of bacteria to antibiotics. Using as an example *E. coli* K12 and *E. coli* HB101, we identified the sensitivity of these bacteria to penicillin and ciprofloxacin in less than 3 hours. This approach has a considerable advantage over alternative biosensing techniques due to the application of commercially available GaAs/AlGaAs microstructures, suggesting that related experiments could be realized with low-cost devices.

5.3 Experimental methods

5.3.1 Materials

The biochips were fabricated from an epitaxially grown GaAs/$Al_{0.35}Ga_{0.65}As$ quantum well (QW) wafer (10-413) obtained from Azastra Inc. (Ottawa, Canada). A cross-sectional view of the wafer microstructure is shown in Figure 37a. It comprises 30 pairs of 6 nm thick GaAs QWs and 10 nm thick $Al_{0.35}Ga_{0.65}As$ barriers grown on a 500 nm thick buffer layer of GaAs that was deposited on a semi-insulating GaAs (001) substrate. The QW architecture is capped with a 10 nm thick GaAs layer. The irradiation of such a microstructure with above bandgap radiation, such as that of a 532 nm laser, induces a PL signal dominated by the QW emission at 829 nm, as shown in Figure 37b.

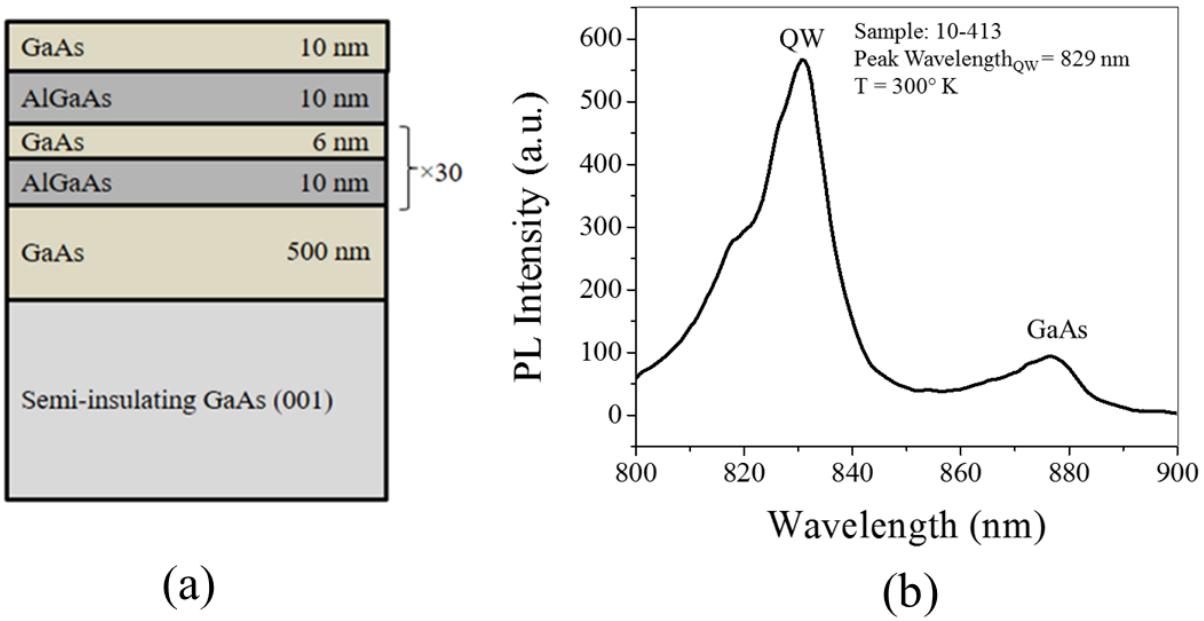

Figure 37. Cross-section of the GaAs/AlGaAs QW microstructure employed for the fabrication of biochips (a), and an example of the PL emission observed at RT from the microstructure irradiated with a 532 nm laser (b).

The solvents used for cleaning the QW wafers were OptiClear, acetone and isopropanol (2-propanol) which were purchased from National Diagnostics (Mississauga, Canada), ACP (Montréal, Canada) and Fisher Scientific (Ottawa, Canada), respectively. Anhydrous ethanol was obtained from Commercial Alcohols Inc. (Brampton, Canada). Ammonium hydroxide (NH_4OH) from Anachemia (Richmond, Canada) was employed to remove oxides from the surface of the wafers. Deionized (DI) water with an electrical resistivity of 18 MΩ.cm was obtained through a domestic purification system connected to the city water supply. Ultra-high purity nitrogen 5.0 UHP (99.999%) used for deoxygenation of anhydrous ethanol, and high purity nitrogen 4.8 HP (99.998%) used for drying the chips were both purchased from Praxair Canada Inc. (Mississauga, Canada). Hexadecane thiol (HDT) and biotinylated polyethylene glycol (PEG) thiol were bought from Sigma-Aldrich (Oakville, Canada) and Prochimia Surfaces (Gdansk, Poland), respectively. A 48% aqueous solution of ammonium sulfide (AS) was obtained from Sigma-Aldrich (Oakville, Canada). Phosphate buffered saline (PBS) solution (10X, pH 7.4) and polyclonal biotinylated antibodies (Ab) against *E. coli* were purchased from Sigma (Oakville, Canada) and ViroStat, Inc (Portland, ME), respectively. Neutravidin (NA) was bought from Molecular Probes (Invitrogen, Burlington, Canada). Penicillin, ciprofloxacin and

Luria Bertani (LB) medium were purchased from Sigma-Aldrich (Oakville, Canada). Live *E. coli* K12 and *E. coli* HB101 bacteria were obtained from the Department of Biology, Université de Sherbrooke (Quebec, Canada). The bacteria were grown in LB broth and kept overnight at 37° C before starting experiments.

5.3.2 Biofunctionalization of the GaAs/AlGaAs biochips

Chips of 2 mm × 2 mm were separated from the QW wafer and cleaned in an ultrasonic bath sequentially in acetone, OptiClear, acetone, and isopropanol for 5 min each. Thereafter, the chips were dried with compressed high-purity nitrogen and etched in NH_4OH (28%) for 2 min at room temperature to remove native surface oxides. Following this step, the freshly etched chips were rinsed with deoxygenated anhydrous ethanol and immersed for 20 h in 0.13 mM biotinylated PEG thiol and 1.87 mM HDT in deoxygenated anhydrous ethanol. After the thiolation step, the biochips were exposed to AS 0.1% for 15 min and rinsed with deionized (DI) water. Following this step, the samples were incubated for 2 h in NA dissolved in PBS (1X) at 0.2 mg/mL. The preparation process continued by exposure of the NA-coated biochips to 0.1 mg/mL of biotinylated polyclonal *E. coli* antibodies for 1 h at room temperature. Previously, this architecture had been successfully used by us for detection of *E. coli* bacteria (Nazemi et al. 2015).

5.3.3 Methodology of monitoring bacterial growth and their reactions to antibiotics

We investigated growth and antibiotic susceptibility of two strains of *E. coli* bacteria, *E. coli* K12 (penicillin-sensitive) and *E. coli* HB101 (penicillin-resistant). Freshly cultured bacteria were employed to reduce the lag phase and to be able to monitor antibiotic susceptibility in less than 3 h. The procedure to prepare freshly cultured bacteria is described in Supporting Information.

To monitor bacterial growth, Ab-coated biochips were placed in an ULTEM^{TM} flow cell and exposed to 1 mL of freshly cultured bacteria at 2×10^8 CFU/mL that was injected into the flow cell at a flow rate of 0.1 mL/min. The biochips were then incubated for an additional 20 min to

allow capture of bacteria on the surface of the biochips. It was assumed that 30 min was sufficient to achieve this goal as suggested by reports of antigen-antibody binding reactions (Hlady et al. 1990). Thereafter, LB broth was injected into the flow cell for 30 min (with flow rate of 0.1 mL/min) and the biochips were incubated in LB at room temperature for an additional 4 h without any further injection to allow the bacteria to grow. The photocorrosion process was investigated *in situ* using a custom designed quantum semiconductor photonic biosensor (QSPB) reader (Aziziyan et al. 2016) capable of rapidly collecting PL maps of 2 mm × 2 mm biochips excited with a light-emitting diode (LED) operating near 660 nm, i.e., delivering the above QW bandgap (829 nm) radiation. The QSPB reader employed a long pass filter with a transmission wavelength threshold at near 820 nm and a CCD camera to record the PL signals. The biochips were irradiated with 6 s pulses, 35 mW/cm^2 each, delivered in every 60 s period with the help of a computer-programmed shutter. The 829 nm PL emission of photocorroding biochips was recorded for up to 5 h. This procedure is neither technically complicated nor expensive. The cost of a QSPB reader is less than $3k, which in comparison to traditional optical systems for detection of bacteria, such as those based on Raman spectroscopy (Wu et al. 2016) offers an economically attractive approach. The necessary apparatus occupies a footprint of less than 30 cm × 30 cm.

As a reference experiment, one series of the Ab-coated samples were exposed to 1 mL of UV-killed bacteria (the preparation procedure of UV-killed bacteria is explained in Supporting Information) at 2×10^8 cell/mL in the same way that live bacteria had been tested. The susceptibility of the bacteria to penicillin G at 50 μg/mL, or ciprofloxacin at 10 μg/mL, was investigated by adding antibiotic solutions to fresh LB, following the initial 30 min exposure of the biochips to LB. The antibiotic solutions were injected into the flow cell for 15 min at a flow rate of 0.1 mL/min and the biochips were incubated in antibiotics for an additional 225 min without any further injection. To study the effect of penicillin and ciprofloxacin on PL emission of the biochips, we compared the PL plots collected from Ab functionalized biochips exposed for 30 min to PBS (1X) and 4.5 h to LB, with the PL plots of the biochips exposed for 30 min to PBS (1X), 30 min to LB and 4 h to either penicillin or ciprofloxacin in LB solutions. These antibiotics have different mechanisms of bacteria-antibiotic interaction. Penicillin inhibits cell wall synthesis of bacteria (Yocum et al. 1980), which could result in bacterial lysis or

detachment from the surface, whereas ciprofloxacin inhibits DNA synthesis and might not affect the bacterial surface proteins that are involved in capture or cause lysis (LeBel 1988).

A schematic illustration of the experimental setup is presented in Figure 38. The setup consists of the flow cell for holding the biochips, the peristaltic pump, and the QSPB reader for collecting PL of photocorroding biochips. All the experiments have been carried out at ambient temperature and repeated at least three times to provide average value and standard deviation. After finishing the PL-monitored photocorrosion experiments, the biochips were analyzed with an optical microscope (Zeiss, Axiotech) to detect changes in bacterial cell shape and biochip surface coverage (see Supporting Information for details).

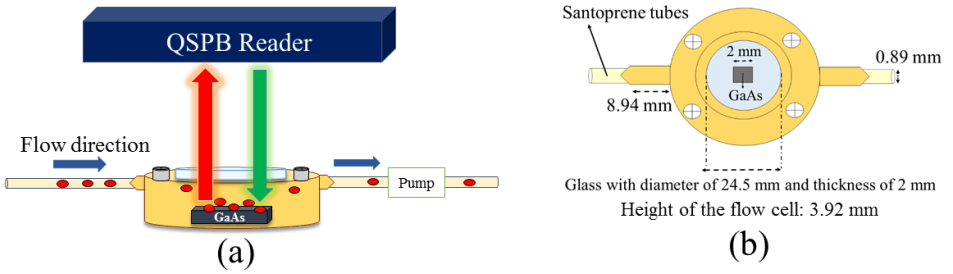

	30 min	4. 5 h
Live bacteria+LB	Live bacteria	LB
UV-treated bacteria+LB	UV-treated bacteria	LB
PBS+LB	PBS	LB

	30 min	30 min	4 h
Live bacteria+LB +Antibiotic	Live bacteria	LB	Penicillin or Ciprofloxacin solution
PBS+LB+ Antibiotic	PBS	LB	Penicillin or Ciprofloxacin solution

(c)

Figure 38. Schematic illustration of the experimental setup (a), top view of the flow cell (b), and time required for different steps of the experiment (c). The biofunctionalized biochips were kept in the flow cell and exposed to bacterial suspension (red ovals) and LB with or without antibiotics while their PL was recorded during the experiment.

5.4 Results and discussion

5.4.1 Photonic monitoring of growth and reaction of *E. coli* K12 to antibiotics

An example of normalized time-dependent PL intensity plots from biochips exposed to penicillin-sensitive live and UV-killed *E. coli* K12 bacteria during incubation in LB without

antibiotics, or with penicillin, or ciprofloxacin is shown in Figure 39. The formation of characteristic maxima in these plots is related to the growth of surface oxides and photocorrosion of the 10 nm thick GaAs cap layer (Nazemi et al. 2015). It can be seen that the maximum of the PL plot from the biochip exposed to live *E. coli* K12 bacteria and LB medium has been delayed to near 240 min, while remaining plots exhibit maxima at less than 180 min. Furthermore, the PL maxima from the biochips exposed to bacteria and antibiotic solutions occurred earlier than those induced by UV-killed bacteria. The average position of the PL maxima for the biochips exposed to live *E. coli* K12 bacteria and LB has been determined at 231 min ±4.9%, UV-killed *E. coli* K12 bacteria and LB at 160 min ±3.5%, live *E. coli* K12 bacteria, LB and ciprofloxacin at 113 min ±8.8% and live *E. coli* K12 bacteria, LB and penicillin at 107 min ±2.6%. Moreover, the average number of bacteria immobilized on the surface of the biochips exposed to live bacteria and LB increased from 929 ±133 bacteria/mm^2 to 3436 ±244 bacteria/mm^2, while this number for UV-killed bacteria was 885 ±168 bacteria/mm^2. In the case of exposure to penicillin and ciprofloxacin, the average number of bacteria immobilized on the surface was 169 ±64 bacteria/mm^2 and 786 ±177 bacteria/mm^2, respectively (see Supporting Information for examples of optical images**)**.

The position of the PL maxima for the biochips without bacteria, but exposed to PBS, LB and penicillin has been determined at 101 min ±4.2%, to PBS, LB and ciprofloxacin at 94 min ±9%, while exposed to PBS and LB has been determined at 83.5 min ±5.9%. Comparable positions of the PL maxima for the biochips exposed to PBS and LB with those of the biochips exposed to PBS, LB and penicillin or ciprofloxacin solutions, suggests that the presence of the investigated antibiotics does not affect the photocorrosion of the GaAs/AlGaAs biochips. This behaviour has been verified also for penicillin and ciprofloxacin solutions at 1 mg/mL.

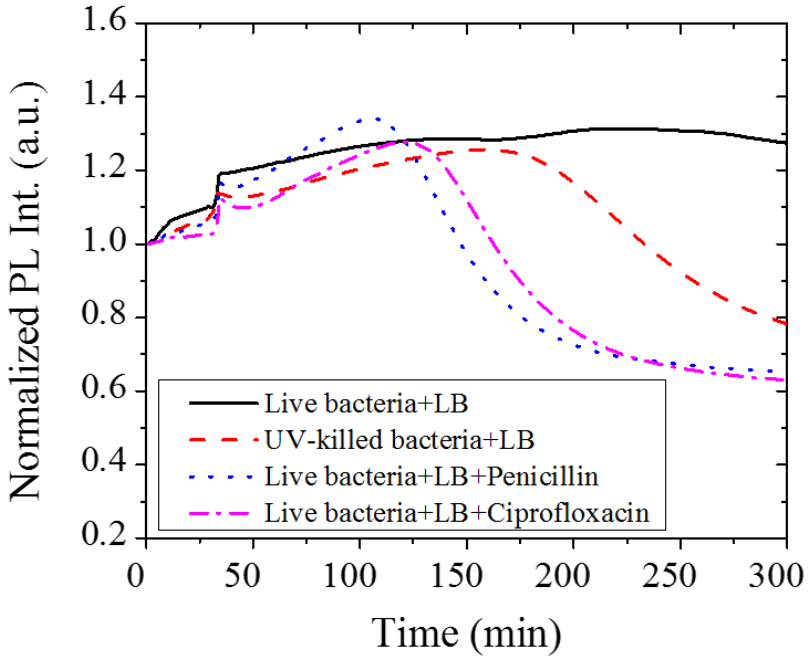

Figure 39. Examples of normalized PL intensity measured *in situ* for biochips exposed to penicillin-sensitive live *E. coli* K12 bacteria and LB (solid line), UV-killed *E. coli* K12 bacteria and LB (dashed line), live *E. coli* K12 bacteria, LB and penicillin (dotted line), and live *E. coli* K12 bacteria, LB and ciprofloxacin (dashed-dotted line).

5.4.2 Photonic monitoring of growth and reaction of *E. coli* HB101 to antibiotics

Figure 40 shows an example of normalized time-dependent PL plots of the biochips exposed to penicillin-resistant live *E. coli* HB101 bacteria and LB medium with or without antibiotics (data shown only for 250 min), as described in Sec. 5.3.3. The *E. coli* HB101 bacteria used in this study have the ability to secrete penicillinase enzyme to hydrolyze the penicillin structure which makes them penicillin-resistant (Dever and Dermody 1991). Therefore, the presence of penicillin should not interfere with bacterial growth, as indicated by the almost identically located PL maxima produced by HB101 bacteria exposed to LB (solid line in Figure 40) and to LB and penicillin solution (dotted line). Since *E. coli* HB101 are sensitive to ciprofloxacin, the PL maximum occurred earlier when the bacterial solution was exposed to ciprofloxacin, and is consistent with the inhibition of bacterial growth (dashed-dotted line). According to Figure 40, the maximum of the PL plot from the biochip exposed to live *E. coli* HB101 bacteria and LB

with or without penicillin has been delayed to near 160 min, while the PL plot from the biochip exposed to bacteria and ciprofloxacin exhibits maximum at less than 120 min. The position of the PL maxima for the biochips exposed to live *E. coli* HB101 bacteria and LB was at 155 min ±4.6%, live *E. coli* HB101 bacteria, LB and penicillin at 147 min ±3.8% and live *E. coli* HB101 bacteria, LB and ciprofloxacin at 111 min ±7.6%. The exposure to LB without and with penicillin resulted in this case in the average number of bacteria immobilized on the surface of the biochips increased from 821 ±96 bacteria/mm^2 to 2843±203 bacteria/mm^2 and 2605±163 bacteria/mm^2, respectively, while this number decreased to 739±190 bacteria/mm^2 when the biochips were exposed to bacteria and ciprofloxacin (see Supporting Information for examples of optical microscopy images).

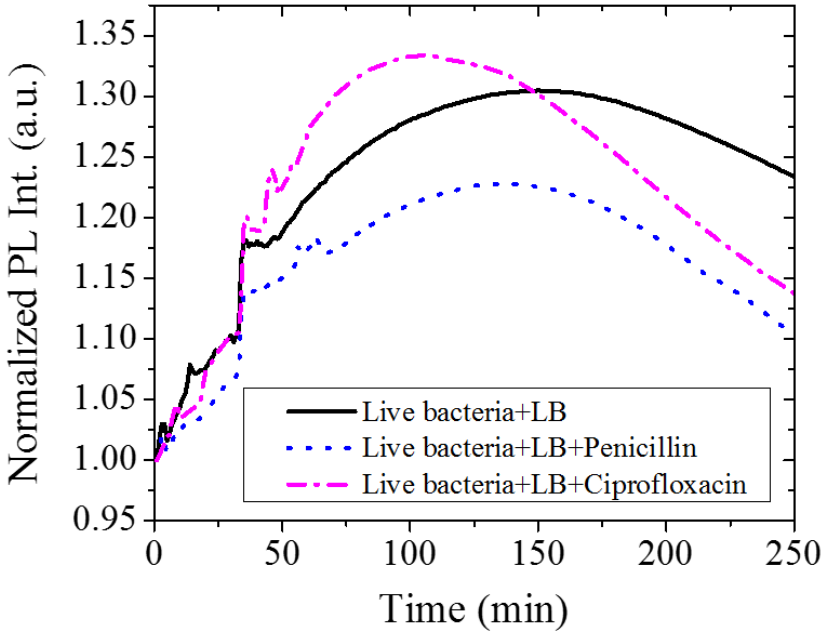

Figure 40. Examples of normalized PL intensity measured *in situ* for biochips exposed to penicillin resistant, ciprofloxacin sensitive *E. coli* HB101 bacteria and LB (solid line), live *E. coli* HB101 bacteria, LB and penicillin (dotted line), and live *E. coli* HB101 bacteria, LB and ciprofloxacin (dashed-dotted line).

In Figure 41, we summarize the positions of the PL maxima for the biochips exposed to live *E. coli* K12 or *E. coli* HB101 and LB with or without antibiotics. The comparable position of the PL maxima for the biochips exposed to *E. coli* HB101 and LB with those exposed to *E. coli* HB101, LB and penicillin is consistent with the resistance of these bacteria to penicillin. In the

case of exposure of the biochips to *E. coli* K12, LB and penicillin, we observed PL maxima sooner in comparison with the *E. coli* K12 growth control tests, which showed the sensitivity of these bacteria to penicillin. The advance in the position of the PL maxima for the biochips exposed to *E. coli* K12 or *E. coli* HB101, LB and ciprofloxacin in comparison with growth control tests demonstrates the sensitivity of both bacteria to ciprofloxacin.

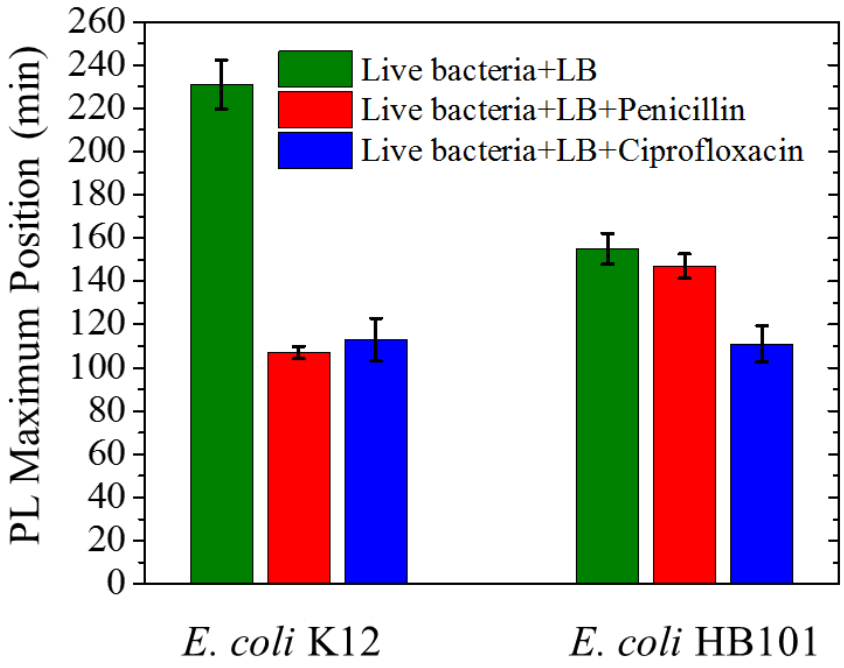

Figure 41. PL maxima positions observed for Ab-coated biochips exposed to penicillin-sensitive *E. coli* K12 or penicillin-resistant *E. coli* HB101 and LB without or with antibiotics.

5.4.3 Effect of photoelectrochemical reactions on PL of GaAs/AlGaAs biochips

The dynamics of temporal PL plots shown in Figure 39 and Figure 40 depends on the power of the 660 nm LED employed for excitation of the biochips, duration of the pulse, and the time allowed between the pulses for the product of photocorrosion to dissipate in the solution. Under the conditions of the current experiment, the built-in electric field in the depletion region of the semiconductor separates photo-excited electrons (e) and holes (h^+). The electric field driven h^+ arriving to the semiconductor surface will induce the corrosion of this material through the transient formation and dissolution of surface oxides dominated by Ga_2O_3 (Choi et al. 2002;

Ruberto et al. 1991). It is the formation of Ga_2O_3 that reduces the density of surface states and decreases the surface recombination velocity of e - h^+, leading to the increased intensity of the PL signal emitted by GaAs surrounded by an aqueous solution (Passlack et al. 1995). As the surface oxides are dissolved into solution and GaAs photocorrodes, a new interface with AlGaAs is formed. This results in a quickly decreasing QW PL signal and formation of a maximum of the temporally dependent PL signal. The formation of this maximum could be accelerated or delayed depending on the electrostatic interaction between the semiconductor and molecules immobilized in its vicinity. For instance, the immobilization of electron donor molecules on the surface of an n-type GaAs (GaAs investigated in this work behaves at room-temperature as an n-type material) will decrease band bending and depletion width of this material (Zhang and Yates 2012), which would result in a decreased concentration of photo-excited h^+ arriving to its surface and, consequently, a delayed photocorrosion process.

The surface of most bacteria at pH greater than 4 is negatively charged, primarily due to the excessive concentration of phosphate and carboxyl groups in comparison to their amino groups (Poortinga et al. 2002). Thus, bacteria suspended in a PBS solution could become decorated with positively charged counter ions present in the solution. The close proximity interaction of these counter ions with the surface of a GaAs/AlGaAs biochip could affect (reduce) transport of photo-excited holes to the semiconductor surface, resulting in a decreased photocorrosion rate of the biochip (delayed formation of the characteristic PL maximum). This characteristic of photocorroding GaAs/AlGaAs nano-heterostructures has been previously explored by us for detection of bacteria tethered to Ab-coated biochips. The dependence of the position of PL maxima vs. different concentrations of bacteria has also been demonstrated in the form of calibration curves (Aziziyan et al. 2016; Nazemi et al. 2015). While immobilization of bacteria could be responsible for electrostatic repulsion of photo-excited h^+ from the surface of the investigated GaAs/AlGaAs microstructures, the growth of these bacteria would further amplify this effect and slow down the photocorrosion rate. The result would be a delayed position of the PL maximum. An alternative mechanism of the biochip interaction with bacteria could involve electric charge transfer, such as that observed between bacteria and indium tin oxide coated glass plates (Poortinga et al. 1999). It is possible that secretion of H^+ ions to create a chemiosmotic or proton motive force associated with bacterial metabolism (Mitchell 2011)

could reduce photocorrosion as the presence of H^+ ions in the vicinity of the biosensor surface could reduce the transport of photo-excited h^+ towards the surface through the electrostatic interaction.

The exposure of Ab-functionalized biochips to UV-killed *E. coli* K12 and LB broth produced PL maximum at t ~180 min (Figure 39), which is delayed in comparison to that corresponding for the penicillin or ciprofloxacin-treated bacteria, but consistent with the much delayed maximum (~ 250 min) observed for the case of growing bacteria. The more rapidly occurring PL maxima for the biochips exposed to *E. coli* K12 and antibiotics, either penicillin or ciprofloxacin, compared with those exposed to UV-killed bacteria might be related to the drastically decreased zeta potential of these bacteria after antibiotic treatment (data not shown), consistent with the literature data concerning effect of different antimicrobial agents on reduction of zeta potential of bacteria (Alves et al. 2010; Nomura et al. 1995). In contrast, we have not observed a significant effect of UV treatment on decreasing the zeta potential of *E. coli* K12 (M. R. Aziziyan, private communication).

The exposure of Ab-functionalized biochips to penicillin-resistant live *E. coli* HB101 bacteria and LB with or without penicillin produced PL maxima coinciding with each other (Figure 40). In contrast, the exposure to ciprofloxacin inhibited the bacterial growth, which resulted in a slightly accelerated photocorrosion (faster occurring PL maximum). Generally, the position of the PL maxima for the biochips exposed to *E. coli* HB101 and LB occurs earlier in comparison to that induced with *E. coli* K12 and LB. This result seems consistent with the weaker zeta potential of *E. coli* HB101 bacteria in 1X PBS (-18 mV) in comparison to that of *E. coli* K12 (-30 mV). Since photocorrosion of the biochips depends on the electrical charge of bacteria, the greater zeta potential of bacteria indicates stronger electrostatic interaction with the biochip and results in a much delayed PL maximum.

For bacterial concentrations lower than 2×10^8 CFU/mL, for which around 800-900 bacteria/mm^2 were observed immobilized on the biochip surface (see Supporting Information), we were not able to monitor bacterial growth. The likely reason for this behaviour is a poisonous effect of As and Ga ions released by the photocorroding biochip to the flow cell, which could affect the viability of bacteria (Harvey and Crundwell 1996; Podol'skaia et al. 2002; Tanaka

2004). We note that a non-irradiated GaAs substrate could support the growth of *E. coli* K12 at concentrations as low as 10^5 CFU/mL (Nazemi et al., 2016). This suggests that under optimized conditions the PL-based monitoring of bacterial reaction to antibiotics should be possible for suspensions with bacteria diluted to less than 2×10^8 CFU/mL.

All the experiments reported here were carried out at ambient temperature, however, it might be possible to operate the biosensor at 37º C. Due to the higher growth rates at 37º C, it is expected that the results of the antibiotic sensitivity of bacteria could then be delivered in a shorter period of time. Our present results were obtained, each time, with a freshly fabricated biochip. During a 5 h long biosensing run, photocorrosion consumed the entire 10 nm thick GaAs cap and, partially at least, the 10 nm thick $Al_{0.35}Ga_{0.65}As$ layer. This left 30 pairs of GaAs/$Al_{0.35}Ga_{0.65}As$ heterostructures (see Figure 37) that, potentially, could be used for other biosensing runs. The advancement of this concept would additionally increase the commercial value of a proposed biosensor, although such an approach exceeds the scope of the research reported in this document.

5.5 Conclusions

We have investigated an innovative method of monitoring growth and reaction of bacteria to antibiotics using PL emission of photocorroding GaAs/AlGaAs QW heterostructures. The method takes advantage of the sensitivity of the photocorrosion effect to the perturbation of the electric field induced by electrically charged bacteria immobilized in the vicinity of a biosensor surface. By monitoring the formation of PL maxima of biofunctionalized GaAs/AlGaAs biochips exposed to different bacterial solutions and antibiotics, we have demonstrated the functionality of this process for monitoring the growth and antibiotic sensitivity of *E. coli* K12 (penicillin-sensitive) and *E. coli* HB101 (penicillin-resistant) bacteria at ambient temperature in less than 3 h. The functionalization of the biochips with antibodies makes the process suitable for specific investigation of different bacteria, although it could also be applied for studying bacteria captured non-specifically, e.g., through covalent binding (Meyer et al. 2010; Nazemi et al. 2016). The reduction in time-to-result can be considered as the main advantage of this method over culture-based techniques, while a relatively simple functionalization process, the

potential for automation of all the steps of the experiment and low-cost of the analysis seem to be attractive for developing clinical diagnostic applications. The method could lead to a significant progress in the pharmaceutical field and help medical personnel to rapidly identify suitable drugs for treating bacterial infections.

5.6 Acknowledgments

This research was supported by the Canada Research Chair in Quantum Semiconductors Program and the Fonds de recherche Nature et Technologie du Québec (FRQNT) project No 2015-PR-184056. The help provided by Dr. Kh. Moumanis (for measuring PL spectral maps of GaAs/AlGaAs samples), M. R. Aziziyan (for zeta potential measurements of bacteria) and technical staff of the Interdisciplinary Institute for Technological Innovation (3IT) are greatly appreciated. We also thank Prof. François Malouin of the Department of Biology, Université de Sherbrooke for kindly supplying *E. coli* K12 and HB101 bacteria.

5.7 Supporting information

5.7.1 Preparation of freshly cultured bacteria

E. coli K12 and *E. coli* HB101 were grown in LB and LB containing penicillin, respectively, and incubated overnight at 37° C before use the following morning in experiments. On the day of the experiments, the bacterial concentration ($N_{bacteria}$) was measured with a cell density meter (Fisher Scientific, model 40) operating at 600 nm. The concentration of the bacterial suspension was estimated using the following formula (Hassen et al. 2016):

$$N_{bacteria} = 10^9 \times R \tag{5.1}$$

where R is the readout of the cell density meter. The bacteria were centrifuged for 25 min at 3000 rpm in LB medium. After that, the medium was removed and the pellets were suspended in PBS (1X) and centrifuged at 3000 rpm for an addition 15 min. Finally, the PBS (1X) was removed and the pellets were resuspended in PBS (1X) at 2×10^8 CFU/mL.

5.7.2 Preparation of UV Killed *E. coli* K12 bacteria

The *E. coli* K12 bacteria were exposed for 2 min to UV light delivering 100 mW/cm^2 radiation of which 95 % was located in the 250-260 nm region. The efficiency of this process to kill all of the *E. coli* bacteria was verified by culture tests (data not shown), showing complete killing consistent with literature reports (Vermeulen et al. 2008).

5.7.3 Optical microscopy of bacteria immobilized on the biochip surface

After finishing the PL measurements, the biochips were analyzed with an optical microscope (Zeiss, Axiotech) operating in a differential interference contrast mode with overhead illumination. This allowed counting bacteria as well as detecting changes in bacterial cell shape. Optical microscopy was also carried out after 30 min exposure of the biochips to bacterial suspension to investigate the initial coverage of the samples with bacteria. No staining or washing was applied before observation of the biochips with the optical microscope. Our intention was to count all the bacteria, so we did not want to wash away the bacteria that were loosely bound to the surface. The biochips were removed from the flow cell and placed on glass slides with the surface that had been exposed to bacteria facing up. The surface coverage of each sample with bacteria was calculated based on analyzing several optical images at total magnification of 500X (each image with a surface area of ~14000 μm^2 per field) and 1000X (each image with a surface area of ~3500 μm^2 per field) collected at 15 or more different sites for the sample and reported per mm^2.

5.7.3.1 Optical microscopy of *E. coli* K12 bacteria immobilized on the biochip surface

Examples of optical images taken after 30 min exposure of the Ab functionalized biochip surfaces to live *E. coli* K12 bacteria, and after an additional 4.5 h exposure in LB broth are shown in Figure 42a and b, respectively, while Figure 42c shows an example of an optical image taken after an Ab functionalized biochip was exposed for 30 min to UV killed *E. coli* K12, followed by a 4.5 h exposure in LB broth. Comparing Figure 42a and Figure 42c reveals that following exposure of *E. coli* K12 to UV light, the shape of the bacteria remained relatively unchanged and little bacterial debris were observed, in agreement with literature data (Challice

and Gorrill 1954). The bacteria initially covered the surface of the biochip with an average density of 929 ±133 bacteria/mm^2. After incubation of the biochip in LB broth for 4.5 h, the average number of bacteria increased to 3436 ±244 bacteria/mm^2. For Ab functionalized GaAs exposed to UV treated bacteria and LB broth, the number of immobilized bacteria was 885 ±168 bacteria/mm^2, which is comparable to the initial coverage and consistent with the expected lack of bacterial growth. When antibiotics were added to the LB medium, the number of immobilized *E. coli* K12 decreased from 929 ±133 to 169 ±64 bacteria/mm^2 for penicillin G, and to 786 ±177 bacteria/mm^2 for ciprofloxacin, as exemplified by Figure 43a and b, respectively. Schematically, the capture, growth and penicillin sensitivity of bacteria on the biosensor surface functionalized with HDT and biotinylated PEG thiols, NA and biotin conjugated antibodies are illustrated in Figure 44. The lower number of bacteria on the biochips exposed to penicillin compared with that on the biochips exposed to ciprofloxacin is likely related to different mechanisms of bacteria-antibiotic interaction. Penicillin inhibits cell wall synthesis of bacteria (Yocum et al. 1980), which could result in bacterial lysis or detachment from the surface, whereas ciprofloxacin inhibits the DNA synthesis and might not affect the bacterial surface proteins that are involved in capture or cause lysis (LeBel 1988).

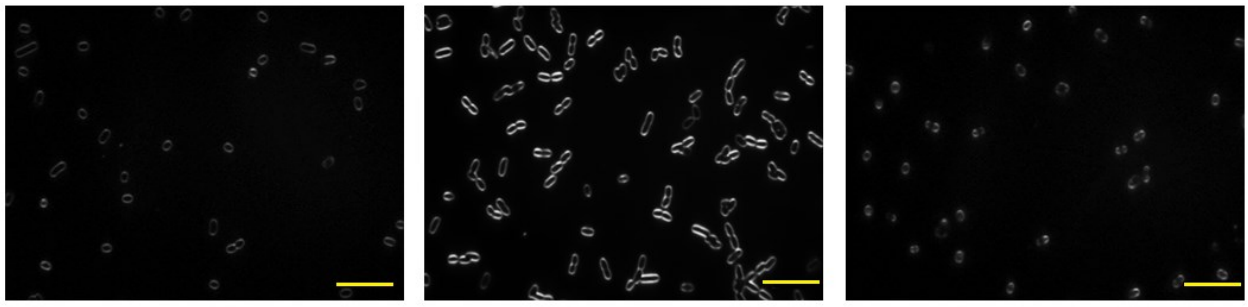

Figure 42. Examples of optical images of *E. coli* K12 immobilized on the biochip surface exposed to live bacteria for 30 min (a), followed by 4.5 h exposure in LB broth (b), and after exposure of the biochip to UV killed bacteria for 30 min, followed by 4.5 h exposure in LB broth (c). The scale bars correspond to 10 µm.

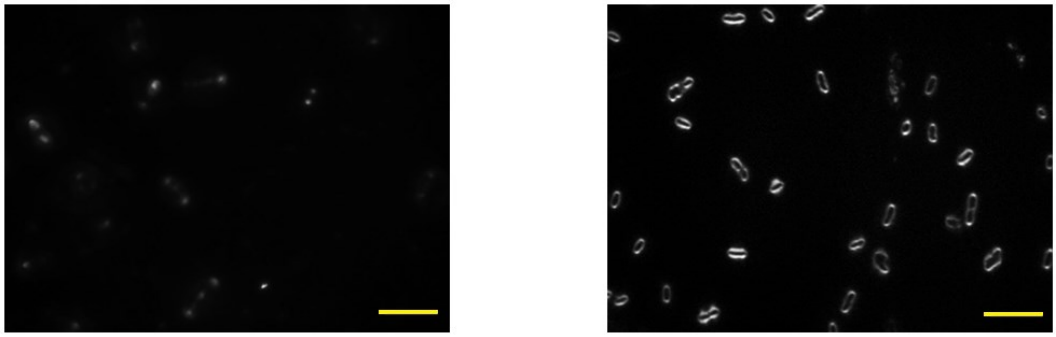

Figure 43. Examples of optical images of *E. coli* K12 immobilized on the biochip surface exposed to live bacteria for 30 min, followed by 30 min exposure in LB and 4 h in LB broth with penicillin at 50 µg/ml (a), and in LB broth where penicillin was replaced with ciprofloxacin at 10 µg/ml (b). The scale bars correspond to 10 µm.

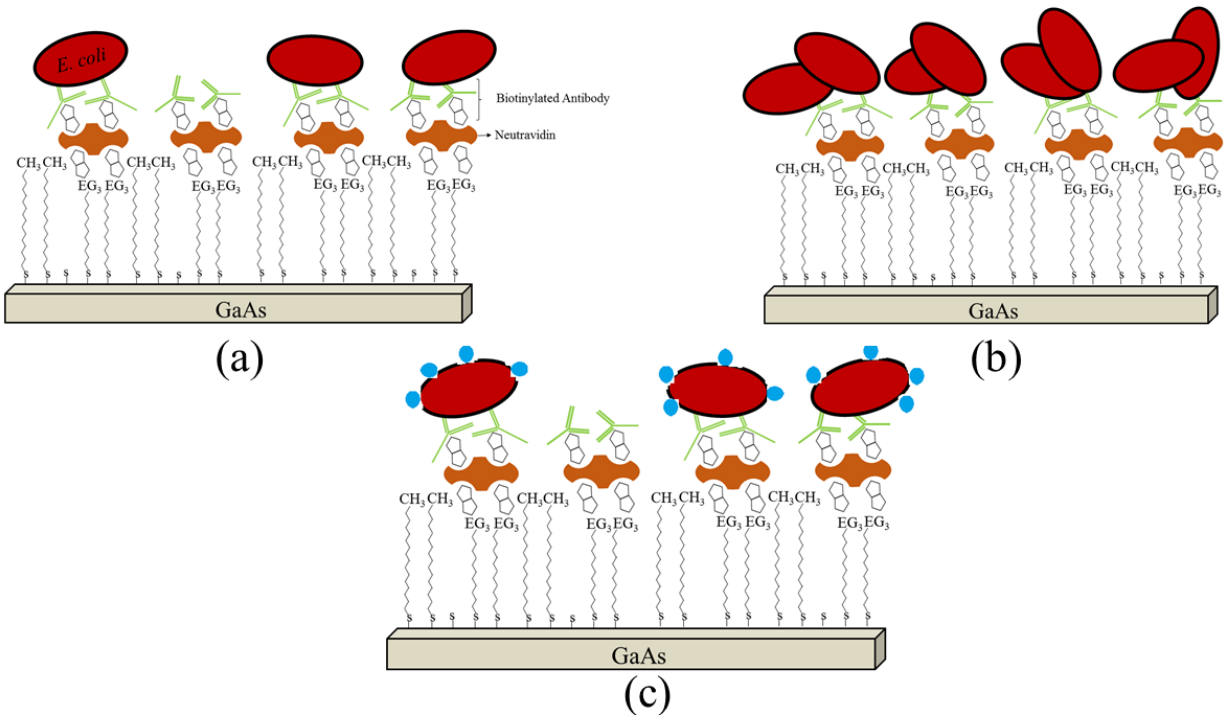

Figure 44. Schematic illustration of the biosensor surface functionalized with PEG SAM, NA and biotin conjugated antibodies employed to tether live bacteria (a), induce growth in the LB broth medium (b), and study the effect of penicillin on the bacteria (c). The blue dots and broken lines around the bacteria in (c) represent the penicillin and the effect of this antibiotic on rupture of bacterial cell walls, respectively.

5.7.3.2 Optical microscopy of *E. coli* HB101 immobilized on the biochip surface

Figure 45 shows examples of optical images taken after exposure of the biochip to live *E. coli* HB101. A 30 min exposure results in surface coverage of the biochip with an average of 821 ±96 bacteria/mm^2 (Figure 45a). After 4.5 h incubation of such a biochip in LB broth, the average density of bacteria increased to 2843±203 bacteria/mm^2 (Figure 45b). Since these bacteria have been genetically modified to be resistant to penicillin (have a plasmid encoding for β-lactamase, also called penicillinase), the exposure of the biochip to a solution of bacteria with penicillin have allowed their growth and the average density of bacteria immobilized on the surface increased to 2605±163 bacteria/mm^2 (see Figure 45c). The exposure of the biochip to a ciprofloxacin solution, however, resulted in inhibition of the bacterial growth and the number of bacteria immobilized on the surface remained constant at about 739±190 bacteria/mm^2 (see Figure 45d).

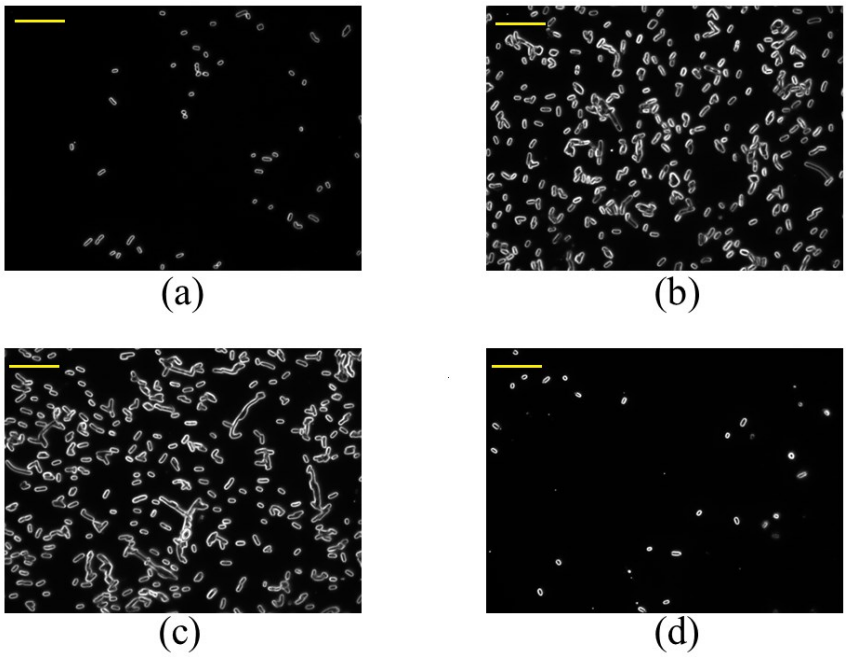

Figure 45. Examples of optical images of *E. coli* HB101 immobilized on the biochip surface exposed for 30 min to live bacteria (a), exposed for 30 min to live bacteria and 4.5 h in LB broth (b), exposed for 30 min to live bacteria followed by 30 min in LB broth and 4 h in LB broth with penicillin at 50 μg/ml (c), and after exposure for 30 min to live bacteria followed by 30 min in LB broth and then 4 h in LB broth with ciprofloxacin at 10 μg/ml (d). The scale bars correspond to 20 μm.

Chapter 6: Complementary experimental results

In this chapter, we discuss photocorrosion of semiconductors and mechanisms of bacterial interactions with semiconductor surfaces. We also present related data that complement the results discussed in Chapters 3-5.

6.1 Mechanism of interaction of bacteria with semiconductor surfaces

When a semiconductor is brought into contact with an electrolyte, there would be a transient charge transfer across the semiconductor/electrolyte interface due to the difference between work function of the semiconductor and electrolyte. The charge transfer causes band bending at the surface of the semiconductor and continues until the Fermi level of the semiconductor and the redox potential of the electrolyte become equal. The band bending is upward in n-type and downward in p-type semiconductors (Rajeshwar 2002). The built-in electric field in the SCR of the semiconductor separates photo-excited electrons (e) and holes (h^+), resulting in a reduced radiative recombination of e-h^+ pairs and, consequently, reduced PL intensity of the semiconductor. For n-type semiconductors the build-in electric field drives holes towards the surface and electrons towards the bulk (Yu and Cardona 2010). The influence of the built-in electric field extends to the electrolyte and causes formation of the Helmholtz layer (stern layer) at the semiconductor/electrolyte interface. The Helmholtz layer consists of the inner Helmholtz layer (IHL) and the outer Helmholtz layer (OHL). The IHL is formed by the ions which are strongly adsorbed to the surface of the semiconductor and the OHL consists of the ions which are bound to the IHL. The diffuse layer is formed by the ions which are loosely bound to the OHL (van de Krol 2011). Figure 46 schematically illustrates the formation of Helmholtz and diffuse layers at the n-type semiconductor/electrolyte interface.

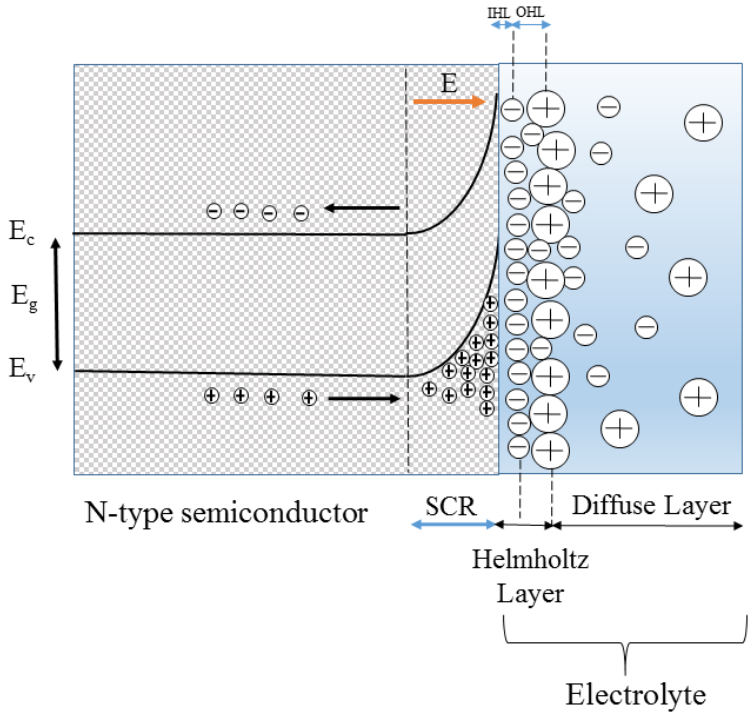

Figure 46. Schematic illustration of formation of Helmholtz (Stern) and diffuse layers at the n-type semiconductor/electrolyte interface. The Helmholtz layer consists of the inner Helmholtz layer (IHL) and the outer Helmholtz layer (OHL). In the figure ⊖ represents the photo-excited electron, ⊕ shows the photo-excited hole, ⊕ and ⊖ show the positively-charged and negatively-charged counter ions, respectively, and E represents the built-in electric field.

Immersion of the semiconductor in the electrolytic solution leads to the corrosion of this material. The corrosion is induced by the holes arriving to the surface of the semiconductor and happens through the transient formation and dissolution of surface oxides. For instance, the corrosion of GaAs in aqueous solutions is described by the following formula (Ruberto et al. 1991),

$$GaAs + 2H_2O + 6h^+ \rightarrow Ga^{3+} + HAsO_2 + 3H^+ \qquad (6.1)$$

Since in n-type semiconductors the built-in electric field drives holes towards the surface, the corrosion process could be photoactivated for these materials. Irradiation of an n-type semiconductor with photons of energy exceeding the bandgap of the semiconductor results in increase of the number of holes arriving to the surface and, consequently, accelerates the corrosion (photocorrosion) process. The rate of photocorrosion is also influenced by other

factors such as ionic strength of the electrolyte, energy of the photons irradiating the semiconductor (Mavi et al. 2004), and electrostatic interactions taking place at the surface of the semiconductor. It has been reported that immobilization of electron donor molecules on the surface of an n-type semiconductor modifies the band bending of this material due to the formation of positively charged ions on the surface (Zhang and Yates 2012). Thus, following this immobilization, holes are repelled from the surface and, consequently, the photocorrosion process is delayed. The same mechanism could happen in the case of exposure of an n-type semiconductor to a bacterial suspension with a pH greater than 4. In this range of pH, the surface of most bacteria is negatively charged (Poortinga et al. 2002). By suspension of bacteria in an electrolytic solution, like PBS (1X), the surface of bacteria could be decorated by positively charged counter ions present in the solution. As schematically illustrated in Figure 47, when the bacteria approach the surface, the strength of the near-surface electric field is reduced and the band bending of the semiconductor is modified. Therefore, transport of photo-excited holes towards the semiconductor surface is reduced and photocorrosion is delayed. We have taken advantage of the dependency of the photocorrosion rate of GaAs/AlGaAs heterostructures on the electrostatic interactions taking place at the surface of these materials to detect bacteria suspended in PBS (1X) (See Chapter 3) and monitor growth and antibiotic susceptibility of bacteria immobilized on the surface of these structures (See Chapter 5).

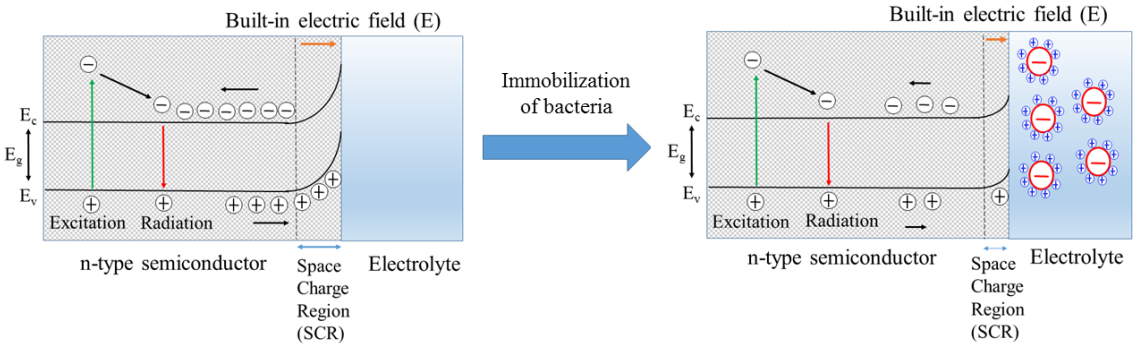

Figure 47. Electron-hole generation in an n-type semiconductor immersed in an electrolyte and irradiated with photons of energy exceeding the bandgap of the semiconductor. Immobilization of negatively charged bacteria decorated with positively charged ions on the surface of the semiconductor decreases the strength of the built-in electric field and reduces the band bending of the semiconductor. Consequently, the concentration of photo-excited holes arriving to the surface decreases and the photocorrosion process is delayed.

6.2 Immobilization of streptavidin-coated microbeads on GaAs surfaces

To investigate the 2-dimensional immobilization efficiency of bacteria on the surface of functionalized GaAs biochips, we employed a model consisting of 3 μm diameter microbeads coated with streptavidin and a network of biotinylated PEG thiol SAMs. More information about the microbeads and biofunctionalization of the GaAs samples is available in Chapter 3. In the experiments discussed in Sec. 3.4.1, the biochips were kept in a flow cell (the flow cell is explained in Chapter 4) and the bead suspension was injected into the flow cell with a flow rate of 0.1 mL/min for 10 min. Following this step, the biochips were exposed to the beads for an additional 20 min without any further injection. For microscopic analysis, the biochips were removed from the flow cell and placed in a Petri dish with the bead exposed surface facing up. The biochips were then rinsed with DI-water while the Petri dish was shaken slightly. This procedure was repeated three times to completely remove beads that were non-specifically attached to the surface (physisorbed beads). Following this step, the biochips were placed on glass slides and analyzed under an optical microscope (Zeiss, Axiotech) equipped with objective lenses of 5X, 10X, 20X, 50X and 100X and an ocular lens with a magnification of 10X. The microscope was able to operate in different modes such as differential interference contrast (DIC) and phase contrast. A CCD camera and the Infinity Capture software were used to take *in-situ* optical images of the biochips. The magnification of the images taken by the camera was the product of the magnification of the objective lens used in the microscope and supplemental 10X digital enlargement. It should be noted that the same procedure was applied for microscopic analysis of bacteria immobilized on the surface of the biochips.

We carried out extra tests in which the dynamics of immobilization of the beads on biofunctionalized surfaces of the biochips was investigated. For that purpose, bead suspensions at concentrations ranging from 5×10^2 to 5×10^6 beads/mL were injected into the flow cell for 100 min at a flow rate of 10 μL/min. The biochips were imaged every minute with the optical microscope and the dynamics of the capture of streptavidin-coated microbeads on the biotinylated surfaces of GaAs samples was investigated. As presented in Figure 48 the number of beads immobilized on the surface increased with time for each concentration of bead

suspensions and detection of beads took more time for low concentrations of beads. We found that the total number of beads immobilized on 100 μm^2 of surface varied from 1.2×10^{-3} to 200 beads for the concentrations mentioned above over 100 min of the experiment. Figure 49 shows some examples of bead immobilization on the surface of the biochip exposed to 5×10^6 beads /mL at different stages of the experiment. The video of immobilization of the beads on the surface of the biochip during this period of time is available at https://www.researchgate.net/profile/Jan Dubowski.

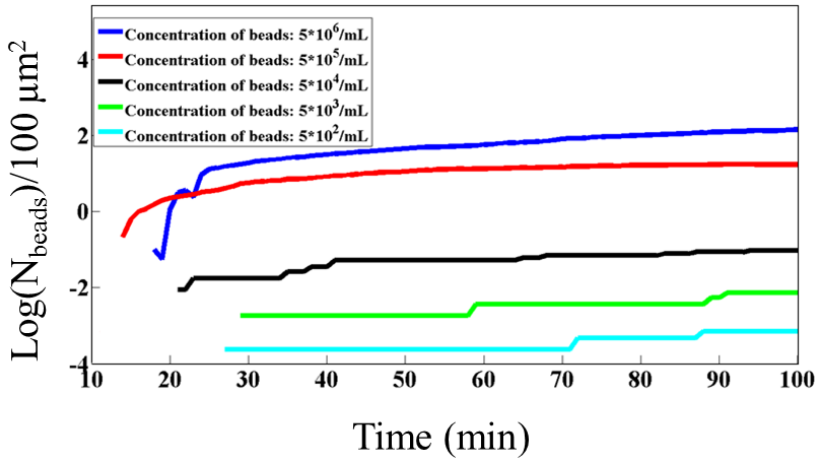

Figure 48. Time dependent surface density of streptavidin-coated microbeads immobilized on biofunctionalized surfaces of GaAs samples.

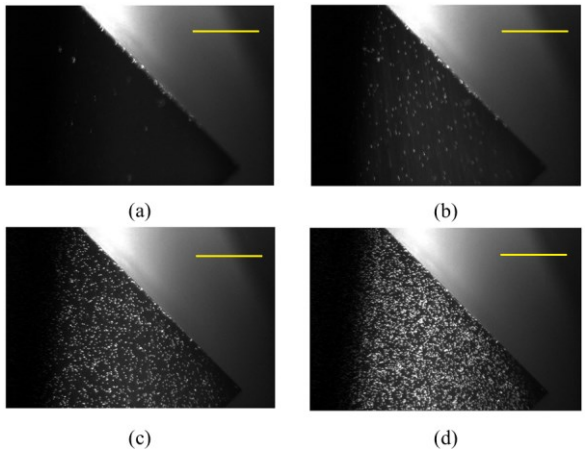

Figure 49. Examples of optical images of microbeads immobilized on a functionalized GaAs biochip after 10 (a), 30 (b), 50 (c) and 100 (d) min exposure to a bead suspension at 5×10^6 beads/mL which was injected into the flow cell at a flow rate of 10 µL/min. Scale bars correspond to 150 µm.

We also studied the effect of velocity of injection (flow rate) on the number of beads immobilized on GaAs surfaces. Figure 50 and Figure 51 show the number of beads immobilized on the GaAs surfaces for two concentrations of bead suspensions, 5×10^3 beads/mL and 5×10^2 beads/mL, respectively, and for two velocities of injection, 10 µL/min and 50 µL/min. It was found that the total number of beads immobilized on the GaAs surface depended on the velocity of injection. Increasing the velocity of injection decreased the time for detection of the first bead, however, it decreased the total number of beads immobilized on the surface as well. The time for detection of the first bead in 5×10^2 beads/mL and 5×10^3 beads/mL was around 10 min for $V_{injection}$= 50 µL/min. This time increased to around 30 min for $V_{injection}$=10 µL/min.

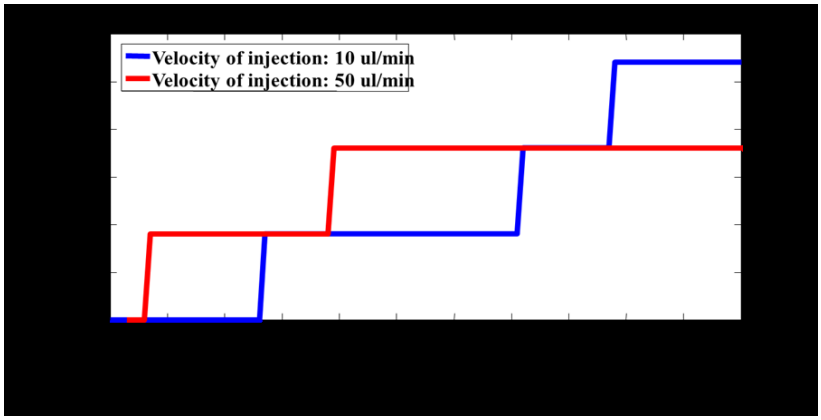

Figure 50. Time dependent surface density of streptavidin-coated microbeads immobilized on biofunctionalized surfaces of GaAs samples. The bead suspensions at 5×10^3 beads/mL were injected into the flow cell with different flow rates (10 µL/min and 50 µL/min).

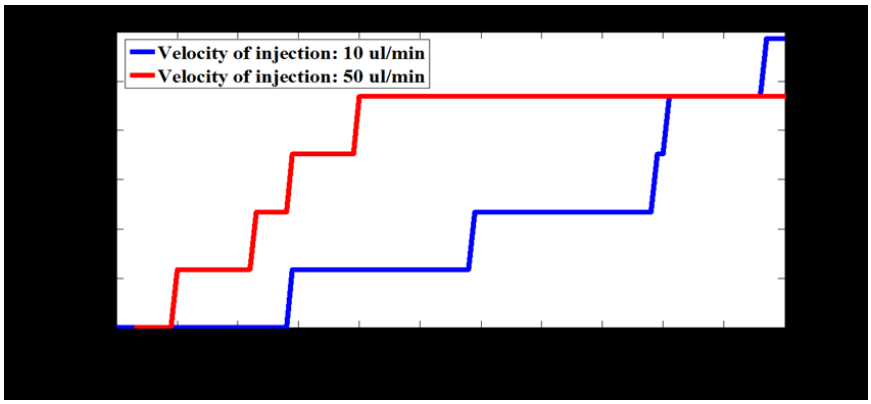

Figure 51. Time dependent surface density of streptavidin-coated microbeads immobilized on biofunctionalized surfaces of GaAs samples. The bead suspensions at 5×10^2 beads/mL were injected into the flow cell with different flow rates (10 µL/min and 50 µL/min).

Capturing of microbeads on GaAs surfaces could be considered as a model of immobilization of bacteria. The goal was to enhance the total number of bacteria immobilized in as short as possible time on GaAs. We noticed that for each concentration, the number of beads immobilized on the surface increased with time. Furthermore, increasing the velocity of injection helps to detect the beads in a shorter time, but excessive velocity of injection decreased the maximum number of beads that could be immobilized. Immobilization of 1 bead/100 μm^2 was observed in 25 min from a solution comprising 5×10^6 beads/mL. For bead concentrations $< 10^5$ beads/mL, it was impossible to observe 1 bead/100 μm^2, even after a 100 min experiment. To make a more realistic model of bacterial immobilization on GaAs surfaces, we suggest to employ beads of smaller size (comparable to the size of bacteria). In addition, antigen-coated beads (Hilton and Parham 2013) and an antibody-based architecture, like the one used for capturing bacteria, could also be employed to create a more accurate model of bacterial immobilization.

6.3 Development of an innovative photo-electrochemical biosensor

An extensive examination of the PL effect in a series of GaAs/AlGaAs nano-heterostructures exposed to PBS and different PBS solutions with bacteria allowed us to observe the effect of PL-monitored photocorrosion of these materials. In order to specifically immobilize bacteria on the surface of the biochips, we functionalized the exterior layer of the GaAs/AlGaAs heterostructures with polyclonal antibodies directed against the bacteria. Irradiation of the heterostructure in an etching fluid using an illumination source, such as a laser, induced photocorrosion of this material. The photocorrosion rate depended on the power of the illumination source and the etching power of the fluid. We noticed that the photocorrosion rate was reducing as the surface concentration of immobilized bacteria was increasing. This observation led to the idea of an innovative biosensor based on photocorrosion of semiconductor nano-heterostructures. As it was explained in Sec. 6.1, the photocorrosion of III-V semiconductors strongly depends on the concentration of photo-excited surface holes. Therefore, immobilization of negatively charged bacteria decorated with positively charged counter ions on the surface of the biochip repels the photo-excited holes from the surface and slows down the photocorrosion process.

Figure 52 shows photo-chemical etching of a freshly etched GaAs/AlGaAs biochip and a biochip immersed in a 0.1% AS solution for 15 min. The GaAs/$Al_xGa_{1-x}As$ (x=0.35) heterostructure used in this study comprised a GaAs cap (10 nm thick) placed on top of a AlGaAs/GaAs microstructure. The AlGaAs layer located below the cap is 100 nm thick, and a 500 nm thick epitaxial layer of GaAs was located below the AlGaAs. The PL of the samples immersed in PBS (1X) was recorded *in situ* using the HI-PLM.

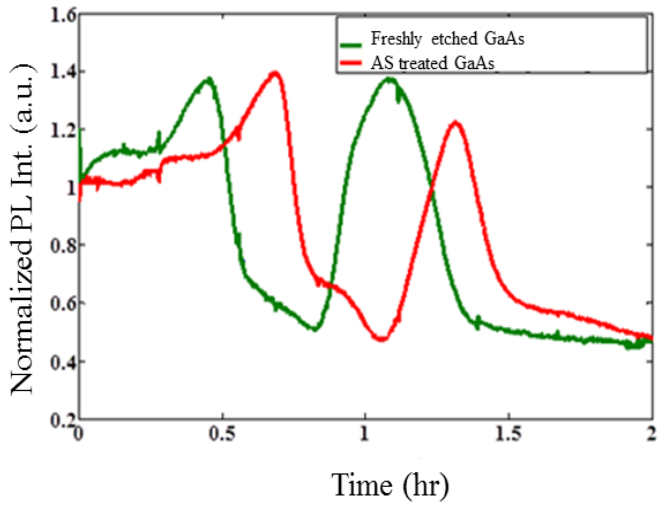

Figure 52. *In situ* PL emission of freshly etched and AS treated biochips in PBS (1X).

As the biochips are immersed in PBS and irradiated with a 532 nm laser (~30 mW/cm^2) the photocorrosion process starts. This process is indicated by the presence of two peaks in the PL spectra of the samples. As the 10-nm thick cap layer of GaAs was etched away, the PL signal increased gradually to reach the maximum at 30 and 45 min for the freshly etched GaAs and AS treated samples, respectively. This was followed by the decrease of the PL signal, which corresponds to the situation where the AlGaAs electrodes are gradually exposed to PBS. The appearance of the second PL peak in these plots was related to the presence of the second GaAs layer that was revealed by the photo-etching process. These results illustrate that the photo-etching process of a freshly etched GaAs is significantly faster than that of S-coated GaAs. We argue that the electrons donated by the S atoms were partially responsible for flattening the GaAs band structure near the surface, which resulted in reduced surface concentration of h^+ and, consequently, in a reduced photo-etching effect. Following this observation, we hypothesized

that postprocessing of antibody-coated biochips with AS would increase the photonic stability of the biochips in PBS solution and allow detection of bacteria at low concentrations. We employed the photocorrosion of GaAs/AlGaAs biochips functionalized with antibody molecules and postprocessed with AS to detect *E. coli* suspended in PBS (1X) at an attractive limit of detection of 10^3 CFU/mL (See Chapter 3 for more information).

It should be noted that for each 2 h long biosensing run discussed in Chapter 3, we employed a new GaAs/AlGaAs biochip. According to the feasibility of revealing the second layer of GaAs in PL measurements (see Figure 52), it might be possible to carry out two biosensing runs with just one biochip. For that purpose, after finishing the first experiment, the biochip should be completely photocorroded to reach the second GaAs layer. By biofunctionalization of the new GaAs layer, a second biosensing run could be carried out. Employing a heterostructure with many heterojunctions, such as the heterostructure used in Chapter 6, would make it possible to carry out more biosensing runs.

These results, along with some other results obtained by QS group members, contributed to the data that supported a patent application aiming to protect the original idea of a photocorrosion-based biosensor (Dubowski et al. 2015).

6.4 Growth of *E. coli* on GaAs (001) surfaces (optical microscopy data)

In our attempt to develop a GaAs-based biosensor to monitor growth and antibiotic susceptibility of bacteria, we investigated the growth of *E. coli* on bare and biofunctionalized surfaces of GaAs (001) samples. It has been reported that some of the common semiconductors such as GaAs and AlGaAs have toxic effects and their toxicity is related to the presence of both As and the counter-elements of As, such as Ga (Tanaka 2004). However, some bacteria have plasmids carrying arsenic resistance determinants (*ars*) which make them resistant to arsenic (Paez-Espino et al. 2009). Diorio et al. (Diorio et al. 1995) discovered a chromosomal arsenic-induced *ars* operon in *E. coli* which makes these bacteria resistant to arsenic at concentrations lower than 0.2 mg/mL. Gallium has recently been found to present antimicrobial activity against

both gram-negative and gram-positive bacteria such as *Pseudomonas aeruginosa* and *S. aureus* (DeLeon et al. 2009; Rzhepishevska et al. 2011). The reason is that the ionic radius of the gallium ion (Ga^{3+}) is similar to ferric iron (Fe^{3+}), so Ga^{3+} could easily replace Fe^{3+} in bacterial metabolism. Since Ga^{3+} cannot reduce, unlike Fe^{3+}, it would block the reactions where a reduced form of Fe^{3+} (Fe^{2+}) is required (DeLeon et al. 2009). Due to the antimicrobial effect of Ga, some researchers have suggested adding Ga to antibiotics such as gentamicin to increase the activity of the antibiotics (Halwani et al. 2008).

In one of our experiments, bare and biofunctionalized GaAs (001) samples were placed upside down on Nutrient agar plates inoculated evenly with 10^5 CFU/mL of a freshly cultured *E. coli* suspension and kept in darkness at 37° C for up to 8 hours. The GaAs samples were biofunctionalized with HDT and biotinylated PEG thiols, neutravidin and biotinylated polyclonal antibodies (see Sec. 4.3.2.1 for more information). The reason for using neutravidin in this bio-architecture instead of streptavidin is that neutravidin offers lower non-specific binding compared with streptavidin (ThermoFisherScientific 2016). Every hour one of the bare samples and one of the antibody-coated samples were removed from the agar plate and analyzed under the optical microscope. We found that the presence of GaAs samples on the agar plate did not inhibit bacterial growth and bacteria were able to grow next to either bare or biofunctionalized surfaces of GaAs. Figure 53 and Figure 54 show examples of optical images of bare and antibody-coated GaAs samples, respectively, after 1, 4 and 8 hours of incubation on the agar plate. As it is exemplified in these figures, the number of bacteria that grew next to the biofunctionalized samples was higher than the number that grew next to the bare samples, however, after 8 hours, the surface of both samples was almost completely covered with bacteria. The time dependent surface density of immobilized bacteria on the bare and functionalized surfaces of GaAs was fitted with exponential curves, as shown in Eq. (6.2). The doubling time of bacteria on the surface of the samples was also estimated using Eq. (6.3). Further discussion of this study is presented in Chapter 4.

$$X_t = X_0 \times \exp(U_{\max} \times (t - t_0)) \tag{6.2}$$

$$R = \frac{ln2}{U_{max}} \tag{6.3}$$

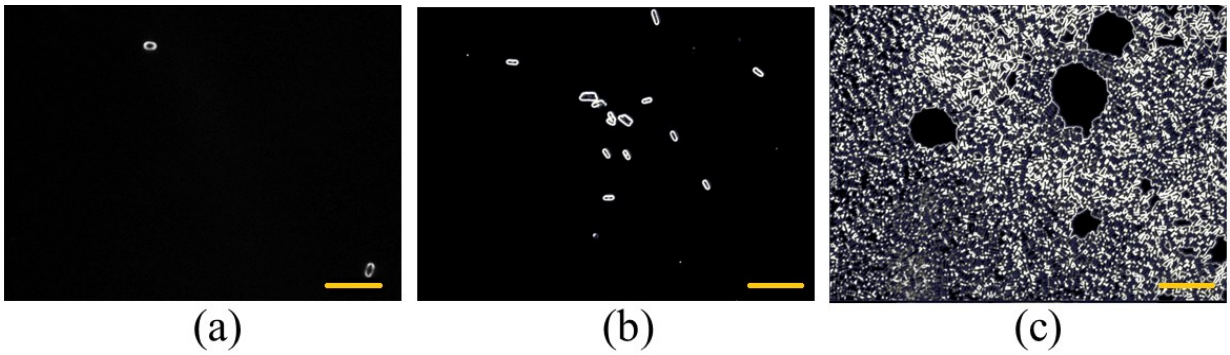

Figure 53. Examples of optical images of *E. coli* immobilized on bare GaAs (001) samples after 1 (a), 4 (b) and 8 (c) hours of exposure of the samples to the Nutrient agar plate inoculated evenly with 100 µL of 10^5 CFU/mL of *E. coli*. The presence of bare GaAs samples in the Nutrient agar plate did not inhibit the bacterial growth. The scale bars correspond to 10 µm.

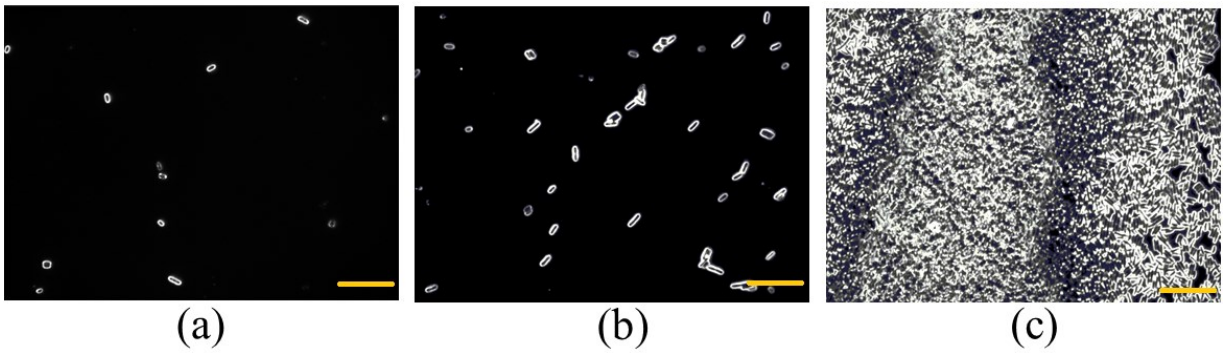

Figure 54. Examples of optical images of *E. coli* immobilized on biofunctionalized GaAs (001) samples after 1 (a), 4 (b) and 8 (c) hours of exposure of the samples to the Nutrient agar plate inoculated evenly with 100 µL of 10^5 CFU/mL of *E. coli*. The presence of biofunctionalized GaAs samples in the Nutrient agar plate did not inhibit the bacterial growth. The scale bars correspond to 10 µm.

In another study, biofunctionalized GaAs (001) samples were kept in a flow cell and exposed for 30 min to freshly cultured *E. coli* suspension and then for 4.5 h to Luria Bertani broth (LB). The biochips were kept in darkness at 37° C during these experiments. The bacteria were immobilized specifically on the GaAs samples functionalized with MHDA-EDC/NHS-Ab. The bacteria were also captured non-specifically on the GaAs samples functionalized with MHDA-EDC/NHS which is a simpler bio-architecture compared with MHDA-EDC/NHS-Ab. The

functionalization procedure of the samples has been described in Sec. 4.3.2.2 and Sec. 4.3.2.3. To investigate the growth of bacteria on GaAs surfaces, the samples were analyzed after 30 min of exposure to bacterial suspensions and after an additional 4.5 h of exposure to LB. It was revealed that bacteria were able to grow on the surface of both samples if their initial concentration was at least 10^5 CFU/mL. However, the initial capture and the growth rate of bacteria depended on the bio-architectures used to capture bacteria. Figure 55 and Figure 56 show examples of GaAs samples functionalized with MHDA-EDC/NHS and MHDA-EDC/NHS-Ab, respectively, after 30 min of exposure to a 10^6 CFU/mL suspension of *E. coli* and after 4.5 h growth of bacteria in LB medium. As it is exemplified in these figures, the initial capture and the subsequent bacterial growth on Ab-coated surfaces was higher than on functionalized surfaces without Ab. The detailed discussion of this study is presented in Chapter 4.

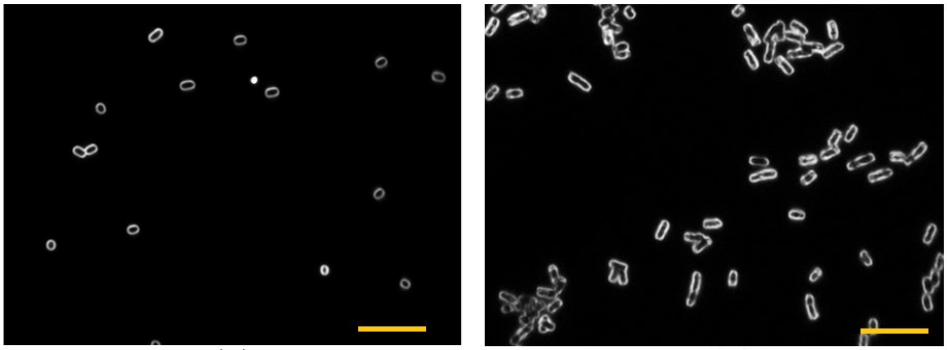

Figure 55.Microscopic images of bacteria directly immobilized on the MHDA-EDC/NHS functionalized surface of GaAs (001) exposed to a 10^6 CFU/mL solution of *E. coli* for 30 min (a) and after 4.5 h growth of bacteria in LB medium (b). The scale bars correspond to 10 µm.

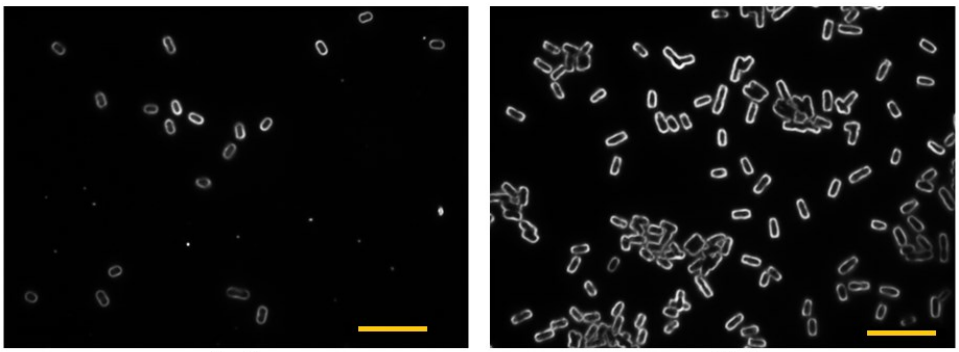

Figure 56. Microscopic images of bacteria immobilized on the MHDA-EDC/NHS-Ab functionalized surface of GaAs (001) exposed to a 10^6 CFU/mL solution of *E. coli* for 30 min (a) and after 4.5 h growth of bacteria in LB medium (b). The scale bars correspond to 10 µm.

6.5 PL emission of GaAs/AlGaAs biochips in growth medium

In order to evaluate growth and antibiotic susceptibility of bacteria using PL of GaAs/AlGaAs heterostructures, investigation of PL emission of these samples in growth medium is necessary.

The wafer used in this study comprised 30 pairs of 6 nm thick GaAs quantum wells (QW) and 10 nm thick AlGaAs barriers grown on a 500 nm thick buffer layer of GaAs that was deposited on a semi-insulating GaAs (001) substrate. The QW architecture was capped with a 10 nm thick GaAs layer. The schematic illustration of the wafer structure is presented in Sec. 5.3.1. The biochips were biofunctionalized with HDT and biotinylated PEG thiols, neutravidin and biotinylated antibodies, following the procedure described in Sec. 5.3.2. The biofunctionalized samples were then kept in a flow cell (the flow cell is explained in Chapter 4) and exposed to PBS (1X) for 30 min and then to LB medium. Figure 57 shows PL emission of the samples recorded with the QSPB reader. The PL measurements were carried out for the samples irradiated with a LED at 660 nm with a power of 35 mW/cm^2 for different duty cycles (DC). As presented in Figure 57, the photocorrosion rate of the biochips and presence of the PL maximum depended on the DC of irradiation. When the time of exposure of the biochip to the LED light increased, for instance 10s/60s compared with 6s/60s, the number of photons irradiating the biochip and the number of photo-excited holes increased as well. Since holes are responsible for initiation and progression of the photocorrosion process, by increasing the number of photo-excited holes the photocorrosion process is accelerated and, consequently, the position of the

PL maximum is advanced. These experiments showed that the photocorrosion of GaAs/AlGaAs heterostructures in LB medium is qualitatively similar to what was observed in PBS (1X). We selected a DC of 6s/60s for our experiments where the biochips were exposed to bacteria and LB with or without antibiotics and the PL emission of the samples was recorded to evaluate growth and antibiotic susceptibility of bacteria (see Chapter 5).

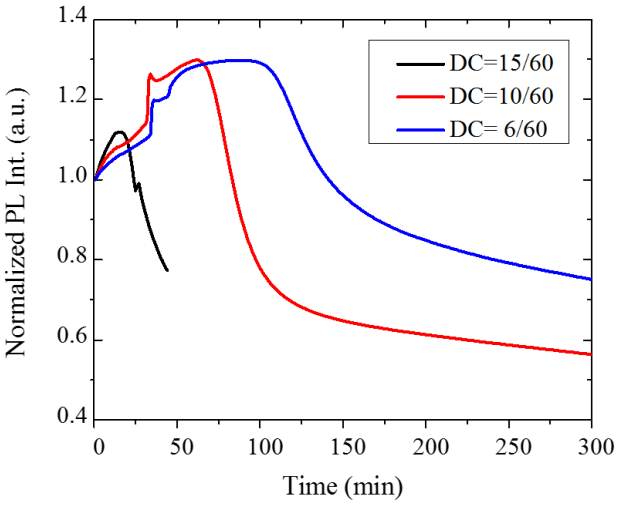

Figure 57. Normalized PL intensity for the biofunctionalized GaAs/AlGaAs samples irradiated in LB medium with a LED light at 660 nm with power of 35 mW/cm^2 and for different duty cycles.

6.6 PL monitoring of bacterial growth at room temperature

Growth of freshly-cultured *E. coli* K12 at an initial concentration of 10^7 CFU/mL on biofunctionalized surfaces of GaAs/AlGaAs biochips was investigated. The wafer used in this study was the same as the one employed in the previous section. The 2 mm × 2 mm biochips were biofunctionalized with HDT and biotinylated PEG thiols, neutravidin and polyclonal biotinylated antibody following the procedure described in Sec. 5.3.2. The polyclonal biotinylated antibody used in this experiment recognized O and K antigenic serotypes of *E. coli*. After the functionalization step, the biochips were kept in a flow cell (the flow cell is explained in Chapter 4) and exposed to bacteria suspended in PBS (1X) at pH 7.4 for 30 min. Following that, LB medium was injected into the flow cell to stimulate the bacteria to grow. The biochips were exposed to LB medium for 4.5 h. The PL of the biochips was recorded during this period

at room temperature with the QSPB reader. The samples were irradiated at 660 nm with power of 35 mW/cm^2 and duty cycle of 6s/60s. As a reference experiment, the PL of the biochips exposed to PBS (1X) for 30 min (instead of bacterial suspension) and LB medium for 4.5 h was also studied. To investigate the growth of bacteria, the biochips were analyzed with the optical microscope after 30 min of exposure to the bacterial suspension and after 4.5 h of bacterial growth in LB medium. Figure 58 shows PL emission of the biochips exposed to PBS (1X) with or without bacteria and LB medium. Examples of optical images of the biochips exposed 30 min to bacteria followed by 4.5 h of exposure to LB are shown in Figure 59. According to Figure 58, the PL maximum for the biochip exposed to bacteria and LB was observed at around 135 min and was delayed compared to that of one exposed to PBS and LB. Based on the optical images, the bacteria initially covered the surface of the biochip with an average density of 410±112 bacteria/mm^2 and the coverage of the surface with bacteria following 4.5 h of exposure to LB was just increased to 500±121 bacteria/mm^2. It was expected that exposure of the bacteria to LB would increase the density of bacteria on the biochip, but numbers of bacteria only increased marginally compared to the seeded density after 4.5 in LB. The reason for observing no bacterial growth could be related to the toxicity of Ga and As ions (Podol'skaia et al. 2002; Rzhepishevska et al. 2011; Tanaka 2004) released from the biochips. The release of these ions is the consequence of the photocorrosion of GaAs/AlGaAs samples, as shown in Eq. (6.1) (Ruberto et al. 1991). The presence of an earlier PL maximum for the biochip exposed to PBS compared with that of one exposed to bacteria could be explained by the effect of bacteria induced retardation of the photocorrosion process resulting in postponing the PL maximum, as explained in Sec. 6.1.

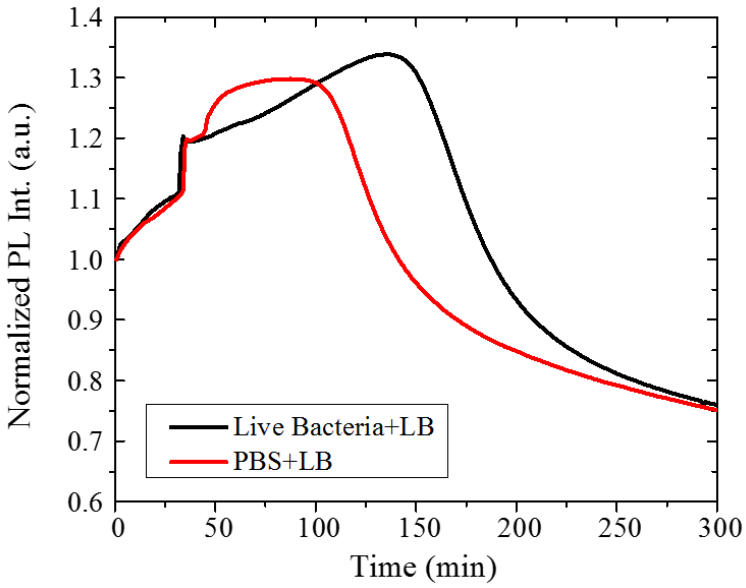

Figure 58. Normalized PL intensity for the biochips exposed to PBS (1X) without or with *E. coli* K12 and LB medium. The PL measurements were carried out at room temperature.

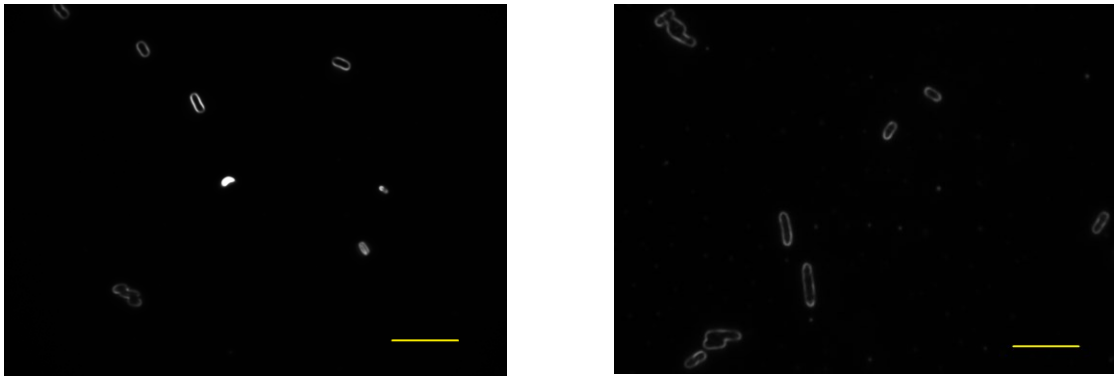

(a) (b)

Figure 59. Microscopic images of bacteria immobilized on the functionalized surfaces of GaAs/AlGaAs biochips exposed to a 10^7 CFU/mL solution of *E. coli* for 30 min (a) and after 4.5 h growth of bacteria in LB medium (b). The scale bars correspond to 10 μm.

It should be mentioned that while in darkness we were able to observe bacterial growth on GaAs surfaces for bacterial concentrations of at least 10^5 CFU/mL, no growth was observed for a bacterial concentration of 10^7 CFU/mL when irradiated biochips were used. As discussed before, the likely reason for this behavior is a poisonous effect of As and Ga ions released by the photocorroding biochip to the flow cell that could affect the viability and/or growth of

bacteria (Podol'skaia et al. 2002; Rzhepishevska et al. 2011; Tanaka 2004). Since the rate of photocorrosion of the biochips is higher under irradiation compared with darkness, the release of As and Ga ions into the flow cell would be higher in this situation, therefore, it will be necessary to work with a higher concentration of bacteria in order to observe their growth, e.g., 2×10^8 CFU/mL. It should be noted that for the concentration of 10^7 CFU/mL the surface coverage with bacteria was around 400 bacteria/mm^2 while for the concentration of 2×10^8 CFU/mL around 900 bacteria/mm^2 were observed immobilized on the biochip surface (see Chapter 5). The minimum concentration of bacteria required in photonic evaluation of bacterial reactivity to antibiotics could be reduced by improving surface functionalization techniques and, consequently, increasing the initial coverage of the surface with bacteria. Alternatively, methods could be devised to reduce the toxic effects of Ga and As like adding protective amounts of Fe ions to the LB or adding ions that would selectively precipitate Ga and/or As. In addition, some methods such as electrophoresis, chemotaxis and filtration could be integrated with this method to concentrate the bacteria on the surface of the biochip and make the biosensor operate at lower concentrations of bacterial suspensions. In the filtration method, bacteria are passed through filters with different pore sizes and selectively separated from solution (Bobbitt and Betts 1992). This technique could be applied in the biosensing field to improve limit of detection (LOD) of biosensors. Following filtration, bacteria would be separated from other particles, concentrated and then exposed to the biosensors. In this technique a calibration curve is needed to correlate the concentration of the filtered suspension to the concentration of the suspension before filtration. Although the biosensor would be exposed to the concentrated suspension of bacteria, the initial concentration of bacteria before filtration, which had been lower than the filtered suspension, would be considered as the LOD of the biosensor. Bernhardt et al. (Bernhardt et al. 1991) employed a 0.22-micron membrane filter to separate *E. coli* and *S. aureus* from human blood and then applied a plate counting method to detect these bacteria. More recently, Wu et al. (Wu et al. 2016) combined a filtration method with surface-enhanced Raman spectroscopy (SERS) to detect *Salmonella* from cantaloupe cubes and *E. coli* O157:H7 from lettuce. They showed that adding the filtration procedure to their SERS method could significantly improve the LOD of the biosensor, e. g., a LOD of 100 CFU/mL was reported for *Salmonella*.

Chemotaxis is a process in which organisms, such as bacteria, change their speed or alter the frequency of turning of their flagella in response to a chemical stimulus. This process allows bacteria to move towards a nutrient, or move away from a noxious chemical (Hauri and Ross 1995). Hassen et al. (Hassen et al. 2016) employed chemotaxis to attract *E. coli* or *L. pneumophila* towards the surface of functionalized GaAs samples and increase immobilization. They attached the enzyme beta-galactosidase to the surface of the biochips included its substrate lactose in the growth medium in order to produce a gradient of glucose/galactose in the vicinity of the GaAs samples to attract bacteria towards the surface. Since the sensitivity of GaAs-based biosensors used for bacterial detection depends on the number of bacteria immobilized on their surfaces (Aziziyan et al. 2016; Duplan et al. 2011; Nazemi et al. 2015), chemotaxis could help to concentrate the bacteria on the surface or in the vicinity of the biosensors and enhance the sensitivity of these devices.

Electrophoresis is the mechanism in which charged particles, such as bacteria, are exposed to an electric field and affected by electrostatic forces which results in movement of the particles in a specific direction. This method has many applications such as DNA and protein analysis (Badcock and Editor 2012). In 1995, capillary electrophoresis (CE) was first combined with biosensing technology (Zhou et al. 1995). In this approach, the CE unit was coupled to the biosensor and caused the desired analytes to move towards the biosensor and allow specific detection (Bossi et al. 2000). For instance, Zhou et al. (Zhou et al. 1995) employed a CE/laser induced fluorescence (LIF) system to detect aspartate and glutamate. Chen et al. (Chen et al. 2005) coupled an amperometric biosensor to a CE system to detect glucose.

6.7 PL monitoring of bacterial growth at 37° C

To accelerate bacterial growth, all the steps of the previous test (Figure 58) were repeated at 37° C. During the PL measurements, the flow cell was placed on a heater whose temperature was set at around 37° C. Figure 60 shows PL emission of the biochips exposed to PBS (1X) with or without bacteria followed by LB medium. Examples of optical images of the samples after 30 min of exposure to the bacteria and after 4.5 h of bacterial growth in LB medium are presented in Figure 61. As expected, bacteria grew at 37°C at a higher rate and the number of bacteria

immobilized on 1 mm^2 of the surface increased from 410±112 to 849±123. However, heating the biochips resulted in acceleration of the photocorrosion process. In spite of the growth of bacteria on the surface of the biochip in this experiment, no difference was observed in the position of the PL maximum for the biochip exposed to bacterial suspension with that of one exposed to PBS (1X). It is was interesting that while at room temperature only the first PL maximum was observed within 5 hours, we were able to distinguish two PL maxima at 37° C. At 37° C, both the 10 nm thick GaAs cap layer and the first 10 nm thick AlGaAs layer were photocorroded as evidenced by PL maxima. The second PL maximum corresponded to the second layer of GaAs which was revealed during the photocorrosion process.

To operate the biosensor at 37° C, the power of the irradiation light and/or the exposure time of the biochips to the light should be reduced to moderate the photocorrosion rate. Working at 37° C which is the optimum temperature for growth of *E. coli* would enable us to monitor the antibiotic sensitivity of bacteria in a shorter period of time and, perhaps, for lower bacterial concentrations.

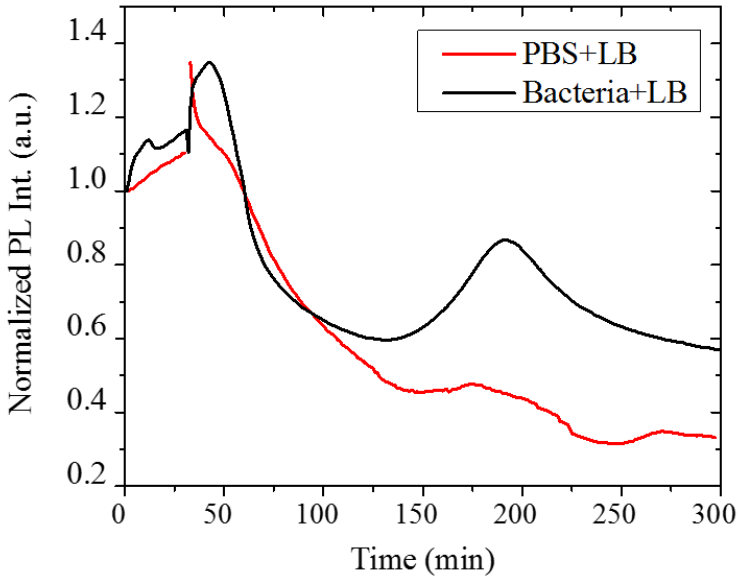

Figure 60. Normalized PL intensity for the biochips exposed to PBS (1X) without or with *E. coli* K12 and LB medium. PL measurements were carried out at 37° C.

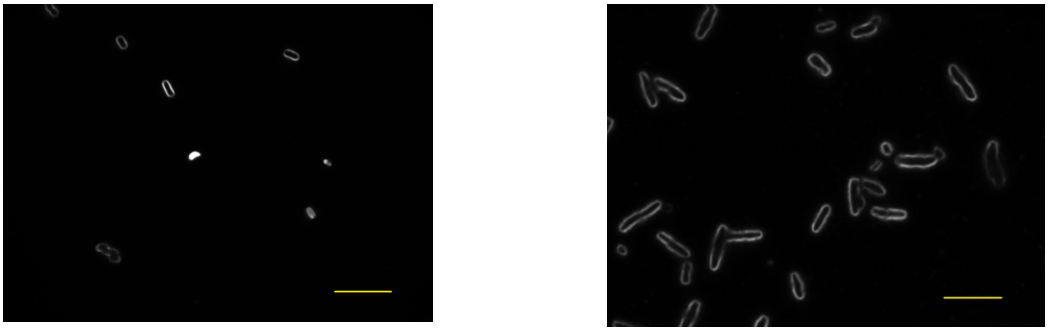

(a) (b)

Figure 61. Microscopic images of bacteria immobilized on the functionalized surfaces of GaAs/AlGaAs biochips exposed to a 10^7 CFU/mL solution of *E. coli* for 30 min (a) and after 4.5 h growth of bacteria at 37° C in LB medium (b). The scale bars correspond to 10 μm.

6.8 Zeta potential measurements of bacteria

We applied the electrophoresis method to measure the zeta potential of freshly-cultured, UV-treated, ciprofloxacin-treated (concentration of ciprofloxacin: 10 μg/mL) and penicillin-treated (concentration of penicillin: 50 μg/mL) *E. coli* K12 suspended in PBS (1X) at a concentration of 10^8 CFU/mL. Zeta potential (ζ) is a parameter defined for dispersed particles that shows the electrostatic potential at the location of the slipping layer of the fluid attached to the particles (Sze et al. 2003). The magnitude of the zeta potential demonstrates the stability of the particles in the dispersion medium, therefore, zeta potential analysis is of great importance in various fields of science. To measure zeta potential, using the electrophoresis technique, particles are suspended in a solvent with a refractive index of *n,* dielectric constant of ε and viscosity of η. The particles are then exposed to an electric field (*E*) and their mobility is measured under the influence of the electric field by using the Doppler effect. For this purpose, a laser light with wavelength of λ and frequency of ν_0 irradiates the particles and the scattered light with a frequency of $\nu_0+\nu_d$ at the angle of θ is measured (see Figure 62). The mobility of the particles was calculated following Eq. (6.4) (Shimko et al. 2014),

$$U = \frac{\lambda.\nu_d}{2.E.n.\mathrm{Sin}(\theta/2)} \tag{6.4}$$

The zeta potential of the particles is then calculated following Eq. (6.5),

$$\zeta = \frac{\eta U}{\varepsilon f(ka)} \tag{6.5}$$

where *f (ka)* is henry coefficient which is normally either 1.5 or 1.0.

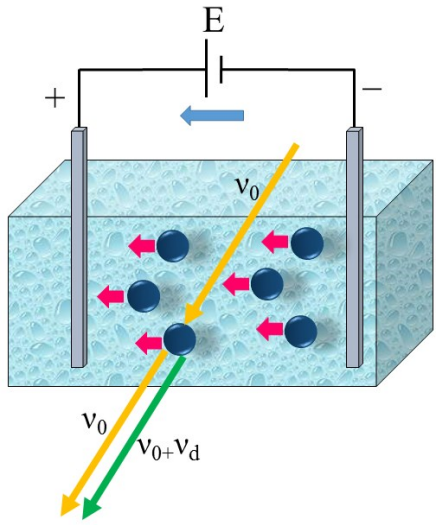

Figure 62. Schematic illustration of a zeta potential analyzer used to measure zeta potential of particles by the electrophoresis method.

Figure 63 shows the zeta potential of live, UV-treated and antibiotic-treated bacteria. According to this Figure, the zeta potential of freshly-cultured and UV-treated bacteria are comparable, while the absolute value of the zeta potential of antibiotic-treated bacteria is significantly lower than freshly-cultured bacteria. These data are in good agreement with the literature concerning the considerable decrease of the absolute value of the zeta potential of bacteria treated with different antimicrobial agents (Alves et al. 2010; Nomura et al. 1995).

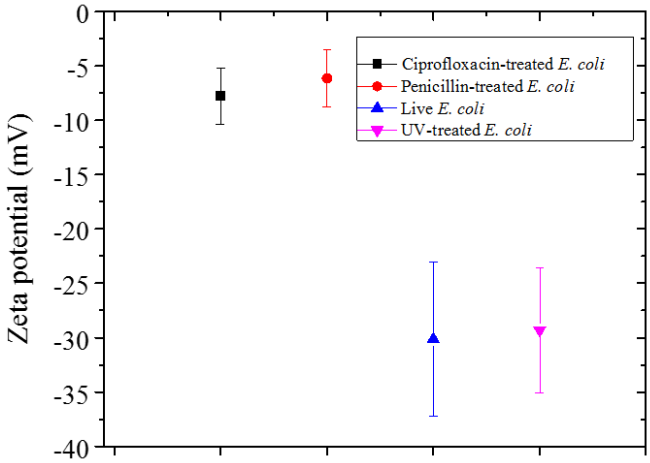

Figure 63. Zeta potential of freshly-cultured, UV-treated, penicillin-treated and ciprofloxacin-treated *E. coli* K12 in PBS (1X). Each experiment was repeated three times to obtain average values with standard deviations.

6.9 PL measurement of Si_3N_4-coated GaAs/AlGaAs biochips in PBS (1X)

The PL emission of Si_3N_4-coated GaAs/AlGaAs biochips in PBS (1X) was investigated. A 40 nm thick Si_3N_4 layer was deposited on a GaAs/AlGaAs wafer using the PECVD technique. The wafer used in this study was the same as the one used in Sec. 6.5. The Si_3N_4-coated samples were cleaned with OptiClear, acetone and isopropanol in an ultrasonic bath (5 min for each). Following this step, the samples were dried under a flow of high-purity compressed nitrogen and etched in a HF solution (2.5%) for 15 seconds. The samples were then incubated in a 25% solution of glutaraldehyde for 1 hour at room temperature. This step was done to provide covalent binding of unconjugated antibodies on the surface of the biochip through the formation of imine bonds (Barrios et al. 2008). Thereafter, the samples were rinsed with PBS (1X) and immersed in a 1 µM solution of polyclonal unconjugated antibodies against *E. coli* for 1 hour at room temperature. The antibody-coated samples were then rinsed with PBS (1X) and DI-water. Following this step, the samples were kept in a flow cell (the flow cell is explained in Chapter 4) and exposed to PBS (1X) of pH 7.4. The PL of the samples was recorded with the QSPB reader for around 20 hours. The biochips were irradiated with a power of 35 mW/cm^2 and a duty cycle of 6s/60s. According to the PL measurement, no photocorrosion occurred for the sample and the PL was stable for a period of 20 hours with variation of less than 3% during this time.

This PL stability is, no doubt, due to the efficient passivation of the surface of the biochip with Si_3N_4 that prevents photocorrosion of the biochip.

In the next experiment, after initial exposure of the biochip to PBS (1X), a suspension of *E. coli* at 10^5 CFU/mL was injected into the flow cell. After injection of the bacterial suspension the PL signal decreased to less than 3% and then recovered to the previous level. The follow-up of this work could be decreasing the thickness of the Si_3N_4 layer to decrease the stability and increase the sensitivity of the biochip.

6.10 Enumeration of bacteria immobilized on the surface of the biochips using fluorescence microscopy

Bacterial immobilization on the surface of biofunctionalized GaAs samples was investigated using an Olympus IX71 fluorescence microscope which was equipped with a xenon arc lamp emitting at 470 and 490 nm. The microscope was connected to a DP71 digital camera and *in-situ* fluorescence images of the samples were taken by using Q-capture software. The GaAs samples were biofunctionalized with HDT and biotinylated PEG thiols, neutravidin and biotinylated antibody, following the procedure described in Sec. 5.3.2. Following this step, the samples were kept in a flow cell (the flow cell is explained in Chapter 4) and exposed for 30 min to bacterial suspensions ranging from 10^3 to 10^5 CFU/mL. Thereafter, PBS (1X) at pH 7.4 was injected into the flow cell to wash away the physisorbed bacteria. Following this step, fluorescent antibody against *E. coli* at a concentration of 1 µM was injected into the flow cell to bind to the bacteria. The samples were exposed to the fluorescent antibody for 1 hour in darkness and then rinsed with DI-water prior to counting bacteria with the fluorescence microscope. The fluorescent images were analyzed with ImageJ software and the number of bacteria immobilized on the samples was calculated for each concentration of bacteria, as presented in Figure 64. According to this figure, the number of bacteria immobilized on the surface of the biochips was low at each concentration of bacteria, e. g., as low as 30 bacteria/mm^2 for 10^3 CFU/mL. It is possible that the fluorescence microscope underestimated the number of bacteria. The reason might be related to the inefficiency of the antibody to bind to all of the bacteria. It is also possible that the fluorescence intensity of some of the labelled bacteria was too low and these bacteria were not counted in the data analysis. However, it should be noted that we might have

overestimated of the number of *E. coli* bacteria using the optical microscope due to the counting of bacteria which were not *E. coli* but had grown in the growth medium.

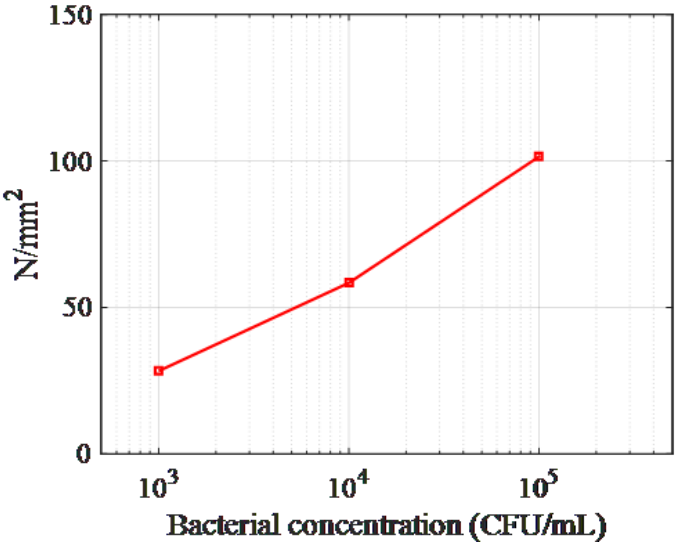

Figure 64. Number of bacteria immobilized on 1 mm^2 of GaAs samples for different concentrations of *E. coli.*

6.11 Acknowledgment

The help of Dr. Kh. Moumanis, Dr. W. M. Hassen and the technical staff of the Interdisciplinary Institute for Technological Innovation (3IT) are greatly appreciated. I also thank Dr. M. A. Jaouad of the Department of Génie Électrique et Informatique, Université de Sherbrooke, for deposition of Si_3N_4 on the surface of GaAs/AlGaAs biochips. I also thank Dr. F. Malouin of the Department of Biology, Université de Sherbrooke for kindly supplying *E. coli* bacteria. The help of M. R. Aziziyan for zeta potential measurements is also appreciated.

CHAPTER 7: Conclusions and perspectives

In the fields of microbiology and medicine it is important to monitor the biological activities of bacteria exposed to specific environments. The conventional methods used for evaluation of antibiotic susceptibility of bacteria are mostly culture-based techniques which are time-consuming and cannot provide same-day results. This delay leads to overtreatment of a wide range of infections which is costly and sometimes inefficient in the case of viral infections. The inappropriate and untargeted use of antibiotics leads to antibiotic resistance and this problem is a significant issue for public health (Gootz 2010). Therefore, a sensitive, rapid and low-cost method for detection of the growth and antibiotic susceptibility of bacteria is needed to improve the phenotypic assay procedures used in pharmaceutical fields.

In this thesis we have developed a PL-based method to monitor growth and antibiotic susceptibility of bacteria immobilized on the surface of biofunctionalized quantum semiconductors. The approach of this project was based on measuring the PL signal which, for specially designed QS microstructures, is highly sensitive to the amount of electric charge accumulated on the surface of such microstructures. We noticed that bacteria growing on the surface of biofunctionalized GaAs/AlGaAs biochips affected the PL of these structures in a way different from antibiotic-treated or UV-killed bacteria. Thus, following this method we were able to distinguish antibiotic-resistant and antibiotic-sensitive bacteria in less than 3 hours. Applying the PL emission of semiconductors to study bacterial reactions to antibiotics is a relatively new approach, therefore, it has several challenges that are discussed in the following paragraphs.

The first challenge in our work was to find an efficient bio-architecture to immobilize bacteria on the surface of GaAs/AlGaAs biochips. Since the sensitivity of the proposed biosensor depends on the density of bacteria immobilized on its surface, the efficiency of concentrating bacteria on the surface or in the vicinity of the biosensor is of great importance. The second challenge was to monitor the effect of bacterial immobilization on the PL emission of GaAs/AlGaAs biochips. After that, we had to investigate the growth of bacteria immobilized on the surface of these structures. Due to the toxicity of Ga and As (DeLeon et al. 2009;

Rzhepishevska et al. 2011; Tanaka 2004), we had to determine the minimum number of bacteria required to permit growth on the surface of the biochips when the samples were kept in darkness or irradiated with a laser (Which increases the release of Ga and As). The last challenge of the work was to investigate the capability of the PL monitoring method to detect the growth and antibiotic susceptibility of bacteria. We had to study if this method is sensitive enough to distinguish antibiotic-resistant from antibiotic-sensitive bacteria.

In the first phase of the project a novel photo-electrochemical biosensor was developed to rapidly detect *E. coli* suspended in PBS (1X). The sensor comprises a PL emitting GaAs/AlGaAs heterostructure, with GaAs as its cap layer, which undergoes photocorrosion when illuminated by a laser. The photocorrosion rate of GaAs and AlGaAs layers depended on the power of the laser and the electrolyte in which the heterostructure was irradiated, such as PBS, water, or LB broth. Photocorrosion was also influenced by the amount of the electric charge immobilized on, or in the vicinity of the surface of the heterostructure. Therefore, monitoring photocorrosion of the heterostructure by using PL emission of a photoluminescent material in the heterostructure would enable us to detect charged molecules, such as bacteria, in the electrolyte and determine their concentrations.

The photocorrosion of GaAs strongly depends on the presence of positively charged minority carriers (h^+) on the surface of this material (Choi et al. 2002; Ruberto et al. 1991). In our experiments where GaAs/AlGaAs biochips were immersed in an electrolytic solution and irradiated with photons, photo-holes were formed near the surface of GaAs which contributed to the formation of surface oxides dominated by Ga_2O_3 (Choi et al. 2002). It is the formation of that oxide that reduced the density of surface states and decreased the SRV of electrons and holes which led to the increasing intensity of the PL signal emitted by GaAs surrounded by an aqueous solution, as reported (Passlack et al. 1995). The surface oxides were dissolved into solution as the GaAs photocorroded. As the GaAs cap material photocorroded, a new interface with AlGaAs was formed, which led to a quickly decreasing PL signal and formation of a maximum on the temporal dependent PL signal. The formation of this maximum could be accelerated or delayed depending on the electrostatic interaction between the semiconductor and molecules immobilized in its vicinity. If an electron-donating molecule arrives at the GaAs

surface, that extra electron will replace the electron that came from the bulk of GaAs. Consequently, the band bending near the surface will decrease (the near surface electric field will become weaker) (Zhang and Yates 2012) and there will be less photocorrosion-inducing photo-holes that could arrive to the surface. It should be noted that the surface of most bacteria is negatively charged at pH greater than 4 (Poortinga et al. 2002). When bacteria are suspended in a solution, like PBS (1X), the bacterial surface would be surrounded by positively charged counter ions present in the solution. Since the GaAs investigated in our work behaved at room-temperature as an n-type material, immobilization of bacteria decorated with positively charged ions on the surface of the biochip should contribute to a reduced transport of photo-excited holes to the surface and decrease the photocorrosion rate of the GaAs/AlGaAs biochips (delay the formation of the characteristic PL maximum). We observed, as shown in Figure 26, Figure 39 and Figure 40, that the greater the bacterial concentration, the more the PL maximum was delayed and, no doubt, the slower would have been the photocorrosion rate.

To immobilize bacteria, the exterior layer (cap layer) of the heterostructure was functionalized with a network of biotinylated antibodies interfaced with biotinylated PEG and HDT thiols through the link provided by neutravidin (b-PEG/HDT/NA/b-Ab). To increase the photonic stability of our biochips in biological environments and to improve the sensitivity of our biosensor, the biofunctionalized biochips were postprocessed with AS. It has been suggested that postprocessing of SAM-coated GaAs samples with a solution of 20% AS for 15 min increases the concentration of sulfur atoms reacting with Ga and As and improves the surface passivation of GaAs samples (Arudra et al. 2012). Consequently, the photonic stability of these biochips was enhanced in aqueous solutions (Arudra et al. 2012). We confirmed this observation for AS solutions at much lower concentrations (0.1%) by showing that this postprocessing caused delayed PL maxima for freshly etched GaAs and helped us to discover that a slowly proceeding photocorrosion becomes sensitive to the electric charge of surface immobilized bacteria (Dubowski et al. 2015). Consequently, we could detect live *E. coli* K12 at a detection limit of 10^3 CFU/mL which was improved from the previously reported 10^4 CFU/mL (Duplan et al. 2011). This method has the potential to lead to effective detection of bacteria at ~1 CFU/mL. Indeed, improving surface functionalization techniques, such as optimization of the amount of antibodies, or applying techniques such as filtration (Wu et al. 2016), chemotaxis

(Hassen et al. 2016) and electrophoresis (Bossi et al. 2000) could help to bring more bacteria to the surface of the biochip and might result in detection of lower concentrations of bacteria. A variety of filtration methods could be applied to concentrate bacterial suspensions (this method is currently employed in our lab to concentrate bacterial suspensions such as *E. coli* suspensions). By exposing the biochips to the concentrated bacteria, lower concentrations of bacteria would be detectable by our proposed biosensor. Chemotaxis is another technique which could help to immobilize more bacteria on the surface and improve LOD of the biosensor. It has been reported that producing a gradient of glucose in the vicinity of the GaAs biochip helps to bring more bacteria toward the surface (Hassen et al. 2016). They employed MUDA/EDC-NHS/Ab/bovine serum albumin (BSA)/β-galactosidase and b-PEG/MHDA/EDC-NHS/β-galactosidase/BSA/NA/b-Ab bio-architectures to create such a gradient. Electrophoresis is another approach which could be applied in our scheme to improve LOD of the biosensor. Since bacteria are electrically charged, a capillary electrophoresis (CE) unit (Bossi et al. 2000) could be coupled to our biosensor to separate bacteria and concentrate them before being injected into the flow cell. Another suggestion to improve LOD of the biosensor is modification of the flow cell (Chen et al. 2007; Jha et al. 2011; Jiang et al. 2014) in which the biochips are exposed to bacterial suspensions. An optimized flow cell should be designed to decrease laminar flow of bacteria and enhance number of bacteria captured by the biochips. The bacterial suspension could also be circulated over the surface of the biochips. Following this approach, bacteria would have more time to be captured by the biofunctionalized surface of the biochips and the number of bacteria immobilized on the surface would probably increase.

In the second phase of the project, we investigated the capture and growth of *E. coli* on bare and biofunctionalized surfaces of GaAs (001) and gold. We found that placing GaAs (001) samples on a Nutrient agar plate inoculated evenly with 10^5 CFU/mL of bacterial suspension did not inhibit bacterial growth, and bacteria were able to grow next to either bare or biofunctionalized surfaces of GaAs samples. In addition, it was revealed that bacteria can grow on the surface of biofunctionalized GaAs (001) samples when the samples were kept in a flow cell and exposed to bacteria and growth medium. However, no bacterial growth was observed on the GaAs surfaces in the flow cell when bacterial suspensions were employed at concentrations lower than 10^5 CFU/mL. This minimum threshold might be related to the toxicity of Ga or As ions released

from the GaAs wafers (Tanaka 2004) and distributed into the flow cell. At concentrations lower than 10^5 CFU/mL, the number of Ga and/or As ions per bacteria might be greater than the number of bacterial protective molecules such as siderophores or Fe ions, reach toxic levels, and affect bacterial viability and/or growth. At higher bacterial concentrations, the amount of Ga or As ions per bacteria might be lower than the bacterial capacity to neutralize them and thus not affect bacterial growth. Moreover, the reason for observing no bacterial growth for concentrations lower than 10^5 CFU/mL might also be related to the inhibition of bacterial growth by the antibodies used to capture the bacteria (Chalghoumi et al. 2009; Lin et al. 1998).

We employed two architectures based on PEG and MHDA thiols. In the first case, b-PEG/HDT/NA/b-Ab bio-architecture was used and in the second case, we employed EDC and NHS linkers to directly bind *E. coli* or to facilitate covalent binding of antibodies to the carboxyl-functionalized surface (MHDA/EDC-NHS or MHDA/EDC-NHS/Ab). It was observed that bacteria can grow on both architectures, however, the bacterial coverage and the bacterial growth rate were higher for the antibody coated surfaces than non-antibody coated ones. We also investigated the efficiency of two antibody-coated architectures, MHDA/EDC-NHS/Ab and b-PEG/HDT/NA/b-Ab, in terms of initial capture of bacteria. We noticed that the surface coverage with bacteria was higher on b-PEG/HDT/NA/b-Ab than MHDA/EDC-NHS/Ab for comparable concentrations of bacteria. Non-specific capture of bacteria with neutravidin might bias the b-PEG/HDT/NA/b-Ab approach.

By increasing the initial coverage of the surface with bacteria, it is possible that we could be able to observe bacterial growth with concentrations lower than 10^5 CFU/mL. The reason is that by increasing the number of bacteria immobilized on the surface, the ratio of Ga or As per bacteria decreases and, consequently, the dose might not reach the toxic levels. In addition, bacteria would be able to communicate with each other and promote other cells to grow. As explained before, increasing the surface coverage with bacteria could be achieved by applying some techniques such as chemotaxis (Hassen et al. 2016), filtration (Wu et al. 2016) or electrophoresis (Bossi et al. 2000).

Following successful growth of bacteria on GaAs surfaces, in the third phase of the project, we used PL emission of photocorroding GaAs/AlGaAs heterostructures to investigate growth and

bacterial reactions to antibiotics. For immobilization of bacteria, we employed the b-PEG/HDT/NA/b-Ab biofunctionalization architecture. This architecture was selected for our experiments because it provided higher efficiency in capturing bacteria compared with the MHDA/EDC-NHS/Ab bio-architecture. After immobilization of bacteria on the surface of the biochips, the samples were exposed to nutrient broth and antibiotic solutions and susceptibility of bacteria to antibiotics was investigated by *in situ* monitoring the PL emission of the heterostructures. As it was proved in the first phase of the project, the position of the PL maximum depended on the electric charge immobilized on the surface of PL emitting GaAs/AlGaAs biochips. The close proximity interaction of positively charged counter ions surrounding the bacteria with the surface of a GaAs/AlGaAs biochip could affect (reduce) transport of photo-excited holes to the semiconductor surface, resulting in a decreased photocorrosion rate of the biochip. Since dissolution of the GaAs cap material results in the appearance of a characteristic maximum in the PL plot collected over time, a decrease in the photocorrosion rate of the biochip results in a delayed formation of the characteristic PL maximum. Based on that, we could provide a calibration curve showing the dependence of the position of the PL maximum on the concentration of the bacterial suspension. This concept was further supported in the third phase of the project where we exposed the bacteria immobilized on the surface of the biochips to growth medium with or without antibiotics and deduced the reactions of bacteria to these environments by monitoring the photocorrosion rate (position of the PL maximum) of the biochips. We observed that while immobilization of bacteria on the surface of the biochip postponed the PL maximum, growth of these bacteria further delayed the PL maximum. When the bacteria grow, the increased number of bacteria on the biochip will increase the negative charge and thus protect the surface from photocorrosion and postpone the PL maximum. Another possible reason could be related to the release of hydrogen (H^+) ions during the metabolic activity of bacteria. H^+ ions are secreted by the bacteria to create a chemiosmotic or proton motive force associated with bacterial metabolism to synthesize ATP (Mitchell 2011). Our assumption is that immobilization of H^+ ions in the vicinity of the biosensor surface results in a reduced transport of photo-excited holes toward the surface and contributes to reduction of the photocorrosion rate. By comparing the position of the PL maximum for the biochip exposed to bacteria and growth medium with that of one exposed to

bacteria and antibiotic solution, the antibiotic sensitivity of the bacteria could be investigated. When bacteria grow, the PL maximum is delayed, but when exposed to an effective antibiotic, their growth is stopped and the PL maximum is advanced. Based on this method, we demonstrated the functionality of our biosensor for monitoring growth and antibiotic susceptibility of *E. coli* K12 (penicillin-sensitive) and *E. coli* HB101 (penicillin-resistant) bacteria at ambient temperature in less than 3 hours. The functionalization of the biochips with antibodies makes the process suitable for specific investigation of different bacteria, although it could also be applied for studying bacteria captured non-specifically, e.g., through covalent binding (Meyer et al. 2010; Nazemi et al. 2016), using adhesive polyphenolic proteins (Meyer et al. 2010) or supported lipid bilayers (SLB) (Afanasenkau and Offenhäusser 2012).

It should be noted that whereas in darkness bacteria were able to grow on GaAs surfaces if their concentration was at least 10^5 CFU/mL, the minimum concentration of bacteria necessary to grow on the biochips irradiated with the laser was at least 2×10^8 CFU/mL. The same suspension is also used to identify the bacteria by MALDI-tof (Wieser et al. 2012). The poisonous effects of gallium and arsenic were less of an issue when the biochips were kept in darkness, and where the release of Ga and As ions was at a lower rate. Photocorrosion provoked by laser illumination of the GaAs biochips gives rise to release of Ga and As ions. By corrosion of the GaAs biochips, Ga and As ions are released into the solution which could affect the viability and/or growth of bacteria. When the GaAs/AlGaAs biochip is irradiated with laser light, the concentration of h^+ near the surface of the biochip increases and, as the result, the photocorrosion rate is accelerated. Therefore, the minimum threshold of bacterial growth is higher when the samples are irradiated with the laser compared with samples kept in the dark.

It is worth mentioning that all the PL measurements for investigation of antibiotic susceptibility of bacteria were carried out at ambient temperature. The reason was that at 37º C the photocorrosion rate of the GaAs/AlGaAs heterostructures was accelerated and no discrimination was observed in the PL emission of the biochips exposed to different environments. However, it might be possible to operate the biosensor at 37º C by reduction of the exposure time of the biochip to the laser light and, consequently, reduce the photocorrosion rate of the biochip. Indeed the PL signals were collected in the period of 5 h for the biochips irradiated with 6 s

pulses with power density of 35 mW/cm^2 delivered every minute (duty cycle of 6s/60s). It could be possible to reduce the exposure time to 1 s (duty cycle of 1s/60s) or decrease the power density of the laser to 20 mW/cm^2. Working at 37º C, which is the optimum temperature for growth of *E. coli*, would enable us to monitor the antibiotic sensitivity of bacteria in a shorter period of time and, perhaps, for lower bacterial concentrations. We might also be able to reduce the time-to-result at room temperature by using GaAs/AlGaAs samples with thinner cap layers (less than 10 nm). This would result in speeding up the photocorrosion process and might allow us to detect differences between growth rates of intact and antibiotic affected bacteria in a shorter period of time. In addition, it is expected that by improving surface functionalization techniques, or by applying some methods such as chemotaxis, filtration and electrophoresis we could increase the initial coverage of the surface with bacteria and, consequently, monitor biological activities of bacteria at lower initial concentrations (less than 2×10^8 CFU/mL). The rapidity of the proposed biosensor, with the time-to-result of 3 h, can be considered as the main advantage of our platform over culture-based methods which are time-consuming and cannot produce same-day results. Although some rapid biosensing techniques such as PCR (Hombach et al. 2010) have been proposed for evaluation of antibiotic susceptibility of bacteria, these genetic methods require background knowledge of resistance genes (Quach et al. 2016) and they lack standardization (Cockerill 1999). Surface plasmon resonance (Chiang et al. 2009) and plasmonic nanohole arrays (Kee et al. 2013) are other methods introduced for rapid evaluation of growth and antimicrobial sensitivity of bacteria. However, the cost and the generally large size of sensitive SPR systems (Lazcka et al. 2007) and the demanding fabrication process necessary to make uniform plasmonic nanoholes (Kee et al. 2013) are inhibitory factors restricting application of these techniques to laboratory environments. Impedance (Rieder et al. 2009; Zavizion et al. 2010) and cytological methods (Quach et al. 2016) have also been developed to assess rapidly antibiotic sensitivity of bacteria. However, these methods often rely on very subtle changes and so may be difficult to bring to hospital laboratories without highly specialized technicians. The PL reader employed in our experiments is relatively inexpensive which shows the practical feasibility of this method. This approach has the potential of being applied in biological laboratories for rapid determination of antibiotic sensitivity of different

bacteria due to its small size, low cost and the potential of being automated for all the steps of the experiment (biofunctionalization of the biochips and PL measurements).

CHAPTER 7: Conclusions et perspectives

Dans les domaines de la microbiologie et de la médecine, il est important de surveiller les activités biologiques des bactéries exposées à des environnements spécifiques. Les méthodes classiques utilisées pour l'évaluation de la sensibilité des bactéries aux antibiotiques sont pour la plupart des techniques fondées sur la culture qui prennent du temps et ne peuvent pas fournir des résultats le même jour. Ce retard conduit au surtraitement d'un large éventail d'infections qui est coûteuse et parfois inefficace dans le cas d'infections virales. L'utilisation inappropriée et non ciblée des antibiotiques conduit à la résistance aux antibiotiques qui est un problème important pour la santé publique (Gootz 2010). Par conséquent, un procédé sensible, rapide et peu coûteux pour la détection de la croissance et de la sensibilité des bactéries aux antibiotique est nécessaire pour améliorer les procédures d'essai phénotypique utilisés dans les domaines pharmaceutiques.

Dans ce thèse, nous avons développé une méthode basée sur la PL pour surveiller la croissance et la sensibilité aux antibiotiques des bactéries immobilisées sur la surface des semi-conducteurs quantiques biofonctionnalisées. L'approche de ce projet a été basée sur la mesure du signal PL par des microstructures QS spécialement conçus. Le PL est très sensibles au niveau de la charge électrique accumulée sur la surface de ces microstructures. Nous avons remarqué que les bactéries qui se développent sur la surface de GaAs/AlGaAs biofonctionnalisèes affectent la PL des biopuces d'une manière différente de bactéries traitées aux antibiotiques ou tuées aux UV. Ainsi, en se servant de cette méthode, nous avons été en mesure de distinguer les bactéries résistantes aux antibiotiques des bactéries sensibles en moins de 3 heures. L'application de l'émission PL de semi-conducteurs pour étudier les réactions bactériennes aux antibiotiques est une approche relativement nouvelle, donc, il a plusieurs défis qui sont abordés dans les paragraphes suivants.

Le premier défi dans notre travail était de trouver un bio-architecture efficace pour immobiliser les bactéries sur la surface de biopuces GaAs/AlGaAs. Etant donné que la sensibilité du biocapteur proposé dépend du nombre de bactéries immobilisées sur sa surface, l'efficacité de la capture des bactéries sur la surface ou au voisinage du biocapteur est d'une grande importance. Le deuxième défi était de surveiller l'effet d'immobilisation bactérienne sur l'émission PL de

biopuces GaAs/AlGaAs. Ensuite, nous avons dû enquêter sur la croissance des bactéries immobilisées sur la surface de ces structures. En raison de la toxicité de Ga et As (DeLeon et al. 2009; Rzhepishevska et al. 2011; Tanaka 2004), il a fallu déterminer le nombre minimal de bactéries nécessaires pour permettre la croissance sur la surface des biopuces lorsque les échantillons ont été conservés dans l'obscurité ou irradié avec un laser (qui augmente la libération de Ga et As). Le dernier défi du travail était d'étudier la capacité de la méthode de surveillance PL à détecter la croissance et la sensibilité des bactéries aux antibiotique. Nous avons dû étudier si cette méthode est suffisamment sensible pour distinguer les bactéries résistantes aux antibiotiques des bactéries sensibles.

Dans la première phase du projet, un nouveau biocapteur photo-électrochimique a été développé pour détecter rapidement *E. coli* en suspension dans le PBS (1X). Le capteur comprend une hétérostructure GaAs/AlGaAs émettant la PL. Le GaAs sert de couche de recouvrement et elle subit la photocorrosion lorsqu'elle est irradiée par un laser. Le taux de photocorrosion des couches de GaAs et de AlGaAs dépend de la puissance du laser et de l'électrolyte dans lequel l'hétérostructure a été irradiée, tel que du PBS, de l'eau ou du bouillon LB. La photocorrosion est également influencée par le niveau de la charge électrique immobilisée sur ou au voisinage de la surface de l'hétérostructure. Par conséquent, la surveillance de la photocorrosion de l'hétérostructure à l'aide de la PL permettrait de détecter la présence de molécules chargées, telles que les bactéries, dans l'électrolyte et de déterminer leurs concentration.

Le photocorrosion de GaAs dépend fortement de la présence de molécules chargées positivement minoritaires (h^+) sur la surface de ce matériel (Choi et al. 2002; Ruberto et al. 1991). Dans nos expériences, où des biopuces GaAs/AlGaAs ont été immergées dans une solution d'électrolyte que nous avons irradié avec des photons, les photo-trous ont été formés à la surface de GaAs, ce qui a contribué à la formation d'oxydes superficiels dominés par Ga_2O_3 (Choi et al. 2002). C'est la formation de cet oxyde qui a réduit la densité des états de surface et provoquer une diminution de la SRV des électrons et des trous qui a conduit à l'intensité croissante du signal PL émis par le GaAs, tel que rapporté (Passlack et al. 1995). Les oxydes de surface ont été dissous dans la solution lorsque le GaAs a photocorrodé. Lors de la photocorrosion du GaAs, une nouvelle interface avec AlGaAs a été formée, qui a conduit a une diminution rapide du signal PL et à la formation d'un maximum sur le signal temporel dépendant

PL. La formation de ce maximum peut être accélérée ou retardée en fonction de l'interaction électrostatique entre le semiconducteur et les molécules immobilisées dans son voisinage. Il a été suggéré que l'immobilisation des molécules de donneur d'électrons sur la surface d'un semiconducteur n-type diminue la bande de flexion et la région d'appauvrissement du semi-conducteur en raison de la formation d'ions chargés positivement sur la surface (Zhang et Yates Jr. 2012). Ainsi, après cette immobilisation, la concentration des trous de surface diminue et, par conséquent, le processus de photocorrosion est retardée. Il convient de noter que la surface de la plupart des bactéries est chargée négativement à un pH supérieur à 4 (Poortinga et al. 2002). Lorsque les bactéries sont mises en suspension dans une solution, comme PBS (1X), la surface bactérienne serait entourée par des contre-ions chargés positivement qui étaient présents dans la solution. Étant donné que le GaAs étudié dans notre travail se comportait, à la température ambiante, comme un matériel n-type, l'immobilisation des bactéries décorées avec des ions chargés positivement sur la surface de la biopuce devrait contribuer à réduire le transport de trous photo-excités à la surface et réduire le taux de photocorrosion des biopuces GaAs/AlGaAs (retarder la formation de la valeur maximale caractéristique PL). Nous avons observé, tel que démontré dans les Figure 26, Figure 39 et Figure 40, que plus la concentration bactérienne était élevée, plus le maximum PL a été retardé et, sans aucun doute, plus le taux de photocorrosion aura été ralentie.

Pour immobiliser les bactéries, la couche extérieure (couche de surface) de l'hétérostructure a été fonctionnalisé avec un réseau d'anticorps biotinylés interfacés avec les thiols PEG et HDT biotinylés via le lien fourni par la neutravidine (b-PEG/HDT/NA/b-Ab). Pour augmenter la stabilité photonique de nos biopuces dans des environnements biologiques et d'améliorer la sensibilité de notre biocapteur, les biopuces biofonctionnalisées ont reçu un post-traitement avec AS. Il a été suggéré que le post-traitement d'échantillons de GaAs SAM-enduits avec une solution d'AS 20% pendant 15 min augmente la concentration des atomes de soufre réagissant avec Ga et As et améliore la passivation de la surface d'échantillons de GaAs (Arudra et al. 2012). Par conséquent, la stabilité photonique de ces biopuces a été améliorée dans des solutions aqueuses (Arudra et al. 2012). Nous avons confirmé cette observation pour les solutions AS à des concentrations beaucoup plus faibles (0.1%) en montrant que ce post-traitement a provoqué un retard maxima PL pour le GaAs fraîchement gravés, et de plus nous avons pu détecter en

direct *E. coli* K12 avec une limite de détection de 10^3 UFC/ml qui était une amélioration sur la valeur 10^4 UFC/ml précédemment rapportée (Duplan et al. 2011). Selon les données PL, il semble que cette méthode a le potentiel de conduire à une détection efficace des bactéries à ~ 1 UFC/ml. En effet, les techniques d'application tels que la chimiotaxie (Hassen et al. 2016), l'électrophorèse (Bossi et al. 2000) et la filtration (Wu et al. 2016) pourrait contribuer à apporter plus de bactéries à la surface de la biopuce et pourrait conduire à la détection de plus faibles concentrations de bactéries. Nous pourrions appliquer la filtration afin de concentrer les suspensions bactériennes (cette méthode est actuellement utilisée dans notre laboratoire pour concentrer des suspensions bactériennes telles que *E. coli*) et ensuite exposer les biopuces aux bactéries concentrées. Selon cette approche, des concentrations plus faibles de bactéries seraient détectables par notre biocapteur proposé. La chimiotaxie est une autre technique qui pourrait aider à immobiliser plus de bactéries sur la surface et améliorer la LOD de bactéries. Il a été rapporté que la production d'un gradient de glucose dans le voisinage de la biopuce GaAs permet d'apporter plus de bactéries vers la surface (Hassen et al. 2016). Ils ont utilisé des bio-architectures de MUDA/EDC-NHS/Ab/albumine de sérum bovin (BSA)/β-galactosidase et b-PEG/MHDA/EDC-NHS/β-galactosidase/BSA/NA/b-Ab pour créer un tel gradient. L'électrophorèse est une autre approche qui pourrait être appliquée dans notre système pour augmenter la sensibilité du biocapteur. Etant donné que les bactéries sont électriquement chargées, une électrophorèse capillaire (CE), (Bossi et al. 2000) peut être couplé à notre biocapteur pour séparer les bactéries et les concentrer avant d'être injecté dans la cellule d'écoulement. Selon cette approche, la sensibilité du biocapteur augmenterait. Une autre suggestion pour augmenter la sensibilité du biocapteur est une modification de la cellule d'écoulement (Chen et al. 2007; Jha et al. 2011; Jiang et al. 2014), dans lequel les biopuces sont exposés à des suspensions bactériennes. Une cellule d'écoulement optimisée devrait être conçue pour diminuer le flux laminaire de bactéries et d'améliorer la quantité de bactéries capturées par les biopuces. La suspension bactérienne pourrait également être distribuée sur la surface des biopuces. Suivant cette approche, les bactéries ont plus de temps à être capturées par la surface biofonctionnalisées des biopuces et le nombre de bactéries immobilisées sur la surface serait probablement augmenté.

Dans la deuxième phase du projet, nous avons étudié la capture et la croissance d'*E. coli* sur des

surfaces nues ou biofonctionnalisées de GaAs (001) et de l'or. Nous avons découvert que le dépôt d'une plaque de GaAs (001) sur une gélose nutritive ensemencée uniformément avec 10^5 UFC/ml de suspension bactérienne n'a pas inhibé la croissance bactérienne, et les bactéries sont capables de croître en contact avec des surfaces nues ou biofonctionnalisées de GaAs. En outre, il a été révélé que les bactéries peuvent se développer sur la surface biofonctionnalisée de GaAs (001) lorsque les échantillons ont été maintenus dans une cellule d'écoulement et exposés à des bactéries dans un milieu de croissance. Cependant, aucune croissance bactérienne n'a été observée sur les surfaces de GaAs dans la cellule d'écoulement lorsque des suspensions bactériennes ont été utilisées à des concentrations inférieures à 10^5 UFC/ml. Ce seuil minimum peut être lié à la toxicité d'ions Ga ou As libérés par les plaquettes de GaAs (Tanaka 2004) et distribué dans la cellule d'écoulement. À des concentrations inférieures à 10^5 UFC/ml, le nombre d'ions Ga et/ou As en solution peut être supérieur au nombre de molécules protectrices bactériennes telles que des sidérophores ou des ions Fe, atteindre des niveaux toxiques et affecter la viabilité et/ou la croissance bactérienne. A des concentrations plus élevées de bactéries, le nombre d'ions Ga ou As peut être inférieure à la capacité des bactéries à les neutraliser et ainsi ne pas nuire à la croissance bactérienne.

Nous avons utilisé deux architectures basées sur les PEG et MHDA thiols. Dans le premier cas, la bio-architecture b-PEG/HDT/NA/b-Ab a été utilisée et dans le second cas, nous avons utilisé EDC et NHS pour lier directement *E. coli* ou pour faciliter la liaison des anticorps par lien covalent à la surface fonctionnalisée (MHDA/EDC-NHS ou MHDA/EDC-NHS/Ab). On a observé que les bactéries peuvent croître sur les deux architectures, cependant, la couverture bactérienne et le taux de croissance des bactéries étaient plus élevés sur les surfaces revêtues d'anticorps en comparaison avec les surfaces nues. Nous avons également étudié l'efficacité des deux architectures recouvertes d'anticorps, MHDA/EDC-NHS/Ab et b-PEG/HDT/NA/b-Ab, en termes de capture initiale des bactéries. Nous avons remarqué que la couverture des surfaces avec des bactéries était plus élevée sur b-PEG/HDT/NA/b-Ab que sur MHDA/EDC-NHS/Ab pour des concentrations comparables de bactéries. Cependant, la capture non spécifique des bactéries par la neutravidine pourrait biaiser l'approche b-PEG/HDT/ NA/b-Ab.

En augmentant la couverture initiale de la surface avec des bactéries, il est possible que l'on pourrait être capable d'observer la croissance bactérienne à des concentrations inférieures à 10^5

UFC/ml. La raison en est que, en augmentant le nombre de bactéries immobilisées sur la surface, le rapport entre Ga et As/bactérie diminue et, par conséquent, la dose peut ne pas atteindre les niveaux toxiques. Comme expliqué précédemment, l'augmentation de la couverture de la surface avec des bactéries peut être obtenue en appliquant des techniques telles que la chimiotaxie (Hassen et al. 2016), la filtration (Wu et al. 2016) ou l'électrophorèse (Bossi et al. 2000).

Après une croissance réussie de bactéries sur les surfaces de GaAs, dans la troisième phase du projet, nous avons étudié la sensibilité des bactéries aux antibiotiques en suivant l'émission PL lors de la photocorrosion des hétérostructures GaAs/AlGaAs. Pour l'immobilisation des bactéries, nous avons utilisé l'architecture b-PEG/HDT/NA/b-Ab. Cette architecture a été sélectionnée pour nos expériences parce qu'il a fourni une plus grande efficacité dans la capture des bactéries par rapport à la bio-architecture MHDA/EDC-NHS/Ab. Après l'immobilisation de bactéries sur la surface des biopuces, les échantillons ont été exposés à un bouillon nutritif et à des solutions d'antibiotiques. La sensibilité des bactéries aux antibiotiques a été étudiée *in situ* par la surveillance de l'émission de PL des hétérostructures. Comme il a été démontré dans la première phase du projet, la position du maximum PL dépendait de la charge électrique immobilisée sur la surface des biopuces. L'interaction étroite de proximité des contre-ions chargés positivement entourant les bactéries avec la surface d'une biopuce GaAs/AlGaAs pourrait affecter (réduire) le transport des trous photo-excités à la surface des semi-conducteurs, ce qui entraînerait un taux de photocorrosion diminué de la biopuce (retardé l'apparition du maximum caractéristique PL). Sur cette base, nous pourrions fournir une courbe d'étalonnage montrant la dépendance de la position du maximum PL sur la concentration de la suspension bactérienne. Ce concept a également été évoqué dans la troisième phase du projet où nous avons exposé les bactéries immobilisées sur la surface des biopuces à un milieu de croissance avec ou sans antibiotiques et déduit les réactions des bactéries à ces environnements en surveillant le taux de photocorrosion (position du PL maximum) des biopuces. Nous avons observé que, bien que l'immobilisation des bactéries à la surface de la biopuce a retardé l'apparition du maximum de PL, la croissance de ces bactéries a retardé encore davantage ce maximum PL. Lorsque les bactéries se développent, l'augmentation du nombre de bactéries sur la biopuce va augmenter la charge négative et donc protéger la surface de la photocorrosion et de reporter le maximum PL.

Une autre raison possible pourrait être lié à la libération des ions hydrogène (H^+) au cours de l'activité métabolique des bactéries. Les ions H^+ sont sécrétées par les bactéries pour créer une force motrice protonique ou chimioosmotique associée au métabolisme bactérien pour synthétiser de l'ATP (Mitchell 2011). Notre hypothèse est que l'immobilisation d'ions H^+ dans le voisinage de la surface du biocapteur résulte en la transport réduit de trous photo-excités vers la surface et contribue à la réduction du taux de photocorrosion. En comparant la position du maximum de la biopuce PL exposés à des bactéries et un milieu de croissance à celle d'une exposition à des bactéries et une solution antibiotique, la sensibilité aux antibiotiques des bactéries pourrait être évaluée. Lorsque les bactéries se développent, le maximum PL est retardé, mais lorsqu'elle est exposée à un antibiotique efficace, leur croissance est stoppée et le maximum PL est avancé. Sur la base de cette méthode, nous avons démontré la fonctionnalité de notre biocapteur pour surveiller la croissance et la sensibilité aux antibiotiques d'*E. coli* K12 (sensible à la pénicilline) et d'*E. coli* HB101 (résistant à la pénicilline) à la température ambiante en moins de 3 heures.

Il convient de noter que, dans l'obscurité, les bactéries sont capables de croître sur les surfaces GaAs si leur concentration est d'au moins 10^5 UFC/ml, la concentration minimale de bactéries nécessaires à la croissance sur les biopuces irradiés par le laser est d'au moins 2×10^8 UFC/ml. Cette même suspension serait également utilisée pour identifier les bactéries par MALDI-TOF (Wieser et al. 2012). Les effets toxiques de gallium et de l'arsenic étaient moins un problème lorsque les biopuces ont été maintenus dans l'obscurité, et que la libération des ions Ga et As était au minimum. La photocorrosion provoquée par illumination laser des biopuces GaAs donne lieu à la libération d'ions Ga et As qui pourrait affecter la viabilité et/ou la croissance des bactéries. Lorsque la biopuce GaAs/AlGaAs est irradié avec une lumière laser, la concentration de h^+ à la surface de la biopuce augmente et, en conséquence, le taux de photocorrosion est accélérée. Par conséquent, le seuil minimal de la croissance bactérienne est plus élevé lorsque les échantillons sont irradiés par le laser par rapport à des échantillons conservés à l'obscurité.

Il est à noter que toutes les mesures PL d'investigation de la sensibilité aux antibiotiques des bactéries ont été réalisées à température ambiante. La raison en est que, à 37º C, le taux de photocorrosion de hétérostructures GaAs/AlGaAs a été accélérée et aucune discrimination n'a été observée dans l'émission PL des biopuces exposés à des environnements différents.

Toutefois, il pourrait être possible de faire fonctionner le biocapteur à 37° C par réduction de la durée d'exposition de la biopuce à la lumière laser et, par conséquent, de réduire le taux de photocorrosion de la biopuce. En effet, les signaux PL ont été recueillies dans la période de 5 h pour les biopuces irradiées avec les impulsions de 6 s avec une densité de puissance de 35 mW/ cm^2 livré chaque minute (cycle de service de 6s/60s). Il pourrait être possible de réduire le temps d'exposition à 1 s (cycle de service de 1s/60s) ou de diminuer la densité de puissance du laser à 20 mW/cm^2. Travailler à 37º C qui est la température optimale pour la croissance d'*E. coli* nous permettrait de surveiller la sensibilité aux antibiotiques des bactéries dans un plus court laps de temps et, peut-être, pour des concentrations bactériennes inférieures. En outre, il est prévu que, en appliquant des méthodes telles que la chimiotaxie, ou l'amélioration des techniques de fonctionnalisation de surface, on peut augmenter la couverture initiale de la surface avec des bactéries et, par conséquent, de contrôler les activités biologiques des bactéries à des concentrations initiales plus faibles (moins de 2×10^8 UFC/ml). La rapidité du biocapteur proposé, avec un temps de résultat de 3 h, peut être considéré comme le principal avantage de notre plate-forme sur les méthodes de culture qui prennent du temps et ne peuvent pas produire des résultats le même jour. Bien que certaines techniques de biologie moléculaire telles que la PCR (Hombach et al. 2010) ont été proposés pour l'évaluation de la sensibilité aux antibiotiques des bactéries, ces méthodes génétiques nécessitent des connaissances de base des gènes de résistance (Quach et al. 2016) et ils manquent de standardisation (Cockerill 1999). La résonance plasmonique de surface (Chiang et al. 2009) et des réseaux de nanotrous plasmoniques (Kee et al. 2013) ont également été introduites pour une évaluation rapide de la croissance et de la sensibilité des bactéries aux antimicrobiens. Cependant, le coût et la grande taille des systèmes SPR sensibles (Lazcka et al. 2007) ainsi que le processus exigeant de fabrication nécessaire pour faire des nanotrous plasmoniques uniformes (Kee et al. 2013) sont des facteurs inhibiteurs limitant l'application de ces techniques à des environnements de laboratoire clinique. L'impédance (Rieder et al. 2009; Zavizion et al. 2010) et les méthodes cytologiques (Quach et al. 2016) ont également été développés pour évaluer rapidement la sensibilité des bactéries aux antibiotiques. Cependant, ces méthodes reposent souvent sur des changements subtils variables et peuvent donc être difficiles à apporter aux laboratoires hospitaliers sans techniciens hautement spécialisés. Le lecteur PL employé dans nos expériences est relativement peu coûteux

qui montre la faisabilité pratique de cette méthode. Cette approche a le potentiel d'être appliquée dans les laboratoires biologiques pour la détermination rapide de la sensibilité aux antibiotiques des bactéries différentes en raison de sa petite taille, son faible coût et le potentiel d'être automatisé pour toutes les étapes de l'expérience (biofonctionnalisation des biopuces et des mesures PL).

REFERENCES

Absolom, D. R., Lamberti, F.V., Policova, Z., Zingg, W., van Oss, C.J., Neumann, A.W. (1983). Surface thermodynamics of bacterial adhesion. *Applied and Environmental Microbiology*, volume 46(1), p. 90-97.

Adamowicz, B., Ikeya, K., Mutoh, M., Saitoh, T., Fujikura, H., Hasegawa, H. (1998). Photoluminescence characterization of air exposed AlGaAs surface and passivated ex situ by ultrathin silicon interface control layer. *Physica E*, volume 2, p. 261-266.

Adams, M., Moss, M. (2008). *Food Microbiology(3rdedtn)*. UK RSC press.

Addis, M., Sisay, D. (2015). A Review on Major Food Borne Bacterial Illnesses. *Journal of Tropical Disease*, volume 3, p. 176.

Adlkofer, K., Duijs, E. F., Findeis, F., Bichler, M., Zrenner, A., Sackmann, E., Abstreiter, G., Tanaka, M. (2002). Enhancement of photoluminescence from near-surface quantum dots by suppression of surface state density. *Physical Chemistry Chemical Physics,* volume 4, p. 785-790.

Adlkofer, K., Shaporenko, A., Zharnikov, M., Grunze, M., Ulman, A., Tanaka, M. (2003). Chemical Engineering of Gallium Arsenide Surfaces with 4'-Methyl-4-mercaptobiphenyl and 4'-Hydroxy-4-mercaptobiphenyl Monolayers. *The Journal of Physical Chemistry B*, volume 107, p. 11737-11741.

Adlkofer, K., Tanaka, M., Hillebrandt, H., Wiegand, G., Sackmann, E., Bolom, T., Deutschmann, R., Abstreiter, G. (2000). Electrochemical passivation of gallium arsenide surface with organic self-assembled monolayers in aqueous electrolytes. *Applied Physics Letters*, volume 76, p. 3313.

Afanasenkau, D., Offenhäusser, A. (2012). Positively charged supported lipid bilayers as a biomimetic platform for neuronal cell culture. *Langmuir*, volume 28(37), p. 13387-13394.

Akerlund, T., Nordstorm, K., Bernander, R. (1995). Analysis of cell size and DNA content in exponentially growing and stationary phase batch cultures of *Escherichia coli*. *Journal of Bacteriology*, volume 177, p. 6791-6797.

Alayo, M. I., Pereyra, I., Scopel, W. L., Fantini, M. C. A. (2002). On the nitrogen and oxygen incorporation in plasma-enhanced chemical vapor deposition (PECVD) SiOxNy films. *Thin Solid Films*, volume 402(1-2), p. 154-161.

Alves, C. S., Melo, M. N., Franquelim, H. G., Ferre, R., Planas, M., Feliu, L., Bardaji, E., Kowalczyk, W., Andreu, D., Santos, N. C., Fernandes, M. X., Castanho, M. A. R. B. (2010). *Escherichia coli* Cell Surface Perturbation and Disruption Induced by Antimicrobial Peptides BP100 and pepR. *The Journal of Biological Chemistry*, volume 285(36), p. 27536–27544.

An, Y. H., Friedman, R. J. (2000). *Handbook of Bacterial Adhesion; Principles, Methods, and Applications*. Humana Press Inc, Totowa, New Jersey.

Arnold, R., Azzam, W., Terfort, A., Wöll, C. (2002). Preparation, Modification, and Crystallinity of Aliphatic and Aromatic Carboxylic Acid Terminated Self-Assembled Monolayers. *Langmuir,* volume 18(10), p. 3980–3992.

Arudra, P., Marshall, G. M., Liu, N., Dubowski, J. J. (2012). Enhanced Photonic Stability of GaAs in Aqueous Electrolyte Using Alkanethiol Self-Assembled Monolayers and Postprocessing with Ammonium Sulfide. *The Journal of Physical Chemistry C*, volume 116, p. 2891−2895.

Arudra, P., Nguiffo-Podie, Y., Frost, E. H., Dubowski, J. J. (2010). Decomposition of Thimerosal and Dynamics of Thiosalicylic Acid Attachment on GaAs(001) Surface Observed with in Situ Photoluminescence. *Journal of Physical Chemistry*, volume C 114, p. 13657-13662.

Atkins, S. D., Clark, I. M. (2004). Fungal molecular diagnostics: a mini review. *Journal of Applied Genetics*, volume 45(1), p. 3-15.

Atlas, R. M. (1988). *Microbiology Fundamentals and Applications*, 2nd ed. Macmillan Publishing Company, New York.

Aziziyan, M. R., Hassen, W. M., Morris, D., Frost, E. H., Dubowski, J. J. (2016). Photonic biosensor based on photocorrosion of GaAs/AlGaAs quantum heterostructures for detection of Legionella pneumophila. *Biointerphases,* volume 11(1), p. 019301.

Babacan, S., Pivarnik, P., Letcher, S., Rand, A. (2002). Piezoelectric Flow Injection Analysis Biosensor for the Detection of *Salmonella Typhimurium*. *Journal of Food Science,* volume 67, p. 314-320.

Badcock, M., Editor, D. (2012). Developments and applications of electrophoresis. Royal Society of Chemistry. http://blogs.rsc.org/ay/2012/01/12/developments-and-applications-of-electrophoresis/.

Bain, C. D., Evall, J., Whitesides, G. M. (1989). Formation of monolayers by the coadsorption of thiols on gold: variation in the head group, tail group, and solvent. *Journal of the American Chemical Society*, volume 111(18), p. 7155-7164.

Bandekar, J. (1992). Amid modes and protien conformation. *Biochimica et Biophysica Acta,* volume 1120, p. 123-143.

Barreiros dos Santos, M., Agusil, J.P., Prieto-Simon, B., Sporer, C., Teixeira, V., Samitier, J. (2013). Highly sensitive detection of pathogen *Escherichia coli* O157:H7 by electrochemical impedance spectroscopy. *Biosensors and Bioelectronics*, volume 45, p. 174-180.

Barrios, C. A., Bañuls, M. J., González-Pedro, V., Gylfason, K. B., Sánchez, B., Griol, A., Maquieira, A., Sohlström, H., Holgado, M., Casquel, R. (2008). Label-free optical biosensing with slot-waveguides. *Optics Letters* , volume 33(7), p. 708-710.

Bartlett, J. M. S., Stirling, D. (2003). A Short History of the Polymerase Chain Reaction. *Methods in Molecular Biology*, volume 226, p. 3-6.

Baumgartner, P., Engel, C., Abstreiter, G., Bohm, G., Weimann, G. (1995). Fabrication of lateral npn-phototransistors with high gain and sub-micrometer spatial resolution. *Applied Physics Letters*, volume 66(6), p. 751.

Baz, M., Abed, Y., Boivin, G. (2007). Characterization of drug-resistant recombinant influenza A/H1N1 viruses selected in vitro with peramivir and zanamivir. *Antiviral Research*, volume 74(2), p. 159-162.

Bennett, P. M. (2008). Plasmid encoded antibiotic resistance: acquisition and transfer of antibiotic resistance genes in bacteria. *British Journal of Pharmacology*, volume 153(Suppl 1), p. S347-S357.

Berg, H. C. (2004). *E. coli in Motion*. Springer, New York.

Bergmans, D. C., Bonten, M. J., Gaillard, C. A., van Tiel, F. H., van der Geest, S., de Leeuw, P. W., Stobberingh, E. E. (1997). Indications for antibiotic use in ICU patients: a one-year prospective surveillance. *Journal of Antimicrobial Chemotherapy,* volume 39(4), p. 527-535.

Bergveld, P. (1970). Development of an Ion-Sensitive Solid-State Device for Neurophysiological Measurements. *IEEE Transactions on Bio-Medical Engineering,* volume BME-17, p. 70-71.

Bergveld, P. (2003). Thirty years of ISFETOLOGY: What happened in the past 30 years and what may happen in the next 30 years. *Sensors and Actuators B: Chemical*, volume 88(1), p. 1-20.

Bernhardt, M., Pennell, D. R., Almer, L. S., Schell, R. F. (1991). Detection of bacteria in blood by centrifugation and filtration. *Journal of Clinical Microbiology,* volume 29(3), p. 422-425.

Besant, J. D., Sargent, E. H., Kelley, S. O. (2015). Rapid electrochemical phenotypic profiling of antibiotic-resistant bacteria. *Lab on a Chip,* volume 15, p. 2799–2807.

Bessolov, V. N., Konenkova, E. V., Lebedev, M. V. (1997). A Comparison of the Effectiveness of GaAs Surface Passivation with Sodium and Ammonium Sulfide Solutions. *Physics of the Solid State*, volume 39, p. 54−57.

Bienaime, A., Leblois, T., Gremaud, N., Chaudon, M.-J., Osta, M. E., Pecqueur, D., Ducoroy, P., Elie-Caille, C. (2013). Influence of a thiolate chemical layer on GaAs (100) biofunctionalization: An original approach coupling atomic force microscopy and mass spectrometry methods. *Materials,* volume 6(11), p. 4946-4966.

Blais, B. W., Leggate, J., Bosley, J., Martinez-Perez, A. (2004). Comparison of fluorogenic and chromogenic assay systems in the detection of *Escherichia coli* O157 by a novel polymyxin-based ELISA. *Letters in Applied Microbiology*, volume 39, p. 516-522.

Bobbitt, J. A., Betts, R. P. (1992). The removal of bacteria from solutions by membrane filtration. *Journal of Microbiological Methods*, volume 16(3), p. 215-220.

Boi, P., Manti, A., Pianetti, A., Sabatini, L., Sisti, D., Rocchi, M. B., Bruscolini, F., Galluzzi, L., Papa, S. (2015). Evaluation of *Escherichia coli* viability by flow cytometry: A method for determining bacterial responses to antibiotic exposure. *Cytometry Part B: Clinical Cytometry*, volume 88(3), p. 149-153.

Borchert, H., Talapin, D. V., McGinley, C., Adam, S., Lobo, A., de Castro, A. R. (2003). *The Journal of Chemical Physics*, volume 119, p. 1800-1807.

Bossi, A., Piletsky, S. A., Righetti, P. G., Turner, A. P. F. (2000). Capillary electrophoresis coupled to biosensor detection. *Journal of Chromatography A*, volume 892(1–2), p. 143-153.

Bott, T. R. (1998). Techniques for reducing the amount of biocide necessary to counteract the effects of biofilm growth in cooling water systems. *Applied Thermal Engineering,* volume 18(11), p/ 1059-1066.

Braga, P. C., Bovio, C., Culici, M., Dal Sasso, M. (2003). Flow Cytometric Assessment of Susceptibilities of Streptococcus pyogenes to Erythromycin and Rokitamycin. *Antimicrobial Agents and Chemotherapy*, volume 47(1), p. 408-412.

Bremera, P. J., Geesey, G. G. (1991). An evaluation of biofilm development utilizing non-destructive attenuated total reflectance Fourier transform infrared spectroscopy. *Biofouling: The Journal of Bioadhesion and Biofilm Research*, volume 3, p. 89–100.

Brooks, B. W., Devenish, J., Lutze-Wallace, C. L., Milnes, D., Robertson, R. H., Berlie-Surujballi, G. (2004). Evaluation of a monoclonal antibody-based enzyme-linked immunosorbent assay for detection of Campylobacter fetus in bovine preputial washing and vaginal mucus samples. *Veterinary Microbiology*, volume 103, p. 77-84.

Budz, H. A., Ali, M. M., Li, Y., LaPierre, R. R. (2010). Photoluminescence model for a hybrid aptamer-GaAs optical biosensor. *Journal of Applied Physics*, volume 107, p. 104702.

Budz, H. A., Biesinger, M. C., LaPierre, R. R. (2009). Passivation of GaAs by octadecanethiol self-assembled monolayers deposited from liquid and vapor phases. *Journal of Vacuum Science and Technology B,* volume 27(2), p. 637-648.

Busscher, H. J., Bos, R., van der Mei, H. C., Handley, P. S. (2000). *Physicochemistry of microbiol adhesion from an overall approach to the limits*. Marcel Dekker, New York.

Busscher, H. J., van Der Mei, R. B. H. C. (1995). Initial microbial adhesion is a determinant for the strength of biofilm adhesion. *Federation of European Microbiological Societies (FEMS) Microbiology Letters,* volume 128(3), p. 229-234.

Busscher, H. J., Weerkamp, A. H., van der Mei, H. C., van Pelt, A. W., de Jong, H. P., Arends, J. (1984). Measurement of the surface free energy of bacterial cell surfaces and its relevance for adhesion. *Applied and Environmental Microbiology,* volume 48(5), p. 980–983.

Cabral, J. P. S. (2010). Water Microbiology. Bacterial Pathogens and Water. *International Journal of Environmental Research and Public Health*, volume 7(10), p. 3657-3703.

Carlet, J., Rambaud, C., Pulcini, C. (2014). Save Antibiotics: a call for action of the World Alliance Against Antibiotic Resistance (WAAAR). *BMC Infectious Diseases,* volume 14(1), p. 1-4.

Carpenter, M. S., Melloch, M. R., Cowans, B. A., Dardas, Z., Delgass, W. N. (1989). Investigations of Ammonium Sulfide Surface Treatments on GaAs. *Journal of Vacuum Science and Technology B*, volume 7, p. 845.

Casey, A. L., Karpanen, T. J., Nightingale, P., Cook, M., Elliott, T. S. J. (2012). Microbiological comparison of a silver-coated and a non-coated needleless intravascular connector in clinical use. *Journal of Hospital Infection,* volume 80(4), p. 299-303.

CDC (2011). Estimates of Foodborne Illness in the United States. Centers for Disease Control and Prevention.

CDC (2013). Antibiotic Resistance Threats in the United States. Centers for Disease Control and Prevention, US Department of Health and Human Services.

CDC (2016a). Antibiotic / Antimicrobial Resistance. Centers for Disease Control and Prevention.

CDC (2016b). Legionella (Legionnaires' Disease and Pontiac Fever). Centers for disease control and prevention.

Chalghoumi, R., Thewis, A., Beckers, Y., Marcq, C., Portetelle, D., Schneider, Y. J. (2009). Adhesion and growth inhibitory effect of chicken egg yolk antibody (IgY) on Salmonella enterica serovars Enteritidis and Typhimurium in vitro. *Foodborne Pathogens and Disease,* volume 6(5), p. 593-604.

Challice, C. E., Gorrill, R. H. (1954). Some observations on the morphological changes in *E. coli* accompanying induction by ultraviolet light. *Biochimica et Biophysica Acta*, volume 14, p. 482-487.

Chen, G., Wang, Y., Yang, P. (2005). Amperometric biosensor coupled to capillary electrophoresis for glucose determination. *Microchimica Acta*, volume 150(3), p. 239-245.

Chen, Z., Mauk, M. G., Wang, J., Abrams, W. R., Corstjens, P. L., Niedbala, R. S., Malamud, D., Bau, H. H. (2007). A microfluidic system for saliva-based detection of infectious diseases. *Annals of the New York Academy of Sciences*, volume 1098, p. 429-436.

Chiang, Y. L., Lin, C. H., Yen, M. Y., Su, Y. D., Chen, S. J., Chen, H. F. (2009). Innovative antimicrobial susceptibility testing method using surface plasmon resonance. *Biosensors and Bioelectronics,* volume 24(7), p. 1905-1910.

Cho, I.-H., Paek, E.-H., Lee, H., Kang, J. Y., Kim, T. S., Paek, S.-H. (2007). Site-directed biotinylation of antibodies for controlled immobilization on solid surfaces. *Analytical Biochemistry,* volume 365(1), p. 14-23.

Choi, J., Jung, Y. G., Kim, J., Kim, S., Jung, Y., Na, H., Kwon, S. (2013). Rapid antibiotic susceptibility testing by tracking single cell growth in a microfluidic agarose channel system. *Lab Chip*, volume 13(2), p. 280-287.

Choi, K. J., Moon, J. K., Park, M. K., Kim, H., Lee, J. (2002). Effects of Photowashing Treatment on Gate Leakage Current of GaAs Metal-Semiconductor Field-Effect Transistors. *Japanese Journal of Applied Physics,* volume 41(5R), p. 2894.

Christensen, G. D., Simpson, W. A., Anglen, J. O., Gainor, B. J. (2000). *Methods for evaluating attached bacetria and biofilms*. *Handbook of bacterial adhesion*. Humana Press Inc., Totowa, NJ.

Clark, L. C., Lyons, C. (1962). Electrode systems for continous monitoring in cardiovascular surgery. *Annals of the New York Academy of Sciences*, volume 102(1), p. 29-45.

Cockerill, F. R. (1999). Genetic methods for assessing antimicrobial resistance. *Antimicrobial Agents and Chemotherapy*, volume 43(2), p. 199-212.

Cohenford, M. A., Rigas, B. (1998). Cytologically normal cells from neoplastic cervical samples display extensive structural abnormalities on IR spectroscopy: Implications for tumor biology. *Proceedings of the National Academy of Sciences of the United States of America,* volume 95(26), p. 15327-15332.

Cotto, A., Looper, J. K., Mota, L. C., Son, A. (2015). Quantitative Polymerase Chain Reaction for Microbial Growth Kinetics of Mixed Culture System. *Journal of Microbiology and Biotechnology*, volume 25(11), p. 1928-1935.

Cuerrier, C. M., Chabot, V., Vigneux, S., Aimez, V., Escher, E., Gobeil, F., Charette, P. G., Grandbois, M. (2008). Surface Plasmon Resonance Monitoring of Cell Monolayer Integrity: Implication of Signaling Pathways Involved in Actin-Driven Morphological Remodeling. *Cellular and Molecular Bioengineering*, volume 1(4), p. 229-239.

Dai, J., Li, Z., Jin, J., Cheng, J., Kong, J., Bi, S. (2008). Study of the solvent effect on the quality of dodecanethiol self-assembled monolayers on polycrystalline gold. *Journal of Electroanalytical Chemistry*, volume 624(1–2), p. 315-322.

Daly, P., Collier, T., Doyle, S. (2002). PCR-ELISA detection of *Escherichia coli* in milk. *Letters in Applied Microbiology*, volume 34(3), p. 222–226.

Dassa, O., Sidorov, V., Paz, Y., Ritter, D. (2006). Coating and Passivation of InP–InGaAs Devices by Organic Self-Assembled Monolayers. *Journal of The Electrochemical Society,* volume 153(1), p. G91-G97

Davis, R., Mauer, L. J. (2010). *Fourier tansform infrared (FT-IR) spectroscopy: A rapid tool for detection and analysis of foodborne pathogenic bacteria*, In: Mendez-Vilas, A. (Ed.), Current Research, Technology and Education Topics in Applied Microbiology and Microbial Biotechnology, p. 1582-1594. Formatex Research Center.

de Freitas, V., Carvalho, E., Mateus, N. (2003). Study of carbohydrate influence on protein-tannin aggregation by nephelometry. *Food Chemistry*, volume 81(4), p. 503-509.

Deininger, R. A., Lee, J. (2005). *Rapid Detection of Bacteria in Drinking Water*. In: Omelchenko, A., Pivovarov, A. A., Swindall, W. J. (Ed.), Modern Tools and Methods of Water Treatment for Improving Living Standards, p. 71-78. Springer, Netherlands.

DeLeon, K., Balldin, F., Watters, C., Hamood, A., Griswold, J., Sreedharan, S., Rumbaugh, K. P. (2009). Gallium maltolate treatment eradicates Pseudomonas aeruginosa infection in thermally injured mice. *Antimicrobial Agents and Chemotherapy*, volume 53(4), p. 1331-1337.

Deupree, S. M. (2009). *Bioanalytical Methods for Investigating Bacterial Adhesion and the Antibacterial Action of Nitric Oxide*. Department of Chemistry. University of North Carolina, Charlotte, North Carolina, USA.

Dever, L. A., Dermody, T. S. (1991). Mechanisms of bacterial resistance to antibiotics. *Archives of Internal Medicine*, volume 151(5), p. 886-895.

Diaspro, A., Chirico, G., Usai, C., Ramoino, P., Dobrucki, J. (2006). *Photobleaching.* In: Pawley, J. B. (Ed.), Handbook of Biological Confocal Microscopy. Springer Science+Business Media, New York.

Ding, X., Dubowski, J. J. (2005). Surface passivation of (001) GaAs with self-assembled monolayers of long-chain thiols. *Society of Photographic Instrumentation Engineers (SPIE) Conference Proceedings*, p. 545-551, Bellingham, WA.

Ding, X., Moumanis, K., Dubowski, J. J., Tay, L., Rowell, N. L. (2006). FTIR and photoluminescence spectroscopy of self-assembled monolayers of long-chain thiols on (001)GaAs. *Journal of Applied Physics*, volume 99, p. 054701.

Diorio, C., Cai, J., Marmor, J., Shinder, R., DuBow, M. S. (1995). An *Escherichia coli* chromosomal ars operon homolog is functional in arsenic detoxification and is conserved in gram-negative bacteria. *Journal of Bacteriology*, volume 177(8), p. 2050-2056.

Dubowski, J. J., Ding, X., Frost, E. H., Escher, E. (2014). Quantum dot template for fast and simultaneous detection of different infectious agents. United States Patent, NO. 11/908,223.

Dubowski, J. J., Nazemi, E., Aithal, S., Huang, X. (2015). Photo-electrochemical biosensor and semiconductor heterostructure-based sensing method. United States Patent, NO. 15/114,660.

Dubowski, J. J., Voznyy, O., Marshall, G. M. (2010). Molecular self-assembly and passivation of GaAs (0 0 1) with alkanethiol monolayers: A view towards bio-functionalization. *Applied Surface Science*, volume 256, p. 5714-5721.

Dufrene, Y. F. (2002). Atomic Force Microscopy, a Powerful Tool in Microbiology. *Journal of Bacteriology*, volume 184, p. 5205-5213.

Duplan, V., Frost, E. H., Dubowski, J. J. (2011). A photoluminescence-based quantum semiconductor biosensor for rapid in situ detection of *Escherichia coli*. *Sensors and Actuators B: Chemical,* volume 160, p. 46-51.

Duplan, V., Miron, Y., Frost, E. H., Grandbois, M., Dubowski, J. J. (2009). Specific immobilization of influenza A virus on GaAs (001) surface. *Journal of Biomedical Optics,* volume 14(5), p. 054042.

Dutta, D., Cole, N., Willcox, M. (2012). Factors influencing bacterial adhesion to contact lenses. *Molecular Vision*, volume 18, p. 14-21.

Ehret, R., Baumann, W., Brischwein, M., Schwinde, A., Stegbauer, K., Wolf, B. (1997). Monitoring of cellular behaviour by impedance measurements on interdigitated electrode structures. *Biosensors and Bioelectronics*, volume 12(1), p. 29-41.

Engel, L. S. (2009). Multidrug-resistant gram-negative bacteria: trends, risk factors, and treatments. *Emergency Medicine Journal*, volume 41, p. 18–27.

Falkinham, J. O., Hilborn, E. D., Arduino, M. J., Pruden, A., Edwards, M. A. (2015). Epidemiology and ecology of opportunistic premise plumbing pathogens: Legionella pneumophila, Mycobacterium avium, and Pseudomonas aeruginosa. *Environmental Health Perspectives,* volume 123, p. 749–758.

Fleming-Dutra, K. E., Hersh, A. L., Shapiro, D. J., et al. (2016). Prevalence of inappropriate antibiotic prescriptions among us ambulatory care visits, 2010-2011. *The Journal of the American Medical Association*, volume 315(17), p. 1864-1873.

Folkers, J. P., Laibinis, P. E., Whitesides, G. M. (1992). Self-Assembled Monolayers of Alkanethiols on Gold: Comparisons of Monolayers Containing Mixtures of Short-and Long-Chain Constituents with CH_3 and CH_2OH Terminal Groups. *Langmuir*, volume 8, p. 1330-1341.

Fratamico, P. M. (2003). Comparison of culture, polymerase chain reaction (PCR), TaqMan Salmonella, and Transia Card Salmonella assays for detection of Salmonella spp. in naturally-

contaminated ground chicken, ground turkey, and ground beef. *Molecular and Cellular Probes,* volume 17, p. 215–221.

Fredborg, M., Andersen, K. R., Jorgensen, E., Droce, A., Olesen, T., Jensen, B. B., Rosenvinge, F. S., Sondergaard, T. E. (2013). Real-time optical antimicrobial susceptibility testing. *Journal of Clinical Microbiology*, volume 51(7), p. 2047-2053.

Fredborg, M., Rosenvinge, F. S., Spillum, E., Kroghsbo, S., Wang, M., Sondergaard, T. E. (2015). Rapid antimicrobial susceptibility testing of clinical isolates by digital time-lapse microscopy. *European Journal of Clinical Microbiology and Infectious Diseases,* volume 34(12), p. 2385-2394.

Frey, B. L., Corn, R. M. (1996). Covalent Attachment and Derivatization of Poly(l-lysine) Monolayers on Gold Surfaces As Characterized by Polarization−Modulation FT-IR Spectroscopy. *Analytical Chemistry*, volume 68(18), p. 3187-3193.

Fu, Z., Rogeli, S., Kieft, T. L. (2005). Rapid detection of *Escherichia coli* O157:H7 by immunomagnetic separation and real-time PCR. *International Journal of Food Microbiology,* volume 99, p. 47-57.

Fujikawa, H., Morozumi, S. (2005). Modeling Surface Growth of Escherichia coli on Agar Plates. *Applied and Environmental Microbiology*, volume 71(12), p. 7920-7926.

Gao, X., Chan, W. C. W., Nie, S. (2002). Quantum-dot nanocrystals for ultrasensitive biological labeling and multicolour optical encoding. *Journal of Biomedical Optics,* volume 7, p. 532–537.

Garbutt, J. (1997). *Essentials of Food Microbiology*, 1st ed. Arnold, London.

Garneau, J. E., Moineau, S. (2011). Bacteriophages of lactic acid bacteria and their impact on milk fermentations. *Microbial Cell Factories,* volume 10(Suppl 1), p. S20-S20.

Garrett, T. R., Bhakoo, M., Zhang, Z. (2008). Bacterial adhesion and biofilms on surfaces. *Porgress in Natural Science*, volume 18(9), p. 1049-1056.

Gasparri, F., Muzio, M. (2003). Monitoring of apoptosis of HL60 cells by Fourier-transform infrared spectroscopy. *Biochemical Journal*, volume 369, p. 239-248.

Ge, B., Wang, F., Sjolund-Karlsson, M., McDermott, P. F. (2013). Antimicrobial resistance in campylobacter: susceptibility testing methods and resistance trends. *Journal of Microbiological Methods*, volume 95(1), p. 57-67.

Gfroerer, T. H. (2006). *Photoluminescence in Analysis of Surfaces and Interfaces*. In: Meyers, R.A. (Ed.), Encyclopedia of analytical chemistry : applications, theory and instrumentation, pp. 9209–9231. John Wiley & Sons, Ltd, Chichester.

Ghafar-Zadeh, E., Sawan, M., Shabani, A., Zourob, M., Chodavarapu, V. (2008). Bacteria Growth Monitoring Through an On-Chip Capacitive Sensor. *IEEE*, Vancouver, BC, Canada.

Gibbons, R. J., Etherden, I., Skobe, Z. (1983). Association of fimbriae with the hydrophobicity of Streptococcus sanguis FC-1 and adherence to salivary pellicles. *Infection and Immunity*, volume 41(1), p. 414-417.

Goldberg, J. (2002). Biofilms and antibiotic resistance: a genetic linkage. *Trends in Microbiology*, volume 10, p. 264.

Golubovich, V. N., Rabotnova, I. L. (1974). Kinetics of growth inhibition by silver ions. *Microbiology,* volume 43, p. 948-950.

Gootz, T. D. (2010). The global problem of antibiotic resistance. *Critical Reviews in Immunology,* volume 30(1), p. 79-93.

Gould, I. M., Bal, A. M. (2013). New antibiotic agents in the pipeline and how they can help overcome microbial resistance. *Virulence*, volume 4(2), p. 185-191.

Griffiths, P. R., de Haseth, J. A. (1986). *Fourier Transform Infrared Spectroscopy*. John Wiley and Sons, New York.

Grisold, A. J., Leitner, E., Muhlbauer, G., Marth, E., Kessler, H. H. (2002). Detection of methicillin-resistant Staphylococcus aureus and simultaneous confirmation by automated nucleic acid extraction and real-time PCR. *Journal of Clinical Microbiology,* volume 40(7), p. 2392-2397.

Gristina, A. G. (1987). Biomaterial-centered infection: microbial adhesion versus tissue integration. *Science,* volume 237(4822), p. 1588-1595.

Gristina, A. G., Costerton, J. W. (1985). Bacterial adherence to biomaterials and tissue. The significance of its role in clinical sepsis, *Journal of Bone and Joint Surgery*, volume 67, p. 264–273.

Grohmann, E., Muth, G., Espinosa, M. (2003). Conjugative Plasmid Transfer in Gram-Positive Bacteria. *Microbiology and Molecular Biology Reviews,* volume 67(2), p. 277-301.

Gudino, M., Miller, W. V. (1981). Application of the enzyme linked immunospecific assay (ELISA) for the detection of platelet antibodies. *Blood*, volume 57, p. 32-37.

Guo-Ping, J., Ruda, H. E. (1998). The origin of Ga_2O_3 passivation for reconstructed GaAs(001) surfaces. *Journal of Applied Physics*, volume 83, p. 5880.

Halwani, M., Yebio, B., Suntres, Z. E., Alipour, M., Azghani, A. O., Omri, A. (2008). Co-encapsulation of gallium with gentamicin in liposomes enhances antimicrobial activity of gentamicin against Pseudomonas aeruginosa. *Journal of Antimicrobial Chemotherapy*, volume 62(6), p. 1291-1297.

Hanna, A., Berg, M., Stout, V., Razatos, A. (2003). Role of Capsular Colanic Acid in Adhesion of Uropathogenic *Escherichia coli*. *Applied and Environmental Microbiology,* volume 69(8), p. 4474-4481.

Harbeke, G., Krausbauer, L., Steigmeier, E. F., Widmer, A. E., Kappert, H. F., Neugebauer, G. (1984). Growth and Physical Properties of LPCVD Polycrystalline Silicon Films. *Journal of the Electrochemical Society,* volume 131(3), p. 675-682.

Harvey, P. I., Crundwell, F. K. (1996). The effect of As(III) on the growth of *Thiobacillus ferrooxidans* in an electrolytic cell under controlled redox Potentials. *Minerals Engineering*, volume 9(10), p. 1059-1068.

Hassen, W. M., Sanyal, H., Hammood, M., Moumanis, K., Frost, E. H., Dubowski, J. J. (2016). Chemotaxis for enhanced immobilization of *Escherichia coli* and *Legionella pneumophila* on biofunctionalized surfaces of GaAs. *Biointerphases,* volume 11(2), p. 021004.

Hauri, D. C., Ross, J. (1995). A model of excitation and adaptation in bacterial chemotaxis. *Biophysical Journal,* volume 68(2), p. 708-722.

He, X., Patfield, S., Hnasko, R., Rasooly, R., Mandrell, R. E. (2013). A Polyclonal Antibody Based Immunoassay Detects Seven Subtypes of Shiga Toxin 2 Produced by *Escherichia coli* in Human and Environmental Samples. *PLOS ONE* , volume 8(10), p. e76368.

Headrick, J. E., Berrie, C. L. (2004). Alternative Method for Fabricating Chemically Functionalized AFM Tips: Silane Modification of HF-Treated Si3N4 Probes. *Langmuir*, volume 20(10), p. 4124-4131.

Healy, T. W., White, L. R. (1978). Ionizable surface group models of aqueous interfaces. *Advances in Colloidal and Interface Science*, volume 9, p. 303.

Herman, J. S., Terry Jr., F. L. (1992). Hydrogen sulfide plasma passivation of gallium arsenide. *Applied Physics Letters*, volume 60, p. 716-717.

Hilton, H. G., Parham, P. (2013). Direct binding to antigen-coated beads refines the specificity and cross-reactivity of four monoclonal antibodies that recognize polymorphic epitopes of HLA class I molecules. *Tissue Antigens,* volume 81(4), p. 212-220.

Hirsch, J. D., Haugland, R. P. (2005). Conjugation of antibodies to biotin. *Methods in Molecular Biology*, volume 295, p. 135-154.

Hlady, V., Lin, J. N., Andrade, J. D. (1990). Spatially resolved detection of antibody–antigen reaction on solid/liquid interface using total internal reflection excited antigen fluorescence and charge-coupled device detection. *Biosensors and Bioelectronics,* volume 5, p. 291–301.

Holmberg, A., Blomstergren, A., Nord, O., Lukacs, M., Lundeberg, J., Uhlén, M. (2005). The biotin-streptavidin interaction can be reversibly broken using water at elevated temperatures. *Electrophoresis,* volume 26, p. 501–510.

Hombach, M., Pfyffer, G. E., Roos, M., Lucke, K. (2010). Detection of methicillin-resistant *Staphylococcus aureus* (MRSA) in specimens from various body sites: performance characteristics of the BD GeneOhm MRSA assay, the Xpert MRSA assay, and broth-enriched culture in an area with a low prevalence of MRSA infections. *Journal of Clinical Microbiology,* volume 48(11), p. 3882-3887.

Huang, X. H., Dubowski, J. J. (2014). Solvent-mediated self-assembly of hexadecanethiol on GaAs (001). *Applied Surface Science*, volume 299, p. 66-72.

Istockphoto LP. (2015). Istock by Getty Images, http://www.istockphoto.com/vector/gram-positive-and-gram-negative-bacteria-gm518294121-49051886?st=_p_penicillin.

Jaouad, A., Aimez, V., Aktik, C. (2004). GaAs passivation by low-frequency plasma- enhanced chemical vapour deposition of silicon nitride. *Electronics Letters*, volume 40.

Jenkinson, H. F. (1986). Cell-surface Proteins of Streptococcus sunguis Associated with Cell Hydrophobicity and Coaggregation Properties. *Journal of General Microbiology,* volume 132, p. 1575-1589.

Jha, A. K., Tripathi, A., Bose, A. (2011). A microfluidic device for bacteria detection in aqueous samples. *Environmental Technology*, volume 32(13-14), p. 1661-1667.

Jiang, X., Jing, W., Zheng, L., Liu, S., Wu, W., Sui, G. (2014). A continuous-flow high-throughput microfluidic device for airborne bacteria PCR detection. *Lab Chip*, volume 14(4), p. 671-676.

Jorgensen, J. H., Ferraro, M. J. (2009). Antimicrobial susceptibility testing: a review of general principles and contemporary practices. *Clinical Infectious Diseases,* volume 49, p. 1749–1755.

Joshi, B., Islam, S. S., Mavi, H. S., Kumari, V., Islam, T., Shukla, A.K., Harsh (2009). Size-selective laser-induced etching of semi-insulating GaAs: Photoluminescence studies. *Physica E: Low-dimensional Systems and Nanostructures,* volume 41(4), p. 690-694.

Joubert, A., Calmes, B., Berruyer, R., Pihet, M., Bouchara, J. P., Simoneau, P., Guillemette, T. (2010). Laser nephelometry applied in an automated microplate system to study filamentous fungus growth. *Biotechniques,* volume 48(5), p. 399-404.

Kaewphinit, T., Santiwatanakul, S., Chansiri, K. (2012). Quartz crystal microbalance DNA based biosensor for diagnosis: A Review. *Sensors and Transducers*, volume 143, p. 44-59.

Kauffman, J. F., Liu, C. S., Karl, M. W. (1998). Surface Recombination Kinetics at the GaAs/Electrolyte Interface via Photoluminescence Efficiency Measurements. *The Journal of Physical Chemistry B*, volume 102, p. 6766-6773.

Komorniczak, M. (2009). Bacterial growth, https://en.wikipedia.org/wiki/Bacterial_growth#/media/File:Bacterial_growth_en.svg.

Kee, J. S., Lim, S. Y., Perera, A. P., Zhang, Y., Park, M. K. (2013). Plasmonic nanohole arrays for monitoring growth of bacteria and antibiotic susceptibility test. *Sensors and Actuators B: Chemical,* volume 182, p. 576– 583.

Kim, C. K., Marshall, G. M., Martin, M., Bisson-Viens, M., Wasilewski, Z., Dubowski, J. J. (2009). Formation dynamics of hexadecanethiol self-assembled monolayers on (001) GaAs observed with photoluminescence and Fourier transform infrared spectroscopies. *Journal of Applied Physics*, volume 106(8), p. 083518.

Kim, T., Kang, J., Lee, J.-H., Yoon, J. (2011). Influence of attached bacteria and biofilm on double-layer capacitance during biofilm monitoring by electrochemical impedance spectroscopy. *Water Research,* volume 45(15), p. 4615-4622.

Kleijin, J. M., van Leeuwen, H. P. (2000). *Electrostatic and electrodynamic properties of biological interfaces*. Marcel Dekker, New York.

Knutton, S. (1995). Electron microscopical methods in adhesion. *Methods in Enzymology*, volume 253, p. 145-158.

Kollef, M. H. (2001). Optimizing antibiotic therapy in the intensive care unit setting. *Critical Care*, volume 5(4), p. 189-195.

Kollef, M. H., Fraser, V. J. (2001). Antibiotic resistance in the intensive care unit. *Annals of Internal Medicine*, volume 134(4), p. 298-314.

Kruchinin, A. A., Tarantov, Y. A., Balova, I. A., Remisova, L. A., Vlasov, Y. G. (1995). Fixation of DNA directly on optical waveguide surfaces for molecular probe biosensor development. *Sensors and Actuators B: Chemical,* volume 29(1-3), p. 324-327.

Kubitschek, H. E. (1990). Cell Volume Increase in *Escherichia coli* after Shifts to Richer Media. *Journal of Bacteriology*, volume 172, p. 94-101.

LaBella, V. P., Krause, M. R., Ding, Z., Thibado, P. M. (2005). Arsenic-rich GaAs(0 0 1) surface structure. *Surface Science Reports*, volume 60, p. 1-53.

Lacour, V., Elie-Caille, C., Leblois, T., Dubowski, J. J. (2016). Regeneration of a thiolated and antibody functionalized GaAs (001) surface using wet chemical processes. *Biointerphases*, volume 11(1), p. 019302.

Lambert, B., Sermage, B., Deveaud, B., Clerot, F., Regreny, A. (1990). Radiative and non-radiative recombination in GaAs-AlGaAs superlattices. *Surface Sience*, volume 228, p. 210-212.

Larryisgood. (2012). Diagram of zeta potential and slipping plane, https://en.wikipedia.org/wiki/Zeta_potential#/media/File:Diagram_of_zeta_potential_and_slipping_planeV2.svg.

Lasia, A. (2014). *Electrochemical Impedance Spectroscopy and its Applications*. Springer Science+Business Media, New York.

Lazcka, O., Del Campo, F. J., Munoz, F. X. (2007). Pathogen detection: A perspective of traditional methods and biosensors. *Biosensors and Bioelectronics*, volume 22, p. 1205-1217.

Lazerand, T., Lishan, D. (2014). Silicon Nitride for MEMS Applications: LPCVD and PECVD Process Comparison. MEMS and Sensors Whitepaper Series Plasma-Therm Website.

Lebedev, M. V. (2001). Role of sulfide ion solvation in the modification of GaAs surface electronic structure. *Semiconductors*, volume 35(11), p. 1291-1299.

LeBel, M. (1988). Ciprofloxacin: chemistry, mechanism of action, resistance, antimicrobial spectrum, pharmacokinetics, clinical trials, and adverse reactions. *Pharmacotherapy*, volume 8(1), p. 3-33.

Lee, J., Dak, P., Lee, Y., Park, H., Choi, W., Alam, M. A., Kim, S. (2014). Two-dimensional layered MoS2 biosensors enable highly sensitive detection of biomolecules. *Scientific Reports,* volume 4, p. 7352.

Lee, K., Lu, G., Facchetti, A., Janes, D. B., Marks, T. J. (2008). Comparative passivation effects of self-assembled mono-and multilayers on GaAs junction field effect transistors. *Applied Physics Letters*, volume 92, p. 123509.

Lee, K., Nair, P. R., Scott, A., Alam, M. A., Janes, D. B. (2009). Device considerations for development of conductance-based biosensors. *Journal of Applied Physics,* volume 105(10), p. 102046.

Leonard, P., Hearty, S., Brennan, J., Dunne, L., Quinn, J., Chakraborty, T., O'Kennedy, R. (2003). Advances in biosensors for detection of pathogens in food and water. *Enzyme and Microbial Technology*, volume 32, p. 3-13.

Lepage, D., Jiménez, A., Carrier, D., Beauvais, J., Dubowski, J. J. (2010). Hyperspectral imaging of diffracted surface plasmons. *Optics Express,* volume 18, p. 27327-27335.

Lewinski, N., Colvin, V., Drezek, R. (2008). Cytotoxicity of nanoparticles. *Small*, volume 4, p. 26–49.

Li, H.-Q. (1997). The Common AFM Modes, http://www.chemistry.uoguelph.ca/educmat/chm729/afm/details.htm.

Li, M., Liu, L., Xi, N., Wang, Y. (2015). Nanoscale monitoring of drug actions on cell membrane using atomic force microscopy. *Acta Pharmacologica Sinica*, volume 36(7), p. 769-782.

Li, Y., Afrasiabi, R., Fathi, F., Wang, N., Xiang, C., Love, R., She, Z., Kraatz, H.-B. (2014). Impedance based detection of pathogenic *E. coli* 0157:H7 using a ferrocene-antimicrobial peptide modified biosensor. *Biosensors and Bioelectronic,* volume 58, p. 193-199.

Lin, D. Q., Brixius, P. J., Hubbuch, J. J., Thommes, J., Kula, M.R. (2003). Biomass/adsorbent electrostatic interactions in expanded bed adsorption: a zeta potential study. *Biotechnology and Bioengineering,* volume 83(2), p. 149-157.

Lin, J., Hogan, J. S., Smith, K. L. (1998). Inhibition of In Vitro Growth of Coliform Bacteria by a Monoclonal Antibody Directed Against Ferric Enterobactin Receptor FepA1. *Journal of Dairy Science*, volume 81(5), p. 1267-1274.

Liu, C., Lei, T., Ino, K., Matsue, T., Tao, N., Li, C.-Z. (2012). Real-time monitoring biomarker expression of carcinoma cells by surface plasmon resonance biosensors. *Chemical Communications*, volume 48, p. 10389–10391.

Liu, C. S., Kauffman, J. F. (1995). Excitation power dependence of photoluminescence enhancement from passivated GaAs. *Applied Physics Letters,* volume 66, p. 3504.

Lo, W.-L., Lai, J. Y., Feinberg, S. E., Izumi, K., Kao, S.-Y., Chang, C.-S., Lin, A., Chiang, H. K. (2011). Raman spectroscopy monitoring of the cellular activities of a tissue-engineered ex vivo produced oral mucosal equivalent. *Journal of Raman Spectroscopy*, volume 42(2), p. 174-178.

Lorenzetti, M., Dogsa, I., Stosicki, T., Stopar, D., Kalin, M., Kobe, S., Novak, S. (2015). The influence of surface modification on bacterial adhesion to titanium-based substrates. *ACS Applied Materials and Interfaces*, volume 7(3), p. 1644-1651.

Luebker, E. R. M., Leung, L. K., Murphy, C. J., Lisensky, G. C., Ellis, A. B. (1991). *Biotechnology: Bridging Research and Applications*, Chapter 7. Kluwer Academic Publishers, Boston.

Lunt, S. R., Ryba, G. N., Santangelo, P. G., Lewis, N. S. (1991a). Chemical studies of the passivation of GaAs surface recombination using sulfides and thiols. *Journal of Applied Physics,* volume 70, p. 7449.

Lunt, S. R., Santangelo, P. G., Lewis, N. S. (1991b). Passivation of GaAs surface recombination with organic thiols. *Journal of Vacuum Science and Technology B*, volume 9(4), p. 2333-2336.

Luong, J. H. T., Male, K. B., Glennon, J. D. (2008). Biosensor technology: Technology push versus market pull. *Biotechnology Advances*, volume 26(5), p. 492-500.

Mach, K. E., Mohan, R., Baron, E. J., Shih, M. C., Gau, V., Wong, P. K., Liao, J. C. (2011). A biosensor platform for rapid antimicrobial susceptibility testing directly from clinical samples. *Journal of Urology*, volume 185(1), p. 148-153.

Mannoor, M. S., Zhang, S., Link, A. J., McAlpine, M. C. (2010). Electrical detection of pathogenic bacteria via immobilized antimicrobial peptides. *Proceedings of the National Academy of Sciences of USA*, pp. 19207–19212.

Mao, S. Y. (2010). Biotinylation of antibodies. *Methods in Molecular Biology,* volume 588, p. 49-52.

Marshall, G. M. (2011). Electro-optic investigation of the n-alkanethiol GaAs (001) interface: surface phenomena and applications to photoluminescence-based biosensing. Electical Engineering. Universite de Sherbrooke, Universite de Sherbrooke.

Marshall, G. M., Lopinski, G. P., Bensebaa, F., Dubowski, J. J. (2011). Electro-optic investigation of the surface trapping efficiency in n-alkanethiol SAM passivated GaAs(001). *Nanotechnology*, volume 22, p. 235704.

Matlock, B. C., Beringer, R. W., Ash, D. L., Allen, M. W., Page, A. F., Analyzing differences in bacterial optical density measurements between spectrophotometers. Thermo Scientific.

Matsumoto, A., Miyahara, Y. (2013). Current and emerging challenges of field effect transistor based bio-sensing. *Nanoscale*, volume 5, p. 10702.

Matthäus, C., Bird, B., Miljković, M., Chernenko, T., Romeo, M., Diem, M. (2008). Infrared and Raman Microscopy in Cell Biology. *Methods in Cell Biology,* volume 89, p. 275-308.

Matthysse, A. G. (1995). Observation and measurement of bacterial adhesion to plants. *Methods in Enzymology*, volume 253, p. 189-206.

Mattoussi, H., Mauro, J. M., Goldman, E. R., Anderson, G. P., Sunder, V. C., Mikulec, F. V., Bawendi, M. G. (2000). Self-Assembly of CdSeZnS Quantum Dot Bioconjugates Using an Engineered Recombinant Protein. *Journal of the American Chemical Society*, volume 122, p. 12142-12150.

Mattox, D. M. (2010). Handbook of Physical Vapor Deposition (PVD) Processing. Elsevier.

Mavi, H. S., Islam, S. S., Rath, S., Chauhan, B. S., Shukla, A. K. (2004). Laser-induced etching of CrO doped GaAs and wavelength dependent photoluminescence. *Materials Chemistry and Physics,* volume 86(2–3), p. 414-419.

McFarland, J. (1907). The Nephelometer: An instrument for estimating the number of bacteria in suspensions used for calculating the opsonic index and for vaccines. *The Journal of the American Medical Association*, volume XLIX, p. 1176-1178.

McGann, P., Snesrud, E., Maybank, R., Corey, B., Ong, A. C., Clifford, R., Hinkle, M., Whitman, T., Lesho, E., Schaecher, K. E. (2016). *Escherichia coli* Harboring mcr-1 and blaCTX-M on a Novel IncF Plasmid: First Report of mcr-1 in the United States. *Antimicrobial Agents and Chemotherapy,* volume 60(7), p. 4420-4421.

McGuiness, C. L., Blasini, D., Masejewski, J. P., Uppili, S., Cabarcos, O. M., Smilgies, D., Allara, D. L. (2007). Molecular self-assembly at bare semiconductor surfaces: Characterization of a homologous series of n-alkanethiolate monolayers on GaAs(001). *Acs Nano,* volume 1(1), p. 30-49.

Medema, G. J., Payment, P., Dufour, A., Robertson, W., Waite, M., Hunter, P., Kirby, R., Anderson, Y. (2003). *Safe drinking water: an ongoing challenge*. In: Dufour, A., Snozzi, M., Koster, W., Bartram, J., Ronchi, E., Fewtrell, L. (Eds.), Microbial safety of drinking water: Improving approaches and methods, p. 11–45. World Health Organization (WHO) and Organization for Economic Cooperation and Development (OECD), London, UK.

Medintz, I. L., Uyeda, H. T., Goldman, E. R., Mattoussi, H. (2005). Quantum dot bioconjugates for imaging, labelling and sensing. *Nature Materials,* volume 4, p. 435-446.

Merritt, K., An, Y. H. (2000). *Factors influencing bacterial adhesion. Handbook of bacteriala adhesion, principles, methdos and applications*. Humana Press Inc., Totowa, NJ.

Meyer, G. J., Lisensky, G. C., Ellis, A. B. (1988). Evidence for adduct formation at the semiconductor-gas interface. Photoluminiscence properties of cadmium selenide in the presence of amins. *Journal of the American Chemical Society*, volume 110, p. 4914-4918.

Meyer, R. L., Zhou, X., Tang, L., Arpanaei, A., Kingshott, P., Besenbacher, F. (2010). Immobilisation of living bacteria for AFM imaging under physiologicalconditions. *Ultramicroscopy,* volume 110(11), p. 1349-1357.

Mitchell, P. (2011). Chemiosmotic coupling in oxidative and photosynthetic phosphorylation. 1966. *Biochimica et Biophysica Acta,* volume 1807(12), p. 1507-1538.

Mittler-Necher, S., Spinkle, J., Liley, M., Nelles, G., Weisser, M., Back, R., Wenz, G., Knoll, W. (1995). Spectroscopic and surface-analytical characterization of self-assembled layers on Au. *Biosensors and Bioelectronics,* volume 10, p. 903-916.

Moina, C., Ybarra, G. (2012). Fundamentals and Applications of Immunosensors, Advances in Immunoassay Technology, Available from: http://www.intechopen.com/books/advances-in-immunoassay-technology/fundamentals-and-applications-ofimmunosensors

Mokkapati, S., Jagadish, C. (2009). III-V compound SC for optoelectronic devices. *Materials Today*, volume 12, p. 22-32.

Mortensen, B. J. (2014). Problems caused by biofilms, http://www.bactoforce.com/wp-content/uploads/2014/09/Problems-caused-by-biofilms.pdf.

Moumanis, K., Ding, X., Dubowski, J. J., Frost, E. H. (2006). Aging and detergent washing effects of the surface of (001) and (110) GaAs passivated with hexadecanethiol. *Journal of Applied Physics,* volume 100(3), p. 034702.

Mukhopadhyay, R., Rosen, B. P., Phung, L. T., Silver, S. (2002). Microbial arsenic: from geocycles to genes and enzymes. *Federation of European Microbiological Societies (FEMS) Microbiology Reviews,* volume 26(3), p. 311-325.

Müller, R., Gröger, G., Hiller, K., Schmalz, G., Ruhl, S. (2007). Fluorescence-based bacterial overlay method for simultaneous in situ quantification of surface-attached bacteria. *Applied and Environmental Microbiology*, volume 73, p. 2653-2660.

Mustafa, D. E., Fan, H., Zhou, X., Tu, H. Y., Zhang, A. D. (2012). Adsorption Behaviour of PEGylated Gold Nanoparticles to Different Surfaces Probed by CV Monitoring. *Advanced Materials Research*, volume 455-456, p. 689-695.

Mwaigwisya, S., Assiri, R. A., O'Grady, J. (2015). Emerging commercial molecular tests for the diagnosis of bloodstream infection. *Expert Review of Molecular Diagnostics,* volume 15(5), p. 681-692.

Naaman, R., Capua, E., Cao, R. (2013). Semiconductor detector for peroxide-based explosives. United States Patent, NO. 13/055,287.

Nagasaki, Y., Kobayashi, H., Katsuyama, Y., Jomura, T., Sakura, T. (2007). Enhanced immunoresponse of antibody/mixed-PEG co-immobilized surface construction of high-performance immunomagnetic ELISA system. *Journal of Colloid and Interface Science*, volume 309, p. 524–530.

Naqvi, S. Z., Kiran, U., Ali, M. I., Jamal, A., Hameed, A., Ahmed, S., Ali, N. (2013). Combined efficacy of biologically synthesized silver nanoparticles and different antibiotics against multidrug-resistant bacteria. *International Journal of Nanomedicine*, volume 8, p. 3187-3195.

Nayak, M., Kotian, A., Marathe, S., Chakravortty, D. (2009). Detection of microorganisms using biosensors—A smarter way towards detection techniques. *Biosensors and Bioelectronics*, volume 25(4), p. 661-667.

Nazemi, E., Aithal, S., Hassen, W. M., Frost, E. H., Dubowski, J. J. (2015). GaAs/AlGaAs heterostructure photonic biosensor for rapid detection of *Escherichia coli* in phosphate buffered saline solution. *Sensors and Actuators B: Chemical,* volume 207, p. 556–562.

Nazemi, E., Hassen, W. M., Frost, E. H., Dubowski, J. J. (2016). Monitoring growth and antibiotic susceptibility of Escherichia coli with photoluminescence of GaAs/AlGaAs quantum well microstructures. *Biosensors and Bioelectronic*s, in print.

Nazemi, E., Hassen, W. M., Frost, E. H., Dubowski, J. J. (2016), Growth of *Escherichia coli* on GaAs (001) surface. Under review.

Nelson, K. E., Gamble, L., Jung, L.S., Boeckl, M. S., Naeemi, E., Golledge, S. L., Sasaki, T., Castner, D. G., Campbell, C. T., Stayton, P. S. (2001). Surface Characterization of Mixed Self-Assembled Monolayers Designed for Streptavidin Immobilization. *Langmuir,* volume 17(9), p. 2807-2816.

Nemati, M., Jenneman, G. E., Voordouw, G. (2001). Mechanistic study of microbial control of hydrogen sulfide production in oil reservoirs. *Biotechnology and Bioengineering,* volume 74(5), p. 424-434.

Newman, J. D., Turner, A. P. F. (2005). Home blood glucose biosensors: a commercial perspective. *Biosensors and Bioelectronics*, volume 20(12), p. 2435-2453.

Nishi, Y., Doering, R. (2007). *Handbook of semiconductor manufacturing technology*. CRC Press

Noble, R. T., Weisberg, S. B. (2005). A review of technologies for rapid detection of bacteria in recreational waters. *Journal of Water and Health*, volume 03, p. 381-392.

Nomura, S., Kuroiwa, A., Nagayama, A. (1995). Changes of surface hydrophobicity and charge of *Staphylococcus aureus* treated with sub-MIC of antibiotics and their effect on the chemiluminescence response of phagocytic cells. *Microbiology*, volume 41, p. 77-81.

Oh, B. K., Lee, Y. K., Lee, W., Bae, Y. M., Lee, W. H., Choi, J. W. (2003). Immunosensor for detection of *Legionella pneumophila* using surface plasmon resonance. *Biosensors and Bioelectronics,* volume 18, p. 605-611.

Ohtake, A. (2008). Surface reconstructions on GaAs(001). *Surface Science Reports*, volume 63(7), p. 295-327.

Olbris, D. J., Ulman, A., Shnidman, Y. (1995). Interplay of wetting and adsorption at mixed self-assembled monolayers. *The Journal of Chemical Physics,* volume 102, p. 6865-6873.

Orth, R. N., Clark, T. G., Craighead, H. G. (2003). Avidin-Biotin Micropatterning Methods for Biosensor Applications. *Biomedical Microdevices,* volume 5(1), p. 29-34.

Paez-Espino, D., Tamames, J., de Lorenzo, V., Canovas, D. (2009). Microbial responses to environmental arsenic. *Biometals,* volume 22(1), p. 117-130.

Passlack, M., Hong, M., Schubert, E. F., Kwo, J. R., Mannaerts, J. P., Chu, S. N. G., Moriya, N., Thiel, F. A. (1995). In situ fabricated Ga2O3–GaAs structures with low interface recombination velocity. *Applied Physics Letters*, volume 66, p. 625-627.

Pau, C., Wells, S. K., Rudolph, D. L., Owen, S. M., Granade, T. C. (2010). A rapid real-time PCR assay for the detection of HIV-1 proviral DNA using double-stranded primer. *Journal of Virological Methods*, volume 164, p. 55–62.

Peng, J., Tsai, W., Chou, C. (2002). Inactivation and removal of Bacillus cereus by sanitizer and detergent. *International Journal of Food Microbiology*, volume 77(1–2), p. 11-18.

Planck, M. (1999). The largest Bacterium: Scientist discovers new bacterial life form off the African coast. Institute for Marine Microbiology.

Podol'skaia, V. I., Gruzina, T. G., Ul'berg, Z. P., Sokolovskaia, A. S., Grishchenko, N. I. (2002). Effect of arsenic on bacterial growth and plasma membrane atpase activity. *Prikladnaia Biokhimiia i Mikrobiologiia*, volume 38(1), p. 57-62.

Poortinga, A. T., Bos, R., Busscher, H. J. (1999). Measurement of charge transfer during bacterial adhesion to an indium tin oxide surface in a parallel plate flow chamber. Journal of Microbiological Methods, volume 38(3), p. 183-189.

Poortinga, A. T., Bos, R., Norde, W., Busscher, H. J. (2002). Electric double layer interactions in bacterial adhesion to surfaces. *Surface Science Reports,* volume 47, p. 1-32.

Pore, R. S. (1994). Antibiotic susceptibility testing by flow cytometry. *Journal of Antimicrobial Chemotherapy*, volume 34, p. 613–627.

Poupard, J. A., Walsh, L. R., Kleger, B. (1994). *Antimicrobial Susceptibility Testing*. Springer, New York.

Quach, D. T., Sakoulas, G., Nizet, V., Pogliano, J., Pogliano, K. (2016). Bacterial Cytological Profiling (BCP) as a Rapid and Accurate Antimicrobial Susceptibility Testing Method for Staphylococcus aureus. *EBioMedicine,* volume 4, p. 95-103.

Quirynen, M., Diericks, K., van Streenberghe, D. (2000). *Mechanisms of Microbial Adhesion and Biofilm formation, Effects of surface roughness and free energy on oral bacetrial adhesion.* Handbook of Bacterial Adhesion: Principles, Methods, and Applications, p. 91-102. Humana Press Inc., Totowa, NJ.

Quirynen, M., van der Mei, H. C., Bollen, C. M., Schotte, A., Marechal, M., Doornbusch, G. I., Naert, I., Busscher, H. J., van Steenberghe, D. (1993). An in vivo study of the influence of the surface roughness of implants on the microbiology of supra- and subgingival plaque. *Journal of Dental Research*, volume 72(9), p. 1304-1309.

Raiteri, R., Grattarola, M., Butt, H., Skladal, P. (2001). Micromechanical cantilever-based biosensors. *Sensors and Actuators A: Chemical*, volume 79, p. 115-126.

Rajeshwar, K. (2002). *Fundamentals of semiconductor electrochemistry and photoelectrochemistry*. In: A. J. Bard, M. Stratmann, Licht, S. (Eds.), Encyclopedia of Electrochemistry: Semiconductor Electrodes and Photoelectrochemistry. Wiley, New York.

Read, A. F., Woods, R. J. (2014). Antibiotic resistance management. *Evolution, Medicine, and Public Health*, volume 147.

Reimschuessel, A. C. (1972). Scanning electron microscopy - Part I. *Journal of Chemical Education*, volume 49(8), p. A413.

Resch-Genger, U., Grabolle, M., Cavaliere-Jaricot, S., Nitschke, R., Nann, T. (2008). Quantum dots versus organic dyes as fluorescent labels. *Nature Methods*, volume 5, p. 763-775.

Reynolds, E.C., Wong, A. (1983). Effect of adsorbed protein on hydroxyapatite zeta potential and Streptococcus mutans adherence. *Infection and Immunity*, volume 39(3), p. 1285-1290.

Rieder, R. J., Zhao, Z., Zavizion, B. (2009). New approach for drug susceptibility testing: monitoring the stress response of mycobacteria. *Antimicrobial Agents and Chemotherapy,* volume 53, p. 4598–4603.

Rigas, B., Morgello, S., Goldman, I. S., Wong, P. T. (1990). Human colorectal cancers display abnormal Fourier-transform infrared spectra. *Proceedings of the National Academy of Sciences USA*, volume 87(20), p. 8140-8144.

Roberts, J. A., Paul, S. K., Akova, M., Bassetti, M., De Waele, J. J., Dimopoulos, G., Kaukonen, K. M., Koulenti, D., Martin, C., Montravers, P., Rello, J., Rhodes, A., Starr, T., Wallis, S. C., Lipman, J. (2014). DALI: defining antibiotic levels in intensive care unit patients: are current beta-lactam antibiotic doses sufficient for critically ill patients?, *Clinical Infectious Diseases,* volume 58(8), p. 1072-1083.

Rolain, J. M., Mallet, M. N., Fournier, P. E., Raoult, D. (2004). Real-time PCR for universal antibiotic susceptibility testing. Journal of Antimicrobial Chemotherapy, volume 54, p. 538–541.

Rosu, D. M., Jones, J. C., Hsu, J. W. P., Kavanagh, K. L., Tsankov, D., Schade, U., Esser, N., Hinrichs, K. (2009). Molecular Orientation in Octanedithiol and Hexadecanethiol Monolayers on GaAs and Au Measured by Infrared Spectroscopic Ellipsometry. *Langmuir*, volume 25(2), p. 919-923.

Roth, B. L., Poot, M., Yue, S. T., Millard, P. J. (1997). Bacterial Viability and Antibiotic Susceptibility Testing with SYTOX Green Nucleic Acid Stain. *Applied and Environmental Microbiology*, volume 63, p. 2421–2431.

Ruberto, M. N., Zhang, X., Scarmozzino, R., Willner, A. E., Podlesnik, D. V., Osgood Jr., R. M. (1991). The laser controlled micrometer scale photoelectrochemical etching of III–V semiconductors. *Journal of The Electrochemical Society*, volume 138, p. 1174-1185.

Ruppé, É., Woerther, P., Barbier, F. (2015). Mechanisms of antimicrobial resistance in Gram-negative bacilli. *Annals of Intensive Care*, volume 5, p. 21.

Rzhepishevska, O., Ekstrand-Hammarstrom, B., Popp, M., Bjorn, E., Bucht, A., Sjostedt, A., Antti, H., Ramstedt, M. (2011). The antibacterial activity of Ga^{3+} is influenced by ligand complexation as well as the bacterial carbon source. *Antimicrobial Agents and Chemotherapy,* volume 55(12), p. 5568-5580.

Schuler, M. M., Marison, I. W. (2012). Real-time monitoring and control of microbial bioprocesses with focus on the specific growth rate: current state and perspectives. *Applied Microbiology and Biotechnology,* volume 94(6), p. 1469-1482.

Schulz, H. N., Brinkhoff, T., Ferdelman, T. G., Hernández Mariné, M., Teske, A., Jørgensen, B. B. (1999). Dense Populations of a Giant Sulfur Bacterium in Namibian Shelf Sediments. *Science,* volume 284(5413), p. 493-495.

Schvartzman, M., Sidorov, V., Ritter, D., Paz, Y. (2001). Surface passivation of (100) InP by organic thiols and polyimide as characterized by steady-state photoluminescence. *Semiconductor Science and Technology*, volume 16(10), p. L68.

Seker, F., Meeker, K., Kuech, T. F., Ellis, A. B. (2000). Surface Chemistry of Prototypical Bulk II-VI and III-V Semiconductors and Implications for Chemical Sensing. *Chemical Reviews*, volume 100, p. 2505-2536.

Sengupta, S., Chattopadhyay, M. K., Grossart, H. P. (2013). The multifaceted roles of antibiotics and antibiotic resistance in nature. *Frontiers in Microbiology*, volume 4, p. 47.

Sharma, R. (2010). Imaging Molecular and Cells. *Nano Science and Technology Institute - Nanotechnology*, volume 3, p. 452-455.

Shimko, A., Povolotckaia, A., Mikhaylova, A. (2014). Saint Petersburg State University, Center for optical and laser research, http://laser.spbu.ru/en/research-eng/dzeta-eng.html.

Shockley, W., Read, W. T. (1952). Statistics of the Recombination of Holes and Electrons. *Physical Review*, volume 87, p. 835-842.

Sin, M. L., Mach, K. E., Wong, P. K., Liao, J. C. (2014). Advances and challenges in biosensor-based diagnosis of infectious diseases. *Expert review of molecular diagnostics*, volume 14(2), p. 225-244.

Sjollema, J., Busscher, H. J. (1989). *Journal of Colloid and Interface Science,* volume 132, p. 382.

Sonnleitner, B., Locher, G., Fiechter, A. (1992). Biomass determination. *Journal of Biotechnology*, volume 25, p. 5-22.

Speers, D. J., Ryan, S., Harnett, G., Chidlow, G. (2003). Diagnosis of malaria aided by polymerase chain reaction in two cases with low-level parasitaemia. *Internal Medicine Journal*, volume 33(12), p. 613-615.

Spellberg, B., Gilbert, D. N. (2014). The future of antibiotics and resistance: a tribute to a career of leadership by John Bartlett. *Clinical Infectious Diseases*, volume 59 Suppl 2, p. S71-75.

Srey, S., Jahid, I. K., Ha, S. (2013). Biofilm formation in food industries: A food safety concern. *Food Control*, volume 31(2), p. 572-585.

Stoffel, A., Kovács, A., Kronast, W., Müller, B. (1996). LPCVD against PECVD for micromechanical applications. *Journal of Micromechanics and Microengineering,* volume 6, p. 20-33.

Streetman, B., Banerjee, S. (1999). *Solid state electronic devices* (5th Edition). Prentice Hall.

Stringer, R. C., Hoehn, D., Grant, S. A. (2008). Quantum dot-based biosensorfor detection of human cardiac Troponin I using a liquid-core waveguide. *IEEE Sensors Journal*, volume 8, p. 295-300.

Su, X., Li, Y. (2004). A self-assembled monolayer-based piezoelectric immunosensor for rapid detection of *Escherichia coli* O157:H7. *Biosensors and Bioelectronics,* volume 19(6), p. 563-574.

Sur, U. K., Lakshminarayanan, V. (2004). A study of the hydrophobic properties of alkanethiol self-assembled monolayers prepared in different solvents. *Journal of Electroanalytical Chemistry*, volume 565(2), p. 343-350.

Syshchyk, O., Skryshevsky, V. A., Soldatkin, O. O., Soldatkin, A. P. (2015). Enzyme biosensor systems based on porous silicon photoluminescence for detection of glucose, urea and heavy metals. *Biosensors and Bioelectronics,* volume 66, p. 89-94.

Sze, A., Erickson, D., Ren, L., Li, D. (2003). Zeta-potential measurement using the Smoluchowski equation and the slope of the current–time relationship in electroosmotic flow. *Journal of Colloid and Interface Science*, volume 261(2), p. 402-410.

Tanaka, A. (2004). Toxicity of indium arsenide, gallium arsenide, and aluminium gallium arsenide. *Toxicology and Applied Pharmacology*, volume 198(3), p. 405-411.

Tang, L., Chun, I. S., Wang, Z. L., Li, J., Li, X., Lu, Y. (2013). DNA Detection Using Plasmonic Enhanced Near-infrared Photoluminescence of Gallium Arsenide. *Analytical Chemistry*, volume 85, p. 9522−9527.

Tarnawski, R., Ulbricht, M. (2011). Amphiphilic gold nanoparticles: Synthesis, characterization and adsorption to PEGylated polymer surfaces. *Colloids and Surfaces A*, volume 374(1–3), p. 13-21.

Taylor, A. D., Yu, Q., Chen, S., Homola, J., Jiang, S. (2005). Comparison of *E. coli* O157:H7 preparation methods used for detection with surface plasmon resonance sensor. *Sensors and Actuators B*, volume 107, p. 202-208.

Thakur, M. S., Ragavan, K. V. (2013). Biosensors in food processing. *Journal of Food Science and Technology,* volume 50(4), p. 625-641.

ThermoFisherScientific (2016). Avidin-Biotin Interaction.

ThermoNicoletCorporation (2001). Introduction to Fourier Transform Infrared Spectrometry. Thermo Nicolet Corporation, USA.

Tinham, P., Bott, T. R. (2003). Biofouling assessment using an infrared monitor. *Water science and Technology*, volume 47(5), p. 39-43.

Tkachev, M., Anand-Kumar, T., Bitler, A., Guliamov, R., Naaman, R. (2013). Enabling Long-Term Operation of GaAs -Based Sensors in Aqueous Solutions. *Engineering*, volume 5, p. 1-12.

Tomkiewicz, P., Arabasz, S., Adamowicz, B., Miczek, M., Mizsei, J., Zahn, D. R. T., Hasegawa, H., Szuber, J. (2009). Surface electronic properties of sulfur-treated GaAs determined by surface photovoltage measurement and its computer simulation. *Surface Science*, volume 603(3), p. 498-502.

Toze, S. (1999). PCR and the detection of microbial pathogens in water and wastewater. *Water Research*, volume 33, p. 3545–3556.

Trueba, F. J., Woldringh, C. L. (1980). Changes in cell diameter during the division cycle of *Escherichia coli*. *Journal of Bacteriology*, volume 142, p. 869–878.

Tsien, H. C., Shockman, G. D., Higgins, M. L. (1978). Structural arrangement of polymers within the wall of Streptococcus faecalis. *Journal of Bacteriology*, volume 133, p. 372.

Turner, A. P. F. (2013). Biosensors: sense and sensibility. *Chemical Society Reviews,* volume 42, p. 3184-3196.

Turner, A. P. F., Karube, I., Wilson, G. S. (1987). *Biosensors, fundamentals and applications*. Oxford University Press, Oxford.

van Belkum, A., Durand, G., Peyret, M., Chatellier, S., Zambardi, G., Schrenzel, J., Shortridge, D., Engelhardt, A., Dunne, W.M., Jr. (2013). Rapid clinical bacteriology and its future impact. *Annals of Laboratory Medicine*, volume 33(1), p. 14-27.

van de Krol, R. (2011). *Principles of Photoelectrochemical Cells. Photoelectrochemical Hydrogen Production*, pp. 13-67. Springer.

van Loosdrecht, M. C., Lyklema, J., Norde, W., Zehnder, A. J. (1990). Influence of interfaces on microbial activity. *Microbiological Reviews,* volume 54(1), p. 75-87.

Velusamy, V., Arshak, K., Korostynska, O., Oliwa, K., Adley, C. (2010). An overview of foodborne pathogen detection: in the perspective of biosensors. *Biotechnology Advances*, volume 28, p. 232–254.

Ventola, C. L. (2015). The Antibiotic Resistance Crisis: Part 1: Causes and Threats. *Pharmacy and Therapeutics*, volume 40(4), p. 277-283.

Vermeulen, N., Keeler, W. J., Nandakumar, K., Leung, K. T. (2008). The bactericidal effect of ultraviolet and visible light on *Escherichia coli*. *Biotechnology and Bioengineering,* volume 99(3), p. 550-556.

Versalovic, J., Carroll, K. C., Funke, G., Jorgensen, J. H., Landry, M. L., Warnock, D. W. (2011). *Manual of Clinical Microbiology*, 10th Edition. American Society for Microbiology Press, Washington.

Villari, P., Motti, E., Farullo, C., Torre, I. (1998). Comparison of conventional culture and PCR methods for the detection of *Legionella pneumophila* in water. *Letters in Applied Microbiology*, volume 27, p. 106–110.

Voznyy, O., Dubowski, J. J. (2008). Structure of Thiol Self-Assembled Monolayers Commensurate with the GaAs(001) Surface. *Langmuir*, volume 24, p. 13299-13305.

Vrettou, C., Tzetis, M., Traeger-Synodinos, J., Palmer, G., Kanavakis, E. (2002). Multiplex sequence variation detection throughout the CFTR gene appropriate for preimplantation genetic diagnosis in populations with heterogeneity of cystic fibrosis mutations. *Molecular Human Reproduction*, volume 8(9), p. 880-886.

Wada, O. (1988). Optoelectronic integration based on GaAs material. *Optical and Quantum Electronic,* volume 20, p. 441-474.

Wang, J., Morton, M. J., Elliott, C. T., Karoonuthaisiri, N., Segatori, L., Biswal, S. L. (2014). Rapid Detection of Pathogenic Bacteria and Screening of Phage-Derived Peptides Using Microcantilevers. *Analytical Chemistry*, volume 86, p. 1671-1678.

Wang, Y., Ye, Z., Ying, Y. (2012). New Trends in Impedimetric Biosensors for the Detection of Foodborne Pathogenic Bacteria. *Sensors,* volume 12, p. 3449-3471.

Wang, Z. L. (2000). Transmission Electron Microscopy of Shape-Controlled Nanocrystals and Their Assemblies. *The Journal of Physical Chemistry B*, volume 104(6), p. 1153-1175.

Wengrovitz, M., Spangler, S., Martin, L. F. (1991). Sonication provides maximal recovery of staphylococcus epidermidis from slime-coated vascular prosthetics. *The American Surgeon*, volume 57(3), p. 161-164.

WHO (2015). Global action plan on antimicrobial resistance. World Health Organization

WHO (2016). Antimicrobial resistance. World Health Organziation (WHO).

Widdel, F. (2007). Theory and measurement of bacterial growth. *Grundpraktikum Mikrobiologie*, volume 4.

Wieliczka, D. M., Ding, X., Dubowski, J. J. (2006). X-ray photoelectron spectroscopy study of self-assembled monolayers of alkanethiols on (001) GaAs. *Journal of Vacuum Science and Technology A*, volume 24(5), p. 1756-1759.

Wieser, A., Schneider, L., Jung, J., Schubert, S. (2012). MALDI-TOF MS in microbiological diagnostics-identification of microorganisms and beyond (mini review). *Applied Microbiology and Biotechnology*, volume 93(3), p. 965-974.

Williams, D. N., Ehrman, S. H., Pulliam Holoman, T. R. (2006). Evaluation of the microbial growth response to inorganic nanoparticles. *Journal of Nanobiotechnology*, volume 4(1), p.1-8.

Wittwer, C. T., Kusukawa, N. (2004). *Molecular Microbiology Diagnostic Principles and Practice*. ASM Press, Washington, DC, USA.

Wolf, G., Crespo, J. G., Reis, M .A. M. (2002). Optical and spectroscopic methods for biofilm examination and monitoring. *Reviews in Environmental Science and Biotechnology*, volume 1(3), p. 227-251.

Wong, Y. Y., Ng, S. P., Si, S. H., Yao, S. Z., Fung, Y. S. (2002). Immunosensor for the differentiation and detection of *Salmonella* species based on a quartz crystal microbalance. *Biosensors and Bioelectronics,* volume 17, p. 676-684.

Wu, X., Han, C., Chen, J., Huang, Y.-W., Zhao, Y. (2016). Rapid Detection of Pathogenic Bacteria from Fresh Produce by Filtration and Surface-Enhanced Raman Spectroscopy. *JOM*, volume 68(4), P. 1156-1162.

Yacobi, B. G. (2003). *Semiconductor materials: An introduction to basic principles*. Springer.

Yocum, R. R., Rasmussen, J. R., Strominger, J. L. (1980). The mechanism of action of penicillin. Penicillin acylates the active site of Bacillus stearothermophilus D-alanine carboxypeptidase. *The Journal of Biological Chemistry,* volume 255(9), p. 3977-3986.

Yoo, E. H., Lee, S. Y. (2010). Glucose biosensors: an overview of use in clinical practice. *Sensors* , volume 10(5), p. 4558-4576.

Yoshioka, K., Sato, Y., Murakami, T., Tanaka, M., Niwa, O. (2010). One-Step Detection of Galectins on Hybrid Monolayer Surface with Protruding Lactoside. *Analytical Chemistry*, volume 82(4), p. 1175-1178.

Yota, J. (2009). Interlevel Dielectric Processes Using PECVD Silicon Nitride, Polyimide, and Polybenzoxazole for GaAs HBT Technology. *Journal of The Electrochemical Society*, volume 156(11), p. G173-G179.

Yotter, R. A., Lee, L. A., Wilson, D. M. (2004). Sensor Technologies for Monitoring Metabolic Activity in Single Cells—Part I: Optical Methods. *IEEE Sensors Journal*, volume 4, p. 395-411.

Yu, P. Y., Cardona, M. (2010). *Fundamentals of Semiconductors*, 4th ed. Springer.

Zagorodko, O., Bouckaert, J., Dumych, T., Bilyy, R., Larroulet, I., Yanguas Serrano, A., Alvarez Dorta, D., Gouin, S. G., Dima, S. O., Oancea, F., Boukherroub, R., Szunerits, S. (2015). Surface Plasmon Resonance (SPR) for the Evaluation of Shear-Force-Dependent Bacterial Adhesion. *Biosensors,* volume 5(2), p. 276-287.

Zariffard, M. R., Saifuddin, M., Sha, B. E., Spear, G. T. (2002). Detection of bacterial vaginosis-related organisms by real-time PCR for Lactobacilli, Gardnerella vaginalis and Mycoplasma

hominis. *Federation of European Microbiological Societies (FEMS) Immunology and Medical Microbiology*, volume 34(4), p. 277-281.

Zavizion, B., Zhao, Z., Nittayajarn, A., Rieder, R. J. (2010). Rapid Microbiological Testing: Monitoring the Development of Bacterial Stress. *PLOS ONE*, volume 5(10), p. e13374.

Zhang, Z., Yates, J. T. (2012). Band Bending in Semiconductors: Chemical and Physical Consequences at Surfaces and Interfaces. *Chemical Reviews,* volume 112(10), p. 5520-5551.

Zhou, S. Y., Zuo, H., Stobaugh, J. F., Lunte, C. E., Lunte, S. M. (1995). Continuous in vivo monitoring of amino acid neurotransmitters by microdialysis sampling with on-line derivatization and capillary electrophoresis separation. *Analytical Chemistry,* volume 67(3), p. 594-599.

Zhou, Y., Kong, Y., Kundu, S., Cirillo, J. D., Liang, H. (2012). Antibacterial activities of gold and silver nanoparticles against Escherichia coli and bacillus Calmette-Guerin. *Journal of Nanobiotechnology*, volume 10, p. 19.